Evaluation of Extended End-Plate Moment Connections Under Seismic Loading

by

John C. Ryan, Jr.

Thesis submitted to the Faculty of the

Virginia Polytechnic Institute and State University

in partial fulfillment of the requirements for the degree of

MASTER OF SCIENCE

In

Civil Engineering

APPROVED:

T.M. Murray, Chairman

W.S. Easterling

R.H. Plaut

September 1999
Blacksburg, Virginia

Key Words: End-Plates, Moment Connections, Cyclic Loading, Metal Building Manufacture's Association

Evaluation of Extended End-Plate Moment Connections Under Seismic Loading

by

John C. Ryan, Jr.

Committee Chairman: Thomas M. Murray
Civil Engineering

(ABSTRACT)

An experimental investigation was conducted to study the extended end-plate moment connections subjected to cyclic loading. Seven specimens representing three end-plate moment connection configurations commonly used in the pre-engineered building industry were used. The connections were designed using yield-line theory to predict end-plate yielding and the modified Kennedy method to predict maximum bolt force calculations including prying action. A displacement controlled loading history was used to load the specimens. The maximum moments obtained experimentally and the experimental bolt forces throughout loading were compared with analytical predictions and finite element model results. The inelastic rotation of connections was calculated and conclusions were drawn on the compliance of these connections with current AISC specifications.

Acknowledgements

I would like to express my deepest appreciation to my committee chairman, Dr. Thomas Murray. His guidance, patience, and ability to take and give a joke will not soon be forgotten. I would also like to thank Dr. Sam Easterling, and Dr. Raymond Plaut for their assistance in developing this thesis.

The time spent in the Structures laboratory was reduced greatly by the assistance given to me by Emmitt Sumner, Dennis Huffman, Brett Farmer, Michelle Rambo-Roddenberry, Joe Howard, Marc Graper, and Clark Brown.

I would like to thank my friends in Blacksburg, and at home in Slidell, Louisiana, for their continued support. In particular a huge debt of gratitude is owed to Amy Dalrymple, Brian Diaz, Tim Mays, and Mark Boorse for gifts of kindness, patience, and time too numerous to count.

I would also like to recognize my sister, Kelly and my two younger brothers, Randy and Patrick, for their encouragement and unconditional love. Finally, I would like to thank my Mom and Dad. None of this would ever have been possible, without their support and consistently sound advice.

TABLE OF CONTENTS

LIST OF FIGURES

LIST OF TABLES

CHAPTER I

INTRODUCTION AND LITERATURE REVIEW

1.1 INTRODUCTION

The study and use of end-plates in moment resisting frames for beam-to-beam splices and beam-to-column connections dates back to the early 1960's. In the United States, these connections were primarily used in pre-engineered metal buildings until the mid 1980's. The pre-engineered, metal building industry, which primarily uses built up steel sections for light one-story buildings, found these connections to be very economical for several reasons. The shop welding required for the end-plates was feasible because of the welding already required for the built up members. Also, the plate material used for the end plates could be cut from the same plate from which the flanges of the built up sections were cut. Further, erection of the metal buildings was relatively simple due to all bolted connections, and therefore advantageous. No field welding was required, allowing construction to be done in cold conditions, and construction time to be reduced.

Eventually, because of more accurate fabrication and better design techniques, the use of moment end-plates has become more economically feasible for use in multi-story buildings. Also, as a result of poor performance of flange-welded moment connections in comparison to the performance of bolted and riveted moment connections in the 1994 Northridge earthquake and the 1995 Kobe earthquake, end-plate moment connections are under serious consideration as an alternative to welding in seismic regions. But because

of limited cyclical testing of moment end-plate connections, extensive research sponsored through the Federal Emergency Management Agency (FEMA) has been initiated. The purpose of this testing is to develop a database of stiffness curves, and possibly a design guide for moment end-plates. However, the research sponsored by FEMA does not include the investigation of built up sections. Therefore, the Metal Building Manufacturer's Association (MBMA), a group of private companies involved in the design, fabrication, and erection of pre-engineered metal buildings, along with the American Institute of Steel Construction (AISC), have independently sponsored the testing of practical flush and extended moment end-plates under cyclic loading.

The extended end-plate connection is primarily used for beam-to-column connections. It consists of a plate with bolt holes drilled or punched, and shop welded to a beam section. The connection is completed in the field when the beam end is bolted to a column. The extended end-plate connection is termed "extended" because the plate extends above or below the flange that will be in tension under load. In the case of extended end-plates used for seismic design, the end-plate is extended above and below both beam flanges.

The purpose of this study is to subject three types of extended moment end-plate configurations, Figure 1.1, to cyclic loading through failure, and observe their response. The strength of these end-plates is to be checked against design criteria developed for monotonic loading. The stiffness of the connections is to be observed to qualify the connections in the categories specified by the *Seismic Provisions for Structural Steel*

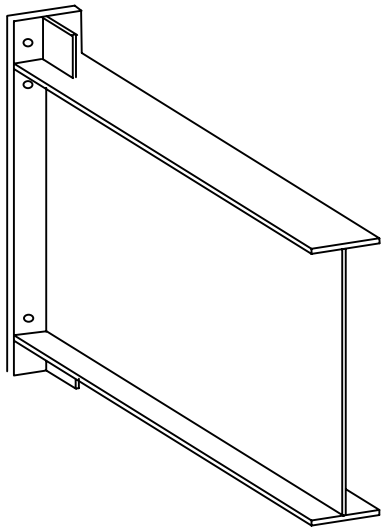

(a) Four Bolt Extended Stiffened

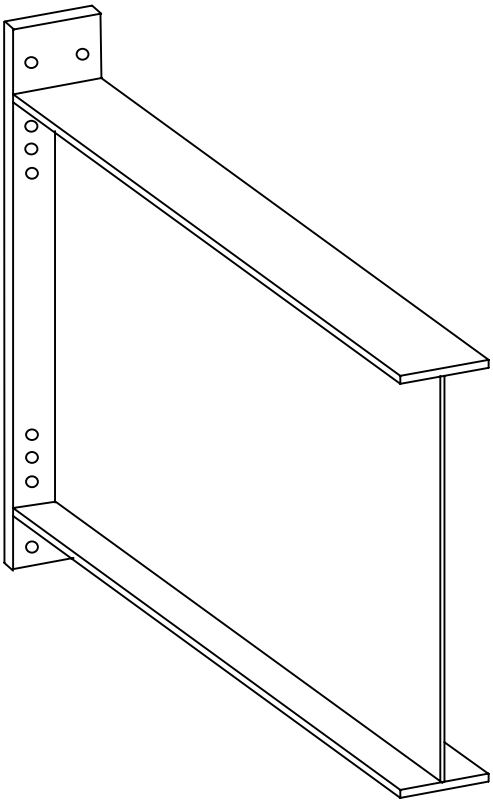

(b) Multiple Row 1/3 Extended

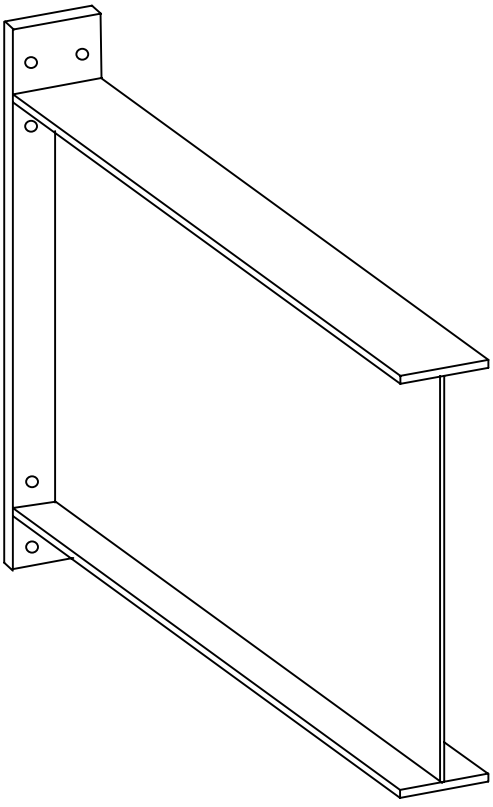

(c) Four Bolt Extended Unstiffened

Figure 1.1 Moment End-Plate Configurations

Buildings (1997), and *Interim Guidelines* (1997). A general outline of these categories is presented in the following Section.

1.2 ROTATIONAL REQUIREMENTS FOR MOMENT CONNECTIONS

Moment connections can be placed in one of two categories according to the AISC *Load and Resistance Factor Design Specification for Structural Steel Buildings* (1993), based on the stiffness of a connection. The connection can either be fully restrained (FR) or partially restrained (PR). AISC (Load 1993) provides criteria for determining construction category.

Additionally there are three types of seismic resisting frames: ordinary moment frames, intermediate moment frames, and special moment frames. Ordinary moment frames are expected to withstand limited inelastic deformation when subjected to the forces resulting from the motions of a design earthquake. A moment connection that qualifies for an ordinary moment frame must exhibit 0.01 radians of inelastic rotation. Intermediate moment frames are expected to withstand moderate inelastic deformation when subjected to the forces resulting from the motions of the design earthquake. To qualify as an intermediate moment frame a connection must exhibit 0.02 radians inelastic rotation. Finally, special moment frames are expected to withstand severe inelastic deformations when subjected to the forces of the design earthquake, and connections for these frames must exhibit 0.03 radians of inelastic rotation (Seismic 1997).

Further, there are rules governing the use of each type of frame, that are dependent on the relative strength of the connection with respect to the beam,. Ordinary moment frames can be designed for FR or PR construction regardless of the relative strength of the end-plate with respect to the beam. However, with the exception of two special cases, FR construction can only be used for intermediate and special moment frames when the design moment strength of the end-plate is greater than the plastic moment strength of the beam. The exceptions are applicable if the flexural strength of the beam is less than the plastic moment capacity of the cross-section. Therefore, FR construction can be used if the beam flange has been reduced, or flange local buckling is the controlling flexural failure mechanism. In these cases, the moment strength of the end-plate can be reduced to the strength of the reduced flange, or the design moment at which the flange buckles. However, the strength of the plate may not be less than 80% of the beam plastic moment strength. Otherwise PR construction must be used for intermediate and special moment frames (FEMA 1997).

1.3 LITERATURE REVIEW

Early experimental analysis was done on bolted rigid connections by Douty and McGuire (1965). Full scale testing of 27 tee-stub connections and seven end-plate moment connections was conducted. Bolt forces induced by tension flange forces were studied for both types of connections. Mathematical models for prying forces were presented for the tee connections. Also, a similar effect of prying was recognized in the end-plate connections. However, the extent of the end-plate testing was inadequate to

obtain prying force relationships. Therefore, in the design method presented for the end-plate connections, bolt forces were assumed to be related to a linear strain model assuming a rigid plate, and prying forces were neglected. Hence, an end-plate thickness that would approach this rigid condition assumption resulted.

Nair et al. (1974) expanded the knowledge of bolt prying forces by conducting a series of 27 tee-stub tests. Both static and fatigue tests were performed for each of the four geometric configurations using a universal testing machine to apply load to the tee sections bolted together with four bolts. The static testing involved loading the specimen to failure, while observing the elongation of the bolts in relation to the load delivered to the specimen. The dynamic tests involved loading the specimen cyclically through up to three million cycles, incrementing the load at a low rate. The elongation of the bolts was observed as well as the load delivered to the specimen. Some of the dynamically loaded specimens were loaded to bolt fracture. From the study, conclusive results were produced, stating that prying forces substantially reduce the ultimate load capacity and fatigue strength of the bolts in bolted tee connections. An empirical relationship between flange forces and prying forces, dependent on the geometry and thickness of the tee flanges, was derived. An equation for bolt forces including prying forces was recommended.

Krishnamurthy (1979) conducted early finite element analysis of moment end-plate connections. This study included thirteen finite element models of “benchmark connections, with dimensions spanning values commonly used in the industry”. The study was limited greatly by the technology of that time. A 2-dimensional/3-dimensional

finite element analysis was conducted to determine adequate correlation between results. If such correlation could be found for the thirteen connections considered, then two-dimensional analysis could be used with factors that correlated to the three-dimensional model of the same connection. According to this paper it would have been impossible to feasibly conduct an exhaustive three-dimensional analysis of end-plate connections because of the time involved in the programming, as well as the computational time required. Additionally, the task of creating a three-dimensional model with every detail and adequate proportions was deemed impossible at that time.

Therefore some simplifying assumptions were made, and a three-dimensional model was created based on a constant strain triangle and eight-node subparametric brick elements. Bolt heads were omitted, and the bolts were modeled as rectangular shanks, having the same cross-sectional area as round bolts. No "contact elements" were used. The bolts were assumed to be in tension, and an effective square area at the compression flange was assumed to be compressed against the column flange.

This study produced stress distribution plots at different loading magnitudes on the plate. Some correlation between the two-dimensional and three-dimensional models was observed. The three-dimensional model had less stiffness than the two-dimensional model because of the "prevention of the transverse variation of deformations and stresses". Seven correlation factors, relating the two different models, were tabulated for each of the thirteen benchmark connections. Krishnamurthy (1979) concluded that prying forces do not exist in moment end-plate connections based on this study.

Krishnamurthay (1979) also conducted a series of beam to column tests in which he concluded that bolt prying was not significant for the end-plate geometries used in his study. However several tests conducted were terminated due to lateral torsional buckling of the beam being tested. Therefore, the end-plate capacities and failure modes for these tests could not have been analyzed. Even so, a procedure developed for moment end-plate design, derived from this study, was adopted by AISC and appears in the AISC Manual.

Kennedy et al. (1981) introduced a method for predicting bolt forces with prying action in end-plate connections. The prediction equations were obtained by assuming an end-plate to be analogous to a split-tee connection. Kennedy et al. assume that a tee-stub or a flange plate goes through three stages of behavior as the load applied to the plate increases. The first stage of behavior, at lower loads, is thick plate behavior. At this stage, no plastic hinges have formed in the plate and prying forces are assumed to be zero. The second stage of plate behavior occurs as two plastic hinges form at the intersections of the plate centerline and each web face. The yielding of the plate marks the thick plate limit and indicates the onset of intermediate plate behavior. The prying force in this stage is between zero and maximum bolt prying force. The final stage of plate behavior, thin plate behavior, is marked by the formation of a second set of hinges at the bolt line. The prying force after thin plate behavior is initiated is equal to the maximum prying force. Kennedy et al. present equations which set thick and thin plate limits as a function of geometric properties of the plate, yield stress values of the plate, and applied flange force.

Finally, bolt prying forces are calculated according to the type of plate behavior determined.

The introduction of yield line theory as the primary analytical tool in predicting end-plate strengths resulted in greater accuracy of predicted strengths, and therefore, more economical plate design. After review of previous work, Mann and Morris (1979) recommended a design procedure for four bolt extended-stiffened end plates to be used in beam-to-column connections. The required end-plate thickness was determined using straight yield-line patterns passing through the bolts. The end-plate thickness achieved by this design procedure was reported to withstand the plastic moment strength of the beam, M_p. The bolts used were then sized as a function of the end-plate thickness. Finally, the required column flange thickness was determined using equations derived by a curved yield line theory.

Srouji et al. (1983) considered the design of four moment end-plate configurations: two-bolt flush, four-bolt flush, four-bolt extended unstiffened, and four-bolt extended stiffened. Design procedures for the required thickness of these end-plate configurations and for the forces in the bolts already existed. However, the difference in results obtained by different procedures was large. Using yield line theory, equations for each of the configurations were derived. Also, bolt prying force prediction equations were developed using variations of methods prescribed by Kennedy et al. (1981), which is referred to as the modified Kennedy method. The analytical models were verified for the two-bolt flush and four-bolt flush configurations through experimental analysis. The

design procedures developed for the extended end plates were verified through comparison to previously acquired experimental data.

For the two-bolt flush configuration, predicted moment capacities correlated closely to moment strengths observed experimentally. Predicted capacities using straight-line yield theory were compared to data obtained experimentally. Seven out of eight tests resulted in predicted versus experimental strength ratios between 0.94 and 1.06. Bolt predictions using the modified Kennedy method were also very close to the forces measured experimentally.

For the four-bolt flush end plate configuration, the predicted versus experimental moment strength ratios were between 0.97 and 1.06. By measuring bolt strain, as in the two-bolt flush tests, bolt forces were also recorded experimentally, and shown to be reasonably close to the predicted bolt forces.

The extended end-plate configurations (stiffened and unstiffened) were compared to experimental tests done by Krishnamurthy (1979). The predicted capacities derived from straight yield line theory correlated well with Krishnamurthy's data except where torsional buckling limit states of end-plate specimens controlled failure.

Kukreti et al. (1982) presented the findings of an analytical study conducted to investigate the behavior of stiffened moment end-plates with two rows of bolts inside and outside the beam tension flange. The tension flange was modeled using finite elements. The assumption was made that the tension flange and the end-plate at the tension flange behaved as a stiffened tee-hanger. A parametric study was done, restricting the

dimensions within practical ranges. Prediction equations were produced based on the data of several models.

Srouji et al. (1983) concluded that the straight yield-line analysis accurately predicts end plate strength for the two-bolt and four-bolt flush end-plate strengths, and that the modified Kennedy method adequately predicts bolt forces for the flush end-plate configurations. The extended unstiffened end-plate study showed that the straight yield-line theory adequately predicted the strengths of the end plates tested by Krishnamurthy (1979) with a few discrepancies.

Morrison et al. (1985) conducted an analytical study to develop a design method for multiple row extended end-plates. The results were verified by full-scale testing The testing program involved the monotonic testing of six beam-to-beam specimens, ranging from 30 in. to 62 in. in depth. The design methods derived and verified by this testing include end-plate thickness requirements based on straight yield-line analysis, as well as bolt force predictions. The method consists of finding a thickness of the end plate based on strength. The thickness is then determined to act as a thick, thin, or intermediate plate under a given load. The bolt forces, including prying action, if present, are then determined using the modified Kennedy method.

Morrison et al. (1986) developed a strength design procedure for four bolt extended stiffened end-plates. This procedure was developed in the same way that the procedure for the multiple row extended moment end-plate design procedure was developed. The beam-to-beam specimens that were tested to verify the procedure were built up sections with nominal depths of 16 in., 20 in., and 24 in.

Murray (1988) reviewed the past literature and design methods for both flush and extended end-plate configurations. Included in Murray's discussion are column-side limit states. Design procedures based on yield-line theory and bolt force limit states are presented.

Tsai and Popov (1990) reported a limited study of four-bolt extended stiffened and four-bolt extended unstiffened moment end plates. The study consisted of three full-scale beam-to-column tests. Two of the tests were unstiffened and one was stiffened. The depths of the hot-rolled beams tested were between 18 in. and 21 in. The specimens were designed based on a hierarchical importance of possible failure modes. The hierarchy of the failure designed for is as follows. First, the beam plastic capacity is to be achieved. Then the inelastic rotational capacity is developed. Next, failure of the end plate in flexure or shear is desired. The failure of the bolts and beam-to-end-plate welds are brittle, and therefore less desirable failure modes. Effort was made in this study to determine adequate bolt strength for cyclical loading.

The purpose of the study was to examine the adequacy of moment end plates, used for static design, under cyclical loading. Data obtained included moment capacity versus rotation, and bolt forces versus applied load, and rotation. Hysteretic plots of moment capacity versus rotation are given.

In the first test, end-plate thickness and bolt diameter were determined using the procedure in AISC (Manual 1989). In this procedure prying forces of the bolts are neglected, and a relatively thick end plate is used to minimize the actual prying forces. The energy dissipation realized by this design was determined to be less than adequate for

seismic design. Almost all of the inelastic deformation achieved by this connection was due to the plastic deformation of the bolts. Consequently, end-plate separation from the column flange was observed as the loading increased. Towards the end of the test, the hysteretic loops developed a slight pinch. The test was terminated when an inner bolt fractured.

In the second test, a stiffened extended end plate was used to distribute the flange force to the bolts more evenly, and to reduce prying forces. Also larger bolts were used. The energy dissipation of this test was determined to be adequate for seismic loading. The inelastic rotation came from local buckling of the beam flanges, which is a desirable, ductile limit state.

In the third test, an unstiffened end-plate was used with relatively larger bolts and a thicker end-plate. The behavior observed was very similar to that seen in the second test.

Tsai and Popov (1990) concluded that moment end-plate connections are a viable substitute for field-welded moment connections in frames designed for seismic loading. However, based on this very limited number of tests, conventional design procedures for statically loaded moment end-plates must be modified to provide more stringent requirements for the connecting bolts. Also, because of the importance of moment end-plate connections, and the lack of sufficient data available, further research was encouraged.

Ghoborah et al. (1990) conducted quasi-static cyclic tests on five extended stiffened end-plates, welded to 14 in. deep hot-rolled sections. The test was designed to

study the effect of continuity plates in the panel zone of the column, and to observe the energy dissipation capacity of the connections. Ghoborah et al. noted, in the two specimens designed without continuity plates in compliance to design procedures suggested by Mann and Morris (1979), that although well behaved hysteretic behavior was observed, severe damage to the column flange occurred. For the three tests in which continuity plates were used, the loading was terminated after extensive beam tip deflection was achieved due to the inelastic deformation of the beam section. It was observed that the majority of the energy was dissipated through inelastic action of the beam. Ghoborah et al. made the following conclusions based on this testing. (1) An unstiffened column connection is not recommended. (2) Bolts should be designed to sustain forces corresponding to 1.3 times the plastic moment capacity of the beam. (3) When designing an unstiffened end-plate, use 1.3 times the plastic moment capacity of the beam as the design moment. (4) However, use 1.0 times the plastic moment capacity of the beam when designing an extended end-plate.

Abel and Murray (1994) developed a design procedure for the four bolt-extended unstiffened moment end-plate connection. The results were consistent with the findings of Srouji et al.(1983), Hendrick et al.(1985), and Morrison et al.(1986). Required end-plate thickness requirements are obtained by an equation derived from yield line theory and bolt forces are predicted using the modified Kennedy method.

Using this strength to thickness of end-plate relationship, predicted strength for actual end-plate thickness was obtained and compared to the experimental strength of several connections. The predicted versus the experimental moment strength ratio of the

plates was found to be between 0.88 and 0.91 for four tests of built up beam sections between 16 in. and 18 in. deep.

Bolt forces were then predicted using the modified Kennedy method for prying forces modified for end-plates. For the experiments, the bolts were gauged to determine the bolt forces throughout testing. The flange force was found to be distributed evenly to all four bolts at the tension flange. The ratio of the applied moment during testing, at the time the bolts were observed to have the pre-determined bolt proof load, versus the predicted moment at the time that the bolts were to have the bolt proof load, were between 0.97 and 1.05.

Sherbourne and Bahaari (1997) developed a methodology based on three-dimensional finite element design, to analytically evaluate the moment rotation relationships for moment end-plate connections. ANSYS 4.4 was the software package used. The purpose for this research was to provide designers with a method of determining stiffness for these connections. It was apparent at the time that the ability of designers to produce a moment-rotation curve for moment end-plate connections was limited.

Because of advancements in computer technology, Sherbourne and Bahaari's models included plate elements for the flange, webs, and stiffeners of the column and beam, as well as taking into account the bolt shank, nut, head of the bolt, and contact regions. However, bolt pre-stressing was not included.

It was determined that the behavior of a moment end-plate throughout an entire loading history, up to and including failure, can be feasibly and accurately modeled by

three-dimensional finite element analysis. This is particularly useful when one of the plates in contact, either the column flange or the end plate, is thin. The analysis of such a plate is inaccurate when using two-dimensional models.

An additional advantage to the use of the three-dimensional model is the separation of the column, bolt, plate, and beam stiffness contributions to the overall behavior of the connection.

Meng, (1996) tested extended end-plate moment connections under cyclic loading. The end-plates were tested using hot-rolled beam sections ranging from 18 in. to 36 in. in depth. A design procedure for four bolt extended moment end-plate connections, developed by Abel and Murray (1994) for monotonic loading was used to design the test specimens. The design procedure was verified for moment end-plates under cyclic loading through these tests. Also, weld access holes were determined to be the cause of unacceptable stress concentrations leading to premature failure of the specimens in which they were used. Other end-plates were tested without the weld access holes, and performed well. Hence, the fabrication of four bolt extended end-plates without weld access holes was recommended. Also four bolt extended moment end-plates were found acceptable for use in high seismic regions for the size of the members tested.

Ribeiro et al. (1998) discussed results of an experimental study of beam-to-column moment end-plate connections. This study includes testing of twelve cruciform built-up sections to validate design criteria used for rolled shapes for the design of built-up

sections. Specimens were designed, specifically to check the method proposed by Krishnamurthy (1979). The following observations among others were made:

1. Applied moments were about 20% greater than the plastic moment capacities predicted.
2. The greater the bolt diameter, the greater is the influence of end-plate thickness.
3. Krishnamurthy's method is non-conservative.
4. Bolt rupture occurred in tests in which the Krishnamurthy method predicted otherwise.
5. Results considering the collapse modes of the testing completed led to a hypothesis concerning prying forces which is not accepted by Krishnamurthy.

In 1998, Troup et al. (1998) presented a paper describing finite element modeling of bolted steel connections. ANSYS was also used for this study, which included an extended moment end plate model as well as a tee-stub model. The model utilized a bi-linear stress-strain relationship for the bolts. Also, special contact elements were used between the end-plate and the column flange for the extended end-plate model, and between the tees for the tee model. By using the contact elements between the contact surfaces of the models, the geometric non-linearities that are present between the surfaces as separation occurs due to increased load can be realistically modeled.

Both models were calibrated with experimental test data to show excellent correlation between analytical and experimental stiffness.

Bolt forces were also analyzed. It was found that for the simple four-bolt arrangement about the tension flange, the tee design prediction is accurate. However, for more complex bolt patterns, the distribution of prying forces is not as clear. Therefore, it is suggested that further research be pursued to establish the suitabilty of the tee-stub analogy for complex designs.

Troup, et al. (1998) concluded the following:

1. Tee-stub analogy is a useful benchmark problem providing an indication of the performance of analysis techniques.
2. Shell elements are more accurate for modeling beam and column sections. Thick endplate design provides additional rotational stiffness and moment capacity but may result in bolt fracture.
3. Thin end plates provide enough deformation capacity to allow semi-rigid connection design, but may result in excessive deflection.
4. The moment capacity prediction of Eurocode 3 has been shown to be reasonable, but conservative, for simple end-plate bolt configurations. The code is inaccurate when analyzing more complicated bolt arrangements. If these inaccuracies do not lead to bolt failure, they are acceptable.

Adey, et al. (1998) conducted a study in which 15 extended end-plate connections were subjected to cyclic loading to compare the effects of bolt configuration and welding procedure on the strength and ductility of moment end-plate connections. The end-plates were tested using 14 in., 18 in., and 24 in. beam sections, denoted as S-series, M-series, and B-series, respectively. The S-series and B-series used tests in which the bolt pitches,

bolt diameters, and end-plate thickness used were identical. In all three series, the outside pitch was varied in half of the tests to create a "relaxed" bolt configuration. The other tests, referred to as having a "tight" bolt configuration, had a the same pitch for both inside and outside bolts.

The study concluded that the M-series sustained greater rotation than the B-series connections, and was therefore more ductile, and that larger pitches resulted in greater energy dissipation.

Also, Adey et al. (1998) developed design equation by modifying work done by Whittaker and Walpole to more accurately match the S-series tests. Upon completion of S, M, and B-series testing, maximum moment values achieved were used as design strengths for several design methods, including the modified version of Whittaker and Walpole. End-plate thicknesses calculated from these design methods were compared to the actual end-plate thicknesses used for tests. The modified Whittaker and Walpole method was most accurate in back calculating the thickness. However, this was the only method which accommodated the connections with inner bolt pitches differing from the outer bolt pitches. For the other methods an average pitch was used.

1.4 OBJECTIVE AND SCOPE OF RESEARCH

The purpose of this research is to investigate the behavior of extended moment end-plate connections under quasi-static cyclic loading. Seven full scale, single-sided beam to column tests were conducted, using built-up beams and columns. Three extended end plate configurations were used: four bolt extended stiffened, multiple row 1/3 extended,

and four bolt extended unstiffened (see Figure 1.1). The inelastic rotational capacity of each configuration was found. Also design procedures utilizing yield-line analysis, and bolt force predictions with prying action, were checked against test results.

CHAPTER II

EXTENDED END-PLATE MOMENT CONNECTION DESIGN

2.1 OVERVIEW

To design moment end-plate connections for this study, four components of the connection were considered: the beam, the end-plate, the bolts, and the column. First a beam section was chosen with an appropriate flexural strength. Once the flexural strength of the beam was determined, the end-plate was designed for the required strength using yield-line theory. After determining the thickness of the end-plate, the bolt sizes were chosen using bolt force equations derived from the modified Kennedy split-tee model. Finally, the column was checked for strength using guidelines presented by AISC (Manual 1994).

In this chapter, yield-line theory is presented in general terms, followed by its direct application to the four bolt extended stiffened end-plate, the multi-row 1/3 extended end-plate, and the four bolt extended unstiffened end-plate. The method for calculating bolt forces using the "Split-Tee Analogy" of Kennedy et al. (1981) is then presented, followed by its direct application to the same end-plate configurations. The flexural strength prediction of the beam is beyond the scope of this research, and is therefore not presented. The column flanges were detailed such that the strength was greater than that of the connected end-plate.

2.2 END-PLATE STRENGTH PREDICTIONS

2.2.1 General Yield-Line Theory

Yield-line theory was first introduced to analyze reinforced concrete slabs, and has more recently been adopted for use in the strength analysis and design of moment end-plates. A yield-line is a continuous formation of plastic hinges along a straight or curved line. An end-plate is assumed to reach failure when the yield-lines form a kinematically valid collapse mechanism. The elastic deformations of an end-plate are assumed to be negligible in comparison to its plastic deformations. Therefore the yield-line development is assumed to divide the end-plate into plane regions.

Derivations of both curved and straight yield lines have been introduced. However, straight yield-lines have been shown to be more accurate for the end-plates tested in this research. To establish the locations of the straight yield lines, the following guidelines must be followed:

1. Axes of rotation generally lie along lines of support.
2. Yield lines pass through the intersection of the axes of rotation of adjacent plate segments.
3. Along every yield line , the bending moment is assumed to be constant and is as the plastic moment of the plate.

The analysis of a yield-line mechanism can be performed by either the equilibrium method or the virtual work method. The virtual work method is simpler than the

equilibrium method, and is therefore preferred. In the virtual work method, the end-plate is assumed to rotate about the center of the compression flange of the beam section. Small angle rotation is assumed. The external work, done by rotating the plate through a small arbitrary rotation, is set equal to the internal work, done at the plastic hinges formed over the yield lines, which accommodates the total rotation of the plate. For a specified yield-line pattern and loading, a certain plastic moment will be required along the hinge lines. For the same loading, other patterns may result in a larger required plastic moment capacity. Hence, the controlling pattern is the one which requires the largest required plastic moment. Or conversely, for a given plastic moment capacity, the controlling mechanism is the one which produces the lowest failure load. This implies that the yield-line theory is an upper bound procedure and the least upper bound solution must be found.

To determine an end-plate plastic moment capacity, or failure load, yield line mechanisms are arbitrarily chosen in accordance with the three guidelines presented above. Next, the external work of a unit rotation of the end-plate is found and set equal to the internal work of the relative rotation of the plane sections divided by yield lines. This equation can either be solved for the unknown load acting through the unit rotation or the resisting moment of the end-plate. The results of this procedure for reasonable yield-line mechanisms are compared. The controlling yield line mechanism is that which corresponds to the greatest plastic moment capacity or the smallest failure load.

The following formulation of yield-line analysis is taken from Hendrick et al. (1985). The internal energy stored in a particular yield-line mechanism is the sum of the

internal energy stored in each yield line forming the mechanism. The internal energy stored in any given yield line is obtained by multiplying the normal moment on the yield line with the normal rotation of the yield line. Thus the energy stored, W_{in} , in the n^{th} yield line of length L_n is:

$$W_{in} = \int_{L_n} m_p \theta_n \, ds \tag{2.1}$$

where θ_n is the relative rotation of line n and ds is the elemental length of line n. The internal energy stored in a yield-line mechanism can be written as:

$$W_i = \sum_{n=1}^{N} \int_{L_n} m_p \theta_n \, ds \tag{2.2}$$

$$= \sum_{n=1}^{N} m_p \theta_n L_n$$

where N is the number of yield lines in the mechanism.

For complicated yield-line patterns the expressions for the relative rotation are somewhat tedious to obtain; therefore it is more convenient to resolve the slopes and moments in the x- and y-directions. This results in the following form of Equation 2.2:

$$W_i = \sum_{n=1}^{N} (m_{px} \theta_{nx} L_x + m_{px} \theta_{ny} L_y) \tag{2.3}$$

where m_{px} and m_{py} are the x- and y-components of the normal moment capacity per unit length, L_x and L_y are the x- and y-components of the yield line length, and θ_{nx} and θ_{ny} are the x-and y-components of the relative normal rotation of yield line n.

2.2.2 Four Bolt Extended Stiffened Moment End-Plates

The yield-line analysis presented here for the four bolt extended stiffened moment end-plates is taken from a study done by Srouji (1983).

One of two yield-line patterns can control the strength of the four bolt extended stiffened moment connection depending on the distance which the end-plate extends beyond the outside bolt line, d_e, and the dimension s. The two mechanisms are shown in Figure 2.1. The first mechanism, in which a hinge forms near the outside edge of the end-plate, is shown as Case 1. The second mechanism, in which a hinge does not form near the outside edge of the end plate, is shown as Case 2. The dimension, s, is found by differentiating the internal work expression with respect to s and equating it to zero. The expression for s is as follows:

$$s = \frac{1}{2}\sqrt{b_f g} \tag{2.4}$$

The equations for the internal work, W_i , end-plate capacity , M_{pl}, and required plate thickness for a given load, t_p, for each case is as follows:

Case 1, when $s<d_e$:

$$W_i = \frac{4m_p}{h}\left[\frac{b_f}{2}\left(\frac{1}{p_f}+\frac{1}{s}\right)+(p_f+s)\left(\frac{2}{g}\right)\right]\left[(h-p_t)+(h+p_f)\right] \tag{2.5}$$

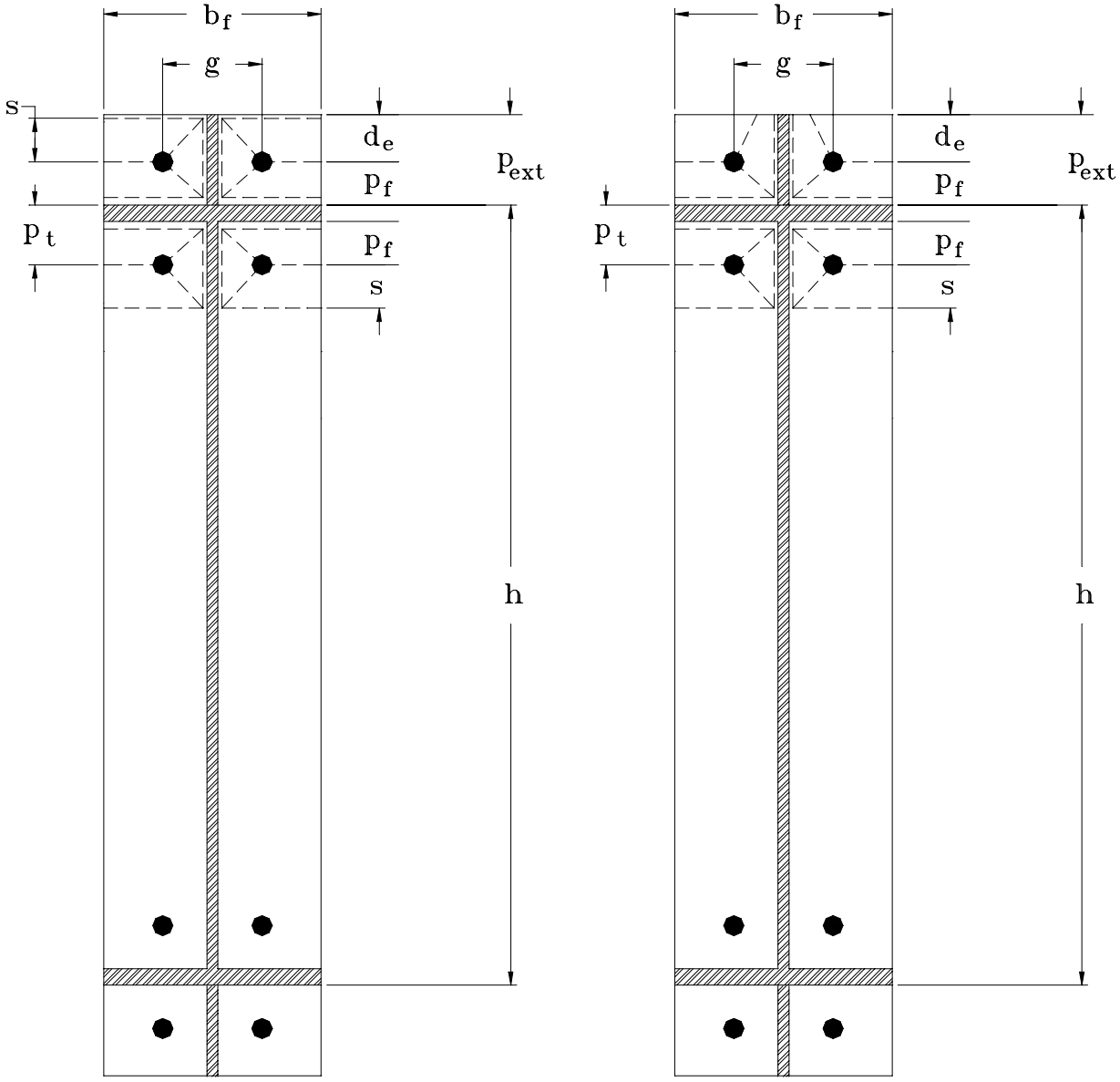

(a) Case 1 when $s < d_e$

(b) Case 2 when $s > d_e$

Figure 2.1 Yield-Line Mechanism for the Four Bolt Extended Stiffened Moment End-Plate Connection From Srouji, et al.(1983)

$$M_{pl} = 4m_p\left[\frac{b_f}{2}\left(\frac{1}{p_f}+\frac{1}{s}\right)+(p_f+s)\left(\frac{2}{g}\right)\right][(h-p_t)+(h+p_f)] \tag{2.6}$$

$$t_p = \left[\frac{M_u/F_{py}}{\left[\frac{b_f}{2}\left(\frac{1}{p_f}+\frac{1}{s}\right)+(p_f+s)\left(\frac{2}{g}\right)\right][(h-p_t)+(h+p_f)]}\right]^{1/2} \tag{2.7}$$

Case 2, when $s>d_e$:

$$W_i = \frac{4m_p}{h}\left[\frac{b_f}{2}\left(\frac{1}{p_f}+\frac{1}{2s}\right)+(p_f+d_e)\left(\frac{2}{g}\right)\right][(h-p_t)+(h+p_f)] \tag{2.8}$$

$$M_{pl} = 4m_p\left[\frac{b_f}{2}\left(\frac{1}{p_f}+\frac{1}{2s}\right)+(p_f+d_e)\left(\frac{2}{g}\right)\right][(h-p_t)+(h+p_f)] \tag{2.9}$$

$$t_p = \left[\frac{M_u/F_{py}}{\left[\frac{b_f}{2}\left(\frac{1}{p_f}+\frac{1}{2s}\right)+(p_f+d_e)\left(\frac{2}{g}\right)\right][(h-p_t)+(h+p_f)]}\right]^{1/2} \tag{2.10}$$

where*:*

$$m_p = \frac{F_{py}t_p^{\,2}}{4} \tag{2.11}$$

and F_{py} is the end-plate yield stress.

2.2.3 Multiple Row 1/3 Extended Moment End-Plates

The yield-line analysis presented here for the multiple row extended end-plate is taken from a study done by Morrison et al. (1986).

One of two yield line mechanisms, depending on the hole spacing, controls the strength prediction of the multiple row 1/3 extended configuration. The two mechanisms differ by the location of a single pair of yield lines, inside the flange. The hinge can occur along the line from the outermost bolt, lying inside the flange, to the web, a vertical distance of u, defined below, from the innermost bolt line. Or, the hinge can occur along the line between the innermost bolt to the intersection of the web and the tension flange. The two mechanisms are shown in Figure 2.2. For each of these mechanisms, there are two patterns which can form, depending on the length of the end-plate extending from the outer bolt line to the edge of the end-plate, similar to Case 1 and Case 2 of the four bolt extended stiffened yield line patterns. However, it can be shown for the specimens in this study that $s>d_e$ for all cases. Therefore the figures of these patterns are not included. The equations for the internal work, W_i, end-plate capacity, M_{pl}, and required end-plate thickness, t_p, for a desired ultimate load are as follows for Mechanism 1 and Mechanism 2:

Mechanism 1:

$$Wi = \frac{4m_p}{h}\left[\frac{b_f}{2}\left(\frac{1}{2}+\frac{h}{p_f}+\frac{h-p_t}{p_f}+\frac{h-p_{t3}}{u}\right)+2\left(p_f+p_{b1,3}+u\left(\frac{h-p_t}{g}\right)\right)\right] \qquad (2.12)$$

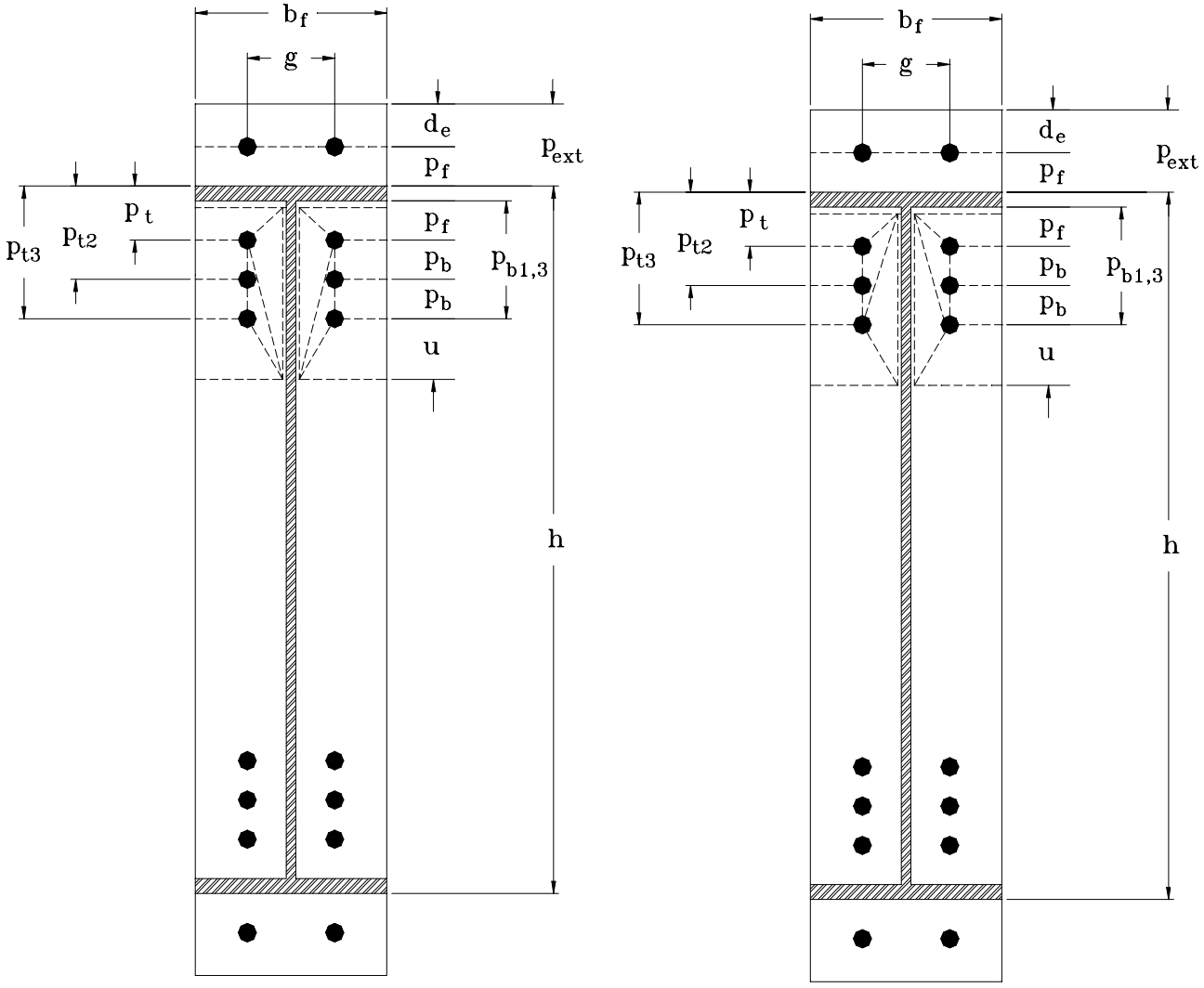

(a) Mechanism 1

(b) Mechanism 2

Figure 2.2 Yield-Line Mechanism for the Multiple Row 1/3 Extended Moment End-Plate Connection After Morrison, et al.(1986).

$$M_{pl} = 4m_p\left[\frac{b_f}{2}\left(\frac{1}{2}+\frac{h}{p_f}+\frac{h-p_t}{p_f}+\frac{h-p_{t3}}{u}\right)+2\left(p_f+p_{b1,3}+u\right)\left(\frac{h-p_t}{g}\right)\right] \tag{2.13}$$

$$t_p = \left[\frac{M_u/F_{py}}{\left[\frac{b_f}{2}\left(\frac{1}{2}+\frac{h}{p_f}+\frac{h-p_t}{p_f}+\frac{h-p_{t3}}{u}\right)+2\left(p_f+p_{b1,3}+u\right)\left(\frac{h-p_t}{g}\right)\right]}\right]^{1/2} \tag{2.14}$$

where m_p is found using Equation 2.11, and u is found by differentiating the internal work expression, Equation 2.12, with respect to u, and setting it equal to zero to find:

$$u = \frac{1}{2}\sqrt{b_f g\left(\frac{h-p_{t3}}{h-p_t}\right)} \tag{2.15}$$

Mechanism 2:

$$Wi = \frac{4m_p}{h}\left[\frac{b_f}{2}\left(\frac{1}{2}+\frac{h}{p_f}+\frac{h-p_t}{p_f}+\frac{h-p_{t3}}{u}\right)+\frac{2}{g}\left(p_f+p_{b1,3}\right)\left(h-t_f\right)+\left(\frac{2u}{g}\right)\left(h-p_{3t}\right)+\frac{g}{2}\right] \tag{2.16}$$

$$M_{pl} = 4m_p\left[\frac{b_f}{2}\left(\frac{1}{2}+\frac{h}{p_f}+\frac{h-p_t}{p_f}+\frac{h-p_{t3}}{u}\right)+\frac{2}{g}\left(p_f+p_{b1,3}\right)\left(h-t_f\right)+\left(\frac{2u}{g}\right)\left(h-p_{3t}\right)+\frac{g}{2}\right] \tag{2.17}$$

$$t_p = \left[\frac{M_u / F_{py}}{\left[\frac{b_f}{2}\left(1 + \frac{h}{p_f} + \frac{h - p_t}{p_f} + \frac{h - p_{t3}}{u} + \frac{h + p_f}{2s}\right) + \frac{2}{g}(p_f + p_{b1,3})(h - t_f) + \left(\frac{2u}{g}\right)(h - p_{3t}) + \frac{2}{g}(d_e + p_f)(h + p_f) + \frac{g}{2} \right]} \right]^{1/2}$$

(2.18)

where m_p is found using Equation 2.11, and u is found by differentiating the internal work expression, Equation 2.16, with respect to u, and setting it equal to zero to find:

$$u = \frac{1}{2}\sqrt{b_f g} \tag{2.19}$$

2.2.4 Four Bolt Extended Unstiffened Moment End-Plates

The yield-line analysis presented here for the four bolt extended unstiffened end-plate is taken from a study done by Abel et al. (1994) and presented here. One yield-line mechanism controls the strength of this end-plate configuration. The pattern for this mechanism is shown in Figure 2.3. The equations for the internal work, W_i end-plate capacity, M_{pl}, and required end-plate thickness, t_p, for a desired ultimate load are as follows:

$$W_i = \frac{4m_p}{h}\left[\frac{b_f}{2}\left(\frac{1}{p_f} + \frac{1}{s}\right) + (p_f + s)\left(\frac{2}{g}\right)(h - p_t) + \frac{b_f}{2}\left(\frac{1}{2} + \frac{h}{p_f}\right)\right] \tag{2.20}$$

$$M_{pl} = 4m_p\left[\frac{b_f}{2}\left(\frac{1}{p_f} + \frac{1}{s}\right) + (p_f + s)\left(\frac{2}{g}\right)(h - p_t) + \frac{b_f}{2}\left(\frac{1}{2} + \frac{h}{p_f}\right)\right] \tag{2.21}$$

$$t_p = \left[\frac{M_u / F_{py}}{\left[\frac{b_f}{2}\left(\frac{1}{p_f} + \frac{1}{s} \right) + (p_f + s)\left(\frac{2}{g} \right)(h - p_t) + \frac{b_f}{2}\left(\frac{1}{2} + \frac{h}{p_f} \right) \right]} \right]^{1/2} \qquad (2.22)$$

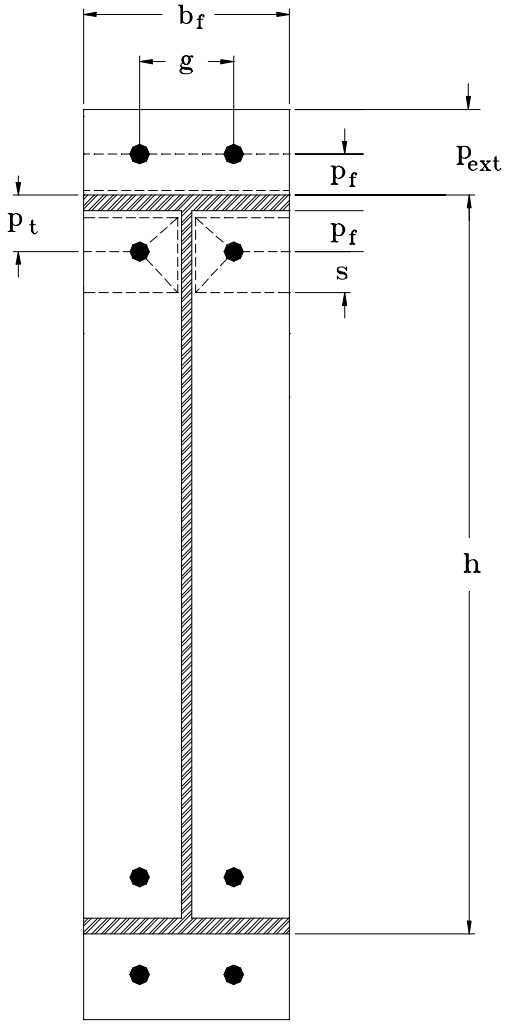

Figure 2.2 Yield-Line Mechanism for the Four Bolt Extended Unstiffened Moment End-Plate Connection After Abel, et al.(1994).

2.3 PREDICTION OF BOLT FORCES INCLUDING PRYING FORCES

2.3.1 Kennedy Method Split-Tee Model

Yield line theory is useful for predicting the strength of the end-plate. However, it completely neglects the forces that are carried into the bolts of the connection. Kennedy et al. (1981) proposed a method for predicting bolt forces including prying forces for split-tee connections. The split-tee has since been assumed to be analogous to the tension region of a moment end-plate connection by Morrison et al.. (1985), Abel and Murray (1994), and Meng (1996). If the web of the beam is neglected and the tension flange is assumed to behave as the web of a tee section, the following method for predicting prying forces is applicable. In Figure 2.4, the distance, a, has been determined

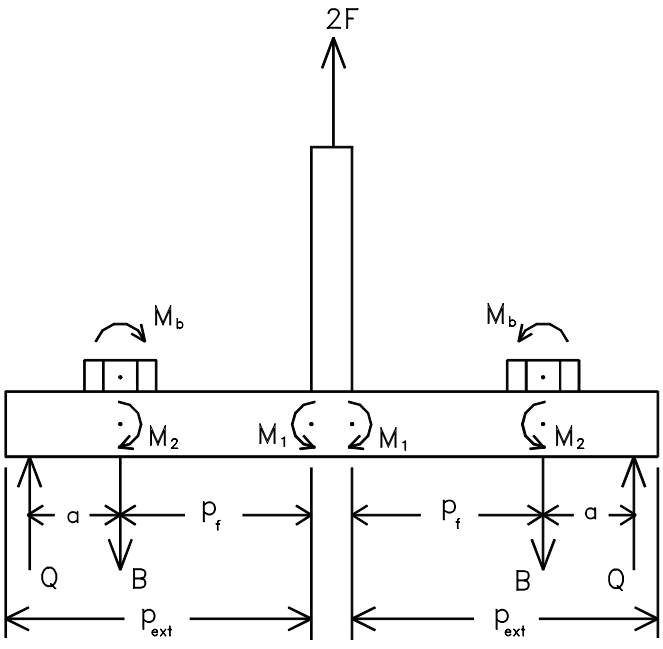

Figure 2.4 Kennedy Method Split-Tee Model

empirically by Hendrick et al. (1985) to be a function of t_p/d_b and is given by:

$$a = 3.682\left(\frac{t_p}{d_b}\right)^3 - 0.085 \tag{2.23}$$

The value for the distance a can not exceed p_{ext}-p_f for the outer portion of the plate.

As noted in Chapter I, the basic assumption of the Kennedy method is that the plate goes through three different stages of behavior as the applied load increases. The first stage of behavior, at lower loads, is thick plate behavior. At this stage, no plastic hinges have formed in the plate and prying forces are assumed to be zero, Figure 2.5(a). The second stage of plate behavior occurs as two plastic hinges form at the intersections of the plate centerline and each web face. The yielding of the plate marks the thick plate limit and indicates the onset of intermediate plate behavior (see Figure 2.5(b)). The prying force in this stage is between zero and maximum bolt prying force. The final stage of plate behavior, thin plate behavior, shown in Figure 2.5(c), is marked by the formation of a second set of hinges at the bolt line. The prying force after thin plate behavior is initiated is equal to the maximum prying force. Once the plate behavior has been established, the bolt force is calculated by summing the portion of the applied flange force assigned to each bolt with the appropriate prying force.

Kennedy et al. (1981) determined that the thick plate behavior of a tee-stem flange was limited to an end-plate thickness, t_p , greater than t_1 from:

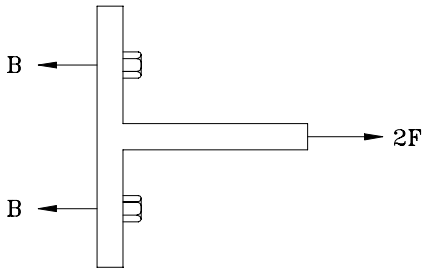

(a) First Stage- Thick Plate Behavior

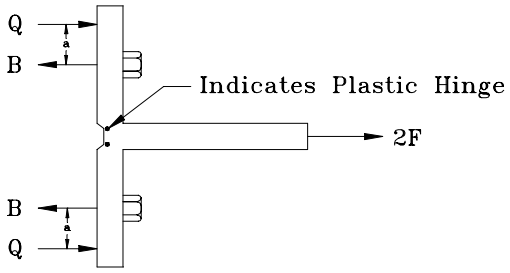

(b) Second Stage-Intermediate Plate Behavior

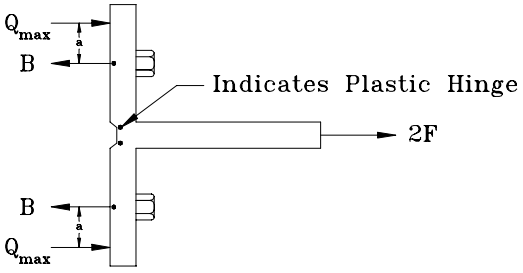

(c) Third Stage Thin Plate Behavior

Figure 2.5 Kennedy Method Split-Tee Behavior After Morrison et al. (1985)

$$t_1 = \sqrt{\frac{4p_f F_f}{b_f \sqrt{F_{py}^2 - 3\left(\frac{F_f}{b_f t_1}\right)^2}}} \tag{2.24}$$

where F_f = total flange force. Solving for t_1 results in the following:

$$t_1 = \sqrt{1.5}\,\frac{F_f}{F_{py} b_f}\sqrt{1+\sqrt{1+\frac{64 p_f^2 b_f^2 F_{py}^2}{9F_f^2}}} \tag{2.25}$$

The thin plate limit, t_{11}, is determined from:

$$t_{11} = \sqrt{\frac{2\left(F_f p_f - \frac{\pi d_b^3 F_{yb}}{16}\right)}{\frac{b_f}{2}\sqrt{F_{py}^2 - 3\left(\frac{F_f}{b_f t_{11}}\right)^2} + w'\sqrt{F_{py}^2 - 3\left(\frac{F_f}{2w' t_{11}}\right)^2}}} \tag{2.26}$$

where w' is the the width of the end-plate per vertical line of bolts minus the bolt hole.

A preliminary value for t_{11} is given by:

$$t_{11} = \sqrt{\frac{2\left(F_f p_f - \frac{\pi d_b^3 F_{yb}}{16}\right)}{F_{py}\left(\frac{0.85 b_f}{2} + 0.8 w'\right)}} \tag{2.27}$$

If the end plate thickness, t_p , is less than or equal to t_{11}, then the end-plate is considered thin. If $t_{11}<t_p< t_1$ then the end-plate is considered to exhibit intermediate plate behavior.

2.3.2 Four Bolt Extended Stiffened Moment End-Plates

Modifications of the Kennedy method for the four bolt extended stiffened end-plate presented here are taken from the experimental investigation done by Morrison et al. (1985). First the connection is idealized in two parts, the inner end-plate and the outer end-plate, Figure 2.6. The outer end-plate consists of the end-plate extension outside the beam tension flange, a portion of the beam tension flange, and the triangular stiffener. The inner end-plate consists of the end-plate within the beam flanges and the remaining beam tension flange. Second, two factors, α and β, are introduced to proportion the flange force into the outer and inner end-plate, respectively. The factors α and β were determined empirically to be 0.4 and 0.6, respectively.

The bolt forces for the outer plate were observed not to include prying forces. Therefore, the outer end-plate is said to behave as a thick plate at all load levels, and the outer end-plate bolt force is calculated as follows:

$$B_o = \alpha F_f/2 \tag{2.28}$$

However, the inner end-plate exhibits prying action at increased load levels. Therefore, to ascertain the magnitude of the bolt forces, the prying forces must first be

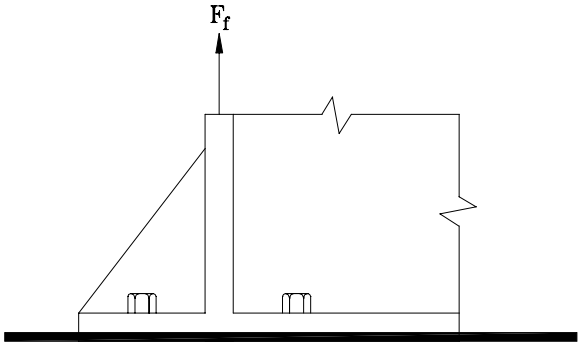

(a) End-Plate at the Beam Flange

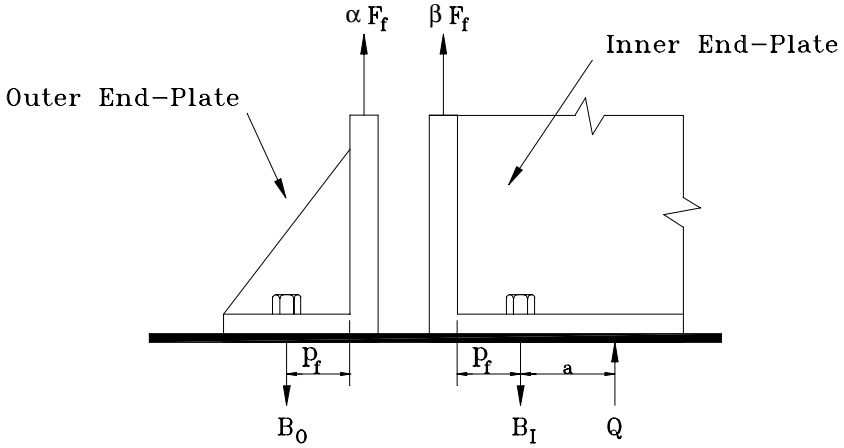

(b) Idealization of the End-Plate at the Beam Flange

Figure 2.6 Modified Kennedy Method Idealized For Four Bolt Extended Stiffened Moment End-Plate Connection After Morrison et al. (1985)

determined. The first step in calculating bolt prying forces is to determine the stage of end-plate behavior. The inner end-plate behavior is determined by comparing the inner flange force, βF_f, with the flange force at the thick plate limit, F_1, and the flange force at the thin plate limit, F_{11}. The flange force at the thick plate limit is:

$$F_1 = \frac{b_f t_p^2 F_{py}}{4p_f \sqrt{1 + \left(3t_p^2 / 16p_f^2\right)}} \tag{2.29}$$

The flange force at the thick plate limit, $F_{11,}$ is:

$$F_{11} = \frac{t_p^2 F_{py} \left[0.85 \left(b_f/2\right) + 0.80\, w'\right] + \left[\left(\pi\ d_b^3 F_{yb}\right)/8\right]}{2p_f} \tag{2.30}$$

If the inner flange force, βF_f, is less than the flange force at the thick plate limit, F_1, the end-plate is considered thick, the bolt prying forces are zero, and the inner bolt force B_I is found as follows:

$$B_I = \beta F_f / 2 \tag{2.31}$$

If the inner flange force, βF_f, is greater than or equal to the flange force at the thick plate limit, F_1, and less than or equal to the flange force at the thin plate limit, F_{11}, the end-plate behavior is intermediate and the prying force is between zero and a maximum. The prying force, Q, for this case is:

$$Q = \frac{\beta F_f p_f}{2a} - \frac{\pi d_b^3 F_{yb}}{32a} - \frac{b_f t_p^2}{8a}\sqrt{F_{py}^2 - 3\left(\frac{\beta F_f}{b_f t_p}\right)^2} \qquad (2.32)$$

Hence, the inner bolt force, B_I, for intermediate end-plate behavior is the inner flange force, βF_f, divided by the number of inner bolts, plus the prying force:

$$B_I = \frac{\beta F_f}{2} + Q \qquad (2.33)$$

Finally, if the inner flange force, βF_f, is greater than the flange force at the thin plate limit, F_{11}, the end plate behavior is thin and prying force is maximum. The prying force, Q_{max}, is as follows:

$$Q_{max} = \frac{w' t_p^2}{4a}\sqrt{F_{py}^2 - 3\left(\frac{F'}{w' t_p}\right)^2} \qquad (2.34)$$

where F' is the lesser of

$$F_{limit} = \frac{F_{11}}{2} \qquad (2.35)$$

and

$$F_{max} = \frac{\beta F_f}{2} \qquad (2.36)$$

Hence, the bolt force, B_I, for thin end-plate behavior is the inner flange force, βF_f, divided by the number of inner bolts, plus the prying force, Q_{max}:

$$B_I = \frac{\beta F_f}{2} + Q_{max} \tag{2.37}$$

The quantities under the radicals in Equations 2.32 and 2.34 can be negative. A negative value for these terms indicates that the end-plate locally yielded in shear before the bolt prying forces could be developed. Thus, the connection is not adequate for the applied load.

2.3.3. Multiple Row 1/3 Extended Moment End-Plates

A discussion on the prying forces in the bolts of the multiple row 1/3 extended stiffened end-plate configuration given here is taken from Morrison et al.. (1986). The assumptions for predicting the prying forces for this connection are similar to those made in predicting the prying forces in the four bolt extended stiffened configuration. Once again the end-plate is idealized as having inner and outer components, as shown in Figure 2.6. Also, the expressions for the flange force at the thick plate limit, F_1, and the flange force at the thin plate limit, F_{11}, are the same as the expressions found for the four bolt extended stiffened moment end-plate, and can be found in Equations 2.29 and 2.30, respectively.

However, because of the additional four bolts added to this connection, the flange force is distributed differently. As shown in Figure 2.7(b), the flange force distributed to the outer end-plate is still αF_f, while the flange force distributed to the inner end-plate

becomes $(\beta_2+\beta_3+\beta_4)F_f$. The values for α, β_2, β_3, and β_4 were empirically determined to

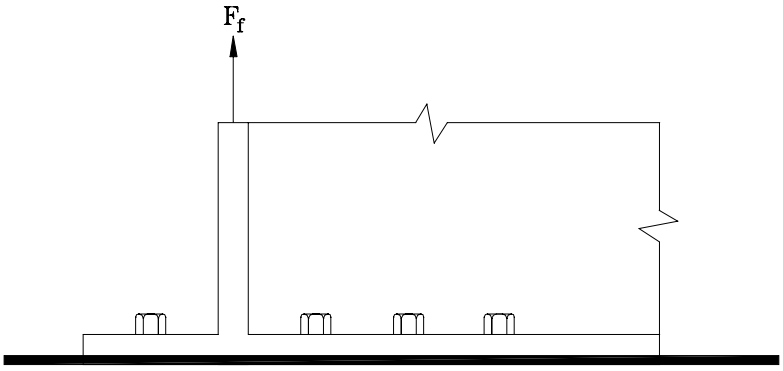

(a) End-Plate at the Beam Flange

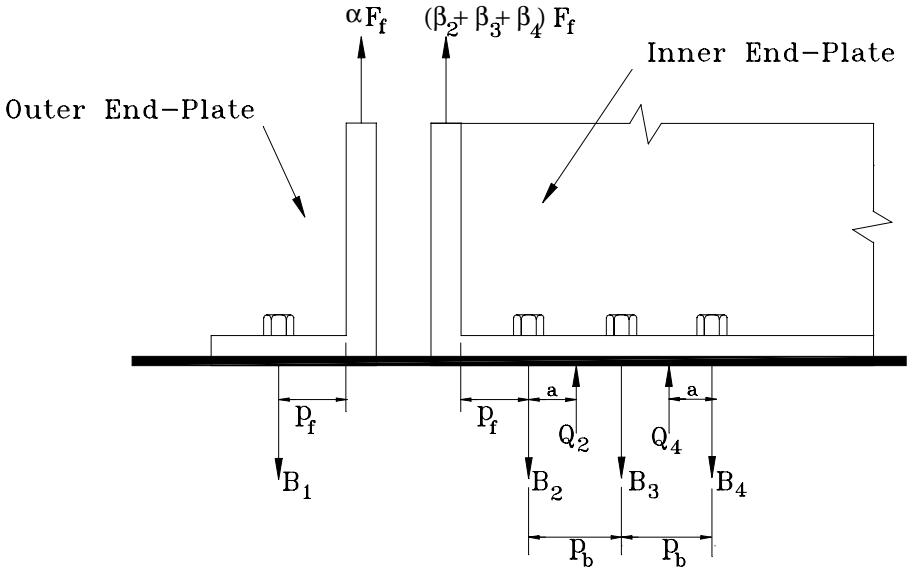

(b) Idealization of the End-Plate at the Beam Flange

Figure 2.7 Modified Kennedy Method Idealized For Multiple Multiple Row 1/3 Extended Moment End-Plate Connection After Morrison et al. (1986)

The outer plate is once again assumed to have no prying action, and is therefore thick for all applied loads. The value for the bolt force, B_1, is then:

$$B_1 = 0.6 \times F_f / 2 \tag{2.38}$$

The inner end-plate does exhibit prying action at increased applied loads. But, because of an inflection point at the middle row of bolts, only bolt force B_2 and bolt force B_4 receive prying force contributions. The middle row of bolts receives no contribution due to prying of the end-plate. Thus, bolt force B_3 is calculated as follows:

$$B_3 = 0.25 \times F_f / 2 \tag{2.39}$$

The explanation for the inner bolt forces, B_2 and B_4, parallels the explanation given for the inner bolt forces explained in Section 2.3.2. The expressions for the inner bolt forces for the multiple row extended 1/3 moment end-plate are as follows:

When $\beta_i F_f < F_1$:

$$B_i = \beta_i F_f / 2 \tag{2.40}$$

When $F_1 < \beta_I F_f < F_{11}$:

$$B_i = \frac{\beta_i F_f}{2} + Q_i \tag{2.41}$$

where Q_i is found as follows:

$$Q_i = \frac{\beta_i F_f p_f}{2a} - \frac{\pi d_b^3 F_{yb}}{32a} - \frac{b_f t_p^2}{8a}\sqrt{F_{py}^2 - 3\left(\frac{\beta_i F_f}{b_f t_p}\right)^2} \tag{2.42}$$

Finally, when $F_{11} < \beta_I F_f$:

$$B_i = \frac{\beta_i F_f}{2} + Q_{i\max} \tag{2.43}$$

where Q_{imax} is found as follows:

$$Q_{imax} = \frac{w' t_p^2}{4a}\sqrt{F_{py}^2 - 3\left(\frac{F'}{w' t_p}\right)^2} \tag{2.44}$$

where F' is the lesser of

$$F_{limit} = \frac{F_{11}}{2} \tag{2.35}$$

and

$$F_{imax} = \frac{\beta_i F_f}{2} \tag{2.36}$$

By setting i = 2 and 4 separately, the bolt force predictions can be calculated for B_2 and B_4 independently.

2.3.4 Four Bolt Extended Unstiffened Moment End-Plate

The bolt force predictions for the four bolt extended unstiffened moment end plate configurations were taken from Abel and Murray (1994). The formulation for the bolt forces, including prying forces (Equations 2.23 to 2.37), for the four bolt extended unstiffened is identical to that of the four bolt extended stiffened, except for the values of α and β. These were both found to be 0.5 for the four bolt extended unstiffened end-plate.

CHAPTER III

TESTING PROGRAM

3.1 EXTENDED END-PLATE TESTING PROGRAM

The experimental work done for this study involved the full-scale testing of seven end-plate connections. The specimens tested were composed of built-up beam and column sections. All beams, columns, end-plates, and stiffeners were fabricated from ASTM specified A572Gr50 steel. All bolts used in this test program were ASTM specified A-325 high-strength structural bolts. Three 24 in. deep beam sections were tested in the four bolt extended stiffened moment end-plate configuration (see Figure 3.1). Three 55 in. deep beam sections were tested in the multiple row 1/3 extended moment end-plate configuration (see Figure 3.2). Also, one 55 in. deep beam section was tested in the four bolt extended unstiffened moment end-plate configuration (see Figure 3.3). The actual dimensions of the specimens are shown in Table 3.1.

The primary purpose of the testing was to find the rotational capacity for the three end-plate configuration under cyclic loading. The end-plates in this study were designed for one of two limit states. The first limit state is a bolt controlled failure mode, where the bolts are designed to fracture before the end-plate yields. The second limit state is an end-plate controlled failure mode, where the end-plate yields significantly before the bolts fracture. Two of the extended stiffened end-plates were designed for the bolt controlled failure mode. The third four bolt extended stiffened end-plate connection, and the remaining four connections, were designed for the end-plate controlled failure mode.

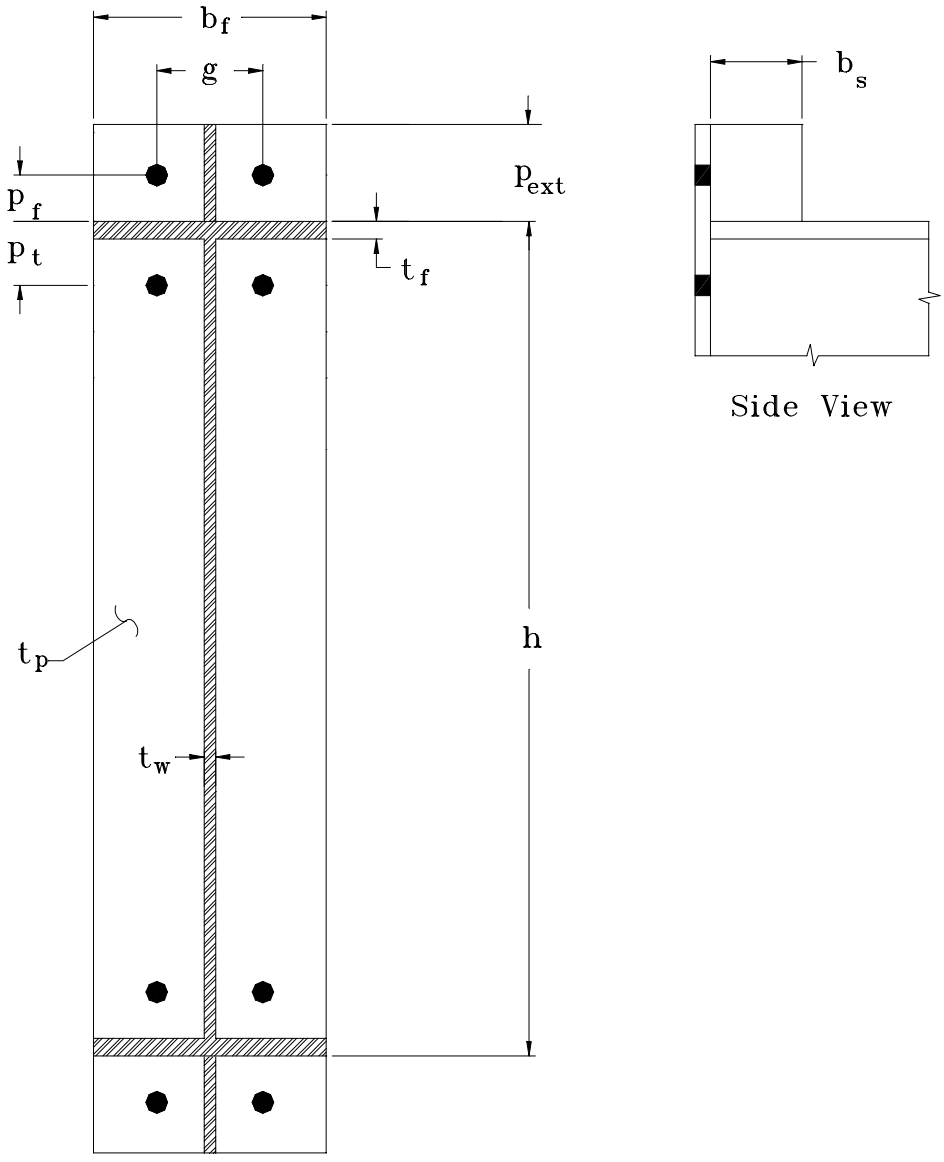

Figure 3.1 Four Bolt Extended Stiffened Moment End-Plate Details

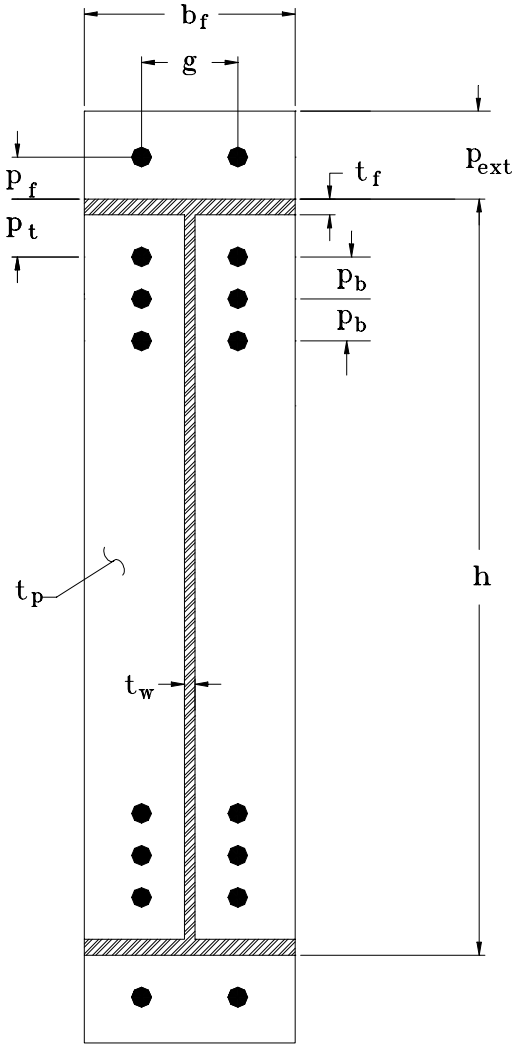

Figure 3.2 Multiple Row 1/3 Extended Moment End-Plate Details

The designation for the connections are given as four terms separated by hyphens. An example of the designation is as follows:

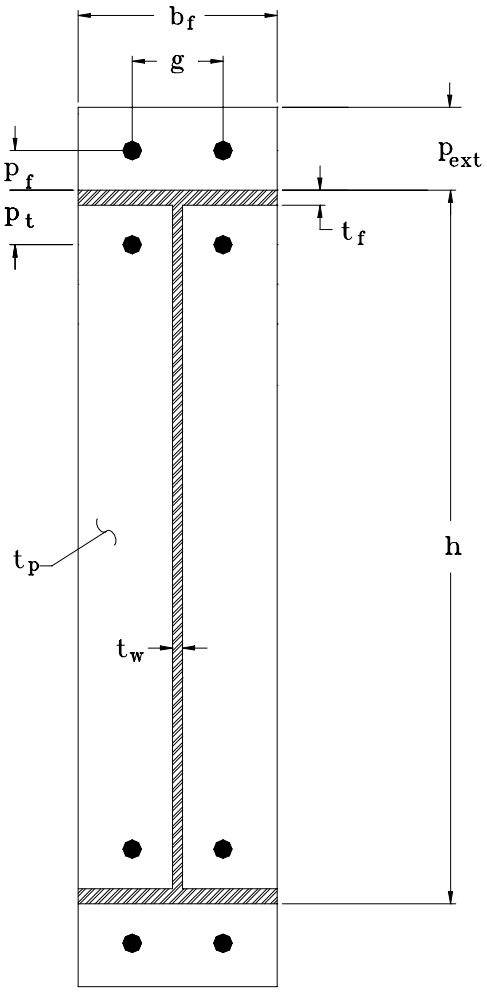

Figure 3.3 Four Bolt Extended Unstiffened
Moment End-Plate Details

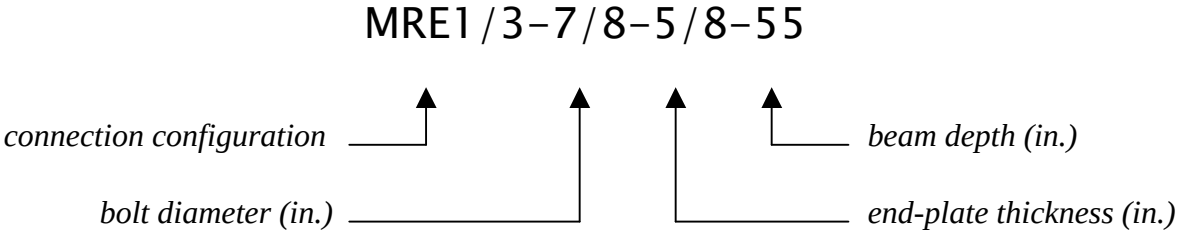

The connection configuration for multiple row 1/3 extended, four bolt extended stiffened, and four bolt extended unstiffened are designated as MRE1/3, 4ES, and 4E, respectively.

Table 3.1 Measured Connection Dimensions

Test Designation	Test	*Bolt*	*End-Plate*						*Beam*				
		d_b (in.)	F_{py} (ksi)	t_p (in.)	p_{ext} (in.)	p_f (in.)	p_b (in.)	g (in.)	h (in.)	b_f (in.)	t_w (in.)	b_s (in.)	L (ft)
ES-1-1/2-24a	1 of 2	1.0	60.7	0.496	2.958	1.323	N/A	3.248	24.0	8.0	0.25	3.5	9.167
ES-1-1/2-24a	2 of 2	1.0	62	0.504	3.208	1.614	N/A	3.293	24.0	8.0	0.25	3.5	9.167
ES-1-1/2-24b	1 of 1	1.0	56	0.501	3.477	1.692	N/A	4.472	24.0	8.0	0.25	3.5	9.167
MRE1/3-7/8-5/8-55	1 of 2	0.875	60.4	0.615	3.498	1.488	3.005	4.015	55.0	8.063	0.350	N/A	10.625
MRE1/3-7/8-5/8-55	2 of 2	0.875	60.4	0.615	3.466	1.483	3.010	4.010	55.0	8.063	0.350	N/A	10.625
MRE1/3-7/8-1/2-55	1 of 1	0.875	62.0	0.498	3.572	1.523	2.610	4.001	55.0	8.015	0.350	N/A	10.625
4E-7/8-1/2-55	1 of 1	0.875	62.0	0.499	3.497	1.522	N/A	4.004	55.0	8.015	0.350	N/A	10.625

Note: See Figures 3.1, 3.2, and 3.3 for definition of dimensions.

3.2 TESTING FRAMES

Two different setups were used for the tests: Test Frame 1 and Test Frame 2 (see Figures 3.4 and 3.5, respectively. Test Frame 1 was used to test the two specimens designated 4ES-1-1/2-24a. Test Frame 2 was used to test the remaining five specimens. In Test Frame 1, load was applied with a 200 kip capacity hydraulic actuator in the vertical plane, in the direction of gravity. In Test Frame 2, load was applied using the same actuator, in the horizontal plane, normal to the direction of gravity. The distance from the point of loading to the face of the connection was chosen such that the shear force at the connection, relative to the moment, would be the shear force realized in an actual connection. Finally, the top and bottom flanges of each specimen were braced such that lateral torsional buckling would not be the controlling limit state. Photographs of Test Frame 1 and Test Frame 2 are shown in Figures 3.6 and 3.7, respectively.

3.3 INSTRUMENTATION

For Test Frame 1, at the beam tip, a 200 kip capacity tension-compression load cell measured force induced at the load point, and linear displacement transducers measured beam deflection at a distance of one foot from the load point, in the direction of the connection. At the column, potentiometers measured the end-plate separation from the column flange at the top and bottom of the end-plate, and two additional linear displacement transducers measured rigid body movement of the test frame and column rotation. Also, linear strip type strain gages measured beam flange strain, and bolt gages were placed inside the shank of the bolts to obtain bolt forces. The

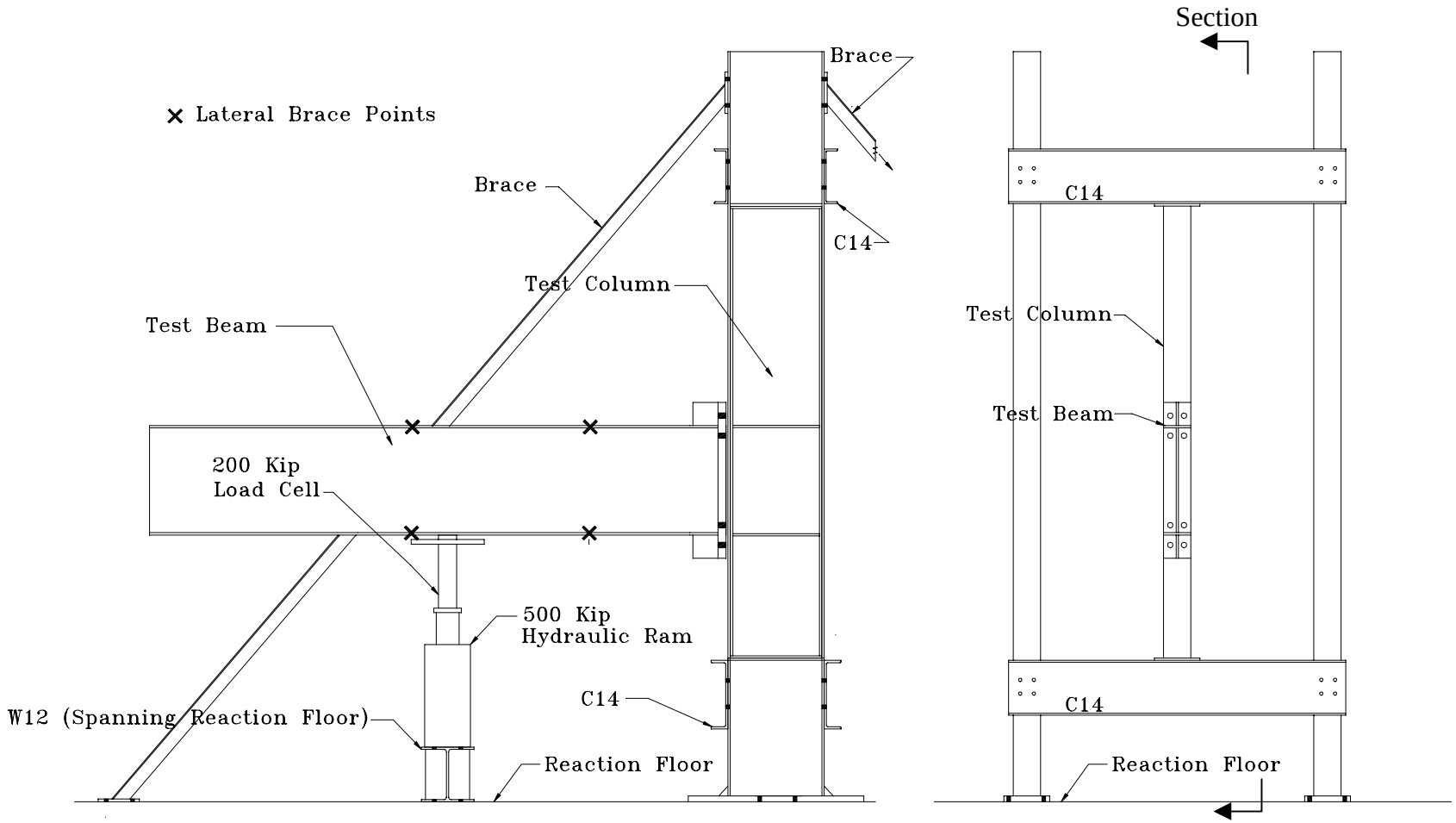

(a) Section

(b) Elevation

Figure 3.4 Test Frame 1

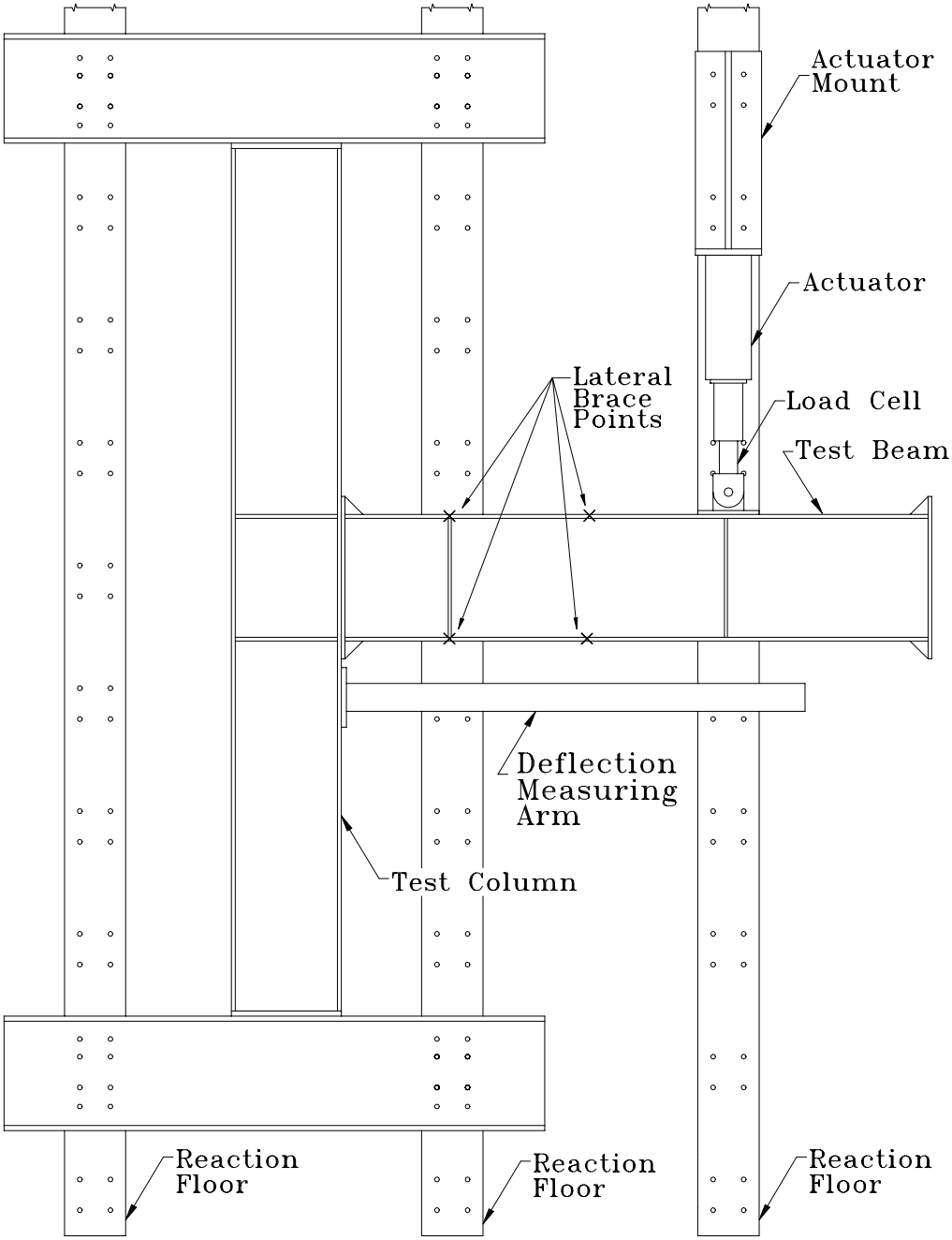

Figure 3.5 Test Frame 2 (Plan View)

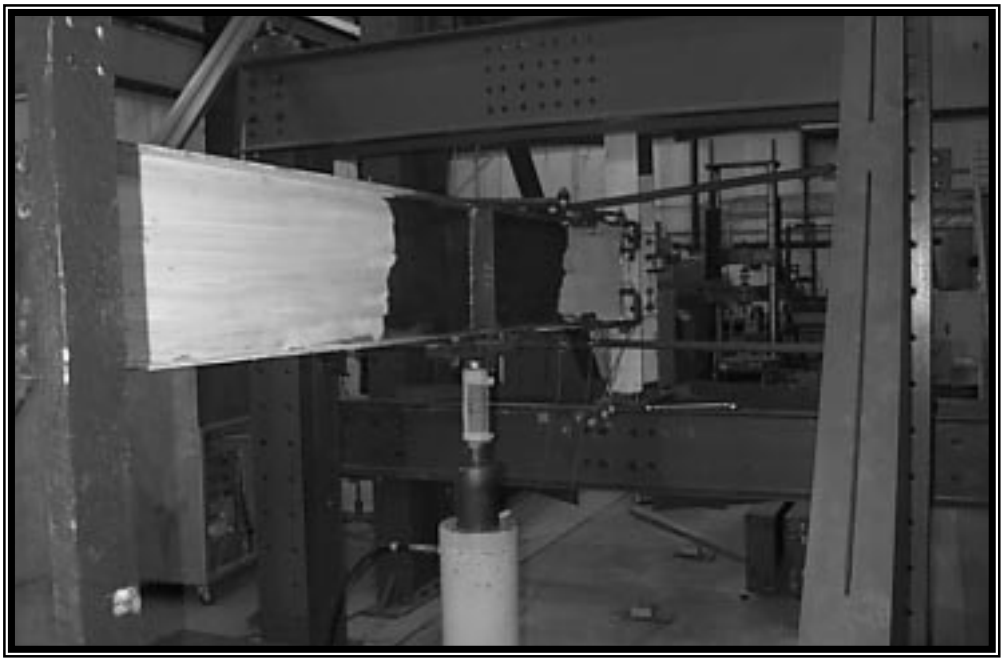

Figure 3.6 Photograph of Test Frame 1

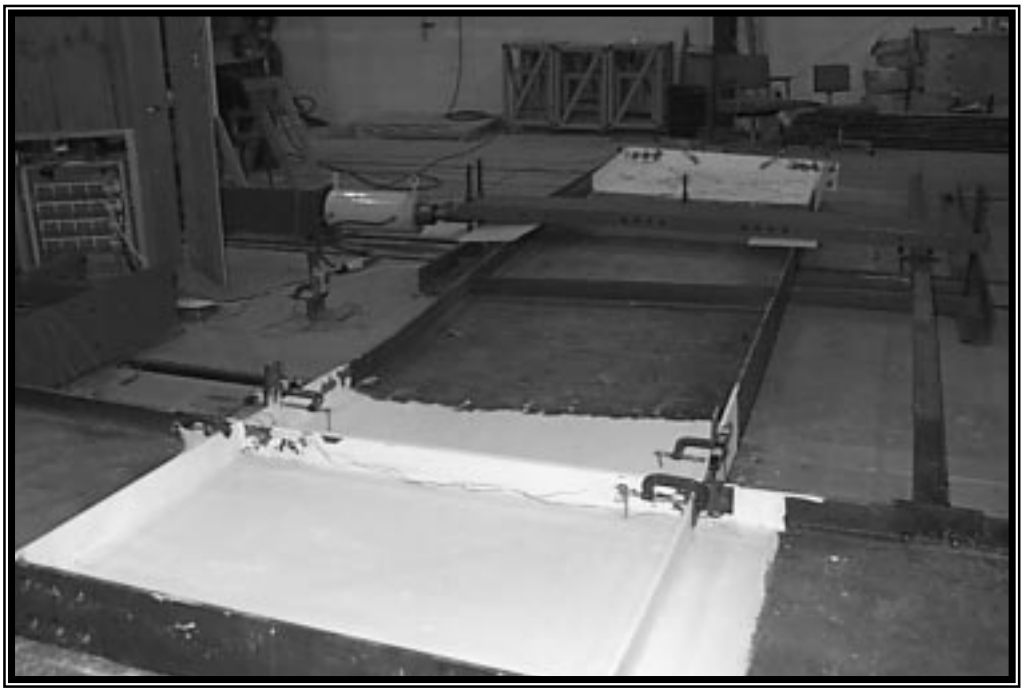

Figure 3.7 Photograph of Test Frame 2

acquisition of bolt strain was useful for determining bolt forces throughout the test, as well as for pre-tensioning the bolts accurately.

The instrumentation used for Test Frame 2 was similar to the instrumentation of Test Frame 1. The only difference was the use of a rigid arm, consisting of a built-up, 14 ft long tubular section with an end-plate welded to one end, and a wheel attached to the other. The arm's end-plate was bolted to the column flange just outside the end plate. It extended, parallel to the beam, beyond the load point, and was supported on the ground at the free end by its wheel. At the load point, the relative displacement of the beam was taken with respect to this arm by a linear displacement transducer. By doing so, both the column rotation and the rigid body rotation of the frame could be accounted for and true beam rotation with respect to the column was obtained.

For both test frames, data readings for each of the instruments discussed above were taken at displacement increments throughout the entire load history of the test. These data points were recorded with a PC-based data acquisition system. The data were transferred via disk media to commercial software for analysis in spreadsheet and graphical analysis software.

3.4 LOADING PROTOCOL

All tests were performed using the loading protocol defined in SAC *Protocol for Fabrication, Inspection, Testing, and Documentation of Beam-Column Connection Tests and Other Experimental Specimens* (Clark 1997). The loading protocol is displacement based and is presented in graphical form, Figure 3.8, and in tabular form, Table 3.2.

TABLE 3.2 SAC Loading Protocol

Load Step #	Peak Deformation, θ	Number of Cycles, *n*
1	0.00375	6
2	0.005	6
3	0.0075	6
4	0.01	4
5	0.015	2
6	0.02	2
7	0.03	2
Continue with increments in θ of 0.01 rad., and perform two cycles at each step		

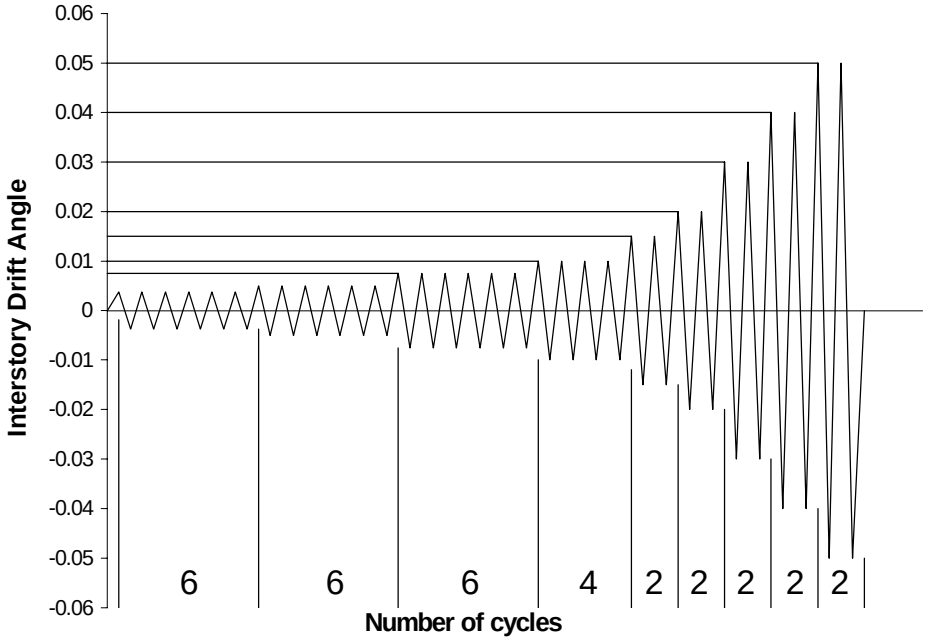

FIGURE 3.8 SAC Loading Protocol

3.5 END-PLATE TENSILE COUPON TESTING

The material used to fabricate all test specimens was A572-Gr50 Steel. The measured yield stress, $F_{y,}$ and ultimate stress, F_u, were found for the material used to fabricate each of the specimens. Procedures in ASTM E8 were used to test 18 in. tensile coupons with a 300 kip capacity universal type testing machine. Because the end-plates were the only component of the connections to yield, only tensile test results from end-plates were tested. The results of these tests are located in Table 3.3.

Table 3.3 End-Plate Tensile Coupon Data

Coupon	Yield Stress (ksi)	Tensile Stress (ksi)	Elongation (%)
4ES-1-1/2-24a	60.7	84.4	25.2
4ES-1-1/2-24a	62.0	85.2	24.7
4ES-1-1/2-24b	56.0	87.3	25.7
MRE1/3-7/8-5/8-55	60.4	85.1	24.9
MRE1/3-7/8-5/8-55	60.4	85.1	24.9
MRE1/3-7/8-1/2-55	62.0	84.6	23.6
4E-7/8-1/2-55	62.0	84.6	23.6

3.6 PRELIMINARY ANALYSIS OF STRENGTH RESULTS

3.6.1 Comparison with Predicted Strengths

The strengths results of the tests were compared to the predicted strengths to determine the accuracy of the prediction methods. Tables 3.4 and 3.5 give the results of these comparisons. The moment strength of the end-plate, M_{pl}, was calculated using yield-line theory; M_q is the moment strength associated with the bolts, calculated using the modified Kennedy method. The values for M_{pl} and M_q were calculated using the measured dimensions presented in Table 3.1 and actual end-plate yield stress, presented in Table 3.3. The values for M_q were found using nominal bolt strengths. The controlling prediction strengths are shaded in gray. The ratios of the predicted moment strengths versus the maximum applied moment strengths are also given. A ratio shaded in gray and equal to unity would indicate an ideal predicted strength. Values of ratios

Table 3.4 Four Bolt Extended Stiffened Preliminary Strength Results

Connection	Test	F_{py} (ksi)	Maximum Moment (ft-kips)			M_{pl}/M_{app}	M_q/M_{app}
			Predicted Strengths		Applied		
			M_{pl}	M_q			
ES-1-1/2-24a	1	60.7	345	286	262	1.32	1.09
ES-1-1/2-24a	2	62.0	326	286	296	1.10	0.97
ES-1-1/2-24b	1	56.0	256	301	458	0.56	0.66

which are less than one indicate conservative predictions, whereas values which are greater than one indicate un-conservative predictions. All predicted versus applied moment strength ratio values for the extended stiffened moment end-plate specimens, with the exception of Specimen *ES-1-1/2-24a Test 1*, are shown to be conservative. Also all MRE1/3 and 4E predicted versus applied moment strength ratio values were conservative.

However, when reviewing the results, it was observed that the maximum moments applied in *ES-1-1/2-24a Test 1* and *ES-1-1/2-24a Test 2* were much less than the maximum moment applied to Specimen *ES-1-1/2-24b*. This difference in strength was considered unlikely because of the similarity between specimen *ES-1-1/2-24a* and specimen *ES-1-1/2-24b*. To check the range of strengths previously applied to moment

Table 3.5 MRE1/3 and Extended Unstiffened Preliminary Strength Results

Connection	Test	F_{py} (ksi)	Maximum Moment (ft-kips)			M_{pl}/M_{app}	M_q/M_{app}
			Predicted Strengths		Applied		
			M_{pl}	M_q			
MRE1/3-7/8-5/8-55	1	60.4	1206	1062	1523	0.79	0.69
MRE1/3-7/8-5/8-55	2	60.4	1221	1062	1720	0.71	0.62
MRE1/3-7/8-1/2-55	1	62.0	778	928	1220	0.64	0.76
4E-7/8-1/2-55	1	62.0	610	650	904	0.67	0.72

end-plate configurations of this type, previous testing programs were reviewed. The work presented in Morrison et al. (1985) and Kline et al. (1989) included monotonic moment end-plate tests with nearly identical dimensions to the specimens *ES-1-1/2-24a* and *ES-1-1/2-24b*.

The review of Morrison et al. (1986) and Kline et al. (1989) produced compelling evidence to support the hypothesis that the maximum load achieved in the experimental data was errantly low for the two *ES-1-1/2-24a* tests when compared to test *ES-1-1/2-24b*. The comparisons are shown in Table 3.6.

Table 3.6 Comparison of Ultimate Applied Moments From Different Testing Programs

Test Specimen	**Reference**	**Loading**	**Initial Bolt Condition**	**M_u (ft-k)**
ES-1-1/2-24	Morrison, 1986	Monotonic	Fully Pretensioned	*349.5
ES-1-1/2-24	Kline, 1989	Monotonic	Snug Tight	468
ES-1-1/2-24a-Test 1	Current Study	Cyclic	Fully Pretensioned	262
ES-1-1/2-24a-Test 2	Current Study	Cyclic	Fully Pretensioned	296
ES-1-1/2-24b	Current Study	Cyclic	Fully Pretensioned	458

* Morrison did not test this specimen to failure.

3.6.2 Need for Finite Element Study

As a result of the inconsistent data obtained in the preliminary strength analysis of the extended stiffened moment end-plate tests, ES tests, a finite element study was conducted, and is presented in Chapter 4. The study also includes a validation of the experimental results obtained in each of the multiple row extended and the four bolt extended unstiffened tests.

CHAPTER IV

FINITE ELEMENT STUDY

4.1 OVERVIEW

A finite element study was done to check the accuracy of the experimental data achieved during the moment end-plate tests. First, finite element models were developed to validate the experimental data obtained during the testing of the multiple row 1/3 extended, MRE 1/3, and the four bolt extended unstiffened, E, end-plate configurations. Then finite element models were developed to investigate the discrepancy in maximum moments applied to the four bolt extended stiffened end-plate configurations. To conduct this study, the author relied heavily on work done by Mays (1999).

4.2 FINITE ELEMENT MODEL

Commercial finite element analysis software, ANSYS, was used to create the model of the moment end-plate connections. Mays (1999) wrote a FORTRAN program to produce the code necessary to create a model of any moment end-plate configuration, bolted to a rigid support. The FORTRAN program requires only the dimensions and strengths of the connection to be entered. The program produces a batch file that can be read directly by the finite element software. An example of a typical mesh is shown in Figure 4.1.

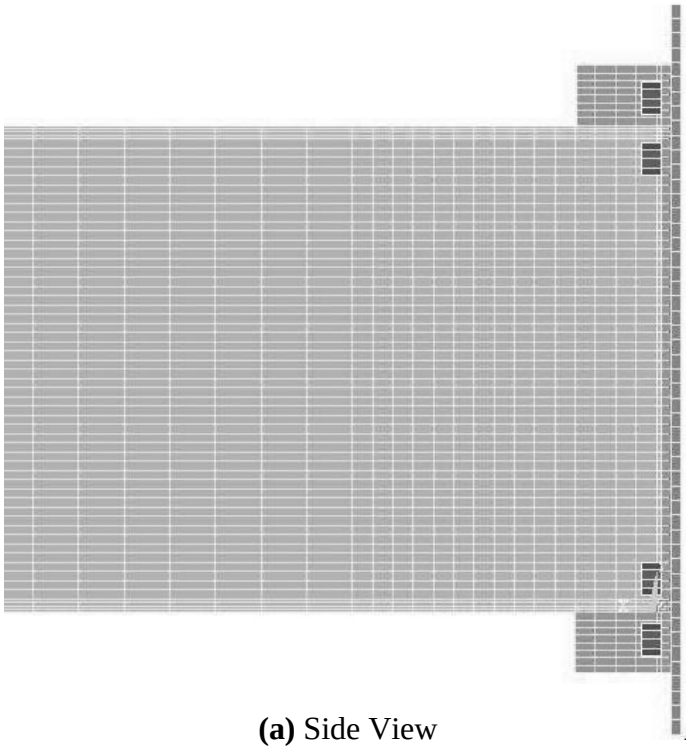

(a) Side View

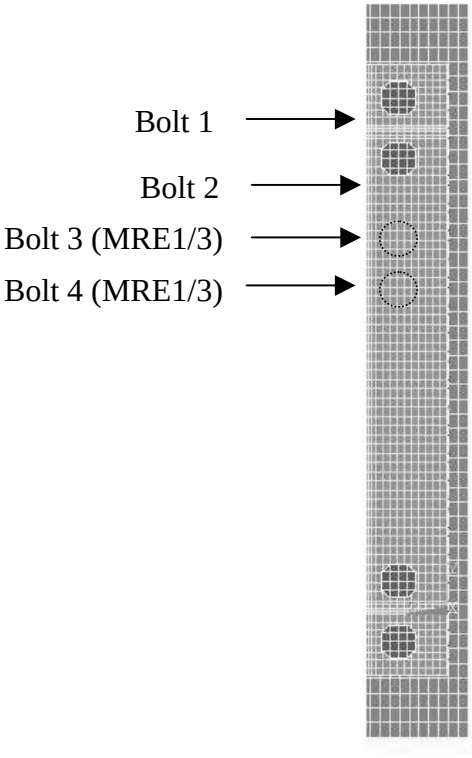

(b) Front View

Figure 4.1 Finite Element Mesh

The following explanation of the finite element model was taken directly from Mays (1999). The finite element models used to analyze these connections are three-dimensional. Symmetry is taken advantage of about a vertical plane, and only half of the structure is analyzed. Solid eight-node brick elements that include plasticity effects are used to model the beam-to-column connection. The beam elements are A572 Grade 50 steel and the yield stress and ultimate stress of all plates are as measured in the experimental analysis. Contact elements are included between the end-plate and the column flange to represent the nonlinear behavior of this complex interaction. Solid twenty-node brick elements that include plasticity effects are used to model the bolts. Constraint equations are introduced to make the bolt heads continuous with the end-plate. Bolt pre-tensioning is applied by prescribed displacements at the end of the bolt shank. These displacements are held constant throughout the loading. The column flange is assumed to be rigid and the nodes along the back of the flange are fixed against all translations. The nodes along the symmetrical surface are fixed against lateral translations. The validation of the mesh refinement for the model used here is presented in Mays (1999).

The models use tri-linear stress-strain equations for the bolts and for the plate material. The tri-linear plots for these stress-strain relationships are shown in Figure 4.2 and Figure 4.3. The values used for F_y and F_u in Figure 4.3 come from tensile coupon testing for each specimen. The terms 11 ε_y and 120 ε_y were obtained by Mays as average strains at which Grade 50 steel has been shown to yield and reach ultimate strength, respectively, in previous work.

For the loading procedure, the bolts are first pre-tensioned. Next, increasing vertical loads are applied at the beam tip in three locations to induce an increasing bending moment at the connection. The beam loading is terminated in this study upon reaching the ultimate strength of the bolts, assumed to be 100 ksi.

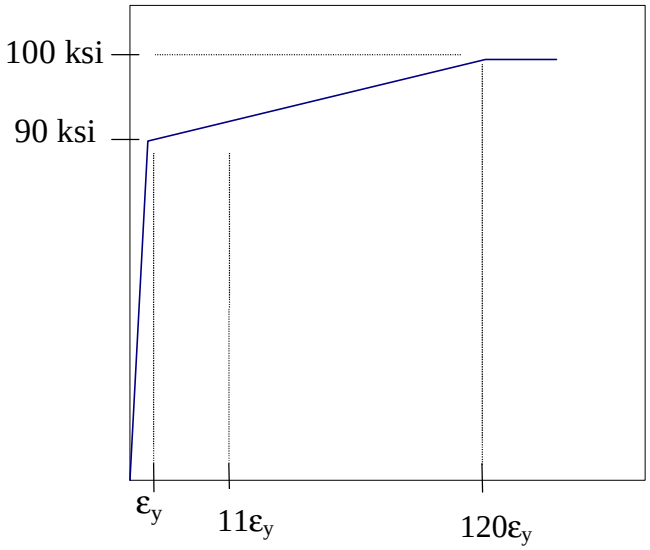

Figure 4.2 Tri-Linear Stress-Strain Relation for Elements Used for Bolts

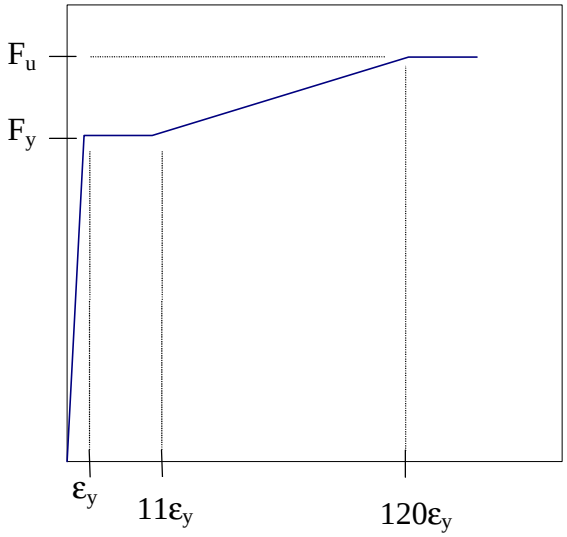

Figure 4.3 Tri-Linear Stress-Strain Relation for Elements Used for Plates

4.3 COMPARISON OF FEM TO EXPERIMENTAL BOLT STRAIN RESULTS

Comparing the finite element model results to the experimental data was fairly complex. The beams of the finite element models were shorter than the beams tested experimentally. Additionally, the column was modeled as a fully rigid flange. Because of these differences, it would have been extremely difficult to compare the load versus beam tip deflection of the finite element model to the load versus beam tip deflection achieved experimentally. However, applied moment at the end-plate versus the bolt forces was easily obtained from the finite element model results and directly comparable to the experimental data. The applied moment at the end-plate versus the bolt forces is, therefore, the focus of this study. The maximum moments obtained in both the finite element models and the experimental tests are also compared.

Because the experimental testing was done cyclically and the finite element study was done monotonically, the envelope curve of the bolt forces for the experimental tests was found and compared to the curve found using the finite element model. The envelope curve was found by plotting bolt strain versus flange force as shown in Figure 4.4. Values were taken from this plot along the loading curve in which load was increased in tension at the flange of the bolt being studied. The bolt strain was then converted to bolt force for strains between equivalent pre-load strain and strains corresponding to 100 ksi. At 100 ksi the bolts are assumed to be perfectly plastic. Therefore, for any bolt force versus applied moment plot, a plateau exists after a bolt strain equivalent to a bolt stress of 100 ksi is reached. The trace of the curve used for comparison is in bold.

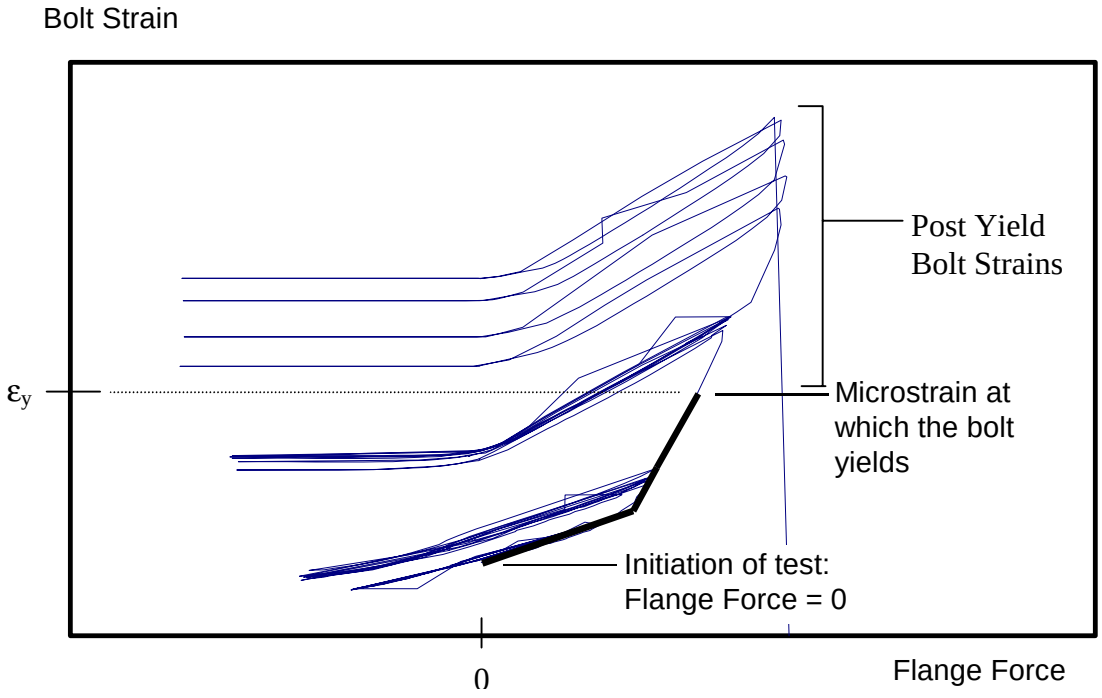

Figure 4.4 Bolt Strain Envelope Curve

4.3.1 Multiple Row 1/3 Extended Moment End-Plates

The first moment end-plate configuration investigated was the multiple row 1/3 extended configuration. The first model used the dimensions and actual yield stresses and ultimate stresses of the test specimen designated *MRE1/3-7/8-5/8-55-Test 2*. The comparison of the finite element results and the experimental results is presented in Figure 4.5. The second model was created using the dimensions and actual yield stresses and ultimate stresses taken from the test specimen designated *MRE1/3-7/8-1/2-55*. The comparison of the results from the second finite element model with experimental results is presented in Figure 4.6. In both finite element models, the bolts were given prescribed

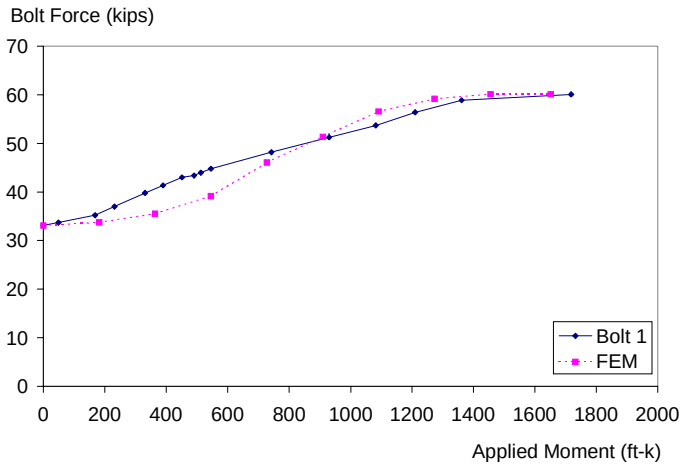

(a) Bolt 1

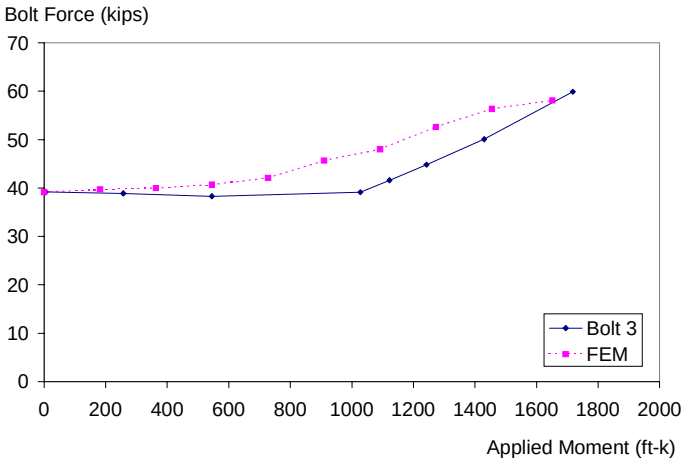

(c) Bolt 3

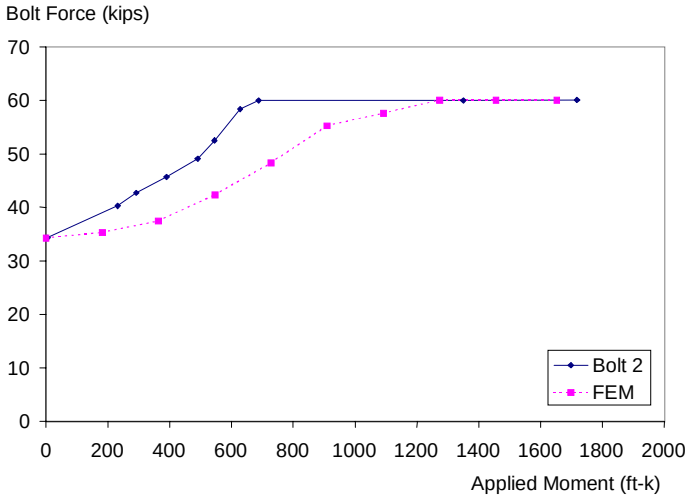

(b) Bolt 2

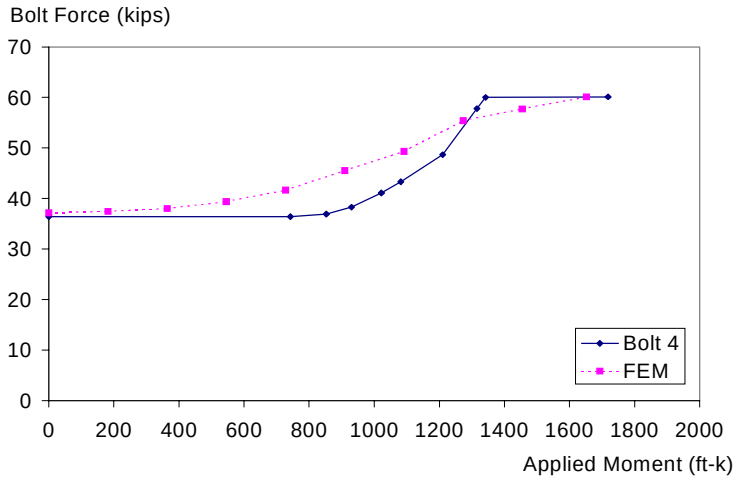

(d) Bolt 4

Figure 4.5 Bolt Force Comparisons for MRE1/3-7/8-5/8-55-Test 2

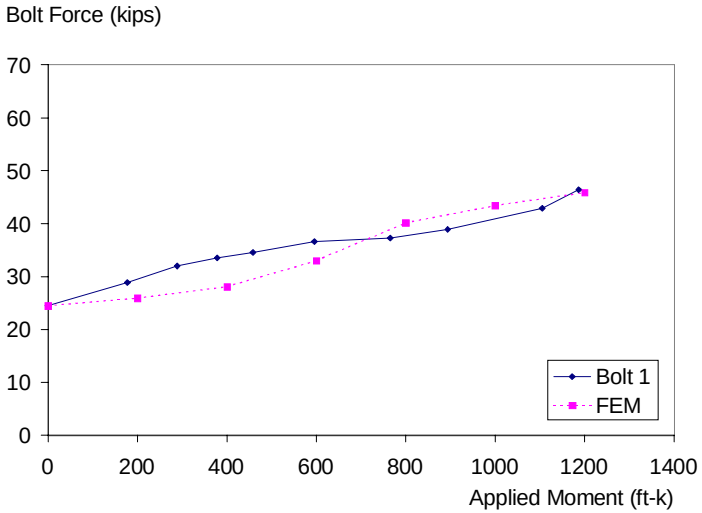

(a) Bolt 1

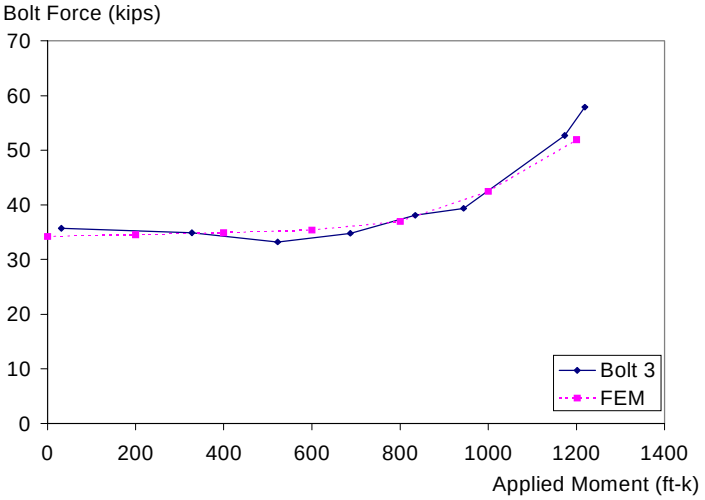

(c) Bolt 3

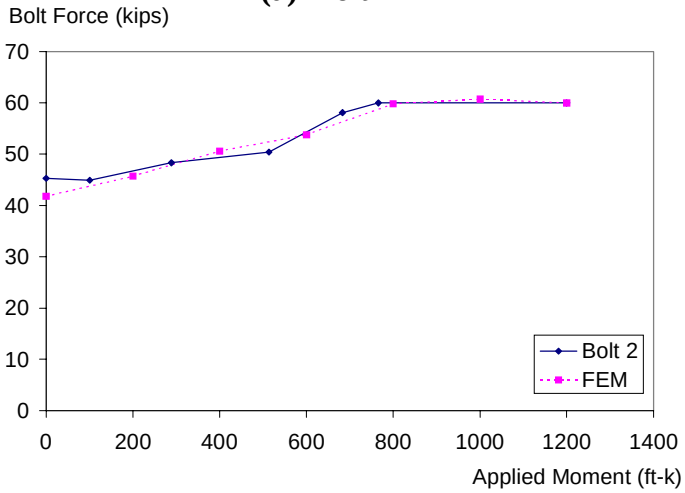

(b) Bolt 2

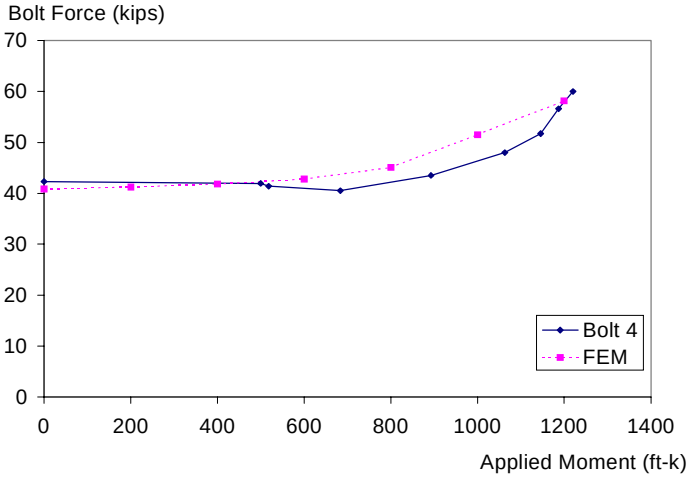

(d) Bolt 4

Figure 4.6 Bolt Force Comparisons for MRE1/3-7/8-1/2-55

is presented in Figure 4.6. In both finite element models, the bolts were given prescribed displacements to induce initial stresses which closely matched the pretension in the experimental specimen. The correlation between experimental and finite element bolt forces is reasonably close for all experimental tests. The maximum moment, M_{FE}, obtained at the end-plate face in the finite element study before the bolt strains of the model diverged is within five percent of M_u for all multiple row 1/3 extended end-plates. M_{FE} and M_u are reported in Table 4.1.

4.3.2 Four Bolt Extended Unstiffened Moment End-Plates

One model was created using dimensions and actual yield stresses and ultimate stresses of the test specimen designated *4E-7/8-5/8-55*. The results are shown in Figure 4.7. Once again the bolt forces found in the experimental study are very close to the bolt forces predicted by the finite element analysis. Also, M_{FE} is within one percent of M_u for this specimen, and is reported in Table 4.1.

4.3.3 Four Bolt Extended Stiffened Moment End-Plates

One finite element model was created using dimensions and actual yield stresses and ultimate stresses of each of the four bolt extended stiffened end-plate specimens used in the experimental study. The results are shown in Figures 4.8, 4.9, and 4.10. The bolt strains of the finite element model diverged after excessive deformation was calculated in the end-plate. The maximum moment obtained in the specimen *ES-1-1/2-24b* was only

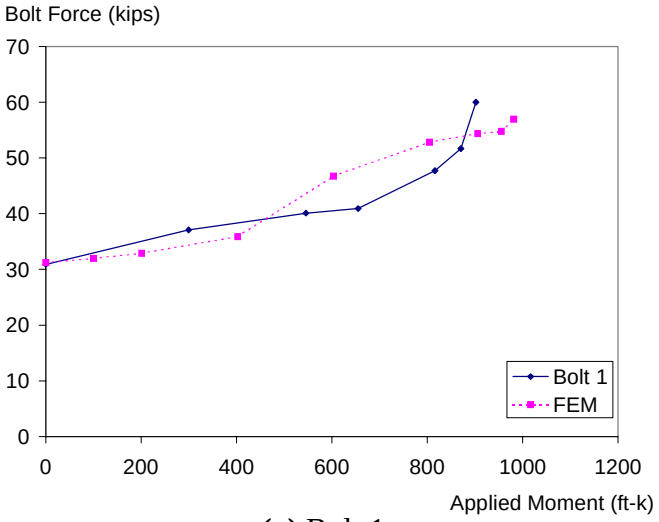

(a) Bolt 1

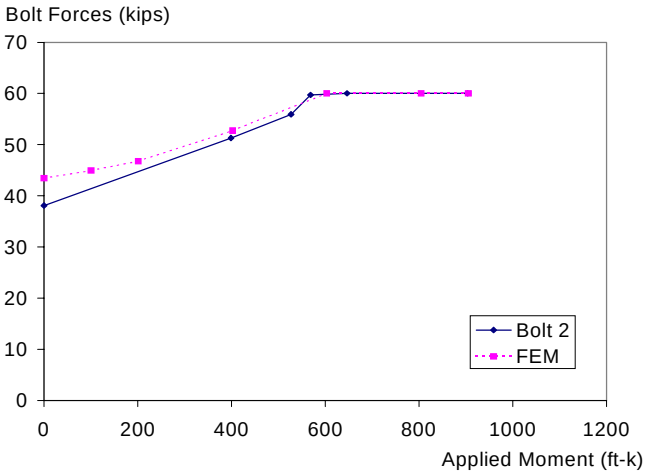

(b) Bolt 2

Figure 4.7 Bolt Force Comparisons for 4E-7/8-1/2-55

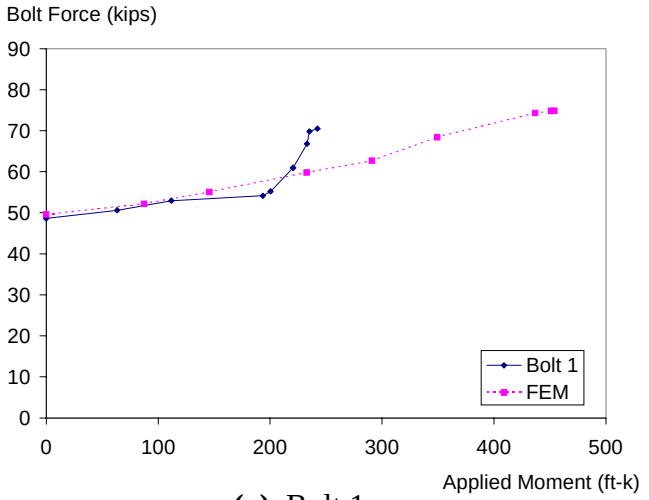

(a) Bolt 1

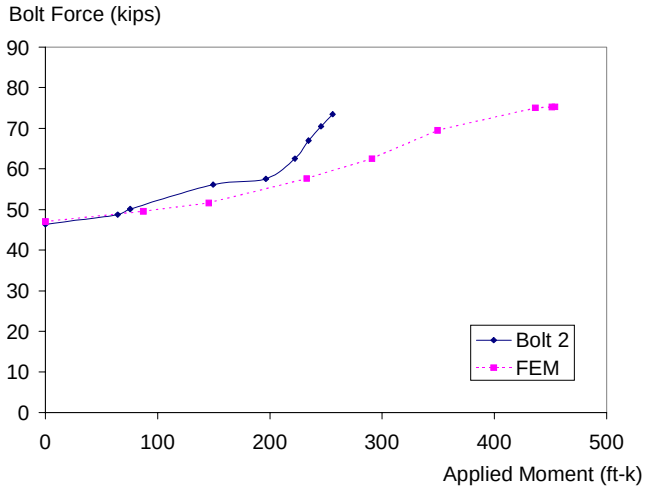

(b) Bolt 2

Figure 4.8 Bolt Force Comparison for ES-1-1/2-24a -Test 1

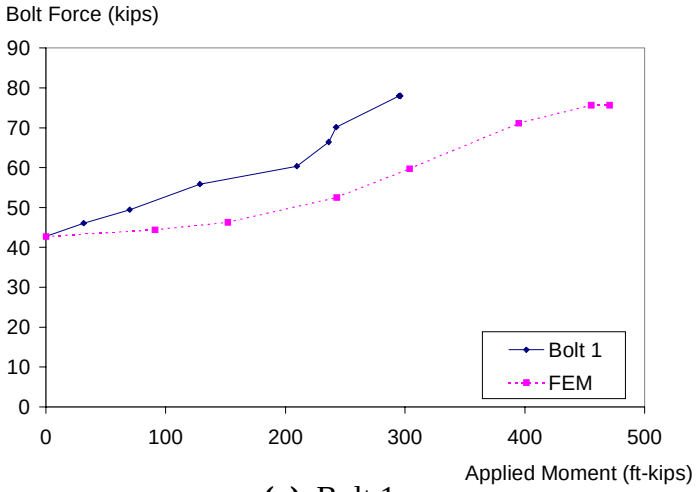

(a) Bolt 1

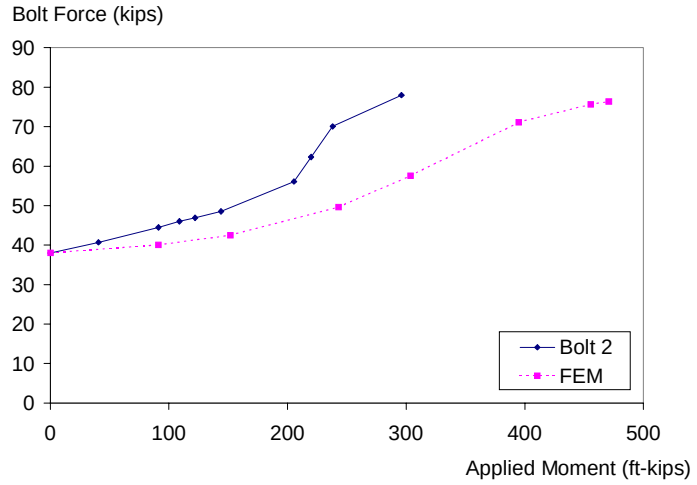

(b) Bolt 2

Figure 4.9 Bolt Force Comparison for ES-1-1/2-24a -Test 2

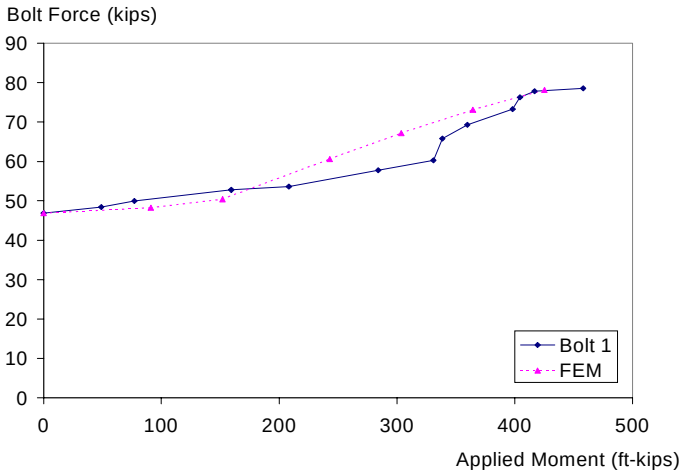

(a) Bolt 1

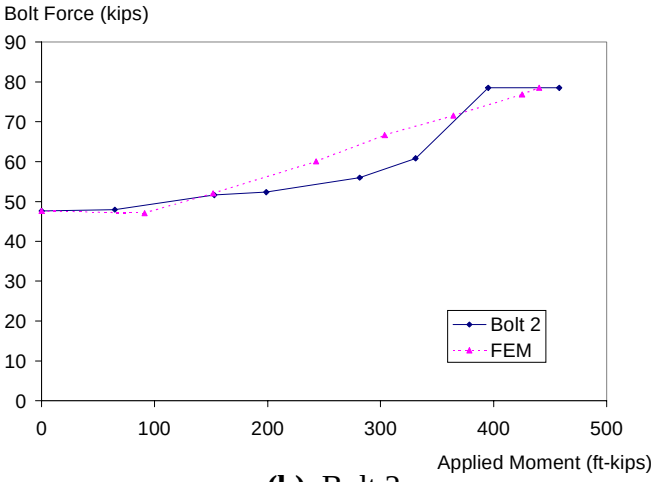

(b) Bolt 2

Figure 4.10 Bolt Force Comparison for ES-1-1/2-24b

eight percent lower than the moment at which the strains of the corresponding finite element model diverged However the maximum moment obtained in the testing of specimens *ES-1-1/2-24a, Test 1* and *Test 2,* was lower than the moment at which the bolt strain of the corresponding finite element model diverged by factors of 1.75 and 1.59, respectively.

Table 4.1 Comparison of Experimental and F.E.M. Ultimate Applied Moment

Specimen	M_{FE} (k-ft)	M_u (k-ft)	M_{FE} / M_U
MRE1/3-7/8-5/8-55	1651	1523	1.09
MRE1/3-7/8-5/8-55	1651	1720	0.96
MRE1/3-7/8-1/2-55	1200	1220	0.98
4E-7/8-1/2-55	905	904	1.01
4ES-1-1/2-24a- Test 1	454	*262	1.75
4ES-1-1/2-24a- Test2	470	*296	1.59
4ES-1-1/2-24b	425	458	0.93

*Values listed are unadjusted for inaccurate load cell.

4.4 Adjustment of Experimental Load Using Finite Element Model

The M_{FE} versus M_U ratios presented in Table 4.1 indicate the close correlation between maximum moment strengths obtained by finite elements and experimental tests for all specimens, with the exception of *ES-1-1/2-24a Test 1 and 2.* Additionally, as is evident in Figures 4.9 and 4.10, the experimental bolt load versus the applied moment

for *ES-1-1/2-24a, Test 1* and *2*, diverges from that found using the finite element model at a much lower load. Because of the close correlation found in all other finite element models with respect to maximum experimental moment strength and experimental bolt forces, the validity of the experimental data was investigated.

It was also learned that the load cell which was used to test flush end-plates by Boorse (1999) was the same load cell used during the testing of the specimens in question. This load cell was determined to be inaccurately calibrated by Boorse (1999). It was also learned that this load cell was over-stressed during a test, subsequent to the loading of *ES-1-1/2-24a Test 1* and *Test 2*. Therefore re-calibrating the load cell and adjusting the data accordingly was not an option.

An explanation of the inaccurate load cell is presented in Boorse (1999). A single correction factor, to be used to adjust the load value throughout loading of the tests, was obtained to correct the inaccurate calibration of the load cell used by Boorse (1999). The correction factor used was obtained by matching the initial stiffness of moment end-plates tested to the initial stiffness of those tested by Srouji (1983). The moment end-plates tested by Srouji had the same configuration as those tested by Boorse, but were tested monotonically. The use of a scalar factor to adjust all load values obtained by the load cell is valid because the load cell produces a linearly changing signal with the change of elongation of the load cell.

However, the use of the finite element model, which has been shown to be accurate in predicting bolt forces throughout loading, produces a more accurate correction factor. Through trial and error, a correction factor of 1.6 was determined for the load data

obtained experimentally in tests of specimen *ES-1-1/2-24a, Test 1* and *Test 2*. The results of applying the 1.6 correction factor are shown Figures 4.11 and 4.12. The plotted bolt forces from the factored experimental results correlate to the bolt force plots found using finite elements much better after applying the factor. The comparisons obtained after applying the factor of 1.6 are much more consistent with other bolt force comparisons made using the experimental data and the finite element model data in this finite element study. The maximum applied moment, M_u, for the extended stiffened end-plate specimens after applying the load factor of 1.6 is reported in Table 4.2. As a result of the close correlation of the bolt forces and maximum moments after applying the correction factor, load data were multiplied by 1.6 throughout the testing of *ES-1-1/2-24a Test 1* and *Test 2.*

Table 4.2 Comparison of Experimental with 1.6 Scaling Factor and FEM Ultimate Applied Moment

Specimen	**M_{FE} (k-ft)**	**M_u (k-ft)**	**M_u / M_{FE}**
4ES-1-1/2-24a-Test 1	454	420	1.08
4ES-1-1/2-24a-Test2	470	474	0.99
4ES-1-1/2-24b	425	458	0.93

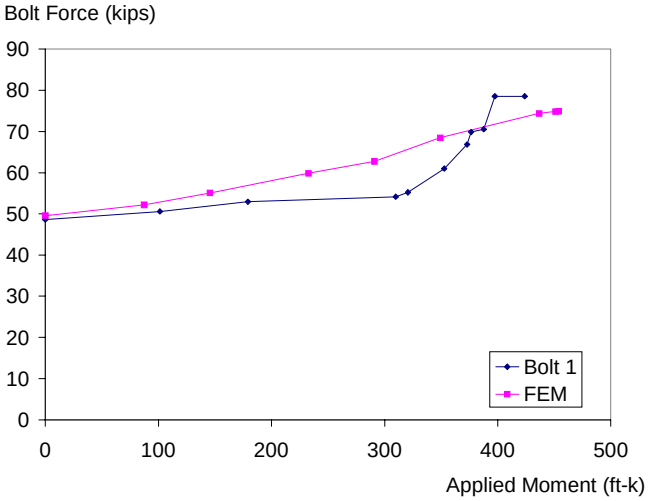

(a) Bolt 1

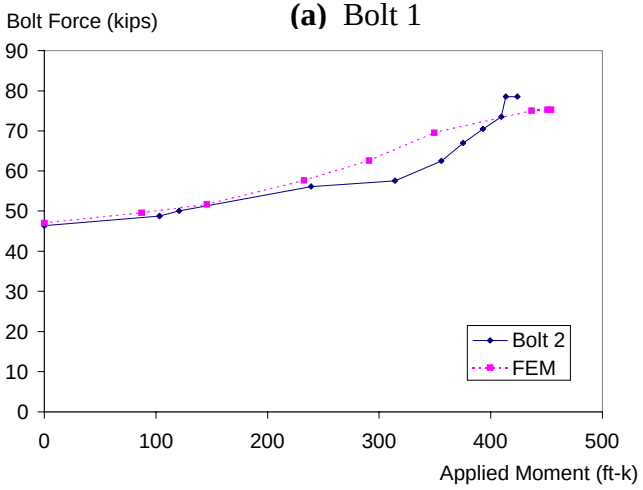

(b) Bolt 2

Figure 4.11 Bolt Force Comparison for ES-1-1/2-24a -Test 1 with 1.6 Scaling Factor

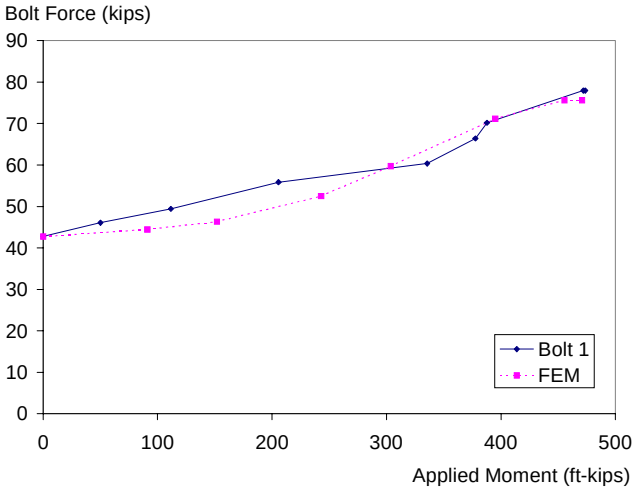

(a) Bolt 1

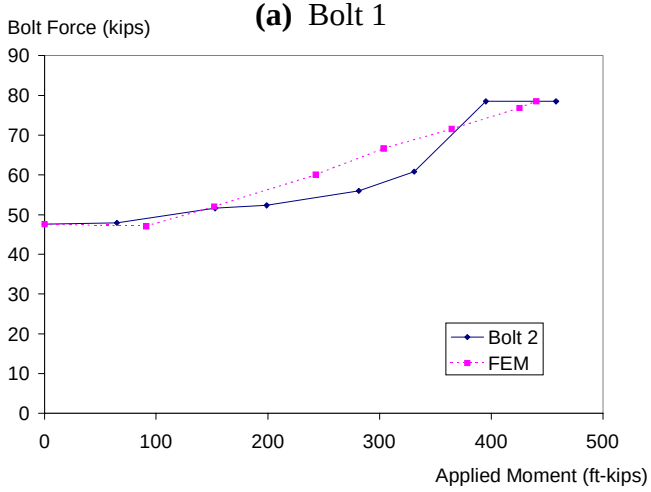

(b) Bolt 2

Figure 4.12 Bolt Force Comparison for ES-1-1/2-24a -Test 2 with 1.6 Scaling Factor

CHAPTER V

ANALYSIS OF EXPERIMENTAL RESULTS

5.1 INTRODUCTION

Included in this chapter are finalized experimental and modified experimental results and the comparison of these results to the predicted strengths. Design of all specimens was done using the methods described in Chapter II. Using the actual dimensions of the specimens given in Table 3.3 and prediction equations presented in Chapter II, the predicted strengths, M_q and M_{pl}, were calculated: M_q is the moment strength of the connection due to the rupturing of the bolts, based on the modified Kennedy method, and M_{pl} is the moment strength of the connection based on the yield line strength of the end-plate. The predicted moment strength, which controls the failure of the connection, is the lower of these two values.

5.2 FOUR BOLT EXTENDED STIFFENED MOMENT END-PLATE CONNECTIONS

5.2.1 Comparison of Experimental and Predicted Strengths

Three tests were conducted using the four bolt extended stiffened end-plate connection. Specimens *ES-1-1/2-24a-Test 1*, and *ES-1-1/2-24a-Test 2* were designed such that M_{pl} controlled. The third specimen, *ES-1-1/2-24b*, was designed such that M_q controlled. The differences between specimens *ES-1-1/2-24a and ES-1-1/2-24b* were the

bolt pitch and gage (See table 3.3). Complete results from the four bolt extended stiffened moment end-plate connection tests are found in Appendix B.

Quasi-static cyclic loading was applied to each specimen according to the SAC loading protocol discussed in Chapter 3. The bolts were pre-tensioned for each test to the pre-load given in AISC (Specification, 1993).

To further comfirm the validity of the 1.6 scaling factor, determined in Section 4.4, the initial stiffnesses of tests *ES-1-1/2-24a,Test 1* and *Test 2*, were compared to the initial stiffness of the moment end-plate connection tested by Morrison (1986). It was found that the uncorrected initial stiffnesses of the two tests done cyclically were much lower than the initial stiffness of the test done by Morrison, (see Figure 5.1). The correlation between the tests done by Morrison and the ES tests done cyclically is much better after the application of the correction factor (see Figure 5.2). Therefore, the 1.6 scaling factor is accepted and all further comparison results have it included.

Maximum strength results from these tests are presented in Table 5.1. The maximum moment strengths of the connections are much greater than the strength predictions from yield-line analysis and the modified Kennedy method. The shaded boxes indicate the controlling limit state for the connection. The maximum experimental moment, M_u, is the maximum applied moment applied throughout the entire test. The results of all ES tests are consistent and very conservative.

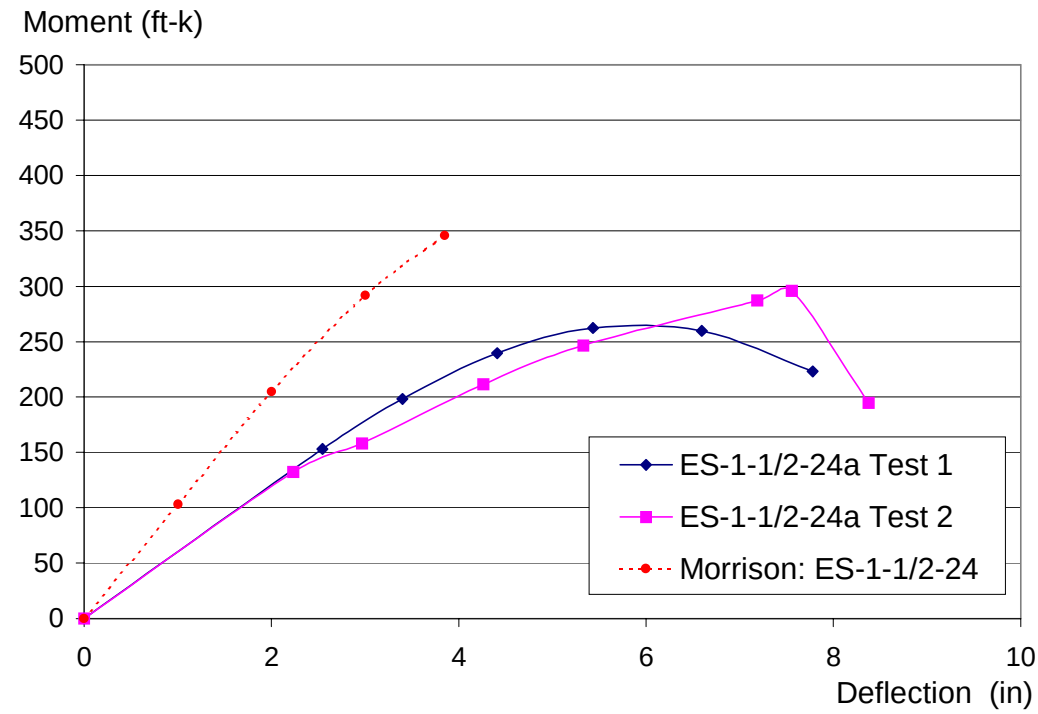

Figure 5.1 Initial Stiffness Comparison to Morrison, 1983
(Before Load Adjustment)

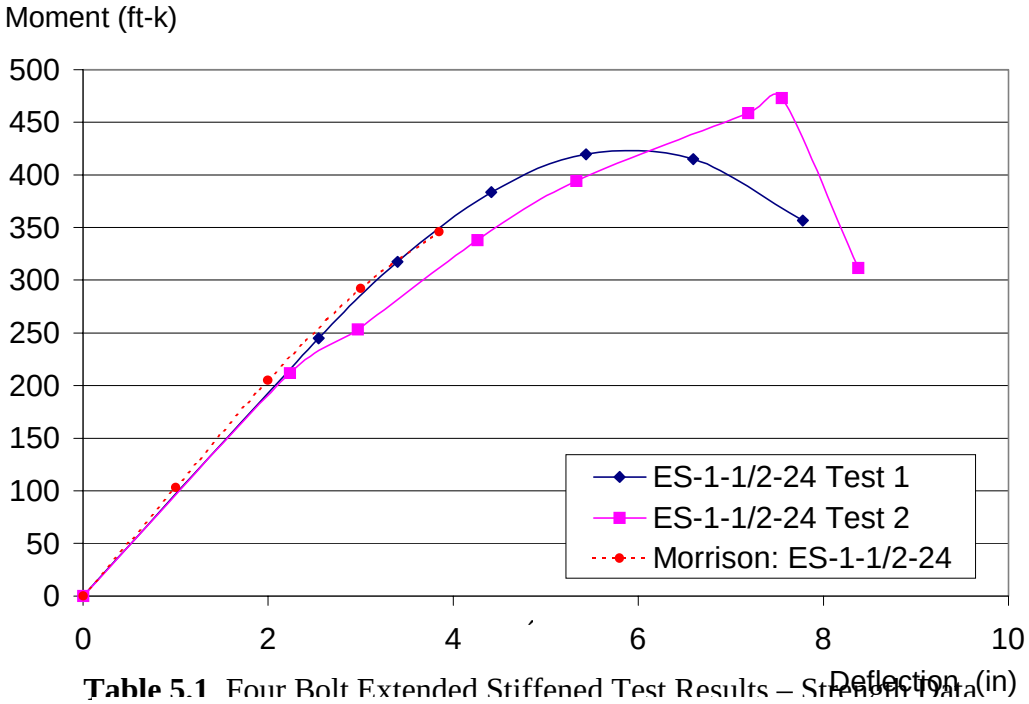

Table 5.1 Four Bolt Extended Stiffened Test Results – Strength Data

Figure 5.2 Initial Stiffness Comparison to Morrison, 1983
(Load Adjusted with 1.6 Correction Factor)

Connection	Test	Maximum Moment (ft-kips)			M_{pl}/M_{app}	M_q/M_{app}	F_{py} (ksi)
		Predicted Strengths		Applied			
		M_{pl}	M_q				
ES-1-1/2-24a	1	345	286	420*	0.82	0.67	60.70
ES-1-1/2-24a	2	326	286	474*	0.69	0.60	62.00
ES-1-1/2-24b	1	256	301	458	0.56	0.66	56.03

*Modified anylitically (see Chapter IV)

5.2.2 Rotational Capability

Rotation results for the four bolt extended stiffened moment end-plate connections are presented in Table 5.2. The total rotation is found by dividing the deflection achieved in the last completed cycle by the distance from the load point to the face of the connection, and subtracting the measured rotation of the test column and the measured rigid body motion of the load frame.

The elastic response of the connection throughout loading is represented by a relationship between moment and total rotation at low loads. This relationship is found by taking a linear interpolation of moment versus total rotation data points from test data obtained prior to any yielding in the connection. The elastic response is then extrapolated for all subsequent loads realized throughout the test. Finally, the inelastic rotation is

found by subtracting the elastic response from the total rotation. Typical total and inelastic rotation curves are presented in Figures 5.3 and 5.4.

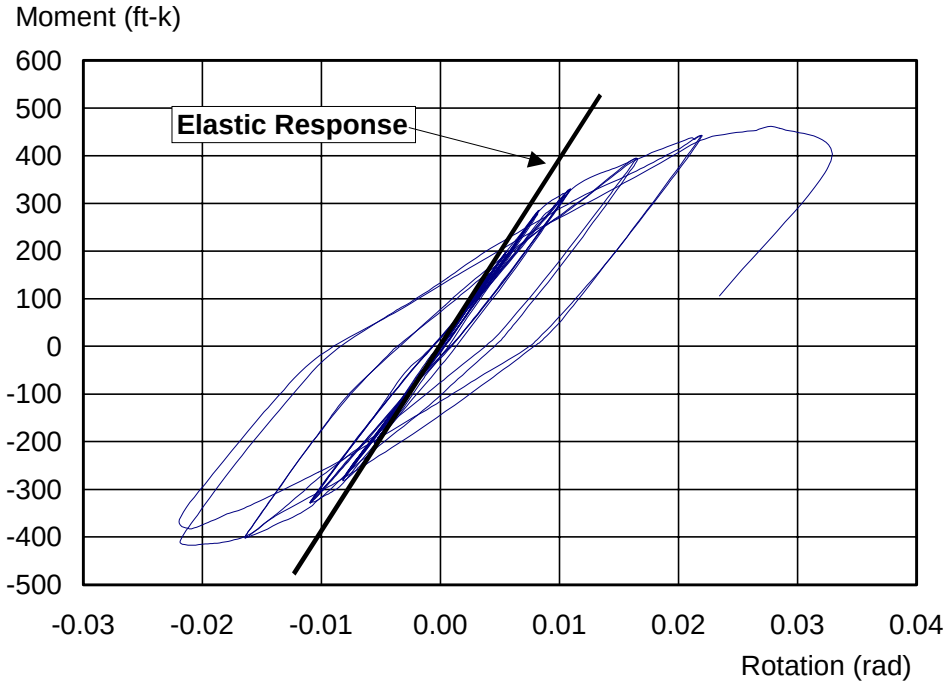

Figure 5.3 Typical Moment Versus Total Rotation Curve

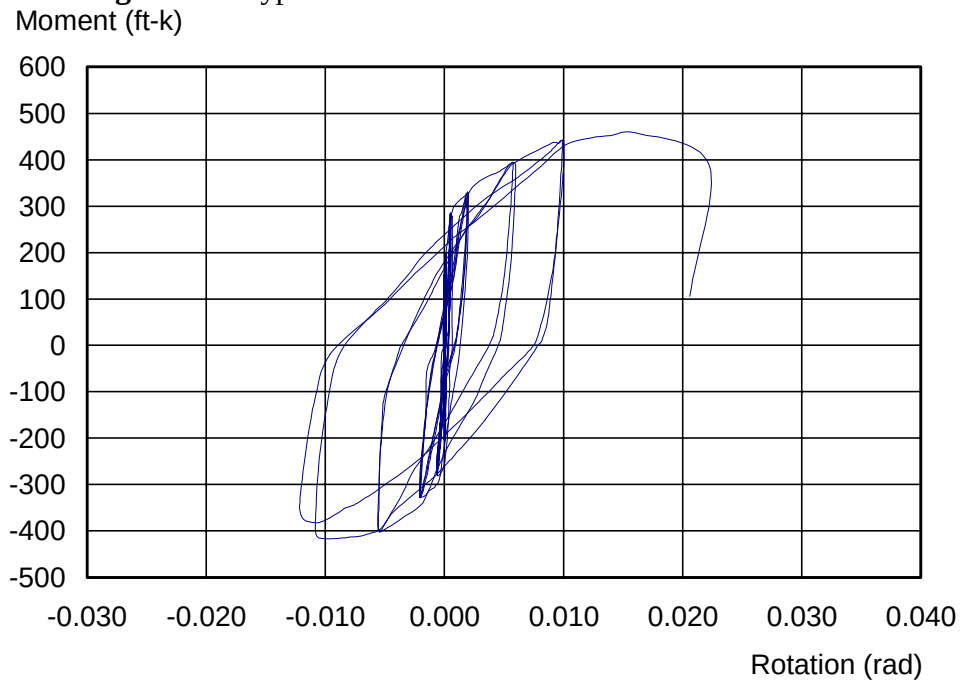

Figure 5.4 Typical Moment Versus Inelastic Rotation Curve

TABLE 5.2 Four Bolt Extended Stiffened Test Results – Rotation Data

Connection	Test	Completed Cycles	Maximum Rotation (rad)		Condition at End of Test
			Total	Inelastic	
ES-1-1/2-24a	1	26	0.022	0.017	End-Plate-to-Web Weld Fracture, and Stiffener to Weld Fracture
ES-1-1/2-24a	2	27	0.034	0.029	End-Plate Fractures at Flange and Web
ES-1-1/2-24b	1	26	0.022	0.012	End-Plate Fracture at Stiffener.

5.2.3 Condition at End of Tests

Each test was terminated when the end-plate connection was no longer able to withstand 30 percent of the maximum load previously applied. Excessive deformation of the plate caused cracks of the end-plates, flanges, webs, or stiffeners adjacent to welds. These fractures are referred to in Table 5.2 as the condition at the end of the test.

After the end-plate yielded and had gone through significant deformation, fractures began to appear in specimen *ES-1-1/2-24a-Test 1*. The first crack was noticed in cycle 24 at the end-plate-to-web interface. The crack led to the complete separation of the end-plate from the web over a 7 in. portion of the web. In cycle 26 the stiffener became completely separated from the flange of the beam on the same side at which the web had separated (see Figure 5.5). This led to a loss of strength, at which time the test was terminated.

(b) Flange-to-End-Plate Weld Fracture

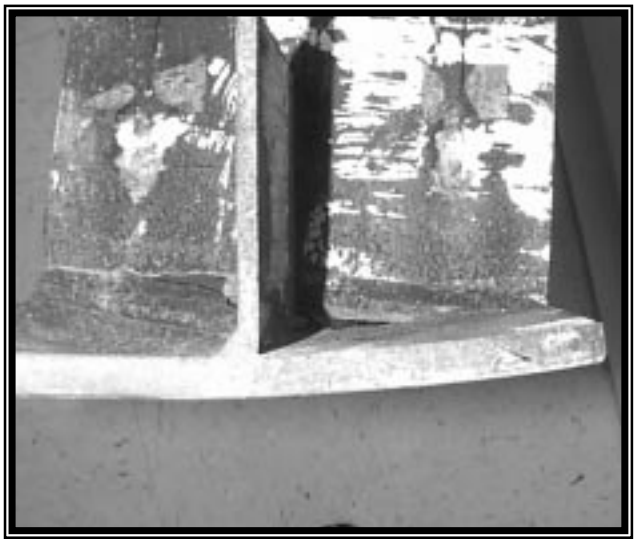

(a) Flange-to-End-Plate Weld Fracture

Figure 5.5 Condition of ES-1-1/2-24a Test 1 at End of Test

A similar set of events led to the loss of strength in specimen *ES-1-1/2-24a-Test 2*. However, the fractures occurred in different locations. The first fracture was observed between the stiffener and the end-plate in cycle 26, followed immediately by local buckling of the adjacent beam flange (see Figure 5.6). In the following cycle this flange separated completely from the end-plate, causing a severe drop in load and termination of the test.

In test *ES-1-1/2-24b* a crack formed between the end-plate at the end-plate-to-stiffener interface from the outside of the flange to the edge of the end-plate resulting in loss of applied load and termination of the test (see Figure 5.7).

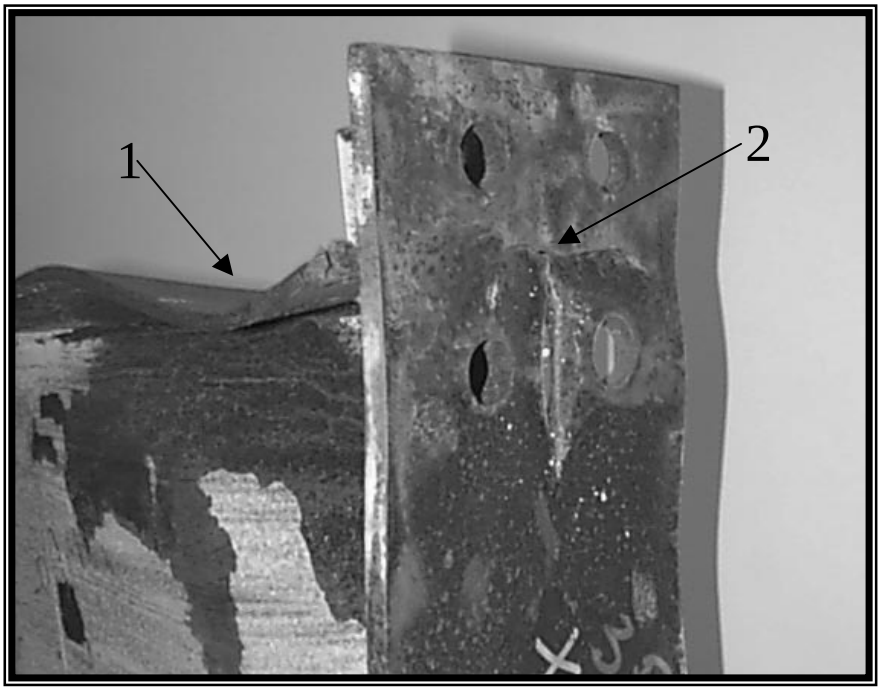

1 Local Flange Buckle
2 Crux of Cruciform Fracture of End-Plate

Figure 5.6 Condition of ES-1-1/2-24a Test 2 at End of Test

(a) Flange-to-End-Plate Fracture at the Weld

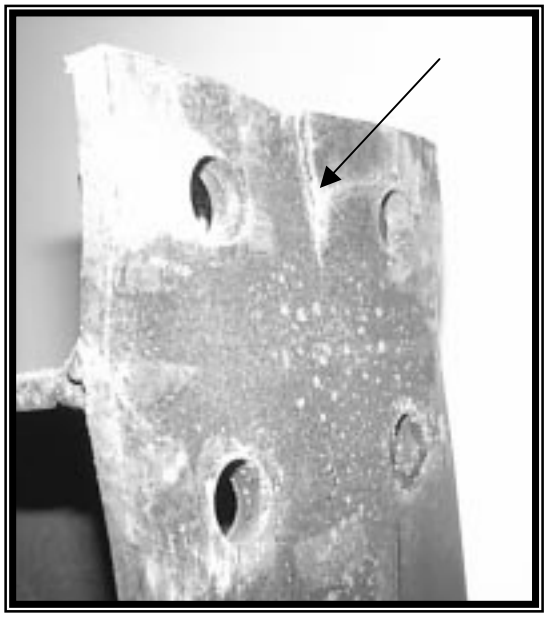

(b) End-Plate Fracture at Stiffener-to-End-Plate Weld

Figure 5.7 Condition of ES-1-1/2-24b at End of Test

5.3 MULTIPLE ROW 1/3 EXTENDED MOMENT END-PLATE CONNECTIONS

5.3.1 Comparison of Experimental and Predicted Strengths

Three tests were conducted using the multiple row 1/3 extended stiffened end-plate connection. These specimens had beam depths equal to 55 in., which is within ten percent of the largest size beams currently used in pre-engineered metal buildings. The first two specimens, MRE1/3-7/8-5/8-55 Tests 1 and 2 were designed such that the strength of the connection due to the strength of end-plate, as predicted by yield-line theory, would be greater than the strength of the connection due to the strength of the bolts. MRE1/3-7/8-1/2-55 was designed such that the strength of the connection due to the strength of the bolts would be greater than that due to the strength of the plate. The parameters varied between specimen MRE1/3-7/8-5/8-55 and specimen MRE 1/3-7/8-1/2-55 were pitch, gage, and end plate thickness. Quasi-static cyclic loading was applied to each specimen according to the SAC loading protocol, presented in Chapter 3. The bolts were pre-tensioned for each test to the pre-load given in AISC (Load, 1993).

Maximum moment results from these tests are presented in Table 5.3. As in Table 5.1, M_{pl} is the moment strength of the connection calculated using yield-line theory, and M_q is the moment strength calculated using the modified Kennedy method. The values for M_{pl} and M_q were calculated using the measured dimensions presented in Table 3.1 and the measured end-plate yield stress (see Table 3.3). The values for M_q were found using nominal bolt strengths. The shaded boxes indicate the controlling limit state for the connection. The maximum experimental moment, M_u, is the maximum applied moment

Table 5.3 MRE1/3 and Extended Unstiffened Test Results– Strength Data

Connection	Test	Maximum Moment (ft-kips)			M_{pl}/M_{app}	M_q/M_{app}	F_{py} (ksi)
		Predicted Strengths		Applied			
		M_{pl}	M_q				
MRE1/3-7/8-5/8-55	1	1206	1062	1523	0.79	0.69	60.40
MRE1/3-7/8-5/8-55	2	1221	1062	1720	0.71	0.62	60.40
MRE1/3-7/8-1/2-55	1	778	928	1220	0.64	0.76	62.00
4E-7/8-1/2-55	1	610	650	904	0.67	0.72	62.00

TABLE 5.4 MRE 1/3 and Extended Unstiffened Test Results – Rotation Data

Connection	Test	Completed Cycles	Maximum Rotation (RAD)		Condition at End of Test
			Total	Inelastic	
MRE1/3-7/8-5/8-55	1	22	0.0129	0.0034	Bolt Fracture
MRE1/3-7/8-5/8-55	2	22	0.0145	0.0015	Bolt Fracture
MRE1/3-7/8-1/2-55	1	22	0.0156	0.0055	Bolt Fracture
E-7/8-1/2-55	1	18	0.0114	0.0046	Bolt Fracture

achieved throughout the entire test. Complete results for the multiple row 1/3 extended tests are found in Appendix C.

5.3.2 Rotational Capability

The maximum total rotation and the maximum inelastic rotation are listed in Table 5.4. The maximum values are taken at the maximum applied moment for all multiple row 1/3 extended moment end-plates tests. The total and inelastic rotation was found for these tests in the same manner that was used for the extended stiffened connections (see Figures 5. 3 and 5.4).

5.3.3 Condition at End of Tests

Bolt fractures occurred in each of the multiple row1/3 and extended moment end-plate specimens. In each case, the initial bolt fracture caused redistribution of load, which in turn caused either additional bolt fractures or severe distortion of the plate. In either case, the specimens could no longer support additional load. Therefore the tests were terminated soon after a bolt fracture occurred because of the loss of specimen strength.

The end-plates of specimens *MRE1/3-7/8-5/8-55-Test 1* and *MRE1/3-7/8-5/8-55-Test 2* yielded partially, but did not appear to incur much inelastic behavior before the bolts ruptured. Photographs of these specimens at the end of the test are shown in Figures 5.8 and 5.9.

The end-plate of specimen *MRE1/3-7/8-1/2-55* incurred greater inelastic distortion than in the other multiple row 1/3 extended tests. Photographs of this specimen after the test are shown in Figure 5.10.

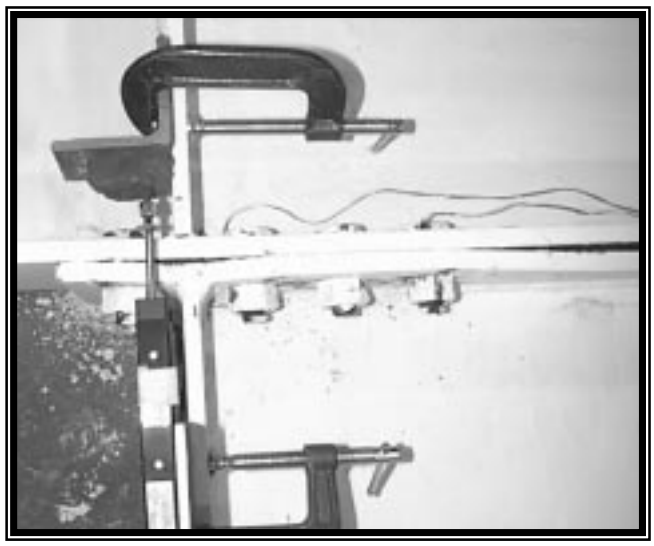

(a) Top Flange

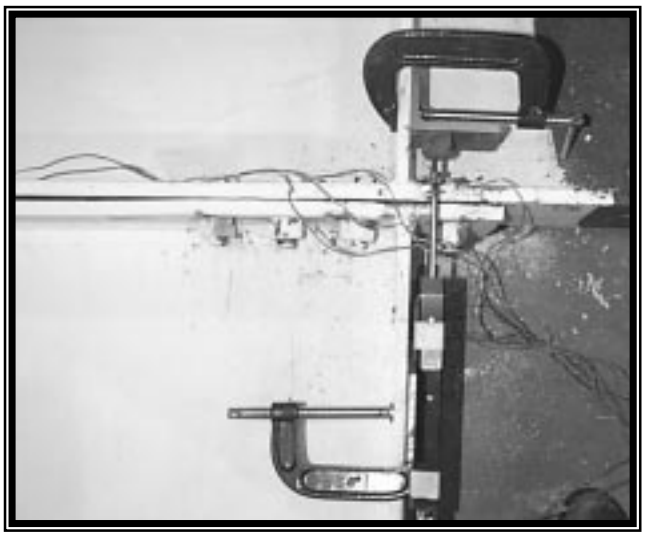

(b) Bottom Flange

Figure 5.8 Condition of MRE1/3-7/8-5/8-55 Test 1 at End of Test

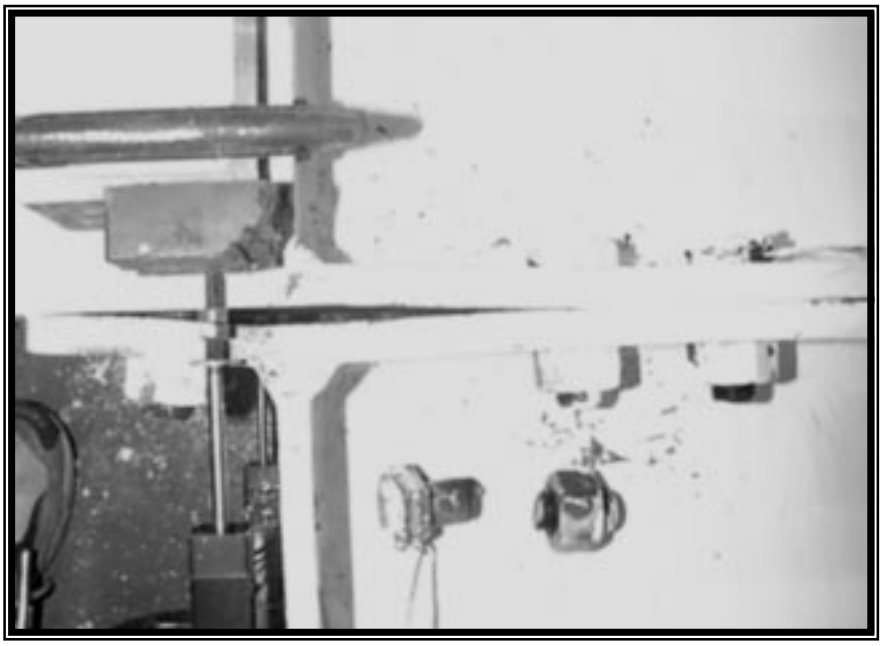

(a) Top Flange

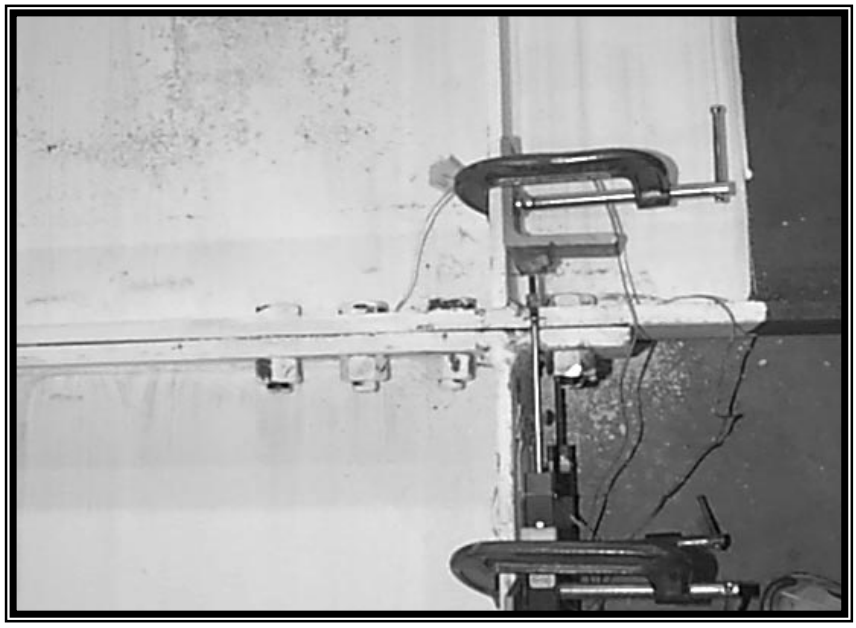

(b) Bottom Flange

Figure 5.9 Condition of MRE1/3-7/8-5/8-55 Test 2 at End of Test

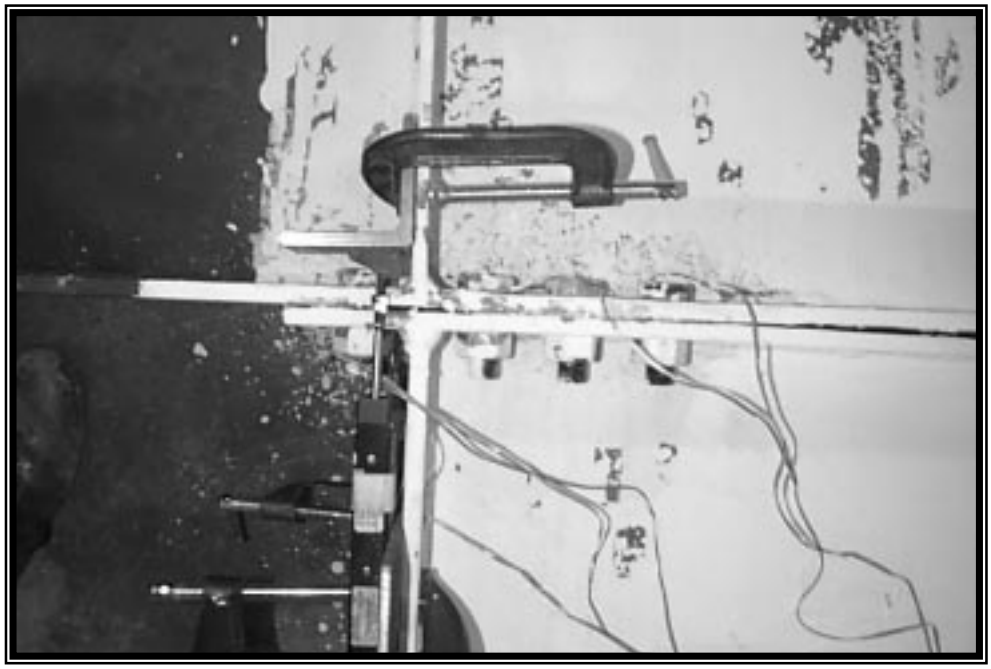

(a) Top Flange

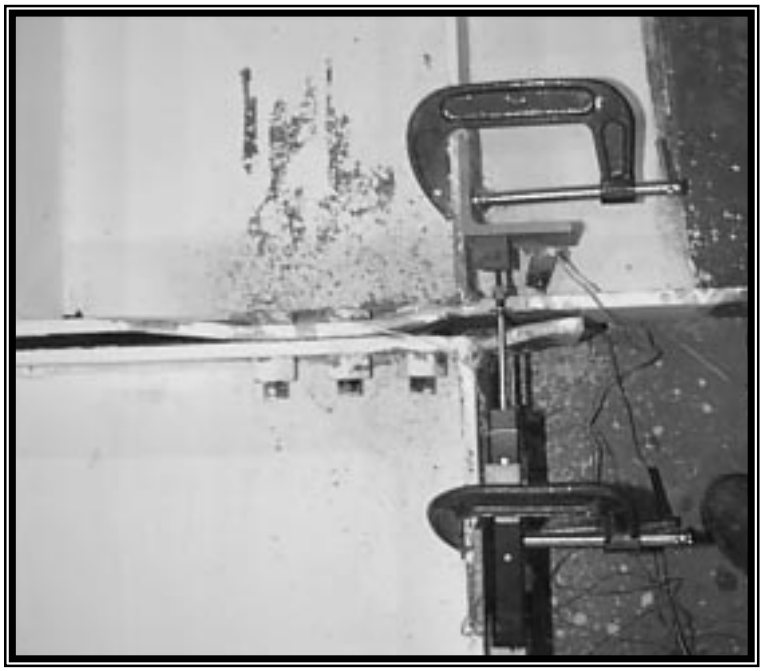

(b) Bottom Flange

Figure 5.10 Condition of MRE1/3-7/8-1/2-55 at End of Test

5.4 FOUR BOLT EXTENDED MOMENT END-PLATE CONNECTIONS

5.4.1 Comparison of Experimental and Predicted Strengths

One test was conducted using the four bolt extended ustiffened moment end-plate connection. The specimen was designed such that the strength of the connection due to the strength of the bolts would be greater than the moment strength of the plate as predicted by yield-line theory. Quasi-static cyclic loading was applied to each specimen according to the SAC loading protocol presented in Chapter 3. The bolts were pre-tensioned for each test to the pre-load given in AISC (Load, 1993). The results of the four bolt extended test are found in Appendix D.

Maximum moment results from these tests are presented in Table 5.3. As in Table 5.1, M_{pl} is the moment strength of the connection calculated using yield-line theory, and M_q is the moment strength calculated using the modified Kennedy method. The values for M_{pl} and M_q were calculated using the measured dimensions presented in Table 3.1 and measured end-plate yield stress (see Table 3.3). The values for M_q were found using nominal bolt strengths. The shaded boxes indicate the controlling limit state for the connection. The maximum experimental moment, M_u, is the maximum applied moment achieved throughout the entire test. The design methods used for this specimen are conservative.

5.4.2 Rotational Capability

The maximum total rotation and the maximum inelastic rotation obtained in the test are presented in Table 5.4. The maximum values are taken at the maximum applied

moment. The total and inelastic rotation was found for this test in the same way that the rotations were found for the extended stiffened connections (see Figures 5. 3 and 5.4).

5.4.3 Condition at End of Test

The four bolt extended moment end-plate test was terminated when the two inside bolts fractured simultaneously. Immediately following the rupture of the two interior bolts, load was distributed to the end-plate directly outside of the flange. At this point a shear fracture of the end-plate was observed (see Figures 5.11 and 5.12). The yielding seen prior to failure was significant.

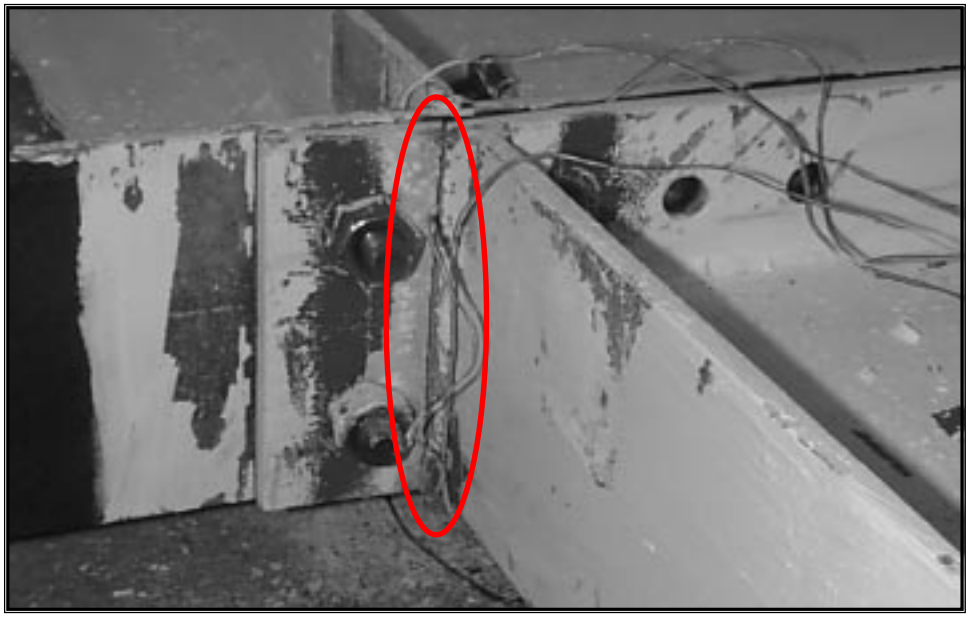

Figure 5.11 Illustration of Shear Failure of End-Plate (E-7/8-5/8-55)

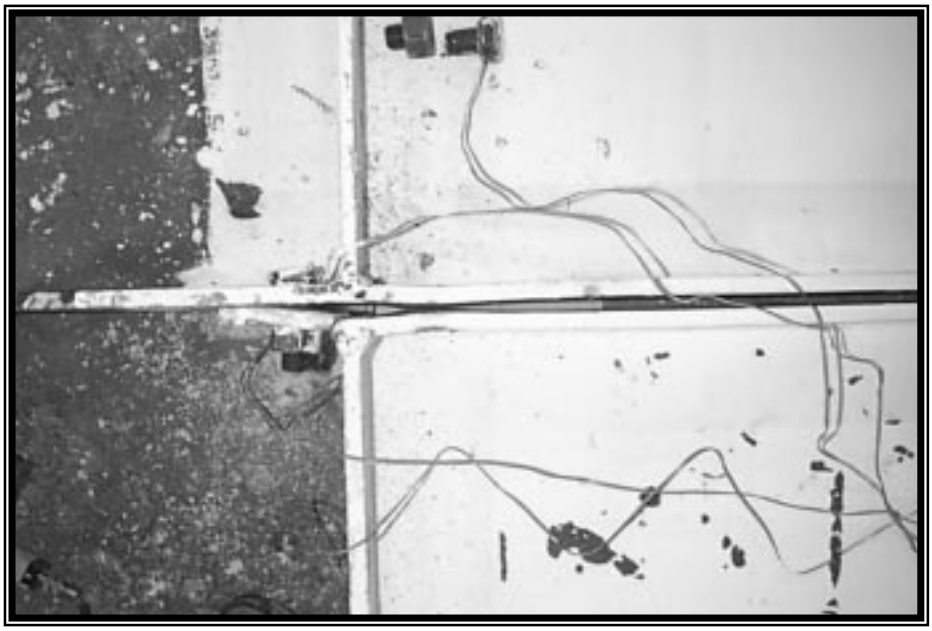

(a) Top Flange

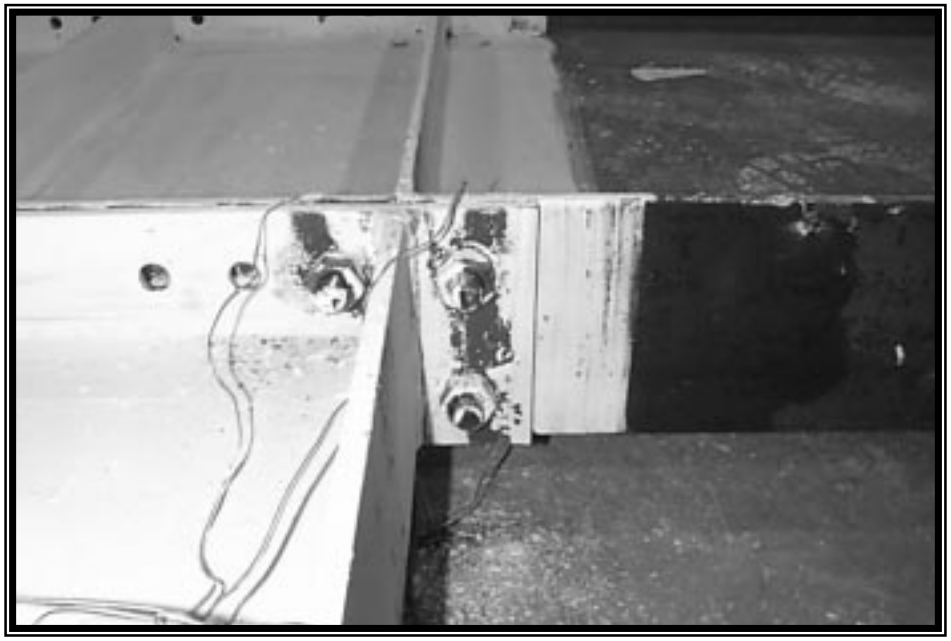

(b) Bottom Flange

Figure 5.12 Condition of 4E-7/8-1/2-55 at End of Test

5.5 SEISMIC FRAME CLASSIFICATION

The inelastic rotational capability of a moment connection is the means by which energy is dissipated during a seismic event if the elastic strength of the frame is overcome by lateral forces. According to AISC (Seismic 1997), steel moment frames are classified in one of three categories depending on the amount of inelastic rotation the connections of the frame can incur. The most restrictive classification, special moment frame, requires 0.03 radians of inelastic rotation from the connections. The intermediate moment frame classification applies to connections that can incur between 0.02 radians and 0.03 radians rotation. Finally, the ordinary moment frame classification applies to connections that can incur between 0.01 and 0.02 radians rotation. All specimens tested were considered for use in seismic frames, based on the inelastic rotation exhibited by the connections. Table 5.5 shows the classification of the connections tested.

Table 5.5 AISC Moment Frame Classification of Connections

Connection	Test	Inelastic Rotation (rad)	Type of Moment Frame For Which Connection May Be Used
ES-1-1/2-24a	1	0.017	Ordinary
ES-1-1/2-24a	2	0.029	Intermediate
ES-1-1/2-24b	1	0.012	Ordinary
MRE1/3-7/8-5/8-55	1	0.003	None
MRE1/3-7/8-5/8-55	2	0.002	None
MRE1/3-7/8-1/2-55	1	0.006	None
4E-7/8-1/2-55	1	0.005	None

CHAPTER VI

SUMMARY AND CONCLUSIONS

6.1 SUMMARY

An experimental investigation was done to study the inelastic rotational capabilities of extended moment end-plates under cyclic loading. Configurations studied were the four bolt extended stiffened, multiple row 1/3 extended, and four bolt extended unstiffened. The design methods used for the design of the moment end-plates configurations were then evaluated.

The procedures used to design the extended moment end-plate connections are discussed in Chapter II. The methods are based on yield-line theory, for determining end-plate thickness, and the modified Kennedy method, for determining bolt diameter. All connections were designed such that the moment strength of the connection was weaker than the plastic moment strength of the cross-section of the beam.

Seven full scale moment end-plate connections were tested using the SAC protocol (1997). Slow cyclic loading was applied until additional load could not be applied. All specimens but one failed as a result of weld fractures, bolt fractures, or end-plate fractures. Specimen *ES-1-1/2-24b* experienced local instability in the beam flange after some weld fractures had already occurred.

As a result of low ultimate moment strength results in the *ES-1-1/1-24a, Tests 1* and *2*, in comparison to monotonic tests in previous experimental studies, and because of evidence indicating a possible load cell problem, a finite element study was conducted. The finite element study was used to obtain a scaling factor to the load cell data, of 1.6 for these tests. The finite element results also correlated well with data obtained in all other specimens studied.

6.2 CONCLUSIONS

6.2.1 Four Bolt Extended Stiffened Moment End-Plate Connections

All extended stiffened moment end-plate configurations demonstrated the ability to incur sufficient inelastic rotation to be used in a moment frame designed for seismic loading. The inelastic rotation achieved in these connections occurred as a result of the inelastic deformation of the bolts and the end-plate. Specimen ES-1-1/2-24a can be qualified as a fully restrained connection for ordinary moment frames. However, AISC (Seismic, 1997) requires that two full scale tests be completed to qualify each connection. Therefore, the testing of Specimen *ES-1-1/2-24b* done in this study does not necessarily qualify a connection of this configuration for use in an ordinary moment frame for seismic design. However, AISC (Seismic, 1997) states that the results of a particular test can be extrapolated to a connection with a beam depth within 10% of the tested specimen and the weight per foot of the beam must be within 25% of the tested specimen. The specification states that extrapolation beyond these limitations is permitted, subject to peer review. But, AISC (Seismic, 1997) was created considering field welded

connections only. Because the seismic specification does not give a range of bolt spacing for which a test results can be extrapolated, the validity of the extrapolation of the results of Specimen *ES-1-1/2-24a* to Specimen *ES-1-1/2-24b* is unclear.

As a result of observing the weld failures of these connections, it is recommended that full-penetration welds be used for beam to end-plate welds, beam-to-stiffener welds and stiffener-to-end-plate welds.

Finally, the design methods used to predict connection strength are shown to be conservative when compared with the experimental strengths for the four bolt extended stiffened moment end-plate connections.

6.2.2 Multiple Row 1/3 and Four Bolt Extended Unstiffened Moment Connections

All multiple row 1/3 extended moment end-plate connections failed to achieve the inelastic rotation to be used in a moment frame designed for seismic loading. The extended stiffened end-plate tested also failed to achieved the inelastic rotation needed for the connection to be used in a moment frame designed for seismic loading. These connections did not exhibit significant rotation because they were 55 in deep. The inelastic rotation in these connections is achieved by the separation of the end plate from the column, as a result of the end-plate and column flange bending. Because this bending is limited by the strength of the bolts due to prying forces, the end-plate separation is also limited, and independent of beam depth. A connection with the same bolt configuration and end-plate thickness as those tested in this study, but using a beam with a lesser depth, would exhibit greater inelastic rotation. The increased inelastic rotation would be directly

proportional to the decreased depth of the beam. Therefore, in order to use this configuration for seismic frames, one of two adjustments in connection design needs to be made. Either the depth of the beam should be decreased, or the connection moment strength should be designed such that it exceeds the plastic moment capacity of the beam.

REFERENCES

Abel, M. and Murray, T. M. (1994). "Analytical and Experimental Investigation of the Extended Unstiffened Moment End-Plate Connection with Four Bolts at Beam Flange," Report No. CE/VPI-ST 93/08, Virginia Polytechnic Institute and State University, Blacksburg, Virginia.

Adey, B. T., Grodin, G.Y., and Cheng, J. J. R. (1998). "Extended End-Plate Moment Connections Under Cyclic Loading," *Journal of Constructional Steel Research*, 46:1-3, Paper No. 133.

Boorgsmiller, J. T. (1995). "Simplified Method For Design of Moment End-Plate Connections," Master of Science Thesis, Virginia Polytechnic Institute and State University, Blacksburg, Virginia.

Boorse, M. R. (1999). "Evaluation of the Inelastic Rotation Capability of Flush End-Plate Moment Connections," Master of Science Thesis, Virginia Polytechnic Institute and State University, Blacksburg, Virginia.

Clark, P., Frank, K., Krawinkler, H, and Shaw, R. (1997) "Protocol for Fabrication, Inspection, Testing, and Documentation of Beam-Column Connection Tests and Other Experimental Specimens", Report No. SAC/BD-97/02, SAC Joint Venture, Sacremento, California.

Douty, R. T., and McGuire, W. (1965). "High Strength Moment Connections," *Journal of Structural Engineering*, Vol. 91, No. 4, pp. 101-128.

Ghobarah, A., Osman, A., and Korol, R. M. (1990),."Behavior of Extended End-Plate Connections Under Cyclic Loading," *Engineering Structures*, Vol. 12, No. 1, pp. 1-27.

Interim Guidelines: Evaluation, Repair, Modification and Design of Welded Steel Moment Frames (1997). FEMA 267 (SAC95-02), Federal Emergency Management Agency, Washington, DC.

Hendrick, D.M., and Kukreti, A.R., and Murray, T.M. (1985). "Unification of Flush End-Plate Design Precedures," Report No. FSEL/MBMA 8305, Unversity of Oklahoma, Norman, Oklahoma.

Kennedy, D. J., and Hafez, M. A. (1982). "A Study of End Plate Connections for Steel Beams," *Canadian Journal of Civil Engineering*, Vol. 11, pp.139-149.

Kennedy, N. A., Vinnakota, S., Sherbourne, A. (1981). "The Split-Tee Analogy in Bolted Splices and Beam-Column Connections", *Joints in Structural Steelwork*, John Wiley and Sons, New York, pp. 2.138-2.157.

Kline, D. P., Murray, T. M., and Rojiani, K. B. (1989). "Performance of Snug-Tight Bolts in Moment End-Plate Connections," MBMA Project 301, Metal Building Manufacturer's Association, Cleveland, Ohio.

Krawinkler, H. and Popov, E. P. (1982). "Seismic Behavior of Moment Connections and Joints," *Journal of the Structural Division, ASCE*. Vol. 108, No. ST2, pp. 373-391.

Krishnamurthy, N. (1979), "Experimental Validation of End-Plate Connection Design", Report Submitted to the American Institute of Steel Construction.

Kukreti, A.R., Murray, T.M., and Ahuja, V. (1982). "Analysis of Stiffened End-Plate Connections with Multiple Bolt Rows at the Beam Flanges," presented at *Sino-American Syposium on Bridge and Structural Engineering*, Beijing, China, September, 13-19, (1982)

Kukreti, A. R., Gheassemieh, M., and Murray, T. M. (1989). "Finite Element Modeling of Large Capacity Stiffened Steel Tee-Hanger Connections," *Computers and Structures*, Vol. 32, No. 2, pp. 409-422.

Load and Resistance Factor Design Specification for Structural Steel Buildings (1993). American Institute of Steel Construction, Chicago, Illinois.

Mann, A. P. and Morris, L. J. (1979). "Limit Design of Extended End-Plate Connections," *Journal of Structural Engineering*, Vol. 105, No. 3, pp. 511-526.

Manual of Steel Construction, Allowable Stress Design 9th ed.*(1989).* American Institute of Steel Construction, Chicago, Illinois.

Manual of Steel Construction: Load and Resistance Factor Design, Volume II (1994). American Institute of Steel Construction, Chicago, Illinois.

Mays, T. W. (1999). Personal Correspondence, Virginia Polytechnic Institute and State University, Blacksburg, Virginia.

Meng, R. (1996), "Design of Moment End-Plate Connections for Seismic Loading". Doctoral Dissertation, Virginia Polytechnic Institute and State University, Blacksburg, Virginia.

Morrison, S. J. Astaneh-Asl, A., and Murray, T. M. (1985). "Analytical and Experimental Investigation of the Extended Stiffened Moment End-Plate Connection with Four Bolts at the Beam Tension Flange," Report No. FSEL/MBMA 86-01, University of Oklahoma, Norman, Oklahoma.

Morrison, S. J. , Astaneh-Asl, A., and Murray, T. M. (1986). "Analytical and Experimental Investigation of the Multiple Row Extended 1/3 Moment End-Plate Connection with Eight Bolts at the Beam Tension Flange," Report No. FSEL/MBMA 86-01, University of Oklahoma, Norman, Oklahoma.

Murray, T. M. (1988). "Recent Developments for the Design of Moment End-Plate Connections," *Journal of Constructional Steel Research*, Vol. 10, pp. 133-162.

Murray, T. M., Kline, D. P., and Rojiani, K.B. (1991). "Use of Snug-Tightened Bolts in End-Plate Connections," *Connections in Steel Structures III: Behavour, Strength and Design: Proceedings of the Second International Workshop*, Pittsburg, Pennsylvania, April 10-12, 1991, Bjorhovde, et al., eds., 1991, 27-34.

Nair, R. S., Birkemoe, P. C., and Munse, W. H. (1974). "High Strength Bolts Subject to Prying," *Journal of Structural Engineering*, Vol. 100, No. 2, pp. 351-372.

Ribeiro, L. F. L., Goncsalves, R. M., and Castigliorni, C. A. (1998), "Beam-to-Column End Plate Connections-An Experimental Analysis," *Journal of Constructional Steel Research*, Vol. 46, No.1-3, Paper No. 304.

Sherbourne, A. N. and Bahaari, M. R. (1994). "3D Simulation of End-Plate Bolted Connections," *Journal of Structural Engineering*, Vol. 120, No. 11, November, pp. 3122-3137.

Sherbourne, A. N. and Bahaari, M. R. (1997). "Finite Element Predictions of End Plate Bolted Connection Behavior. I: Parametric Study," *Journal of Structural Engineering*, Vol. 123, No. 2, pp. 157-164.

Seismic Provisions for Structural Steel Buildings, (1997). American Institute of Steel Construction, Chicago, Illinois.

Seismic Provisions for Structural Steel Buildings, Addendum 1 (1997). American Institute of Steel Construction, Chicago, Illinois.

Srouji, R., Kukreti, A., and Murray, T. M. (1983). "Yield-Line Analysis of End-Plate Connections with Bolt Force Predictions", Report No. FESL/MBMA 83-05, University of Oklahoma, Norman, Oklahoma.

Troup, S., Xiao, R. Y., and Moy, S. S. J. (1998). "Numerical Modelling of Bolted Steel Connections", *Journal of Constructional Steel Research*, Vol. 46, No. 1-3, Paper No. 362.

Tsai, K. C. and Popov, E. P. (1990). "Cyclic Behavior of End-Plate Moment Connections," *Journal of Structural Engineering*, Vol. 116, No. 11, pp. 2917-2930.

APPENDIX A

NOMENCLATURE

a	-	distance from bolt line to location of prying action
AISC	-	American Institute of Steel Construction
B	-	bolt force
B_I	-	inner bolt force (Srouji, 1983)
B_O	-	outer bolt force (Srouji, 1983)
B_I	-	inner bolt force (Srouji, 1983)
B_1	-	outer bolt force (Morrison, 1985)
B_2	-	bolt force of first inner row of bolts (Morrison, 1985)
B_3	-	bolt force of second inner row of bolts (Morrison, 1985)
B_4	-	bolt force of third inner row of bolts (Morrison, 1985)
b_f	-	beam flange width
ds	-	elemental length of line n
d_b	-	bolt diameter
d_e	-	distance from the centerline of the outer bolts to the outer edge of the end-plate
E	-	Young's Modulus of Elasticity
F	-	flange force per bolt
F_f	-	total flange force
F_{py}	-	end-plate material yield stress
F_{yb}	-	yield stress of the bolt
g	-	end-plate bolt gage distance
h	-	beam depth
L_n	-	length of yield line n

MBMA		Metal Building Manufacturer's Association
M_1	-	plastic moment at first hinge line to form
M_2	-	plastic moment at second hinge line to form
M_3	-	plastic moment at third hinge to form
M_{app}	-	applied maximum moment
M_{FE}	-	maximum moment found by using finite element analysis
M_b	-	moment strength of the bolt
m_p	-	plastic moment capacity of plate per unit length equal to $(F_{py}t_p^2)/4$
M_{pl}	-	moment strength of the connection calculated using yield-line theory
M_{pred}	-	predicted moment strength
M_q	-	moment strength of the connection calculated using maximum bolt force predictions
M_U	-	end-plate ultimate moment capacity at beam end
N	-	number of yield lines in a mechanism
n_j	-	the number of cycles to be performed in load step j
p_b	-	distance between interior bolt centerlines
$p_{b1,3}$	-	distance from the first interior bolt centerline to the inner most interior bolt centerline in the configuration with three interior bolt rows
P_{ext}	-	distance from face of beam flange to end of end-plate in Kennedy model
p_f	-	distance from bolt centerline to near face of beam flange
p_t	-	distance from bolt centerline to far face of beam flange
p_{t2}	-	distance from the second interior bolt centerline to the far face of the beam tension flange
p_{t3}	-	distance from the third interior bolt centerline to the far face of the beam tension flange
Q	-	prying force

Q_{max}	-	maximum prying force
s	-	distance from bolt centerline to outermost yield-line
SAC	-	joint venture involving: the Structural Engineers Association of California (SEAOC), Applied Technology Council (ATC), and the California Universities for Research in Earthquake Engineering (CUREe)
t_1	-	thick plate limit
t_{11}	-	thin plate limit
t_p	-	end-plate thickness
u	-	distance from the innermost bolt to the innermost yield line.
w’	-	width of end-plate per bolt at bolt line minus bolt hole diameter
W_e	-	total external work done on the connection
W_i	-	total internal energy stored
δ	-	deformation, a generic quantity including strains, angles of shear distortion, rotations, axial deformations and displacements
δ_y	-	yield deformation
θ	-	interstory drift angle
θ_e	-	elastic rotation
θ_i	-	inelastic rotation
θ_j	-	interstory drift at load step j in SAC protocol
θ_j	-	the peak deformation in load step j
θ_n	-	relative normal rotation of yield-line n
θ_t	-	total rotation

APPENDIX B

FOUR BOLT EXTENDED STIFFENED RESULTS AND TEST DATA

Summary
ES 1-1/2-24a
Test 1

Predicted Capacities:
Moment Strength Predicted by Yield Line Analysis, M_{pl}……345 ft-kips
Yield Stress of End Plate, F_y……...60.7 ksi
Moment Strength Predicted by Bolt Rupture, M_q……282 ft-kips

Strength Results:
Maximum Moment From Test, M_u……..420 ft-kips
M_{pl} / M_u……0.82
M_q / M_u…….0.67

Rotation Results:
Maximum Total Rotation…….0.022 rad
Maximum Inelastic Rotation……0.017 rad

Number of Completed Cycles……..…….26

Condition at End of Test……..End-plate weld fractures

Weld Fractures that occurred during test:

- Stiffener-to-End-Plate weld on top flange
- Flange-to-End-Plate weld on top flange, starting at the web and emanating 2.25 in. to the right of the web and 1.75 in. to the left of the web.
- Web-to-End-Plate weld, starting at top flange and emanating 4.75 in. towards the center of the section.
- Stiffener-to-Flange weld on Bottom Flange
- Flange-to-End-Plate weld on bottom flange, running from the web to the outer right edge of the flange, and from the web to 2.0 in. left of the web.

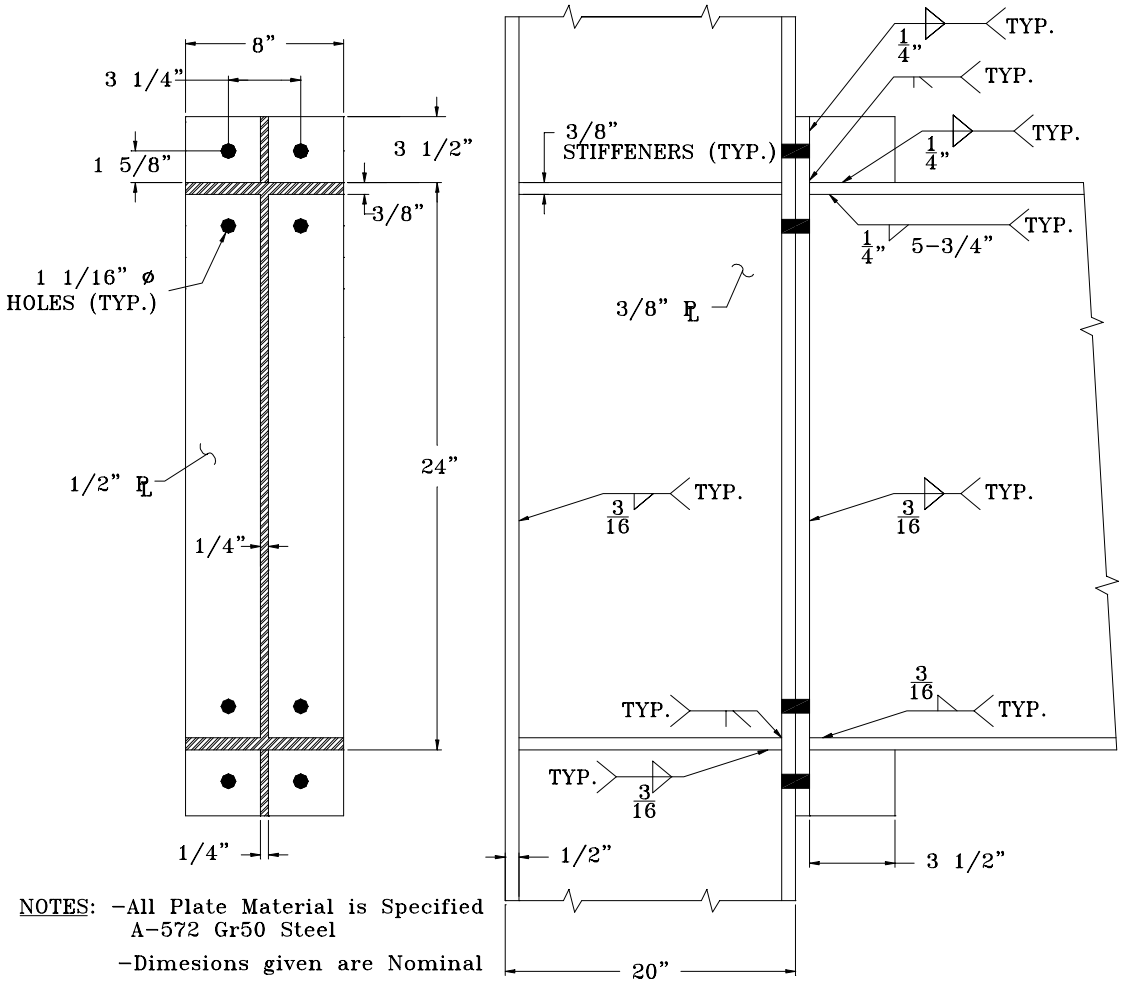

ES-1-1/2-24a Test 1 Connection Details

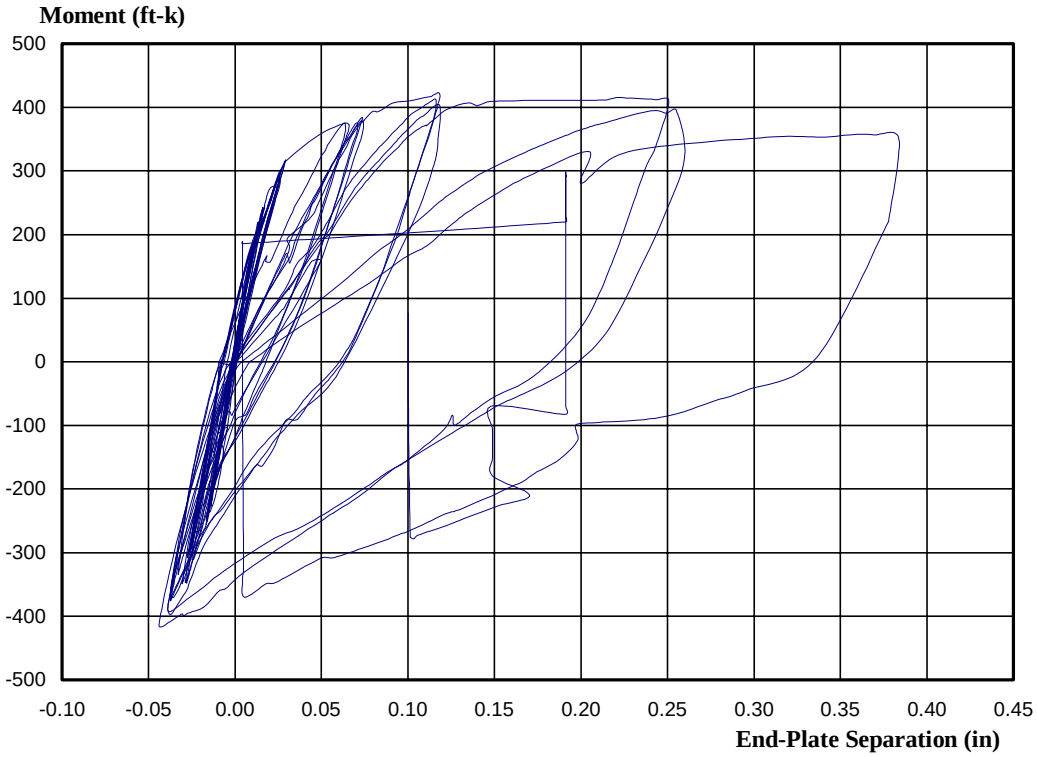

Moment At End-Plate vs. End-Plate Separation at Bottom Flange
ES-1-1/2-24a Test 1

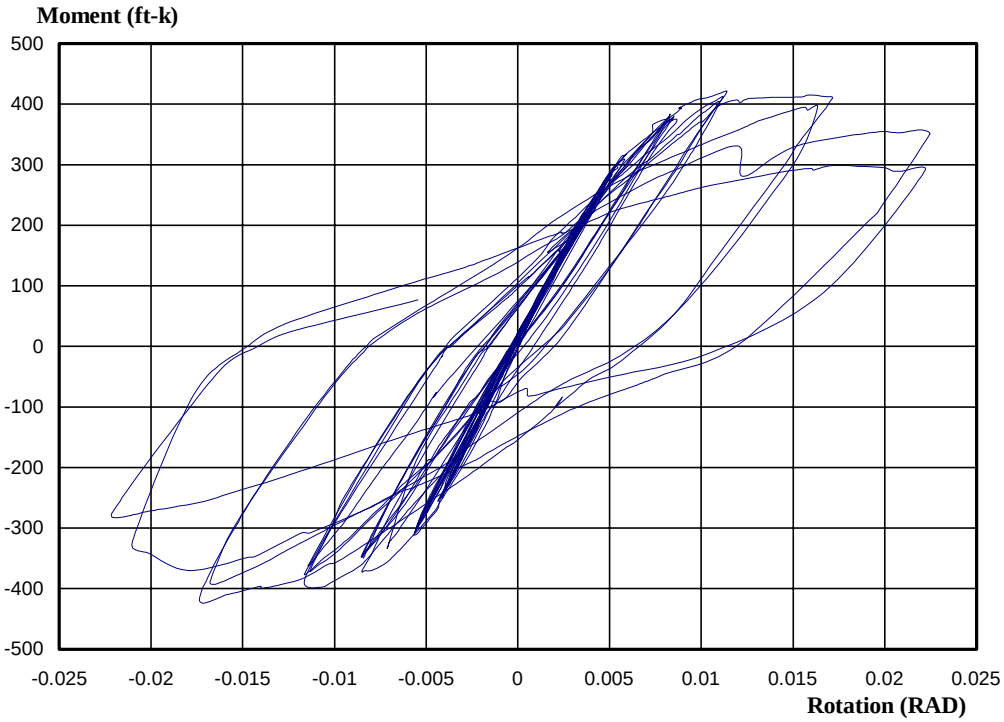

Moment At End-Plate vs. Adjusted Total Rotation at End-Plate
ES-1-1/2-24a Test 1

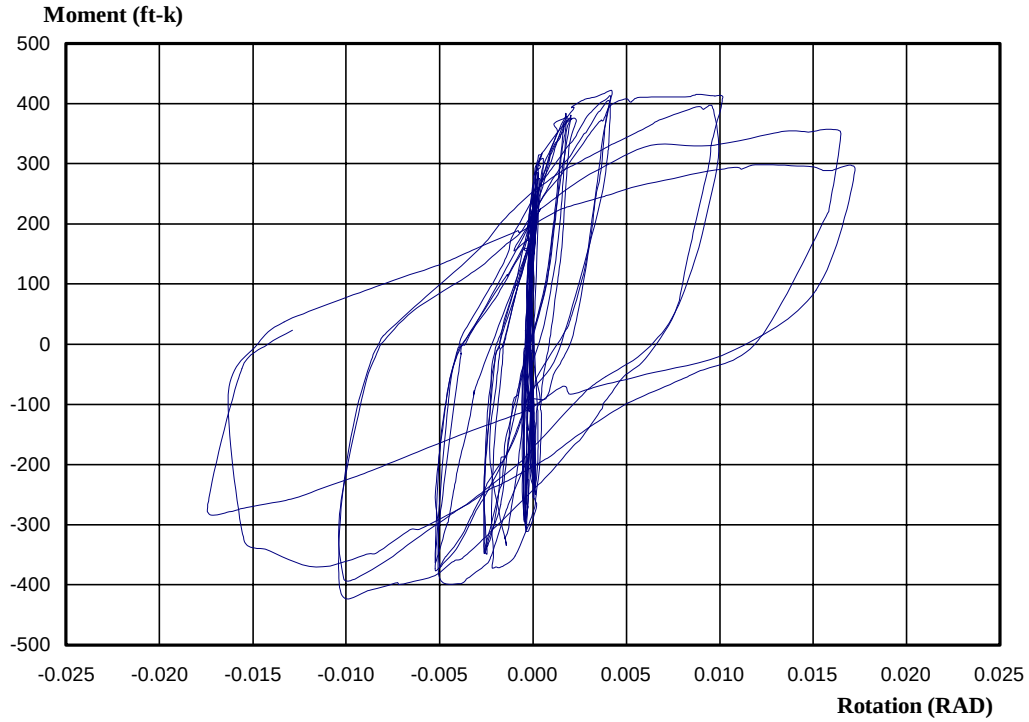

Moment vs. Inelastic Rotation at End-Plate
ES-1-1/2-24a-Test 1

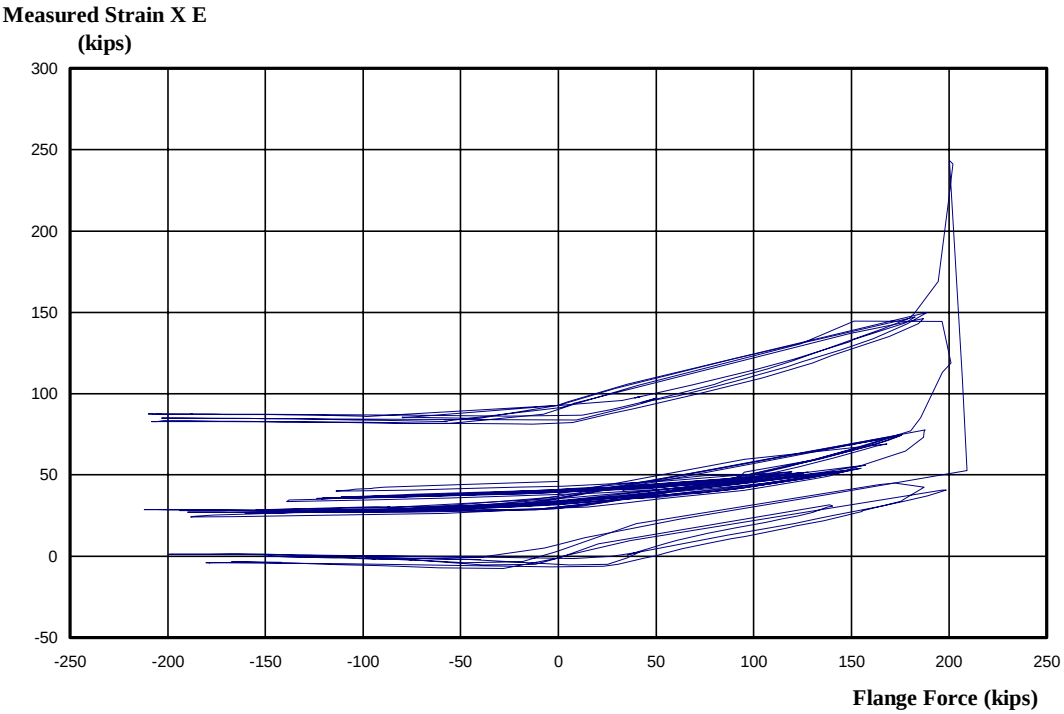

Measured Bolt Strain X E vs. Flange Force-Bolt 1
ES 1-1/2-24a Test 1

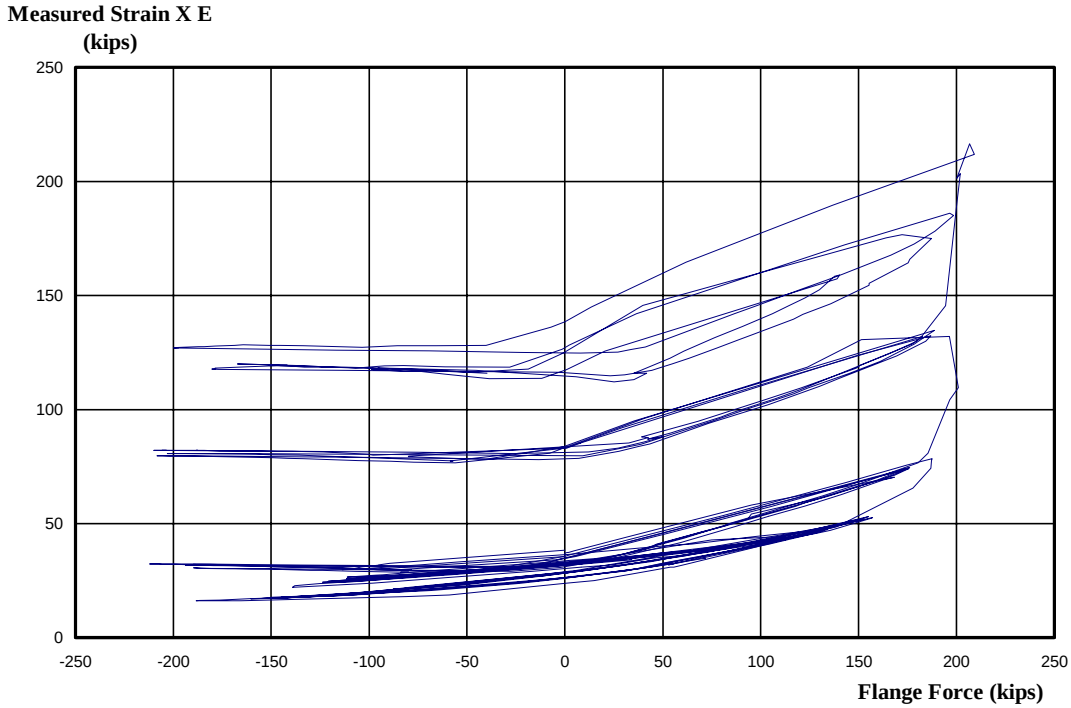

Measured Bolt Strain X E vs. Flange Force-Bolt 2
ES 1-1/2-24a Test 1

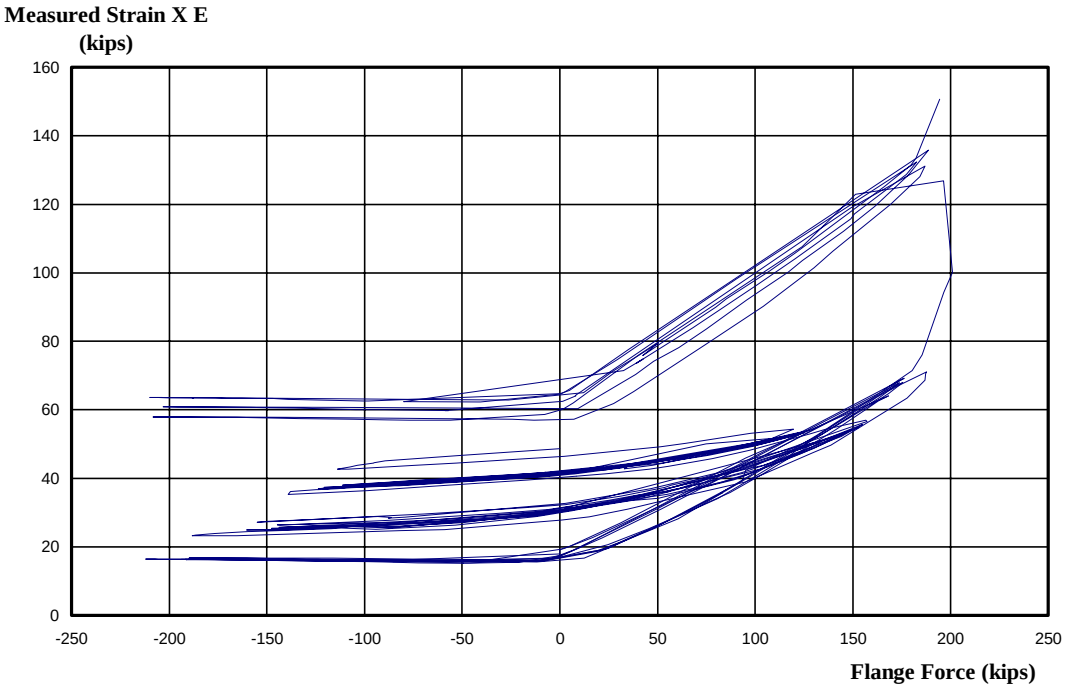

Measured Bolt Strain X E vs. Flange Force-Bolt 3

ES 1-1/2-24a Test 1

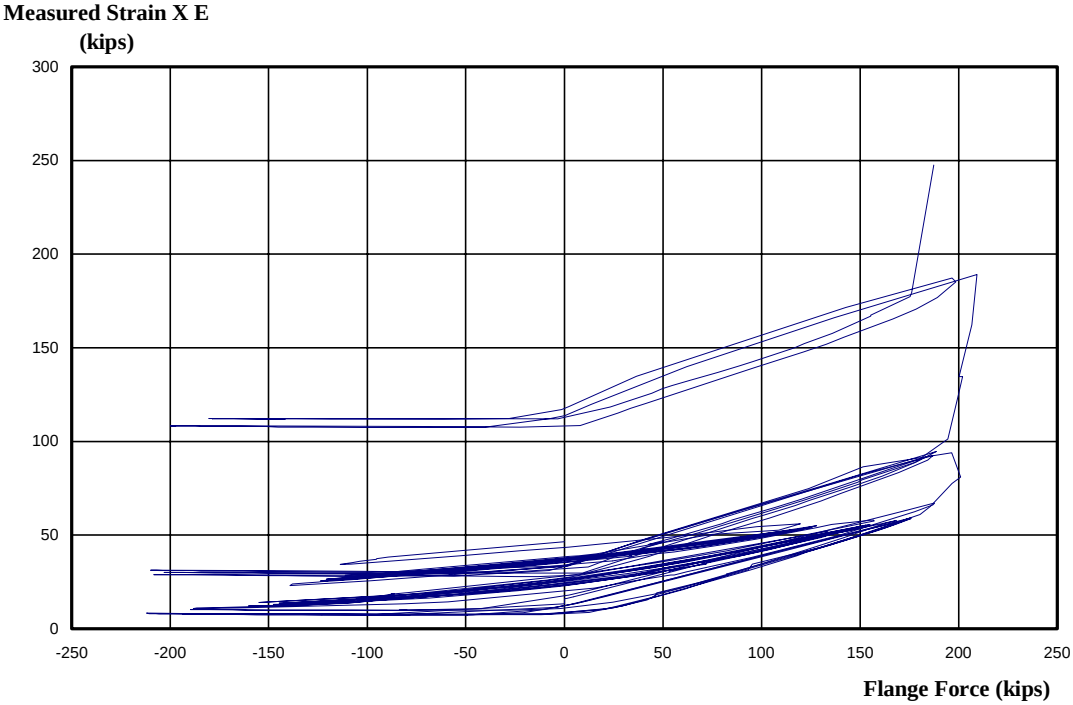

Measured Bolt Strain X E vs. Flange Force-Bolt 4

ES 1-1/2-24a Test 1

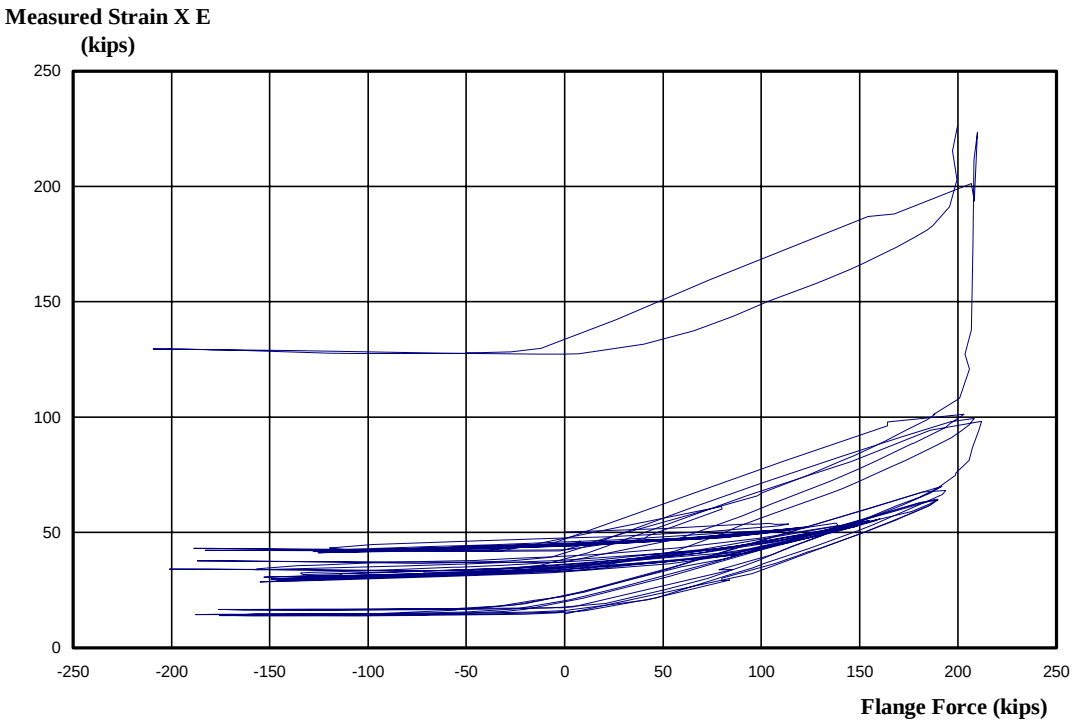

Measured Bolt Strain X E vs. Flange Force-Bolt 5
ES 1-1/2-24a Test 1

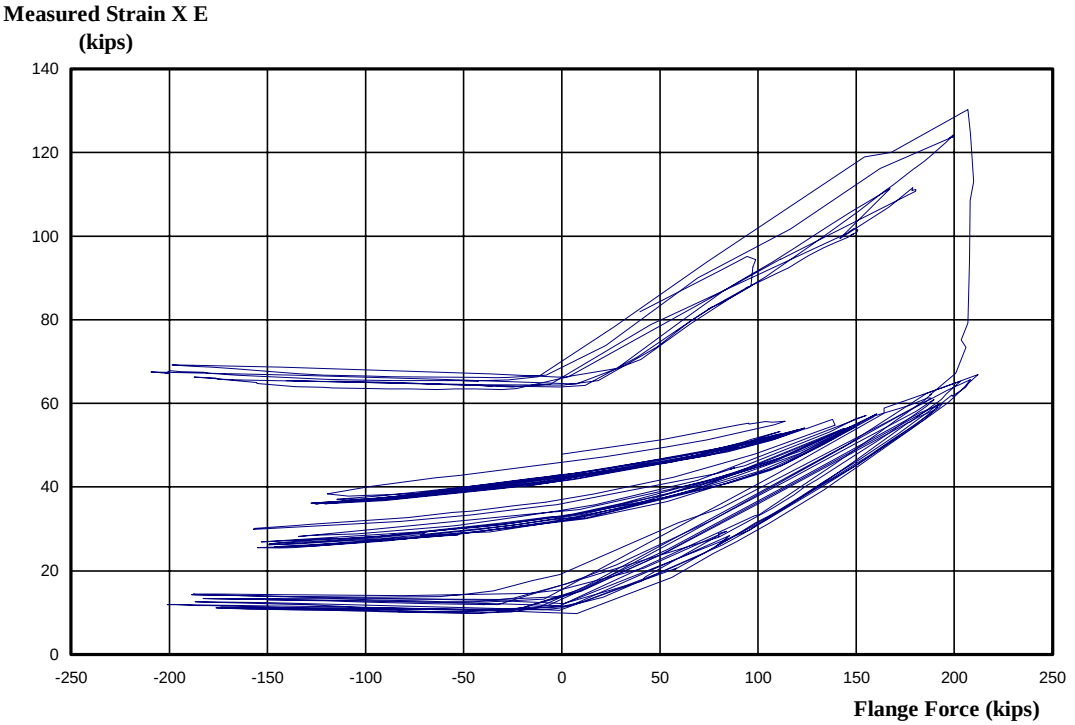

Measured Bolt Strain X E vs. Flange Force-Bolt 6
ES 1-1/2-24a Test 1

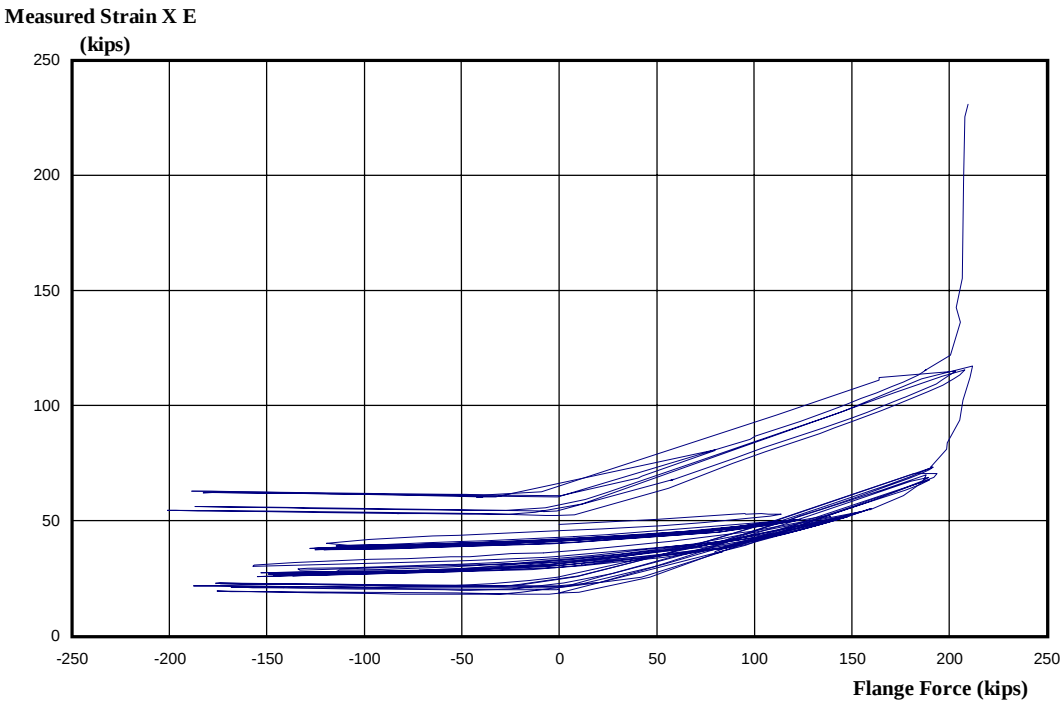

Measured Bolt Strain X E vs. Flange
ES 1-1/2-24a

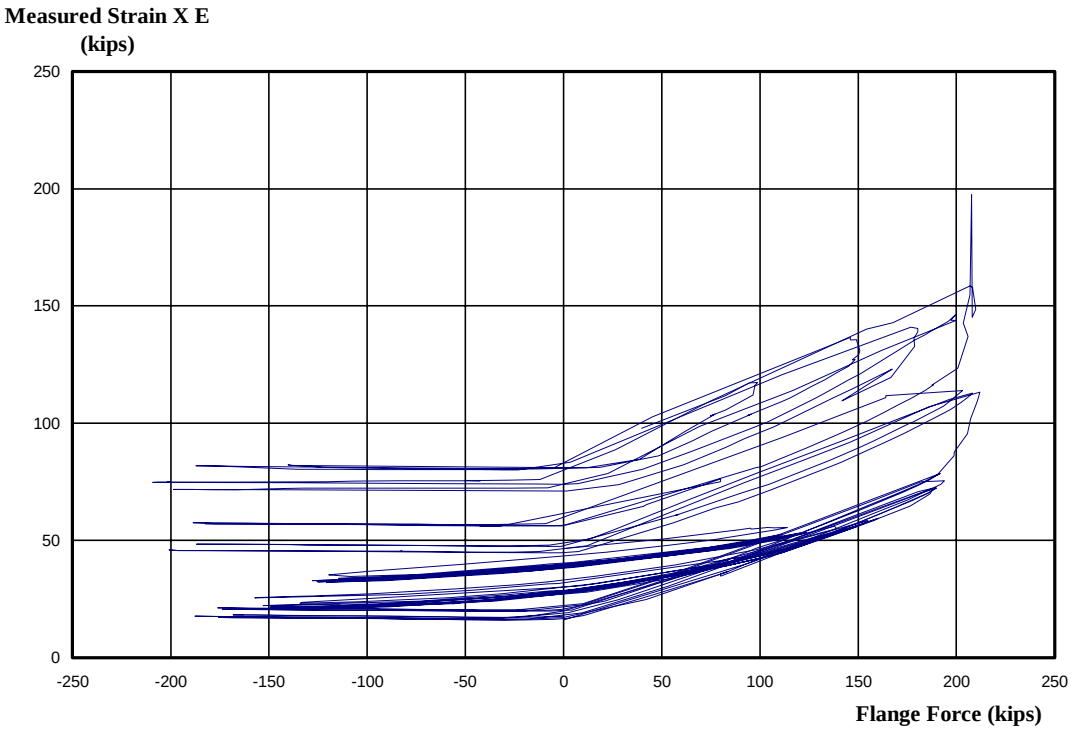

Measured Bolt Strain X E vs. Flange Force-Bolt 8
ES 1-1/2-24a Test 1

Summary
ES 1-1/2-24a
Test 2

Predicted Capacities:

Moment Strength Predicted by Yield Line Analysis, M_{pl} ……326 ft-kips
Yield Stress of End Plate, F_y……..…62.0 ksi
Moment Strength Predicted by Bolt Rupture, M_q ……282 ft-kips

Strength Results:

Maximum Moment From Test, M_u ……..473.6 ft-kips
M_{pl} / M_u……0.69
M_q / M_u…….0.59

Rotation Results:

Maximum Total Rotation…….0.034 rad
Maximum Inelastic Rotation……0.029 rad

Number of Completed Cycles……..…….27

Condition at End of Test ……..End-plate weld fractures

Failures that occurred during test:

- Local buckling of bottom flange.
- Flange-to-End-Plate weld fracture along entire length of bottom flange.
- Stiffener-to-End-Plate weld fracture.

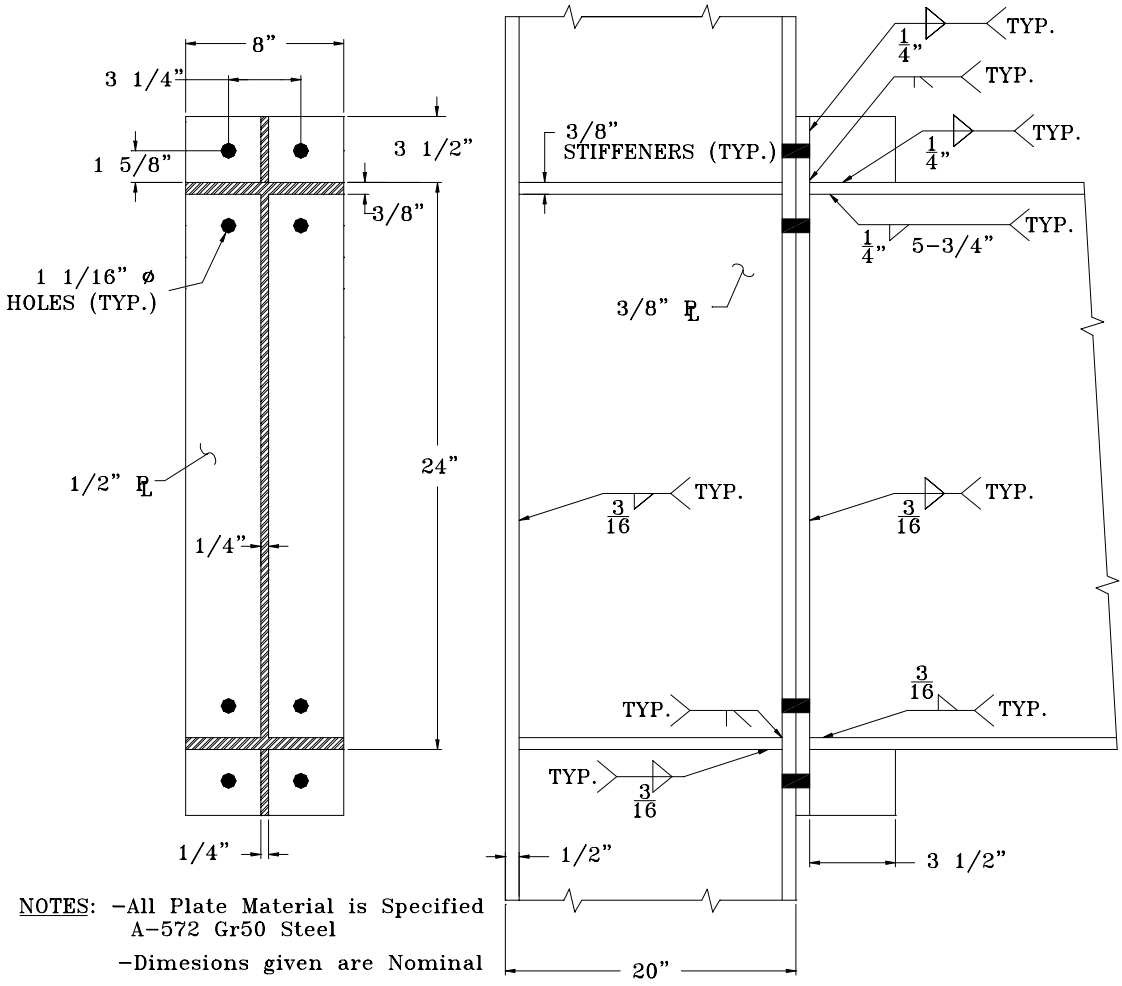

ES-1-1/2-24a Test 2 Connection Details

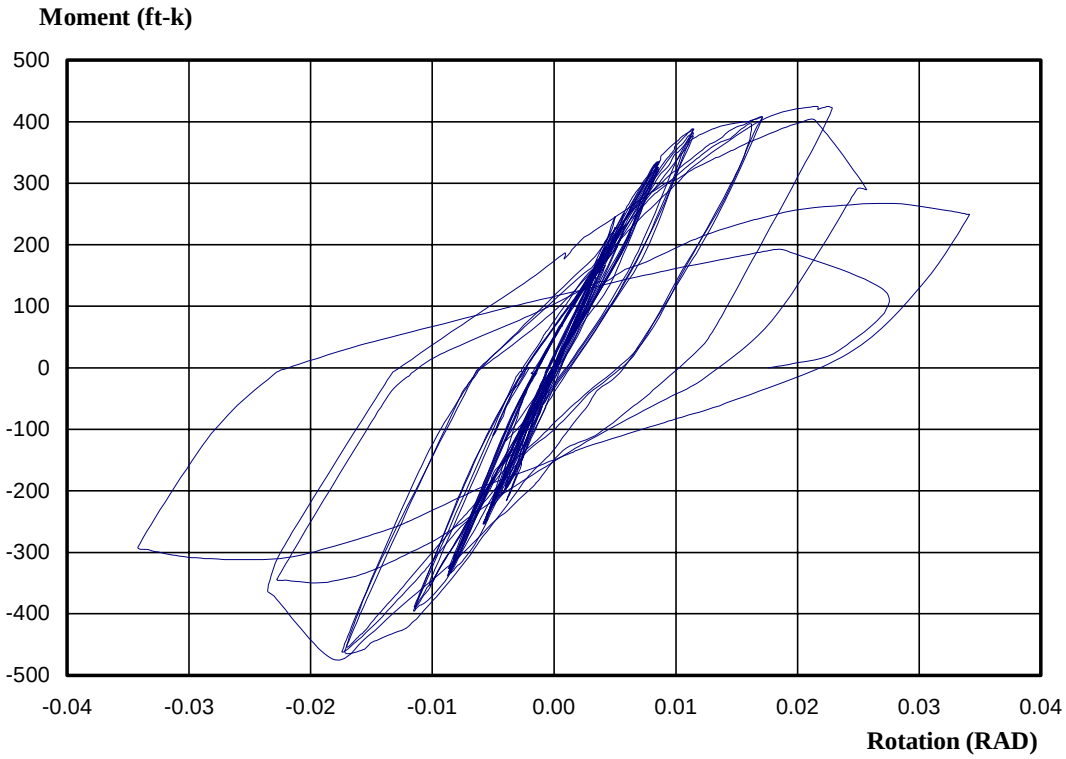

Moment vs. Total Rotation at End-Plate
ES-1-1/2-24a Test 2

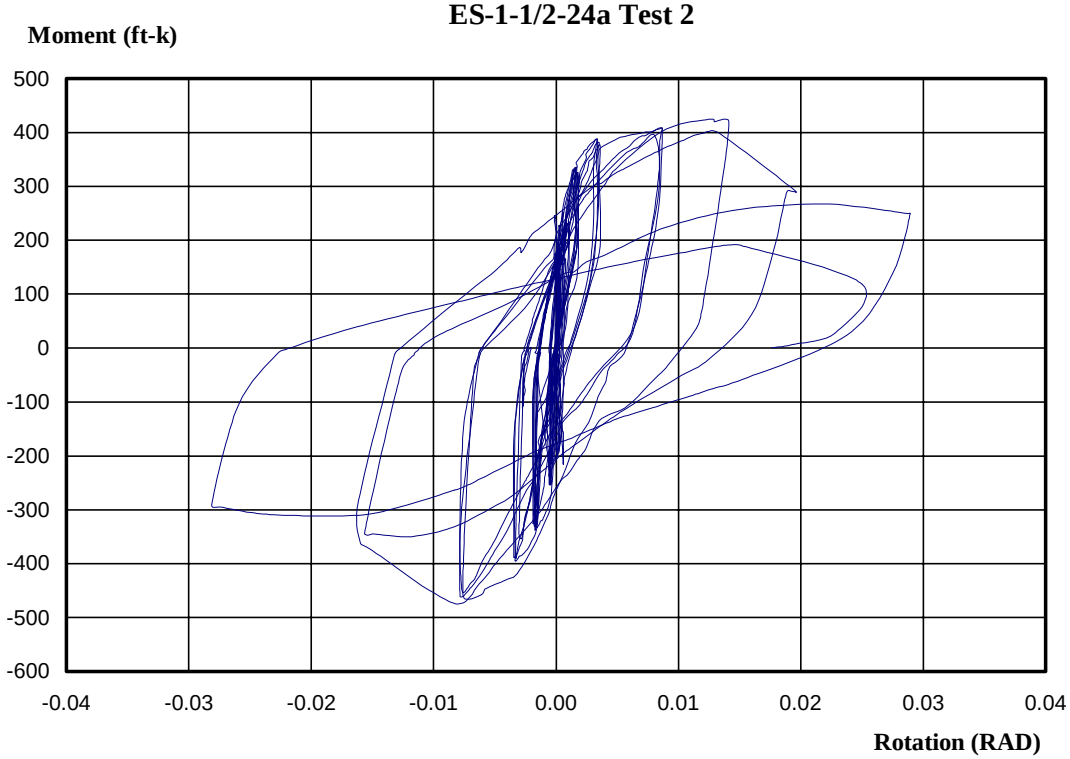

Moment vs. Inelastic Rotaton at End-Plate
ES-1-1/2-24a Test 2

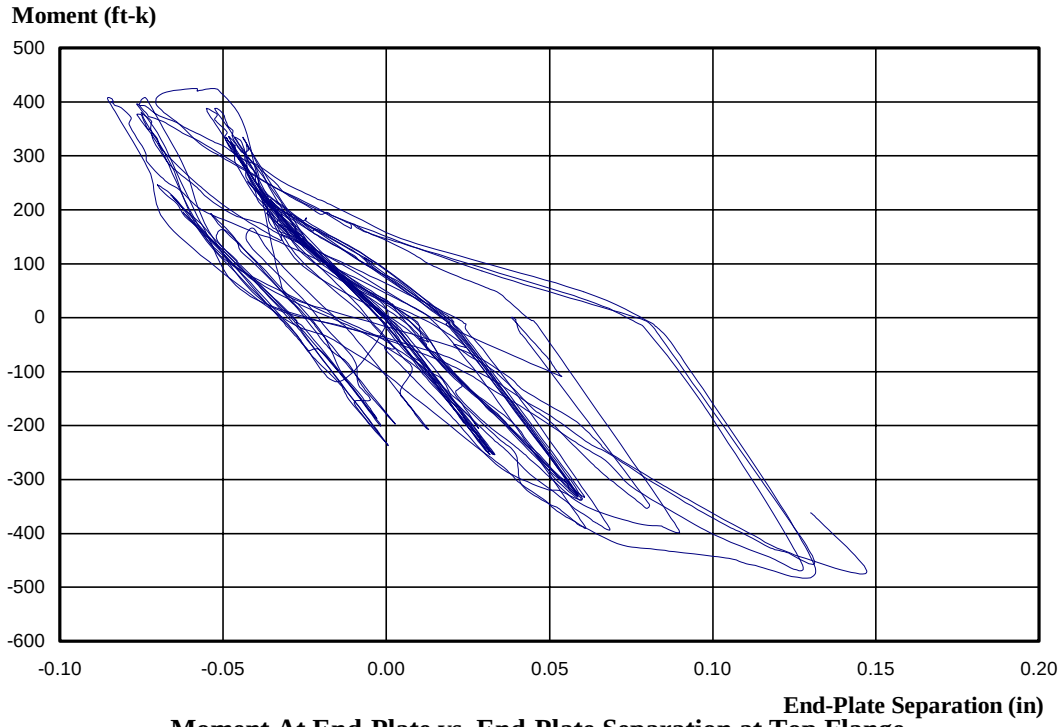

Moment At End-Plate vs. End-Plate Separation at Top Flange
ES-1-1/2-24a Test 2

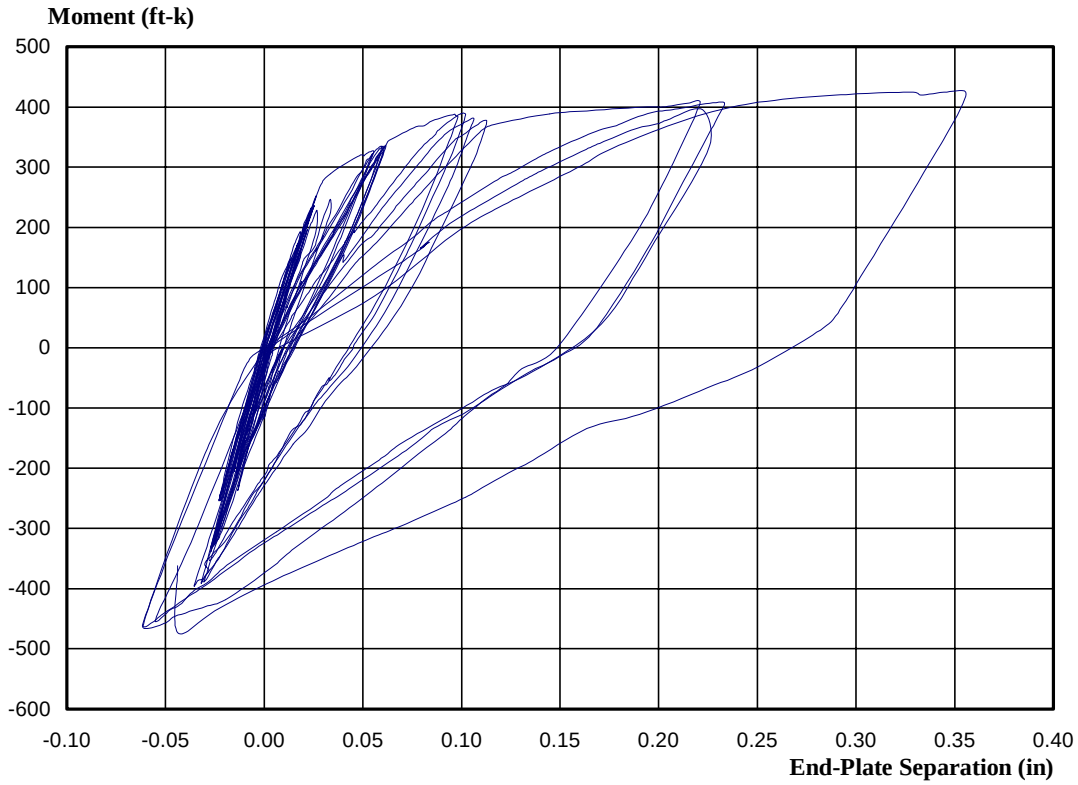

Moment At End-Plate vs. End-Plate Separation at Bottom Flange
ES-1-1/2-24a Test 2

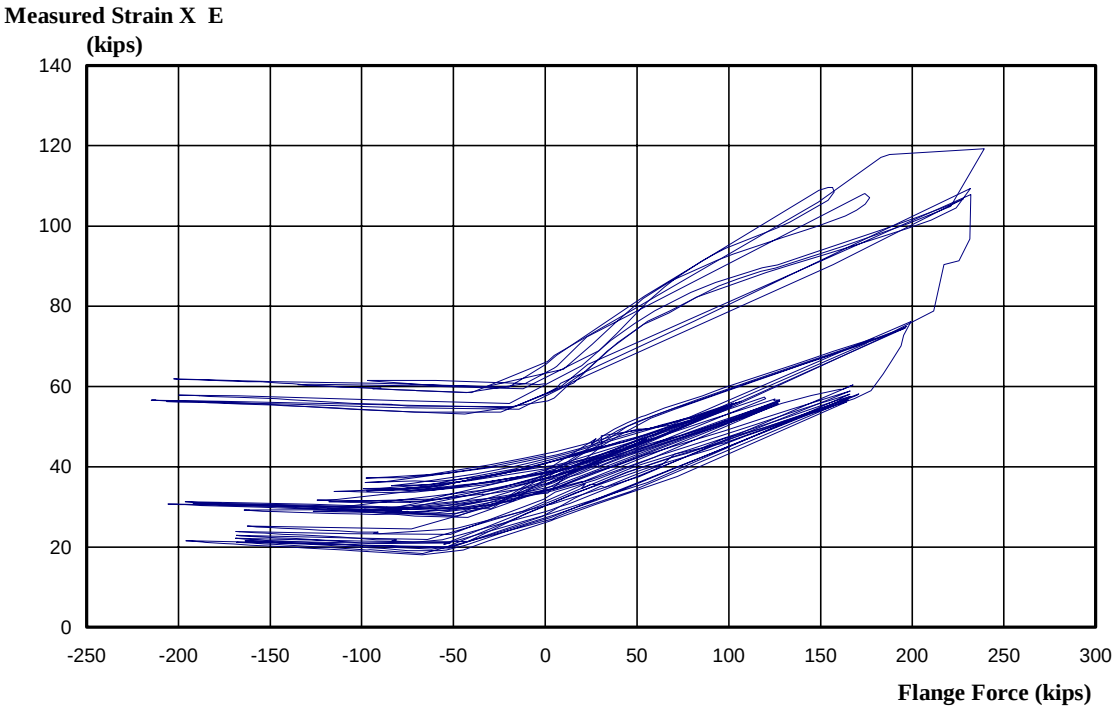

Measured Bolt Strain X E vs. Flange Force-Bolt 1
ES 1-1/2-24a Test 2

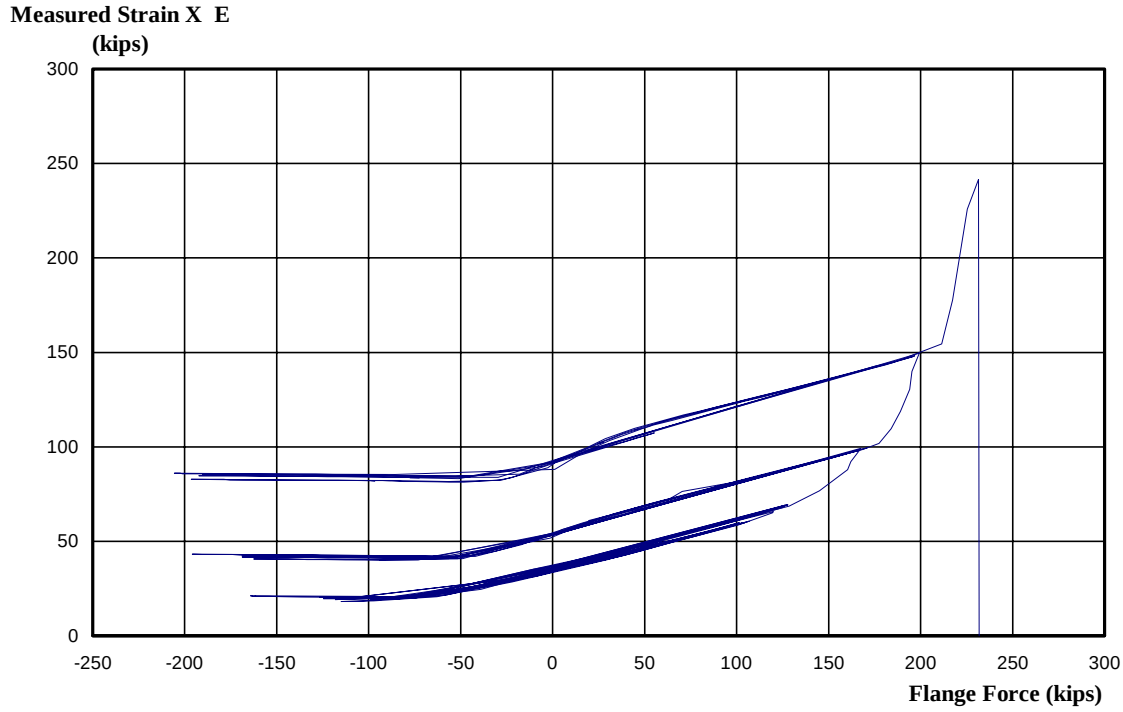

Measured Bolt Strain X E vs. Flange Force-Bolt 2
ES 1-1/2-24a Test 2

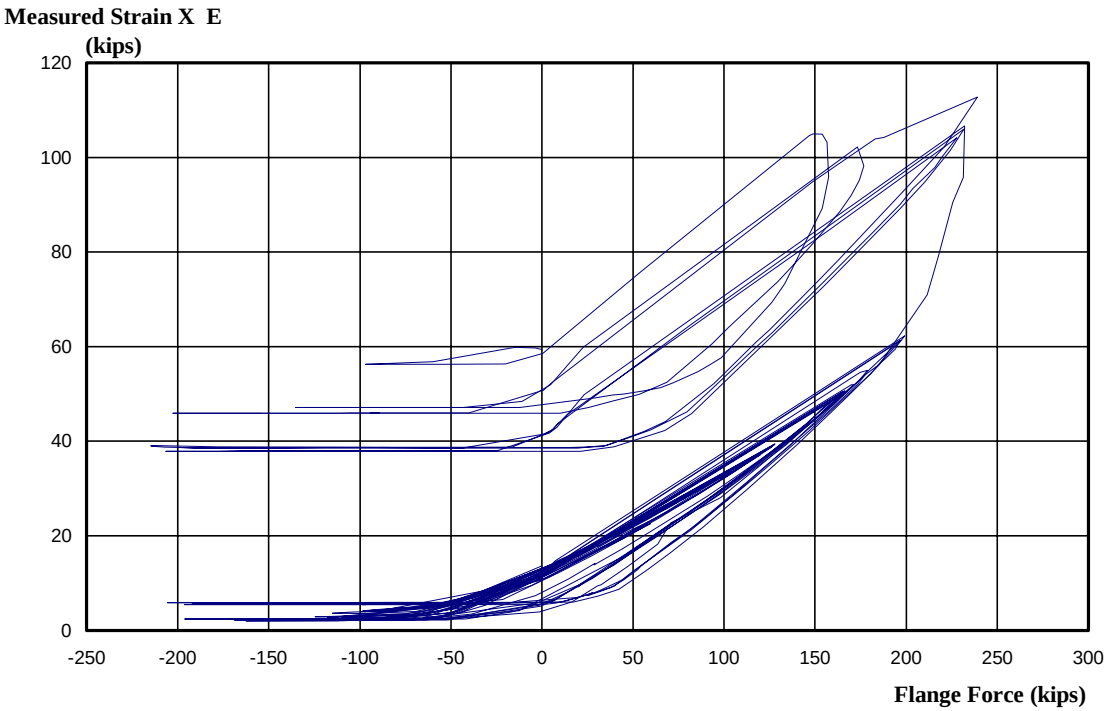

Measured Bolt Strain X E vs. Flange Force-Bolt 3
ES 1-1/2-24a Test 2

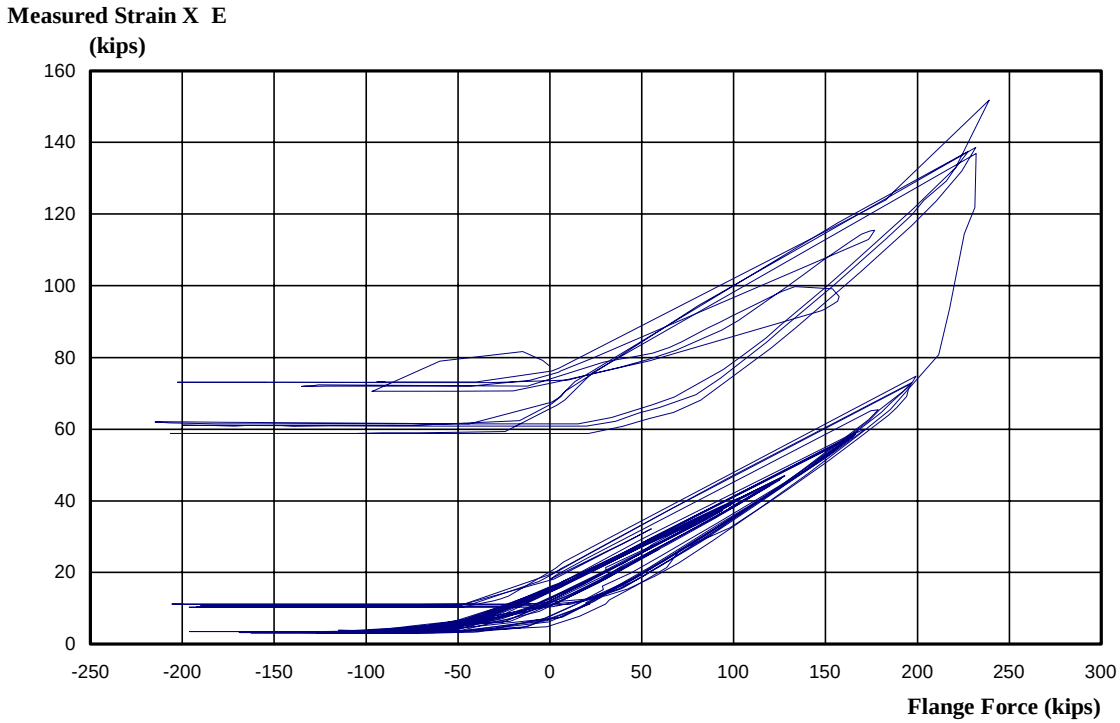

Measured Bolt Strain X E vs. Flange Force-Bolt 4
ES 1-1/2-24a Test 2

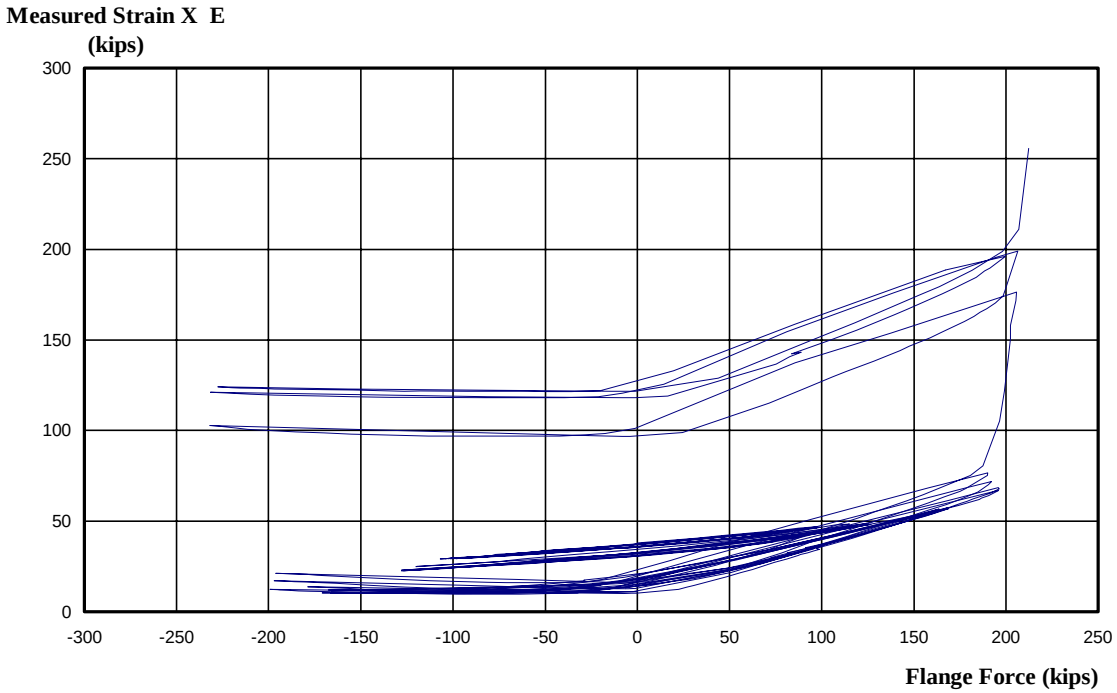

Measured Bolt Strain X E vs. Flange Force-Bolt 5

ES 1-1/2-24a Test 2

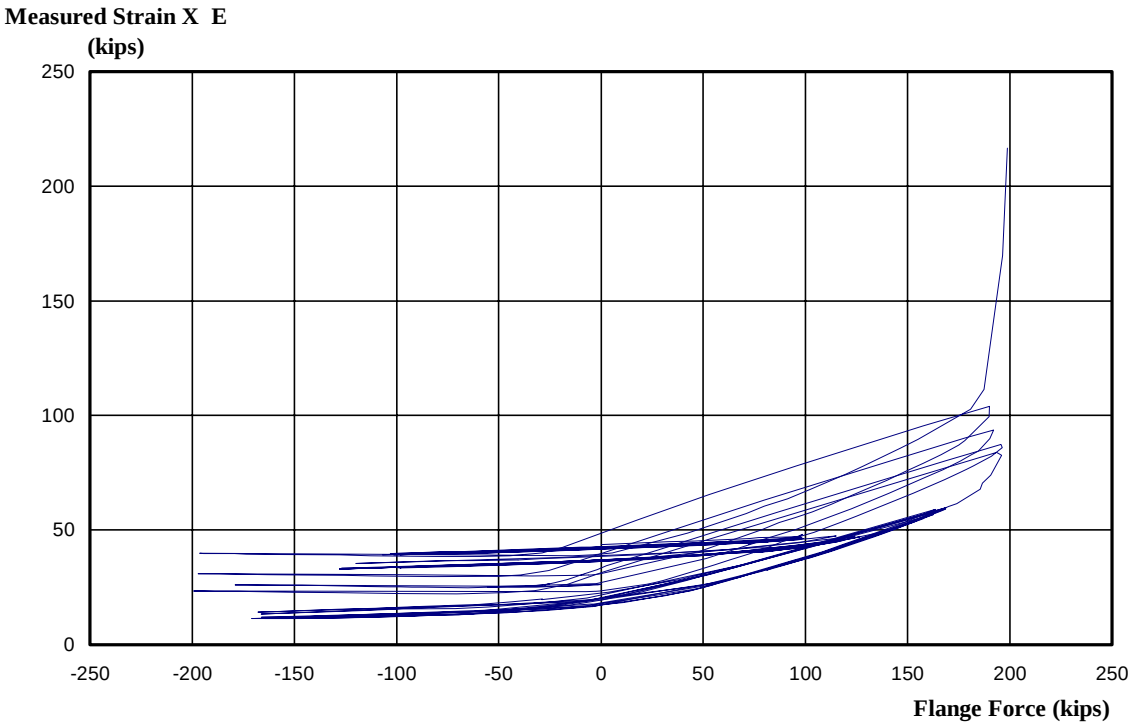

Measured Bolt Strain X E vs. Flange Force-Bolt 6

ES 1-1/2-24a Test 2

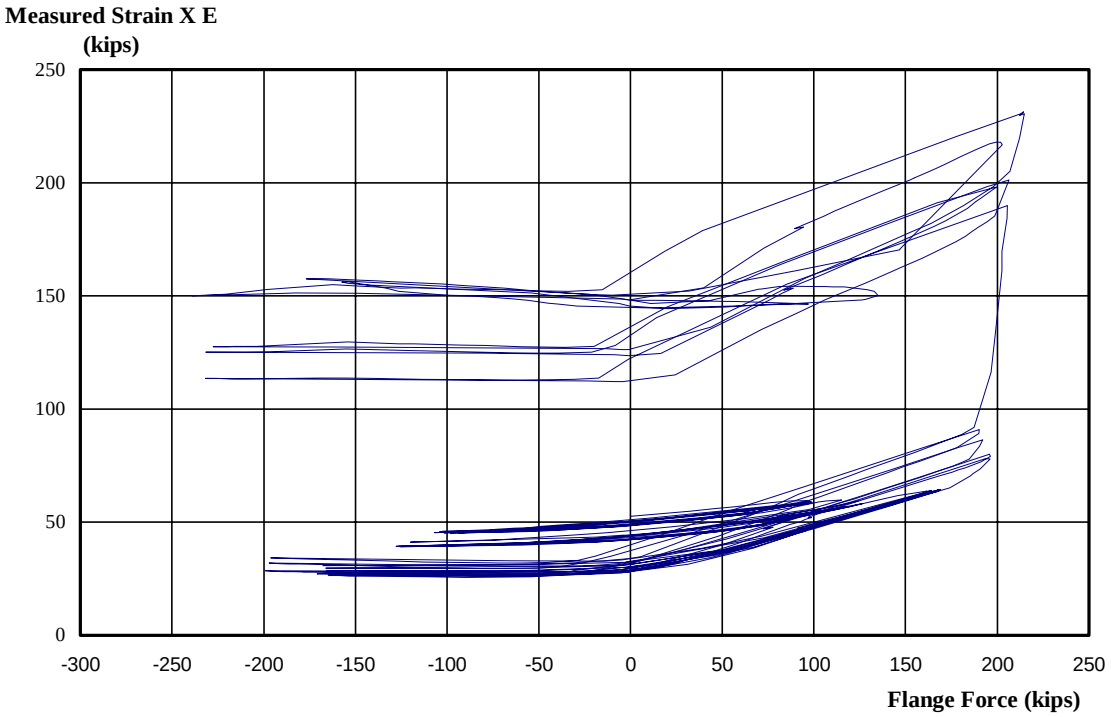

Measured Bolt Strain X E vs. Flange Force-Bolt 7
ES 1-1/2-24a Test 2

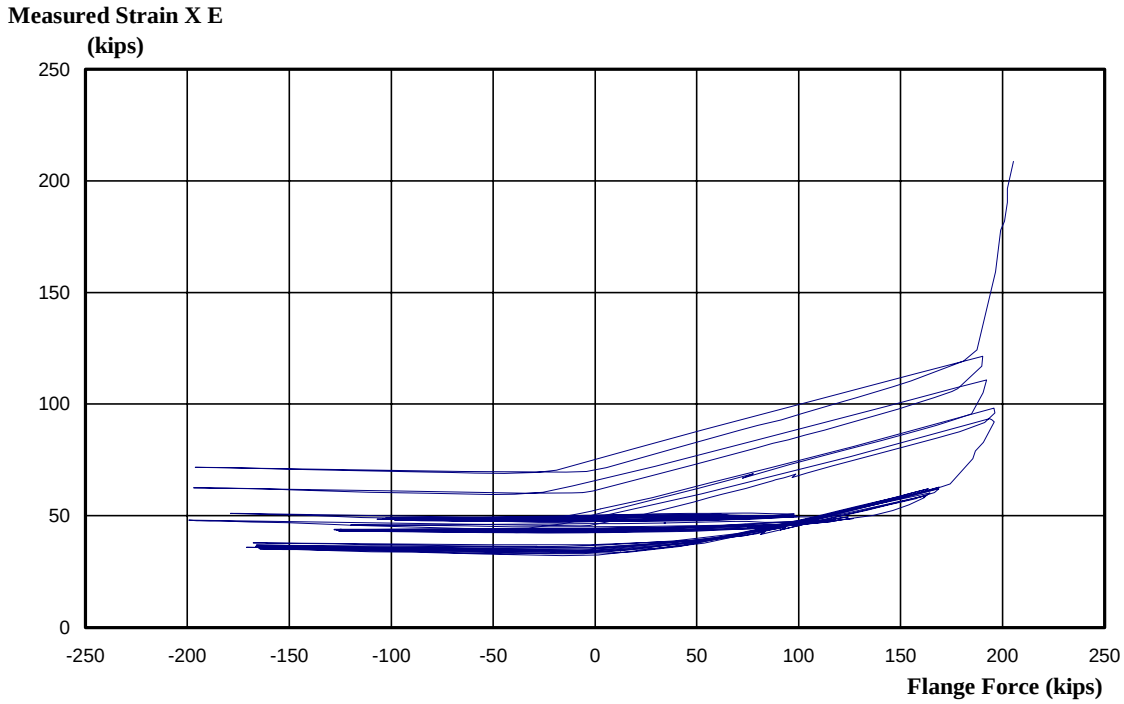

Measured Bolt Strain X E vs. Flange Force-Bolt 8
ES 1-1/2-24a Test 2

Summary
ES 1-1/2-24b
Test 2

Predicted Capacities:
Moment Strength Predicted by Yield Line Analysis, M_{pl} ……256ft-kips
Yield Stress of End Plate, F_y……..…56.0 ksi
Moment Strength Predicted by Bolt Rupture, M_q ……297 ft-kips

Strength Results:
Maximum Moment From Test, M_u ……..457.6 ft-kips
M_{pl} / M_u……0.56
M_q / M_u…….0.64

Rotation Results:
Maximum Total Rotation…….0.022 rad
Maximum Inelastic Rotation……0.012 rad

Number of Completed Cycles…….…….26

Condition at End of Test……..End-plate fractures

Failures that occurred during test:

- Fracture of end-plate at the stiffener-to-end-plate interface, both flanges.

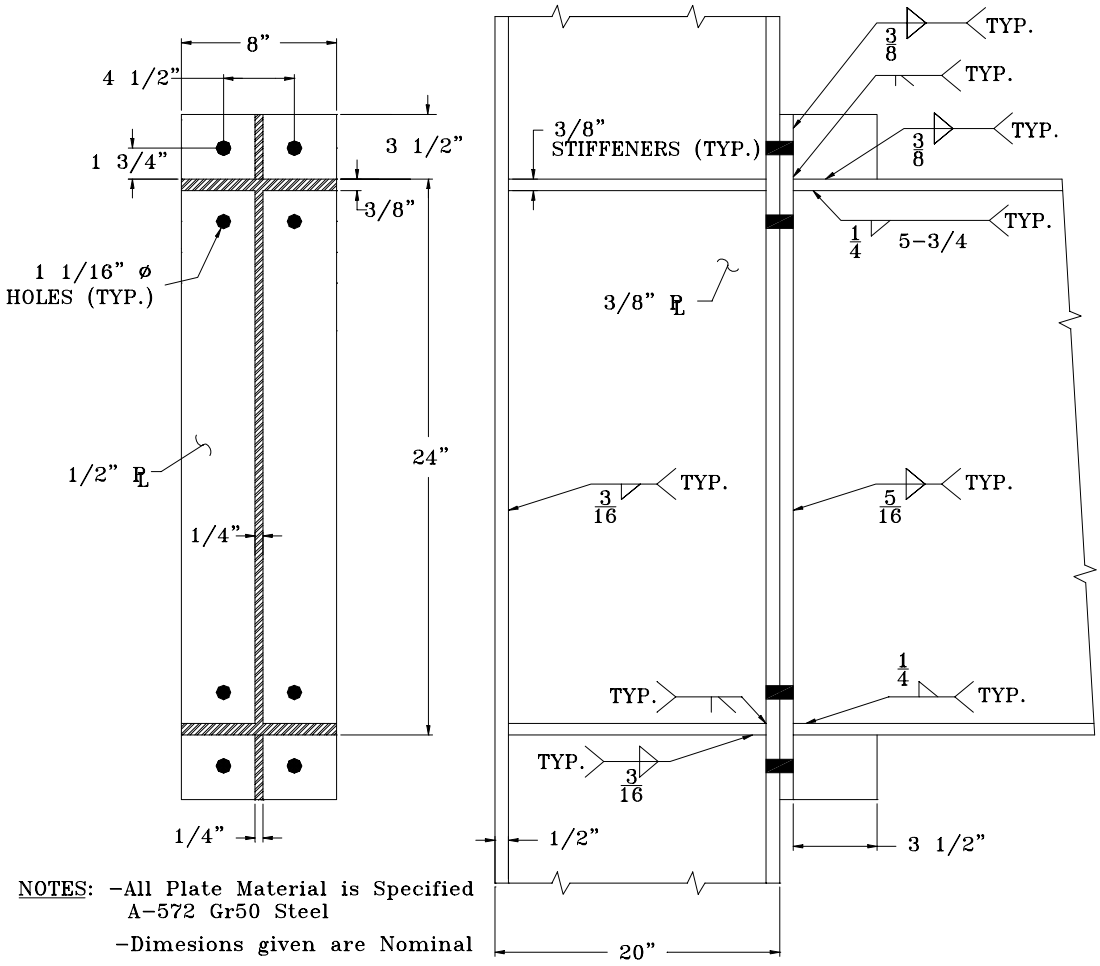

ES-1-1/2-24b Connection Details

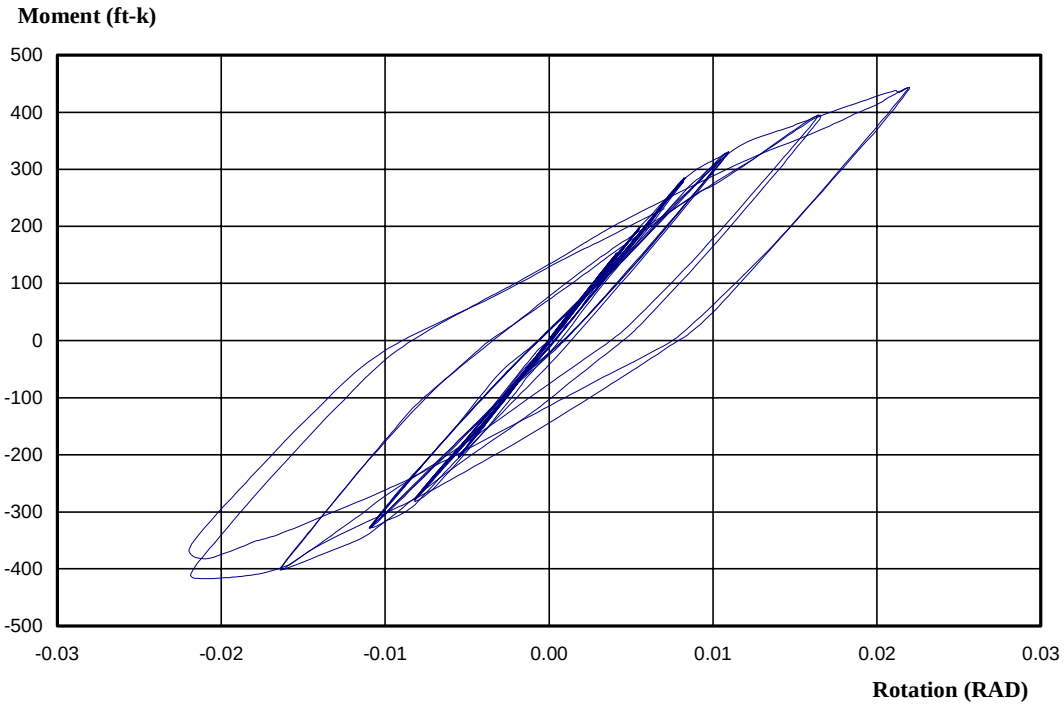

Moment At End-Plate vs. Total Rotation at End-Plate
ES-1-1/2-24b

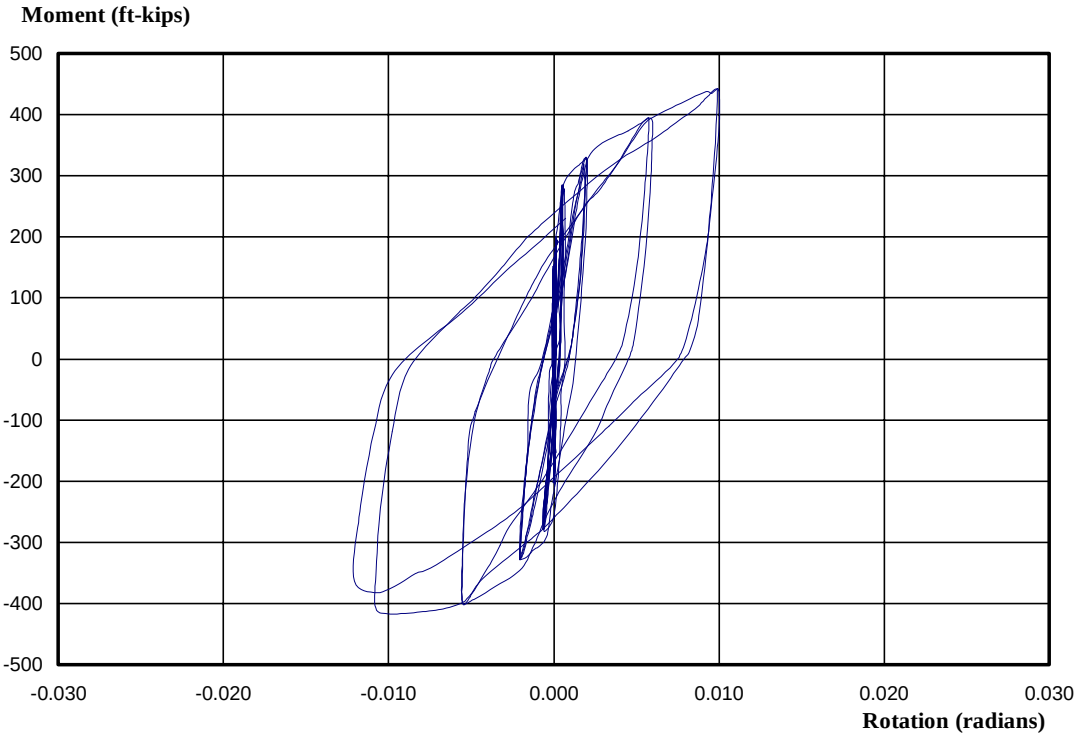

Moment At End-Plate vs. Inelastic Rotation at End-Plate
ES-1-1/2-24b

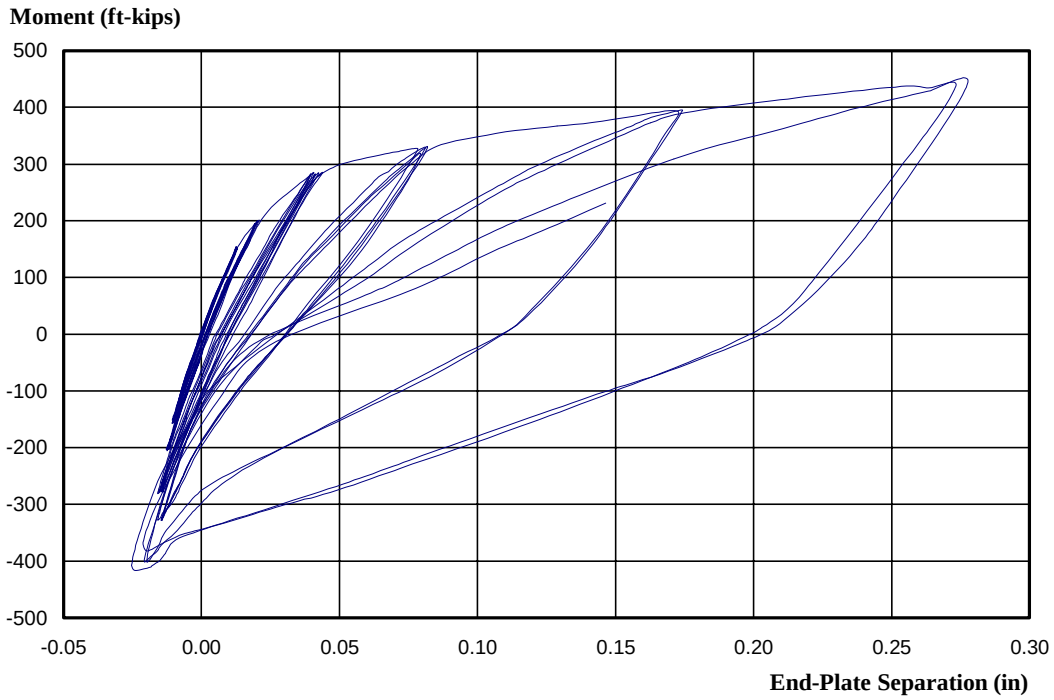

Moment At End-Plate vs. End-Plate Separation at Top Flange
ES-1-1/2-24b

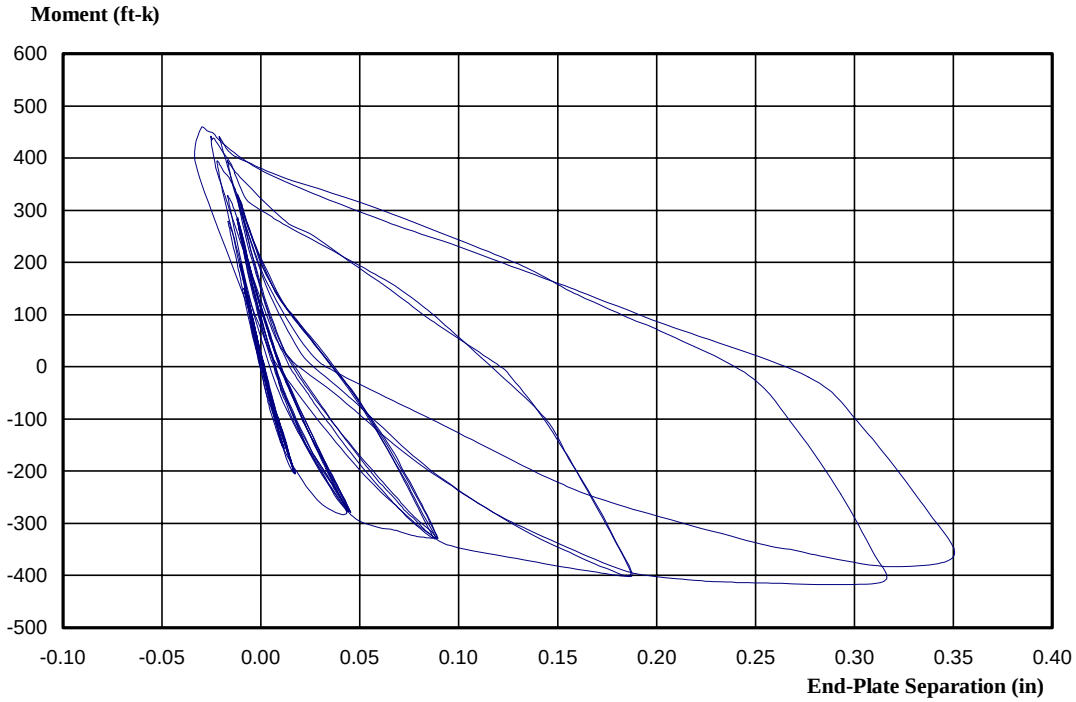

Moment At End-Plate vs. End-Plate Separation at Bottom Flange
ES-1-1/2-24b

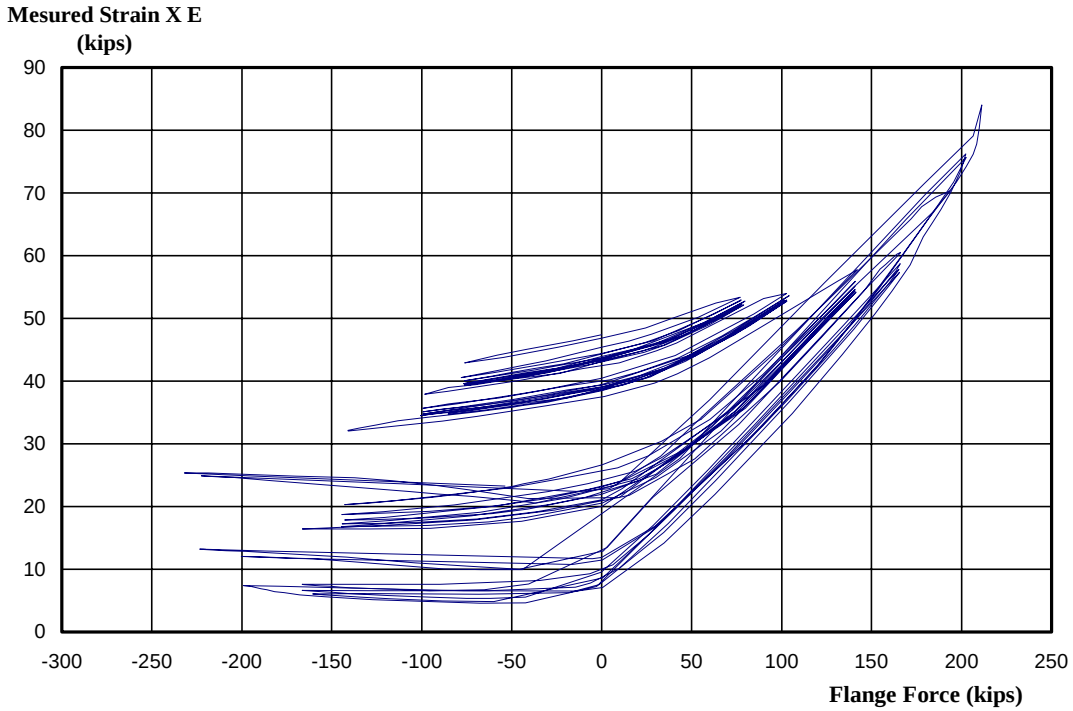

Measured Bolt Strain X E vs. Flange Force-Bolt 1
ES 1-1/2-24b

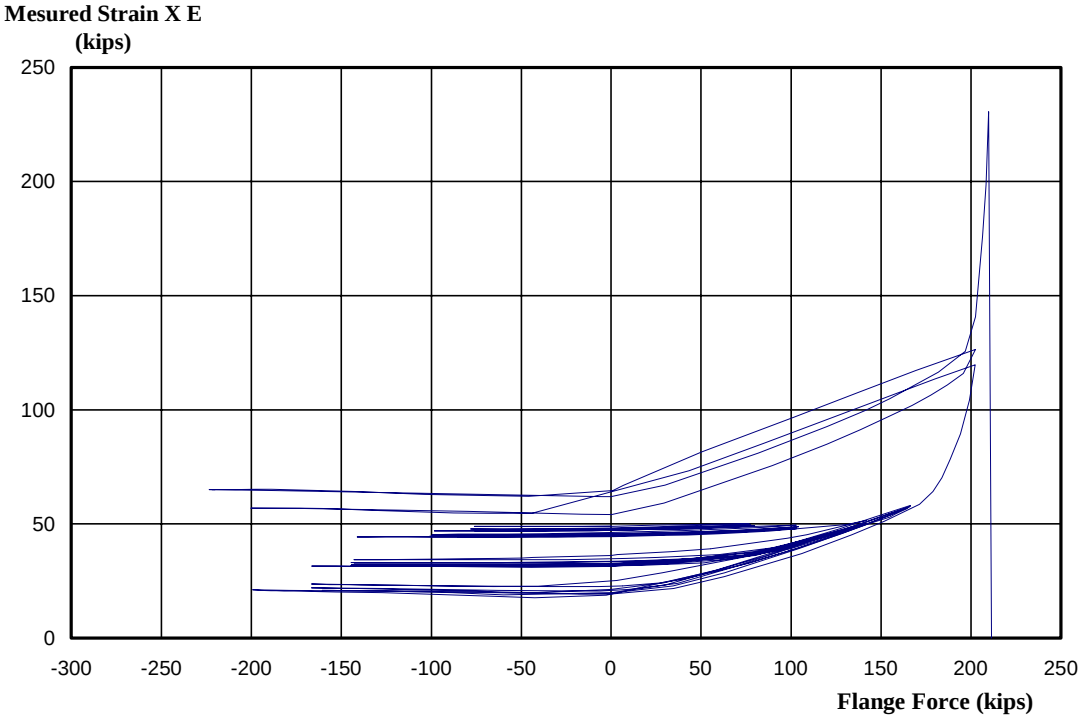

Measured Bolt Strain X E vs. Flange Force-Bolt 3
ES 1-1/2-24b

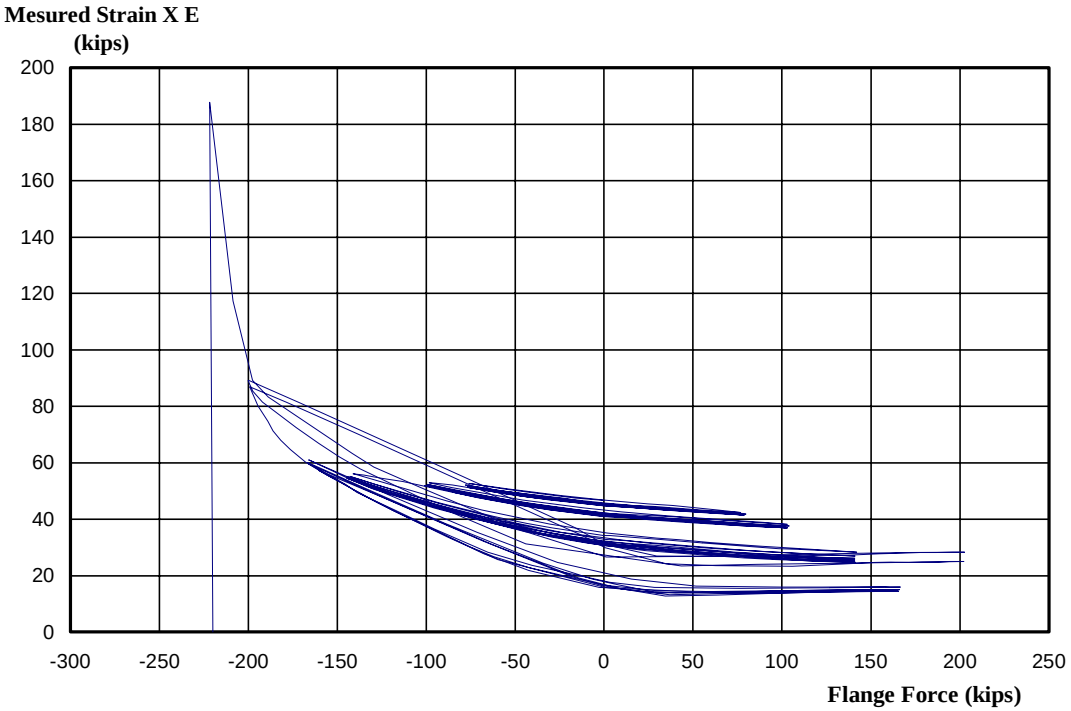

Measured Bolt Strain X E vs. Flange Force-Bolt 5
ES 1-1/2-24b

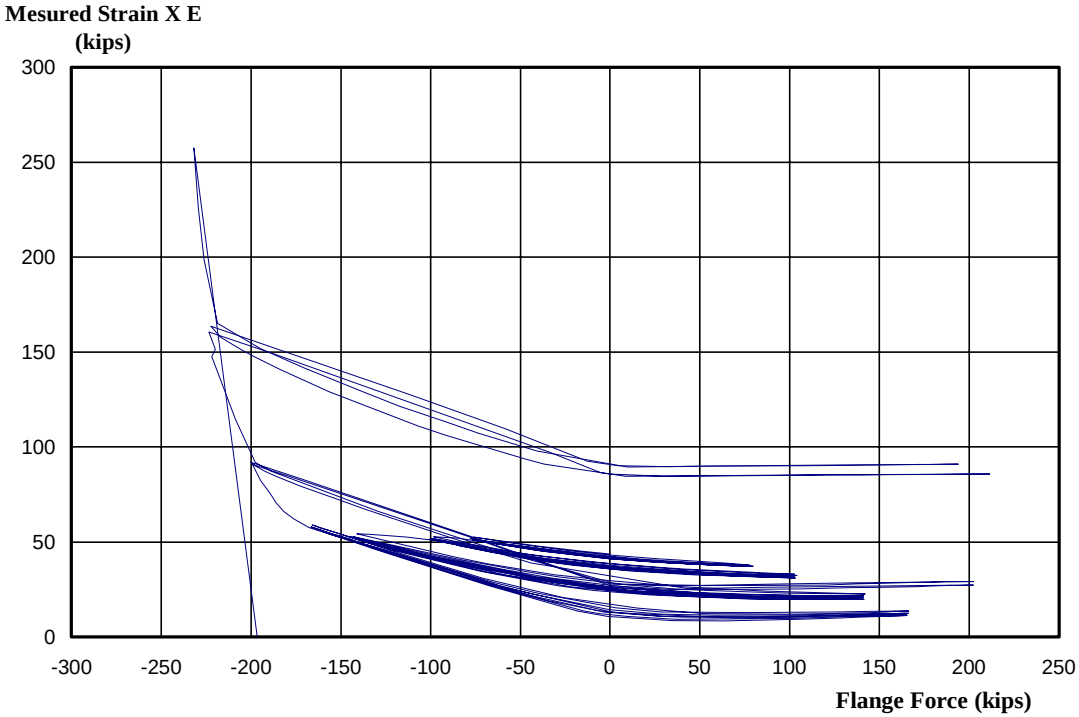

Measured Bolt Strain X E vs. Flange Force-Bolt 7
ES 1-1/2-24b

APPENDIX C

MULTIPLE ROW 1/3 EXTENDED RESULTS AND TEST DATA

Summary
MRE1/3-7/8-5/8-55
Test 1

Predicted Capacities:

Moment Strength Predicted by Yield Line Analysis, M_{pl}……1206 ft-kips

Yield Stress of End Plate, F_y……...60.4 ksi

Moment Strength Predicted by Bolt Rupture, M_q……1358 ft-kips

Strength Results:

Maximum Moment From Test, M_u……..1523 ft-kips

M_{pl} / M_u……0.79

M_q / M_u……0.89

Rotation Results:

Maximum Total Rotation…….0.0129 rad

Maximum Inelastic Rotation……0.0034 rad

Number of Completed Cycles……..…….22

Condition at End of Test……..Bolt Rupture(Bolt #4)

List of Significant Observations During Testing:

- During the first load step (Max Rotation =0.00375 rad) six cycles were completed. The Load vs. Displacement plot remained linear, and the specimen remained in the elastic region of stress. The specimen was observed after the sixth cycle. The white wash indicated no yielding of the specimen.
- During the second load step (Max Rotation = 0.005 rad) six cycles were completed. The observations made were identical to those stated above.
- Six cycles were also completed at the third load step (Max Rotation = 0.0075 rad).
- At the fourth load step (Max Rotation = 0.01 rad) four cycles were completed. Because of various problems with testing equipment during this load step, up to six full cycles at the first load step were done to correct the problems and check the parameters of testing.
- On the first cycle of the fifth load step, additional problems were encountered with the load cell at 140 kips. The data taken during the quarter cycle leading up to the

load cell failure were omitted. Four weeks later, the specimen was loaded again. Bolt rupture occurred at 0.0129 rad rotation. A small amount of end-plate yielding was observed at the outside of the flanges, as well as around the inside bolts. The test was terminated at this point.

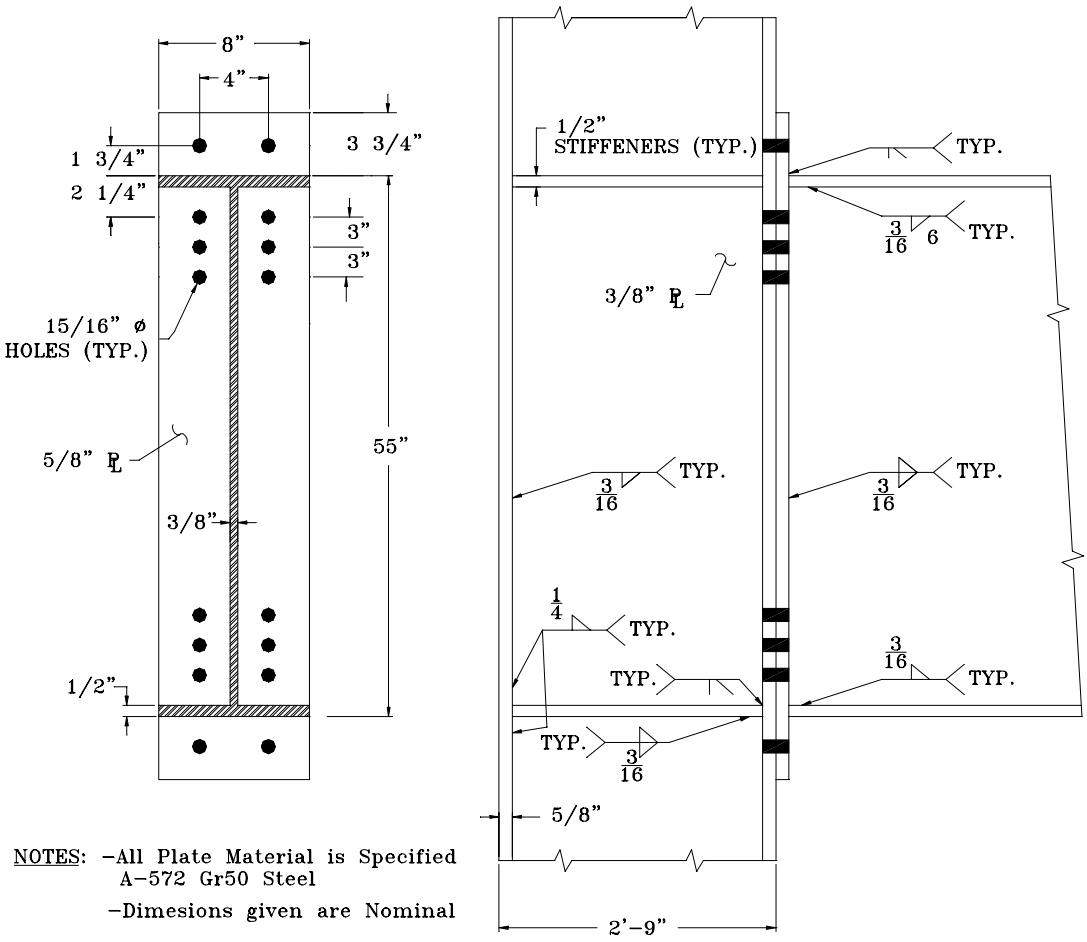

MRE1/3-7/8-5/8-55 Test 1 Connection Details

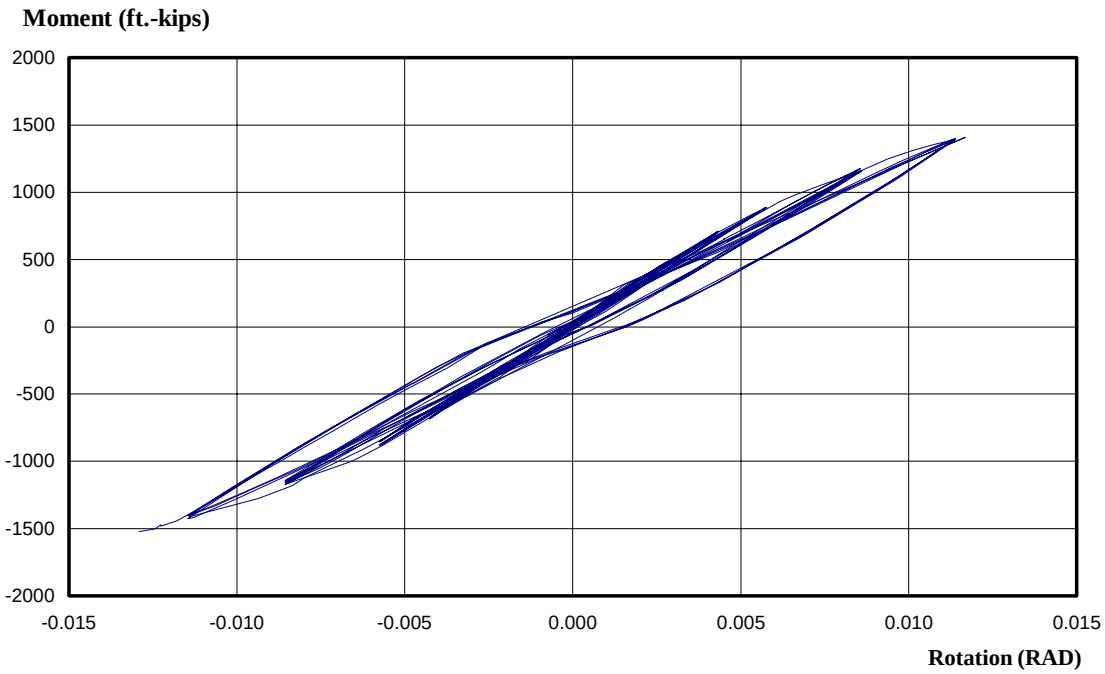

Moment vs. Total Rotation at End Plate
MRE1/3-7/8-5/8-55 Test 1

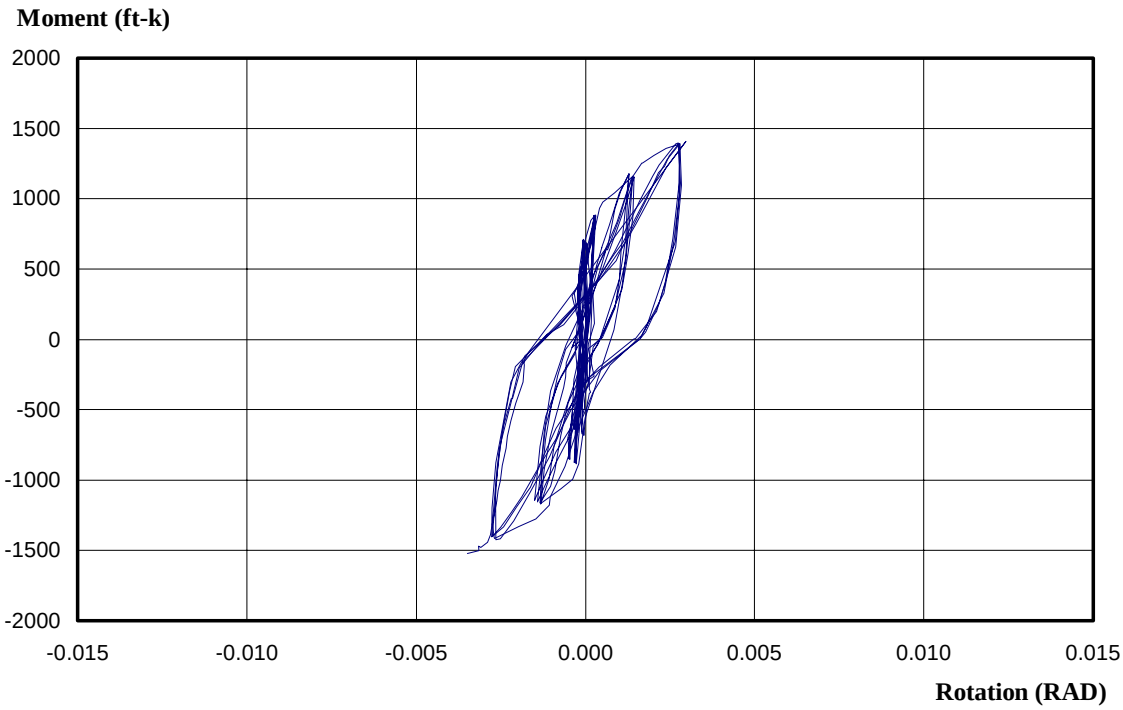

Moment at End Plate vs. Inelastic Rotation at End-Plate
MRE1/3-7/8-5/8-55 Test 1

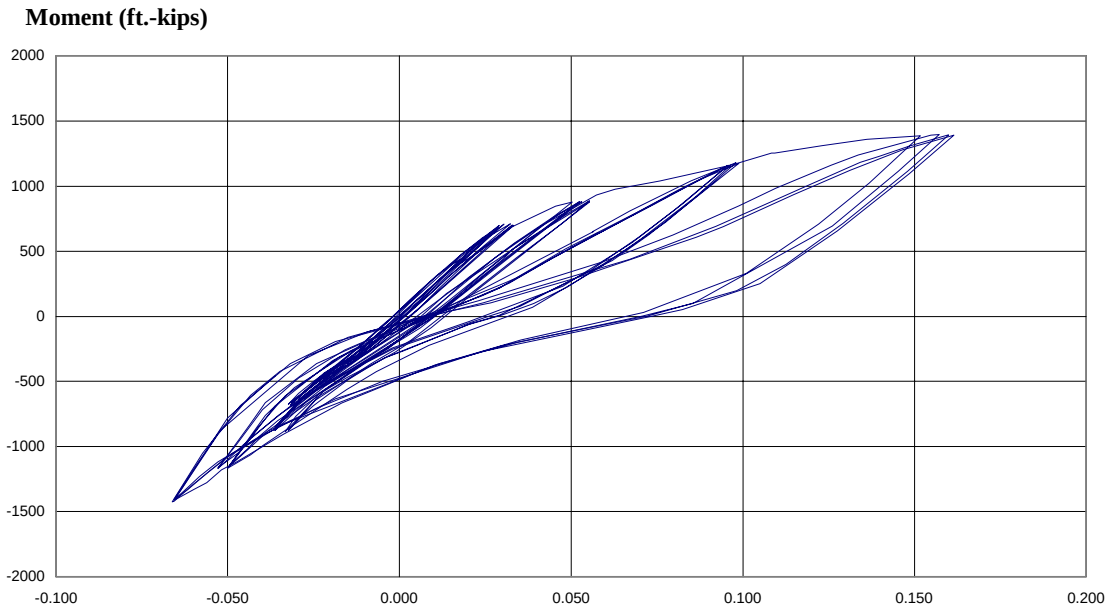

Moment at End-Plate vs. End-Plate Separation at Top Flange
MRE1/3-7/8-5/8-55-Test 1

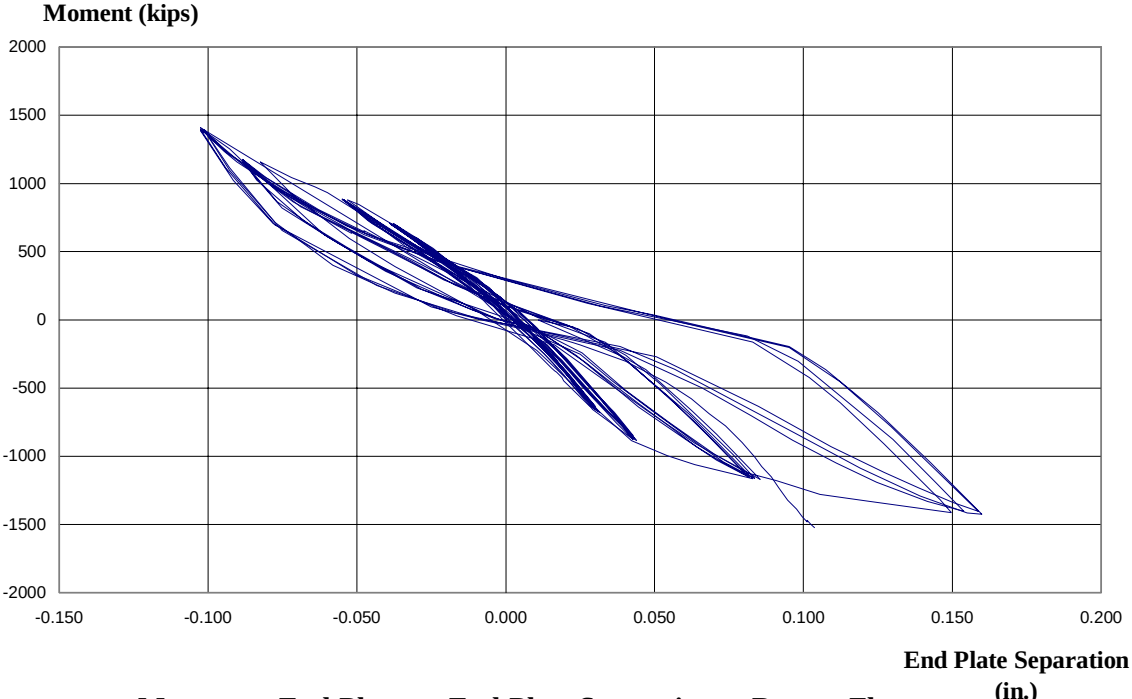

Moment at End-Plate vs. End-Plate Separation at Bottom Flange
MRE1/3-7/8-5/8-55-Test 1

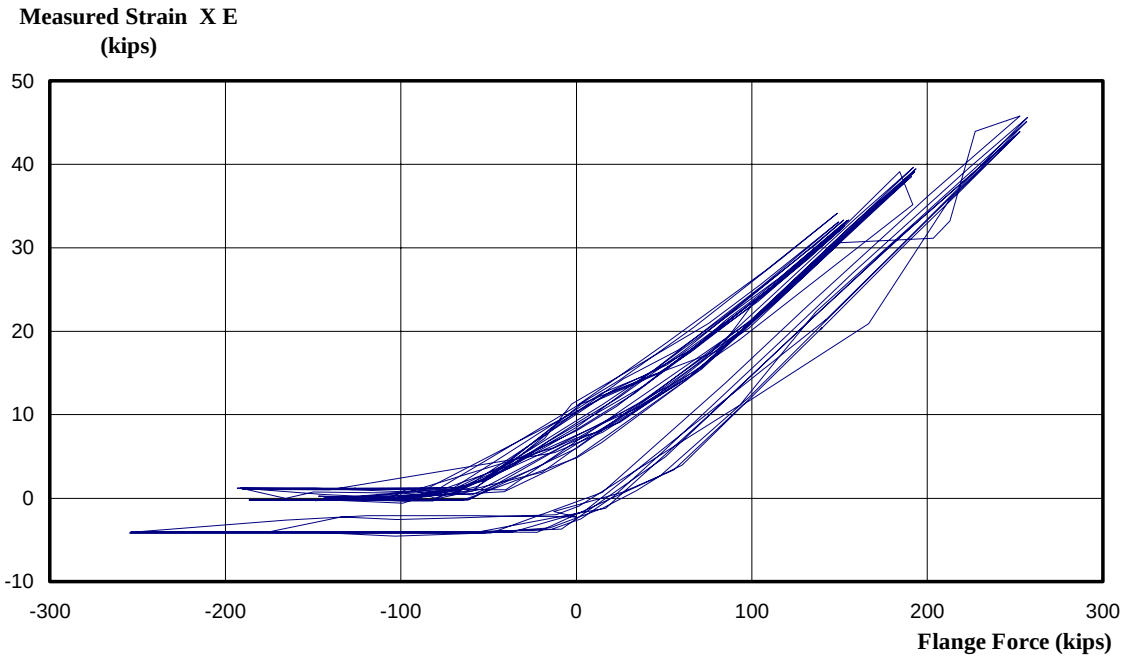

Measured Strain X E vs. Flange Force -Bolt 1
MRE1/3-7/8-5/8-55 Test 1

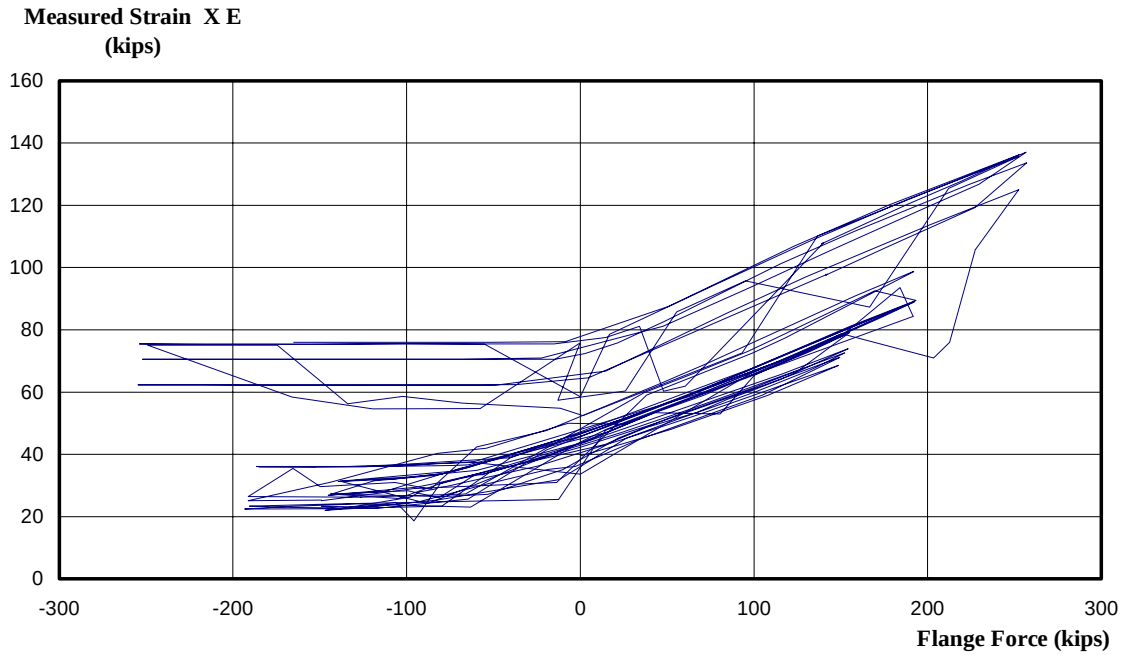

Measured Strain X E vs. Flange Force -Bolt 4
MRE1/3-7/8-5/8-55 Test 1

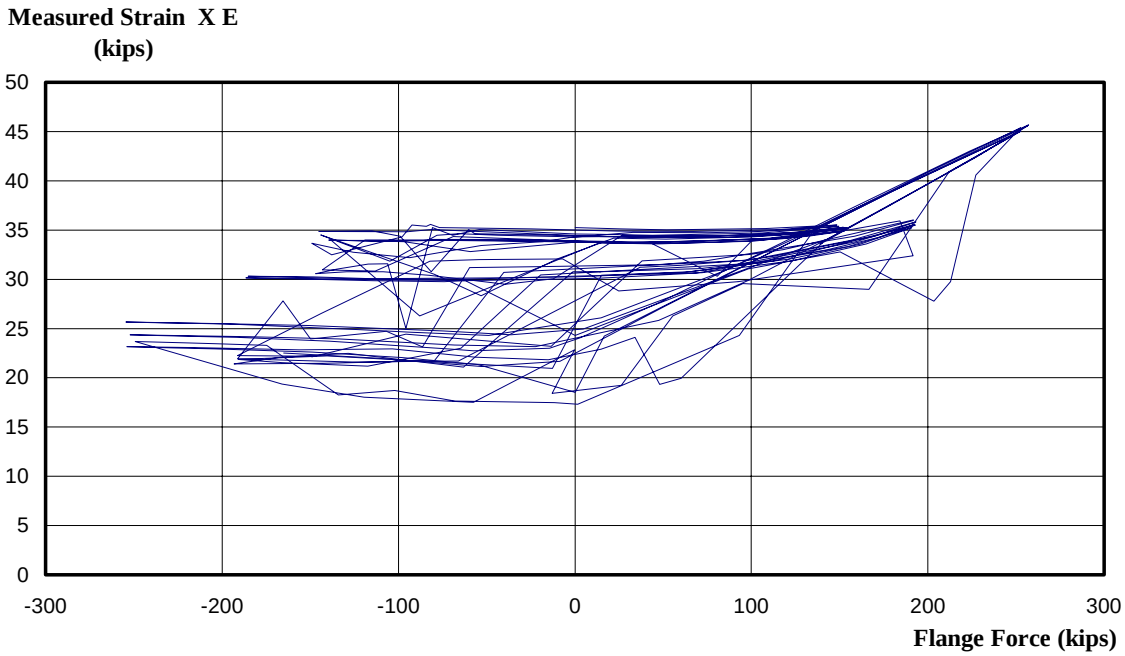

Measured Strain X E vs. Flange Force -Bolt 5
MRE1/3-7/8-5/8-55 Test 1

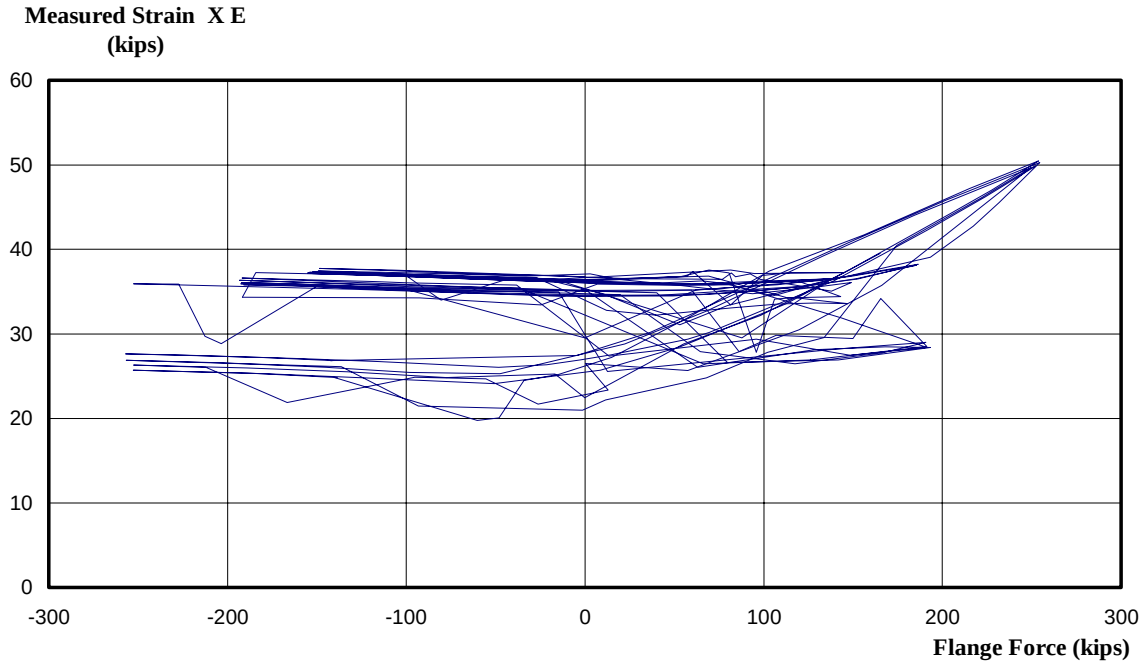

Measured Strain X E vs. Flange Force -Bolt 12
MRE1/3-7/8-5/8-55 Test 1

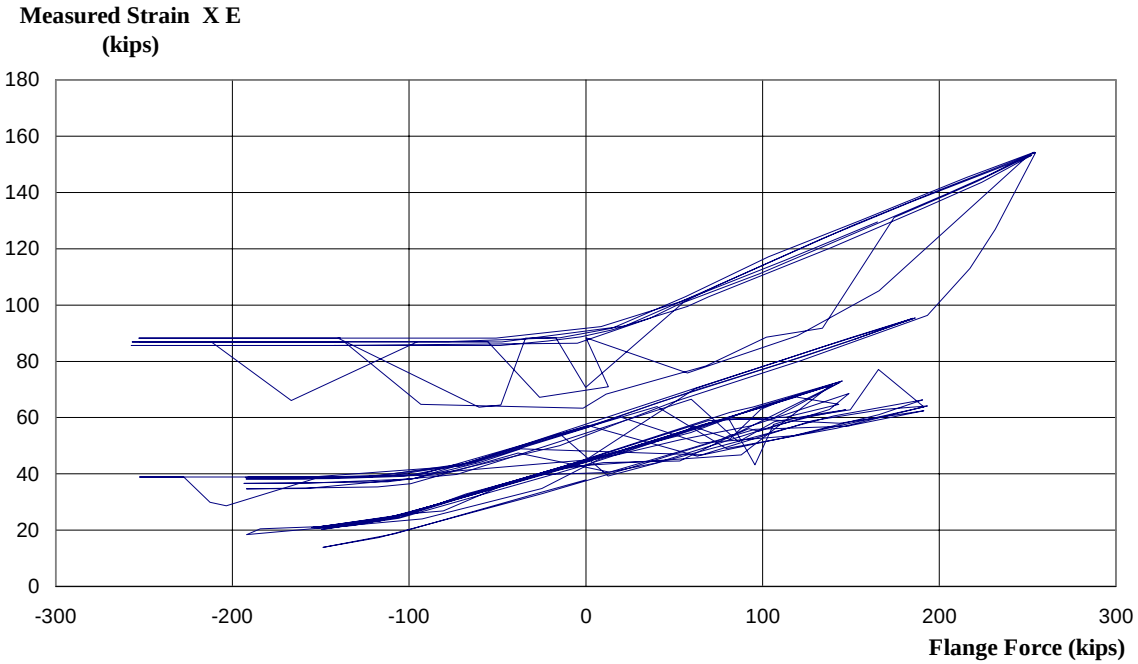

Measured Strain X E vs. Flange Force -Bolt 13
MRE1/3-7/8-5/8-55 Test 1

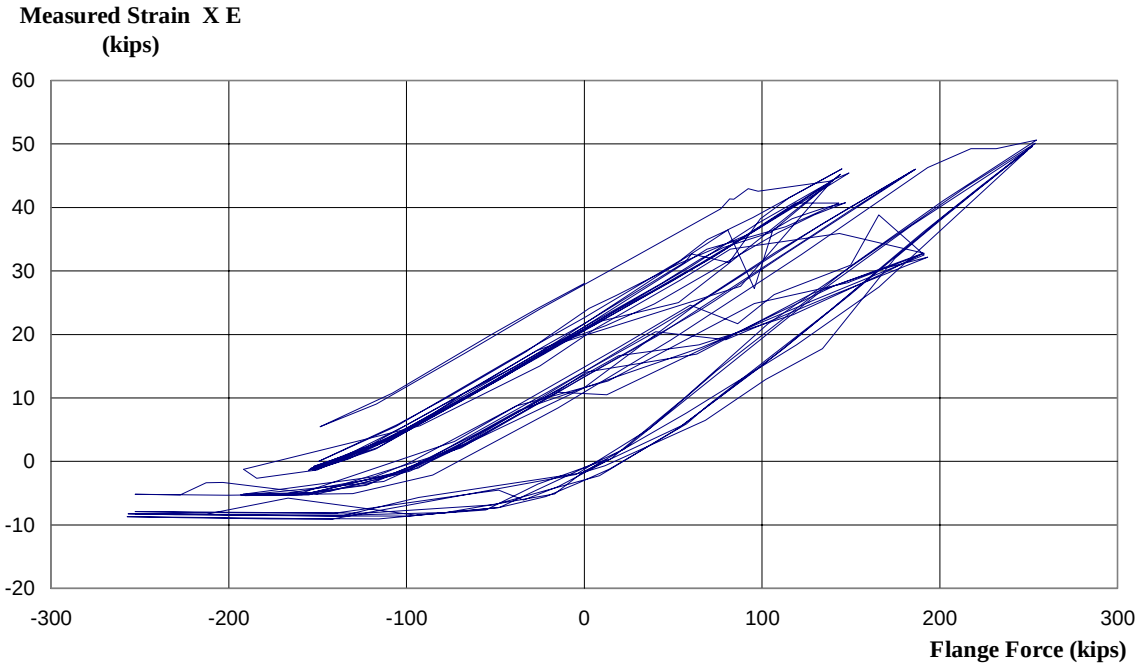

Measured Strain X E vs. Flange Force -Bolt 16
MRE1/3-7/8-5/8-55 Test 1

Summary
MRE1/3-7/8-5/8-55- Test 2

Predicted Capacities:

Moment Strength Predicted by Yield Line Analysis, M_{pl}……..1221 ft-kips

Yield Stress of End Plate, F_y……..…62.0 ksi

Moment Strength Predicted by Bolt Rupture, M_q ……1354 ft-kips

Strength Results:

Maximum Moment From Test, M_u ……..1720 ft-kips

M_{pl} / M_u…….0.71

M_q / M_u……..0.79

Rotation Results:

Maximum Total Rotation……..0.0145 rad

Maximum Inelastic Rotation…….0.0015 rad

Number of Completed Cycles…….…….22

Condition at End of Test..……..Bolt Rupture (Bolt #4)

List of Significant Observations During Testing:

- During the first load step (Max Rotation =0.00375 rad) six cycles were completed. The Load vs. Displacement plot remained linear, and the specimen remained in the elastic region of stress. The specimen was observed after the sixth cycle. The white wash indicated no yielding of the specimen.
- During the second load step (Max Rotation = 0.005 rad) six cycles were completed. The observations made were identical to those stated above. 1/8 inch separation of end-plate from column flange at the girder flange was observed at zero load.
- Six cycles were also completed at the third load step (Max Rotation = 0.0075 rad). White wash at the top side of the connection indicated slight yielding.
- At the fourth load step (Max Rotation = 0.01 rad) four cycles were completed. Greater yielding was seen at both ends of connection on end-plate, outside and inside of the girder flanges.
- On the first cycle of the fifth load step (Max Rotation = 0.015 rad). Bolt rupture occurred at 0.0145 rad rotation. A small amount of end-plate yielding was observed at the outside of the flanges, as well as around the inside bolts. The test

was terminated at this point.

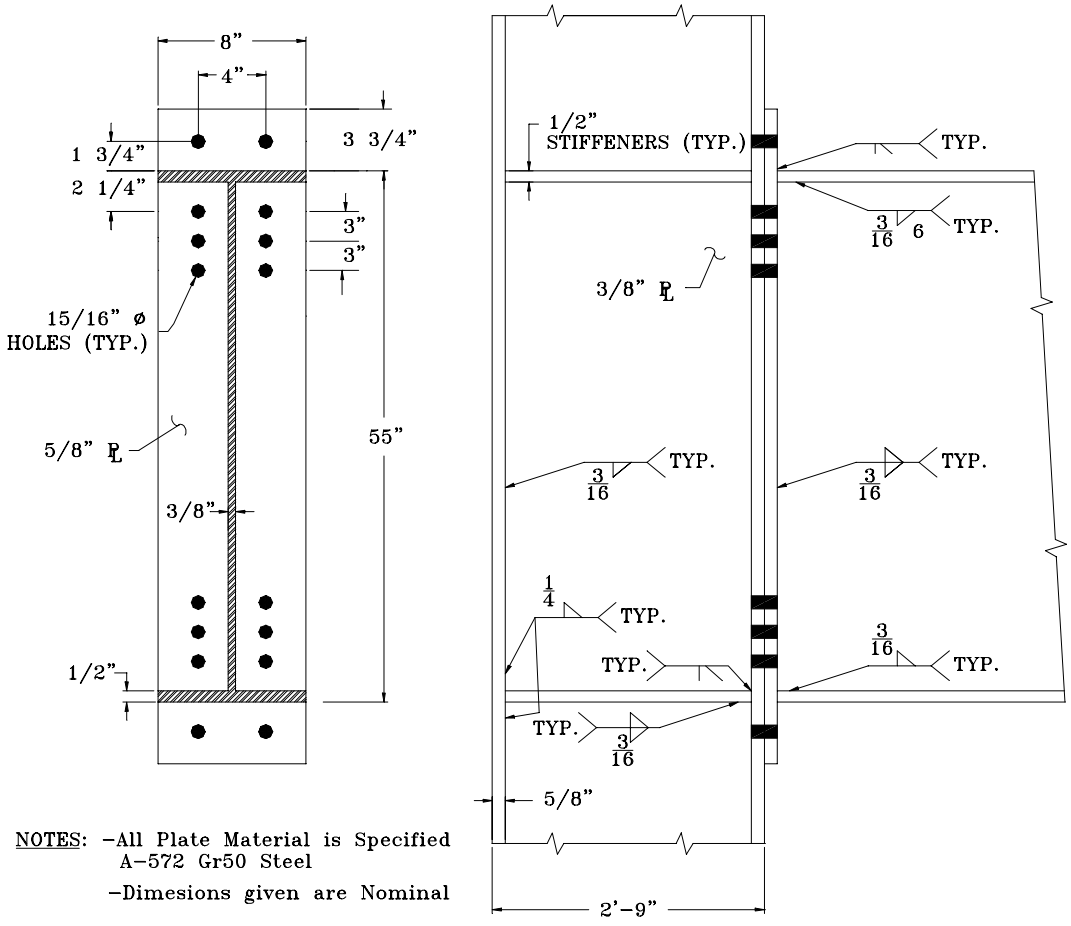

MRE1/3-7/8-5/8-55 Test 2 Connection Details

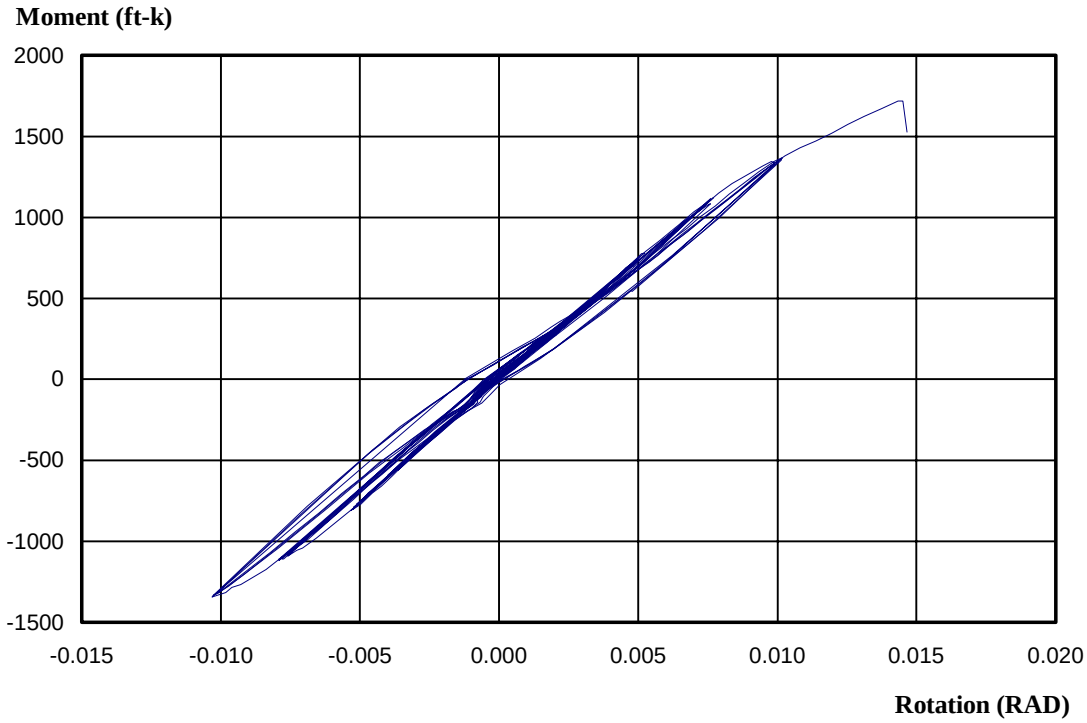

Moment vs. Total Rotation at End-Plate
MRE1/3-7/8-5/8-55 Test 2

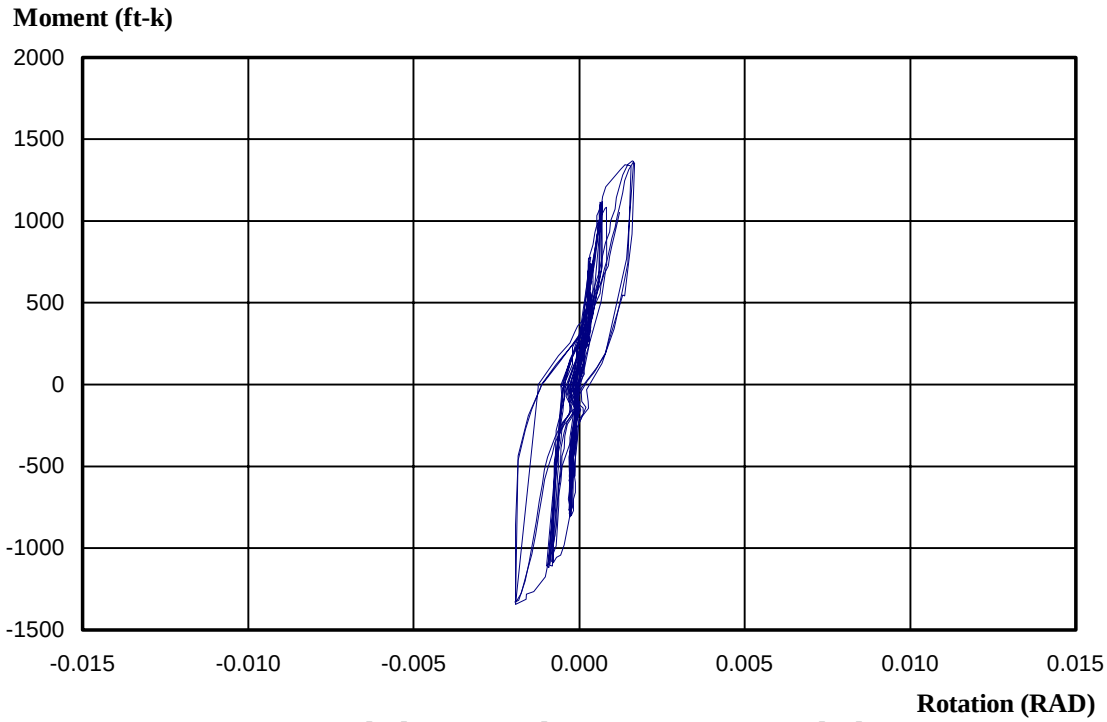

Moment at End Plate vs. Inelastic Rotation at End-Plate
MRE1/3-7/8-5/8-55 Test 2

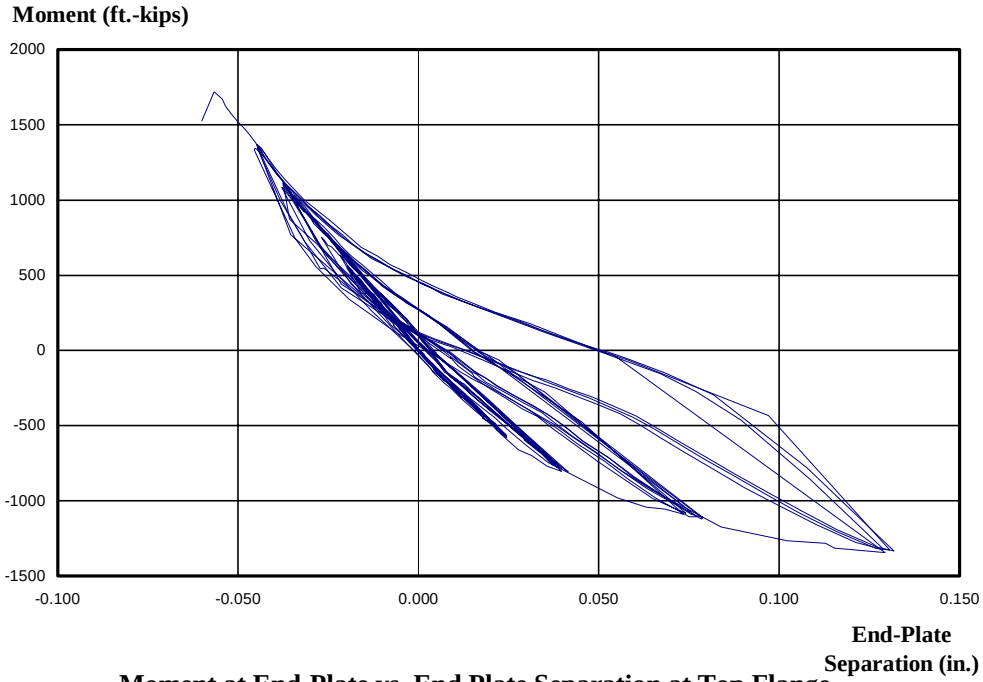

Moment at End-Plate vs. End Plate Separation at Top Flange
MRE1/3-7/8-5/8-55-Test 2

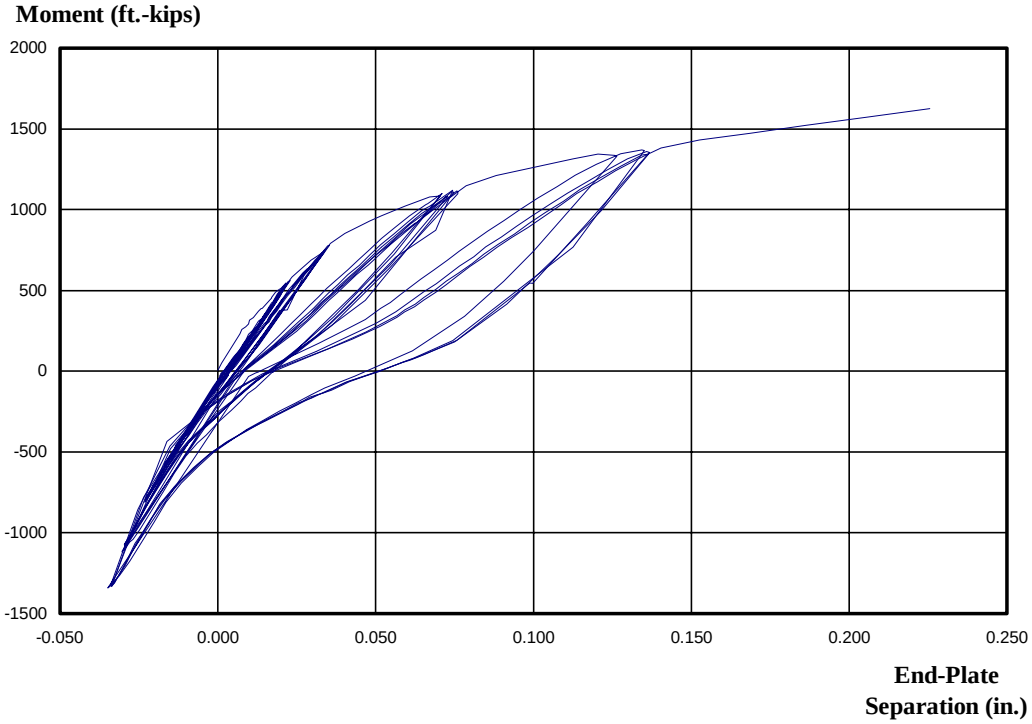

Moment at End-Plate vs. End Plate Separation at Bottom Flange
MRE1/3-7/8-5/8-55-Test 2

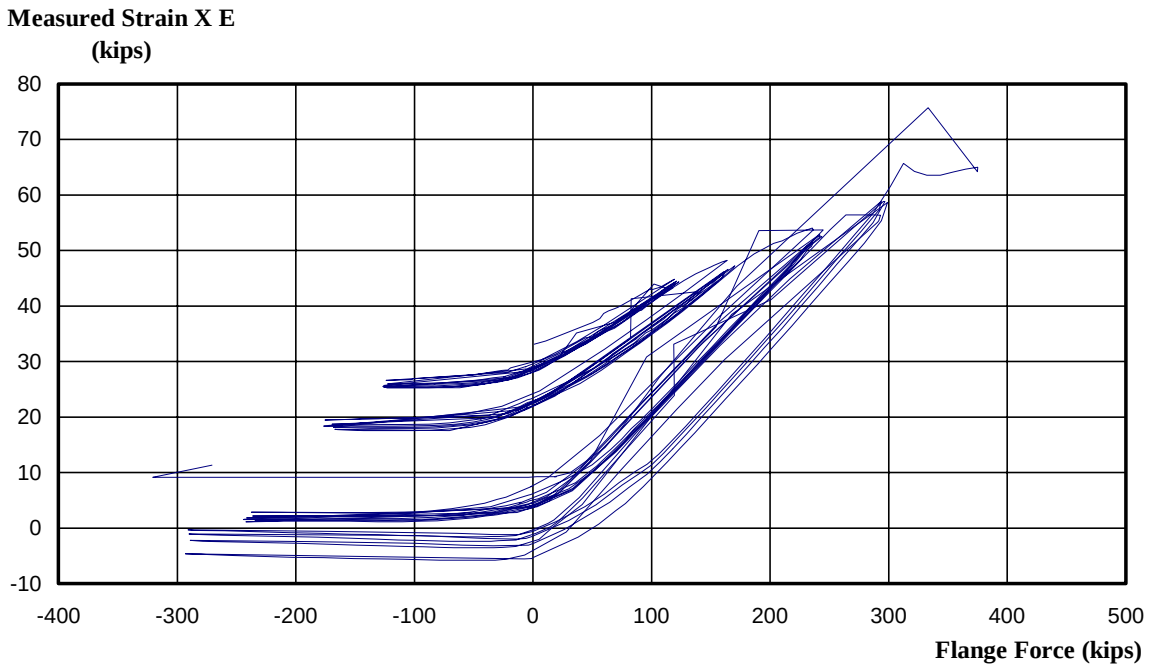

Meaured Bolt Strain X E vs. Flange Force-Bolt 1
MRE1/3-7/8-5/8-55 Test 2

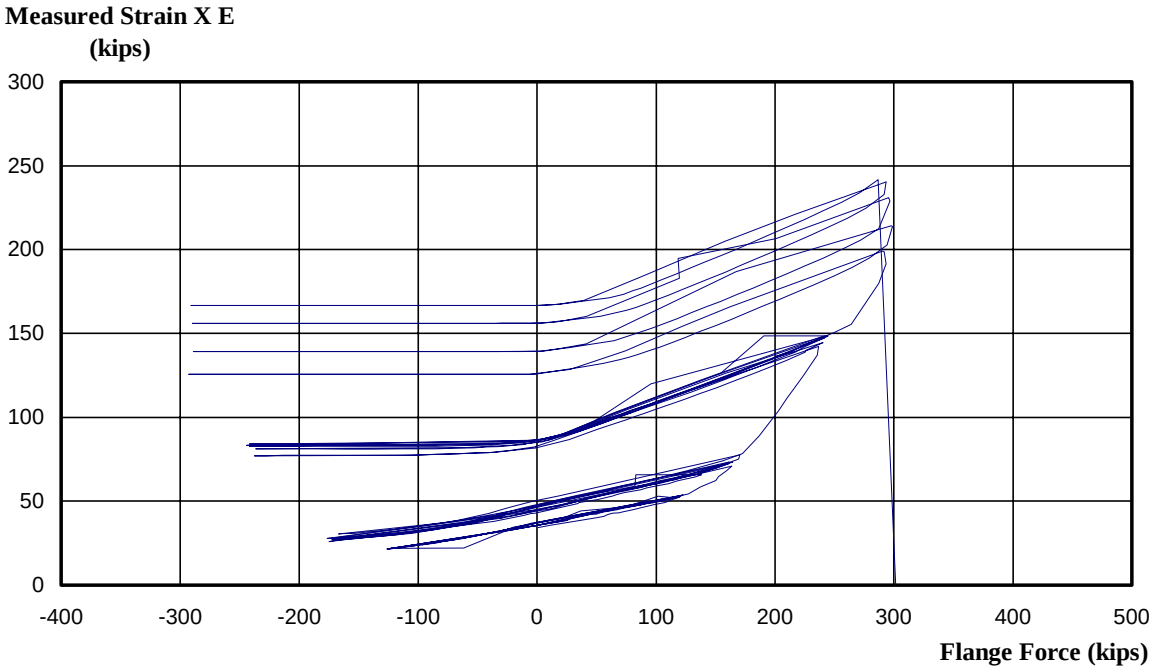

Meaured Bolt Strain X E vs. Flange Force-Bolt 4
MRE1/3-7/8-5/8-55 Test 2

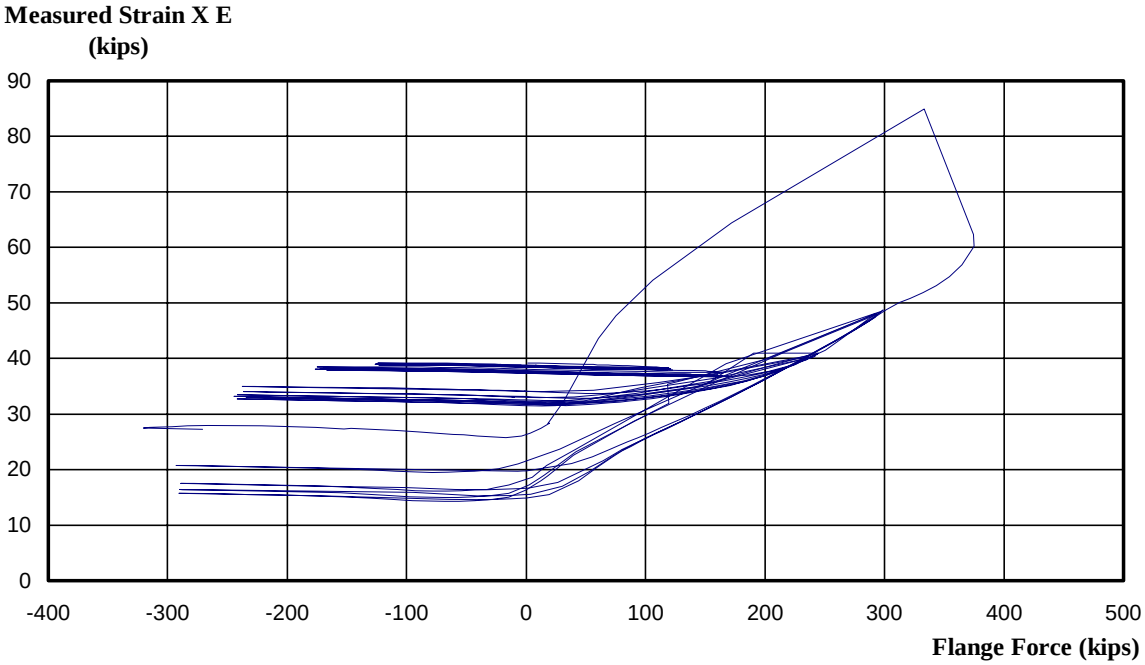

Meaured Bolt Strain X E vs. Flange Force-Bolt 5
MRE1/3-7/8-5/8-55 Test 2

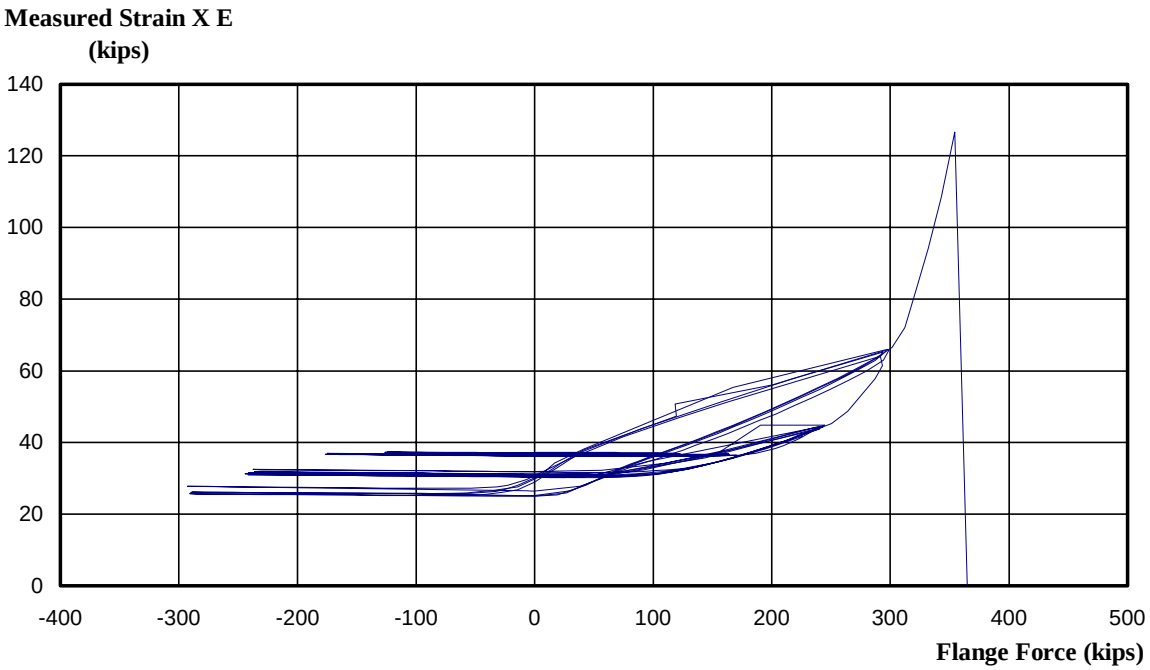

Meaured Bolt Strain X E vs. Flange Force-Bolt 8
MRE1/3-7/8-5/8-55 Test 2

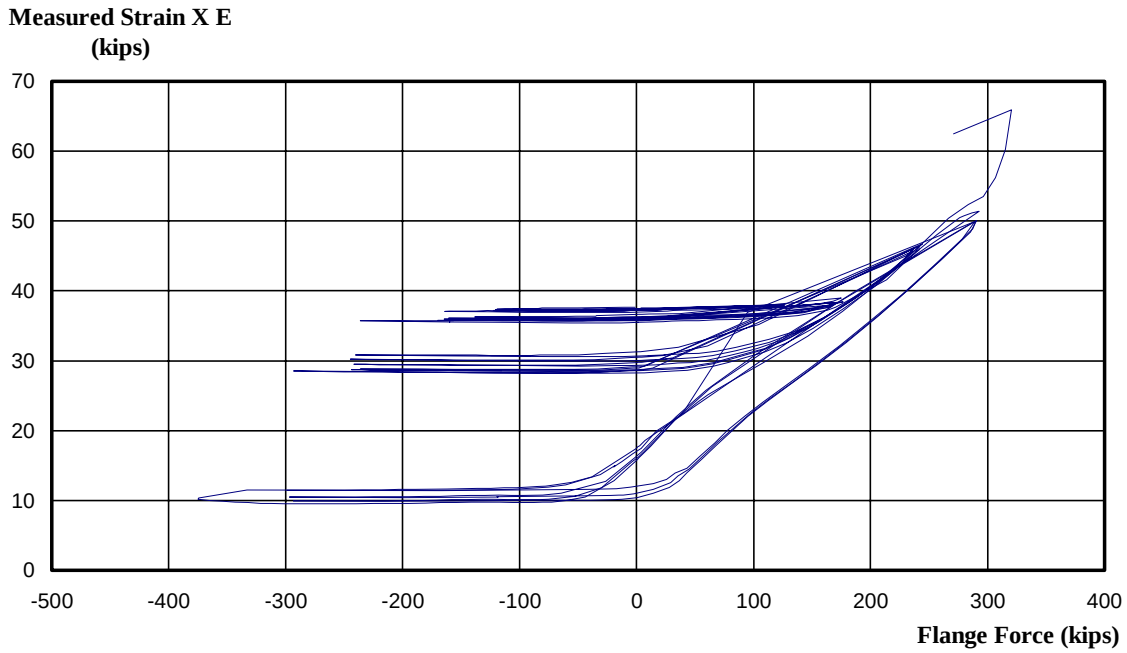

Meaured Bolt Strain X E vs. Flange Force-Bolt 9
MRE1/3-7/8-5/8-55 Test 2

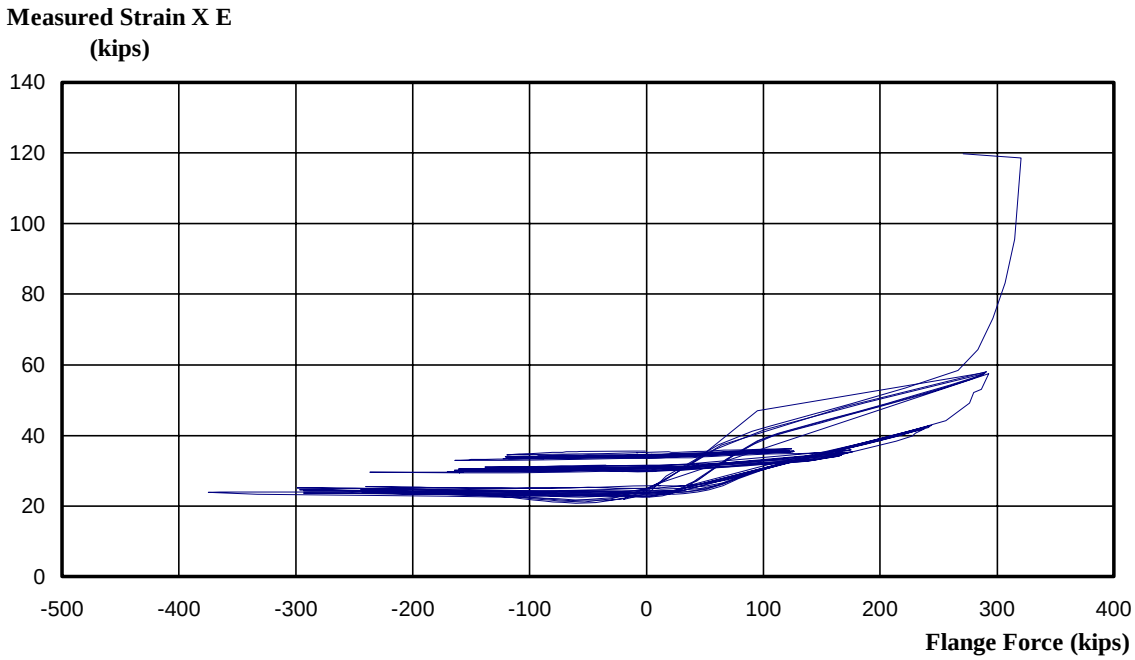

Meaured Bolt Strain X E vs. Flange Force-Bolt 12
MRE1/3-7/8-5/8-55 Test 2

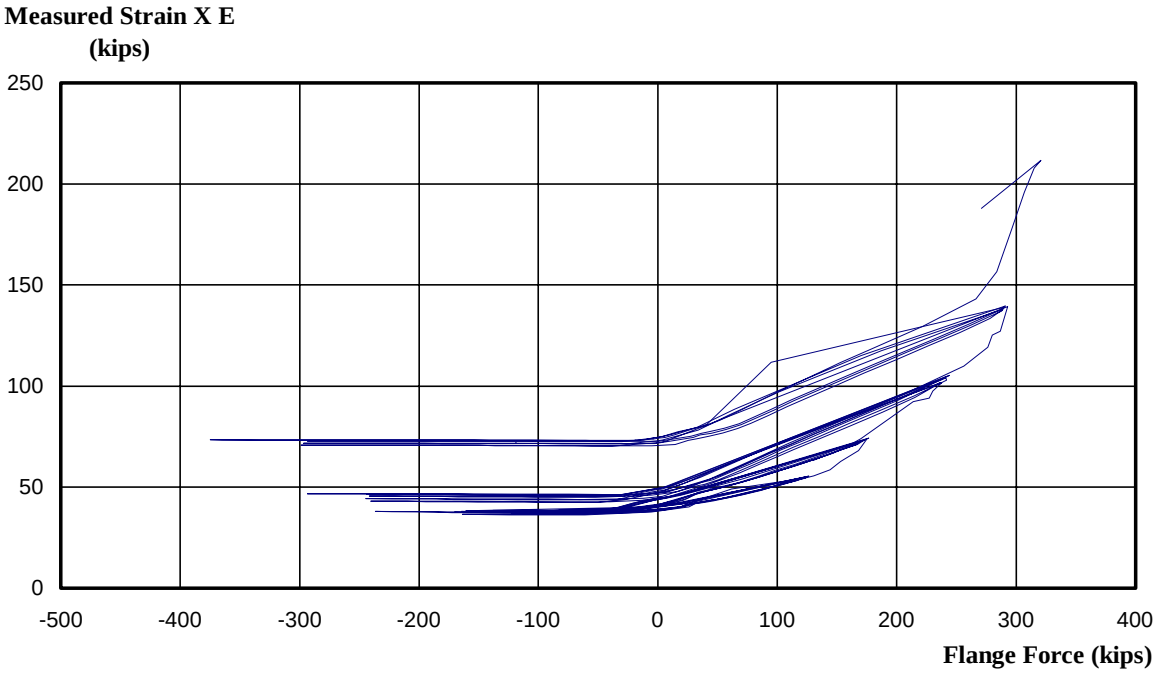

Meaured Bolt Strain X E vs. Flange Force-Bolt 13
MRE1/3-7/8-5/8-55 Test 2

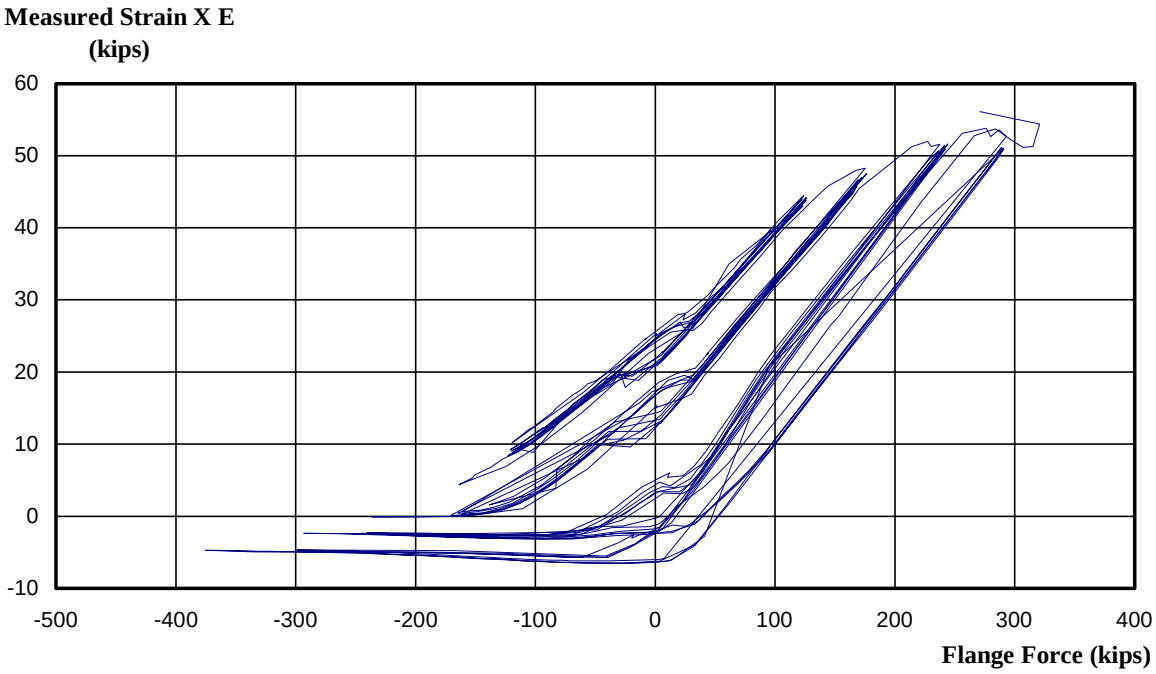

Meaured Bolt Strain X E vs. Flange Force-Bolt 16
MRE1/3-7/8-5/8-55 Test 2

Summary

MRE1/3-7/8-1/2-55

Predicted Capacities:

Moment Strength Predicted by Yield Line Analysis, M_{pl}……..776 ft-kips
Moment Strength Predicted by Bolt Rupture, M_q……1342 ft-kips

Strength Results:

Maximum Moment From Test, M_u……..1220 ft-kips
M_{pl} / M_u…….0.64
M_q / M_u……..0.91

Rotation Results:

Maximum Total Rotation…….0.0156 rad
Maximum Inelastic Rotation……0.0055 rad

Number of Completed Cycles……...…...22

Failure mode……..Bolt Rupture(Bolts #14, #15, and #16)

List of Significant Observations During Testing:

- During the first load step (Max Rotation =0.00375 rad) six cycles were completed. The Load vs. Displacement plot remained linear, and the specimen remained in the elastic region of stress. The specimen was observed after the sixth cycle. The white wash indicated no yielding of the the specimen.
- During the second load step (Max Rotation = 0.005 rad) six cycles were completed. The observations made were identical to those stated above.
- Six cycles were also completed at the third load step (Max Rotation = 0.0075 rad). At the peak of this load step, the Load vs. Deflection plot began to flatten slightly. Also, at the end of the sixth cycle, slight flaking of the white wash was seen at the end-plate on the outside of the flanges. At zero load, a small amount of end-plate separation from the column flange was observed.
- At the fourth load step (Max Rotation = 0.01 rad) four cycles were completed. More extensive yielding of the end-plate was observed at the outside of the flanges. Also yielding was observed inside of the flanges on both the column flange and the end plate around the bolts. The white wash in the panel zone of the column also indicated yielding.
- On the first cycle of the fifth load step, (Max Rotation = 0.015 rad), three bolts

ruptured at 0.0146 rad rotation, taken from the load point to the center of the column. At this point the test was terminated.

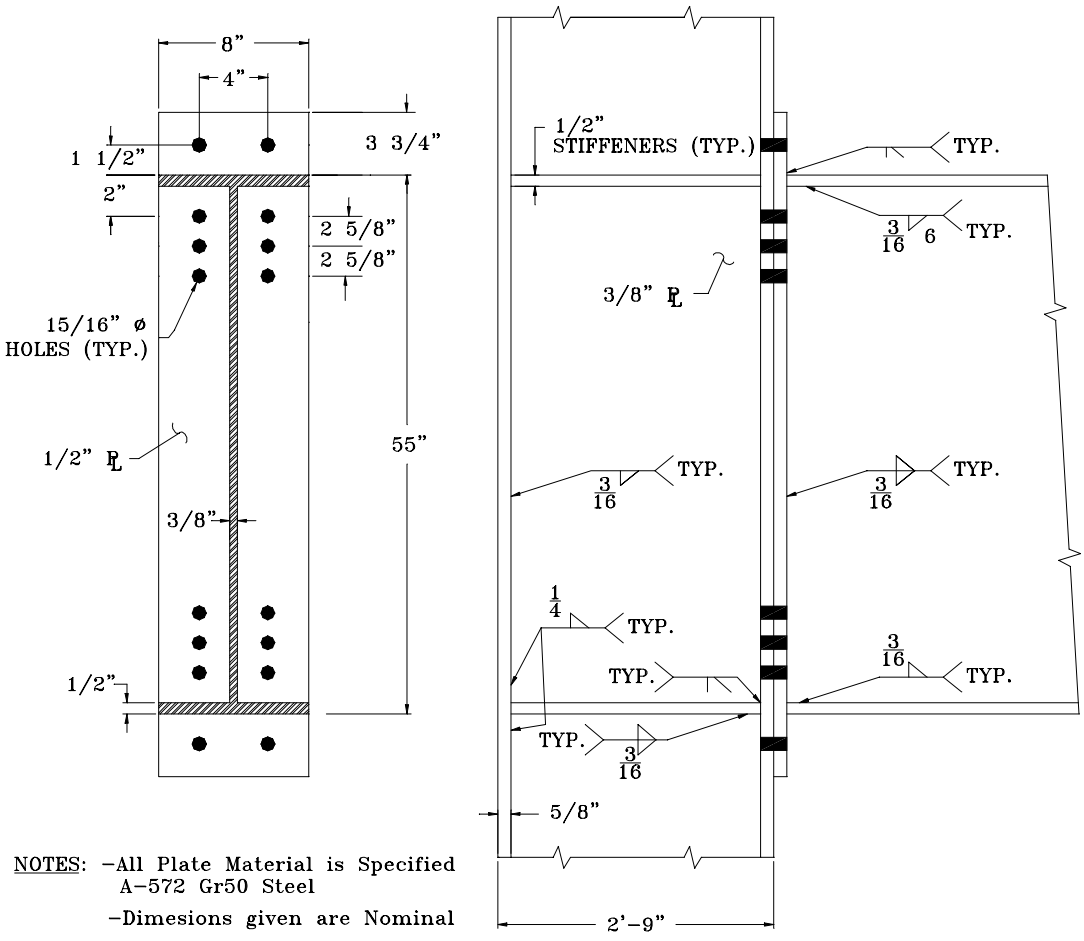

MRE1/2-7/8-1/2-55 Connection Details

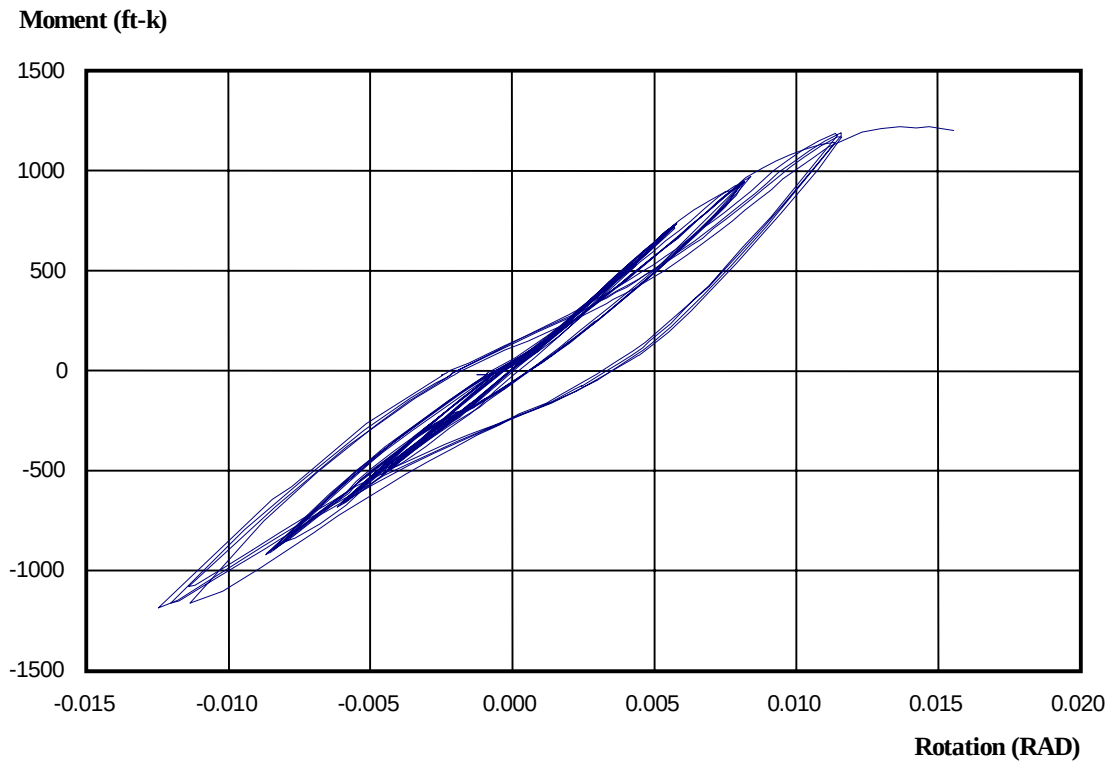

Moment vs. Total Rotation at End-Plate
MRE1/3-7/8-1/2-55

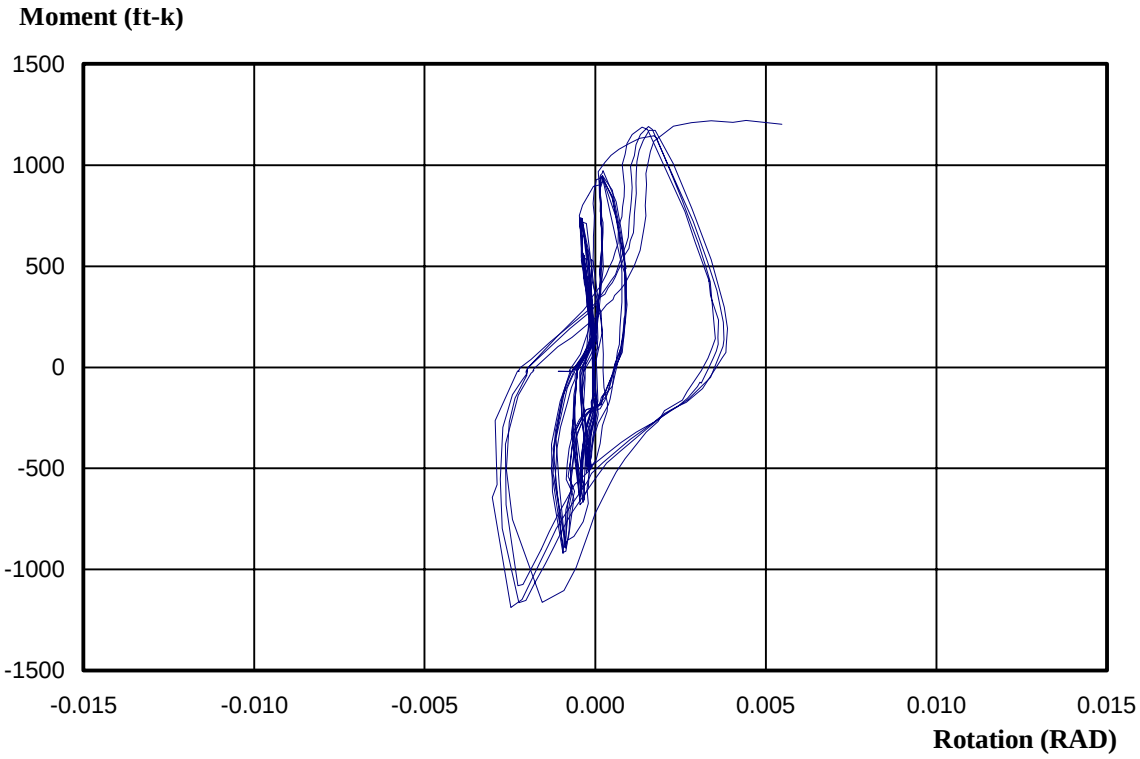

Moment vs. Inelastic Rotation at End-Plate
MRE1/3-7/8-1/2-55

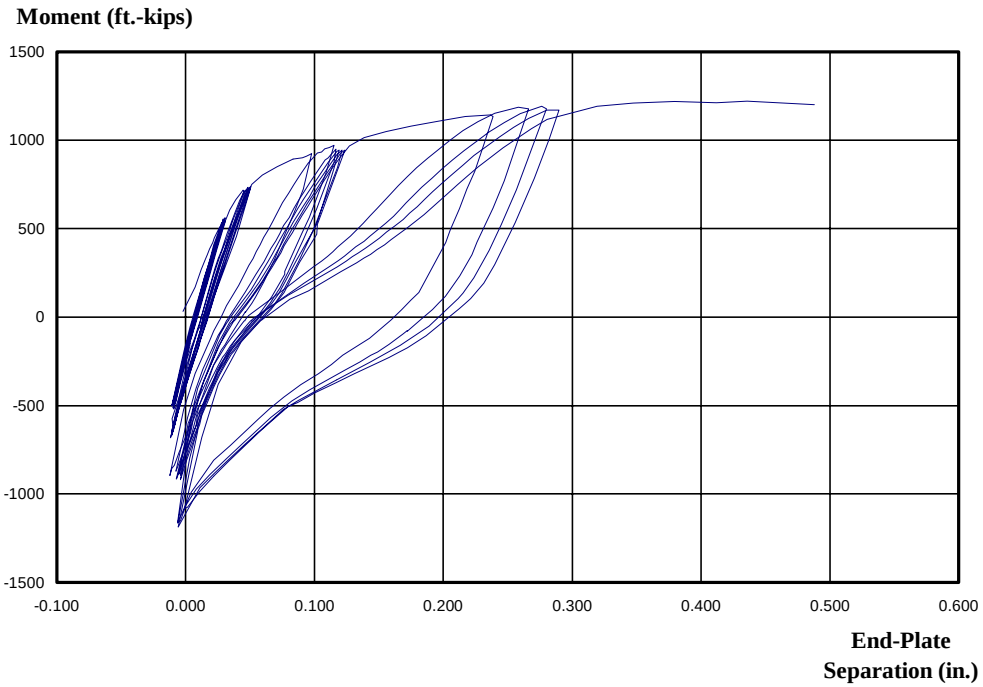

Moment at End-Plate vs. End Plate Separation at Bottom Flange
MRE1/3-7/8-1/2-55

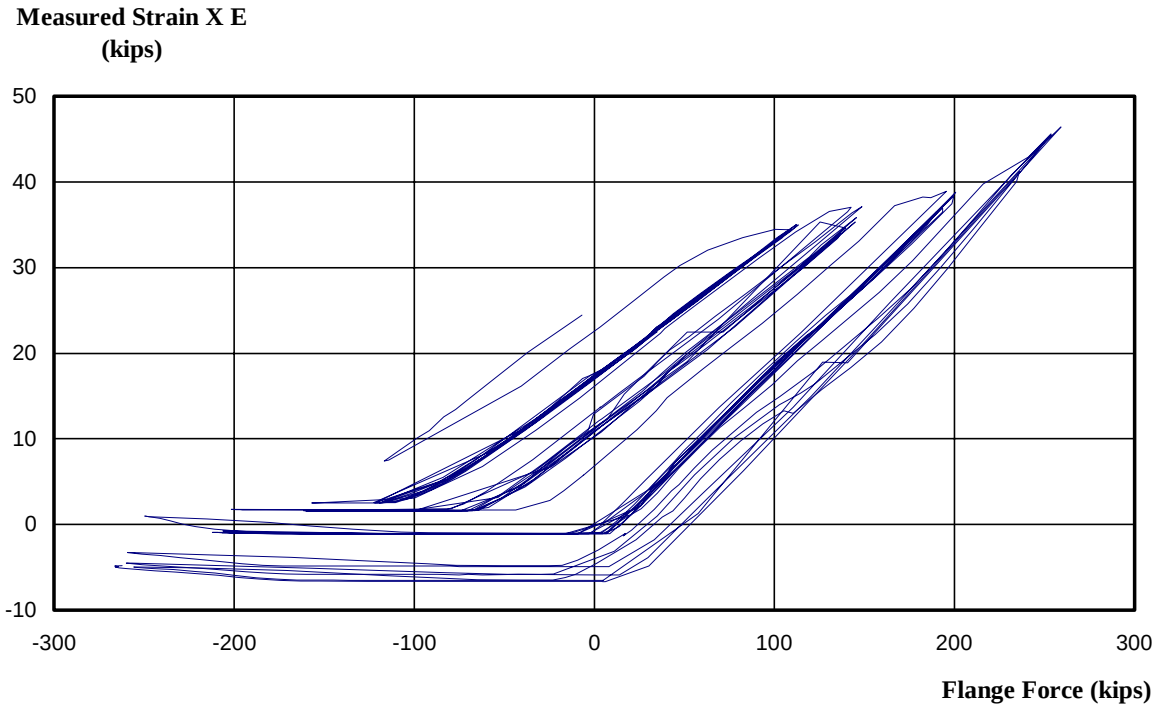

Measured Bolt Strain X E vs. Flange Force-Bolt 1
MRE1/3-7/8-1/2-55

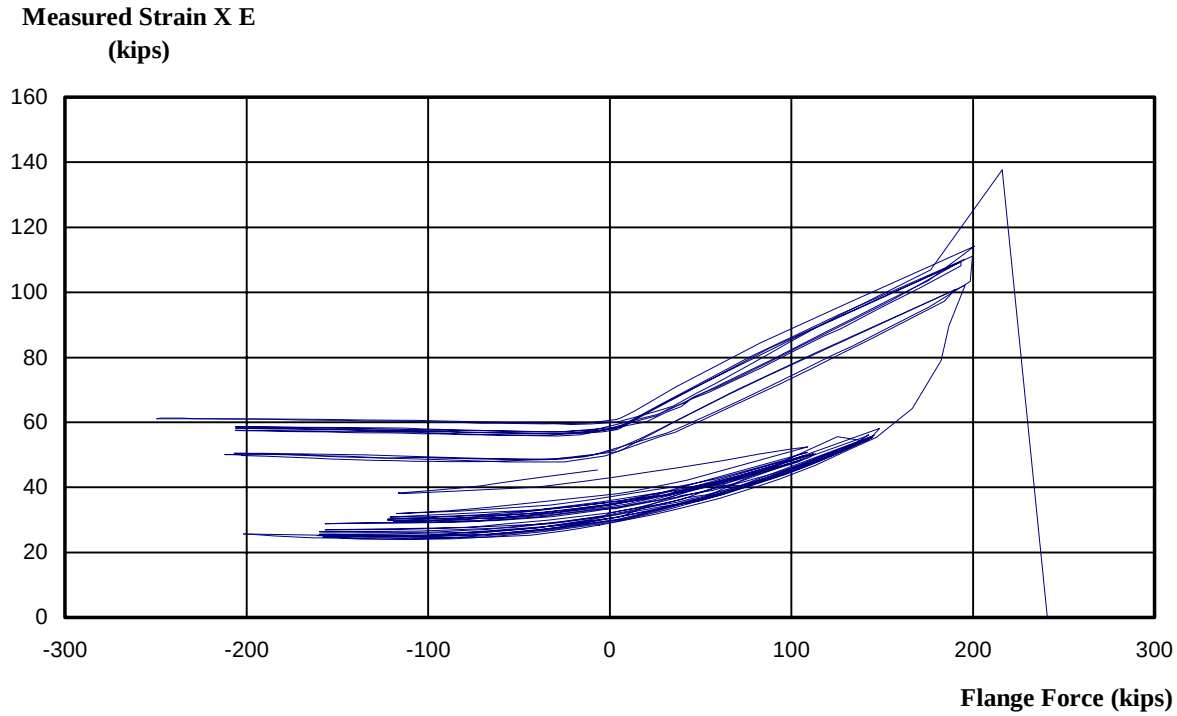

Measured Bolt Strain X E vs. Flange Force-Bolt 1
MRE1/3-7/8-1/2-55

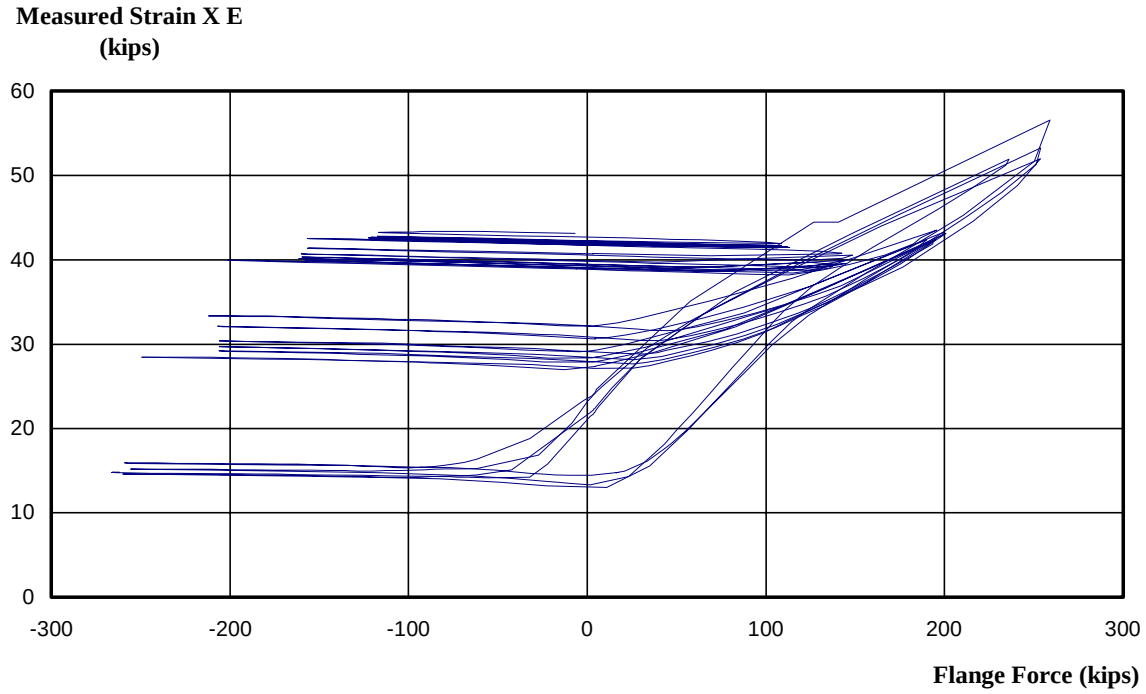

Measured Bolt Strain X E vs. Flange Force-Bolt 8
MRE1/3-7/8-1/2-55

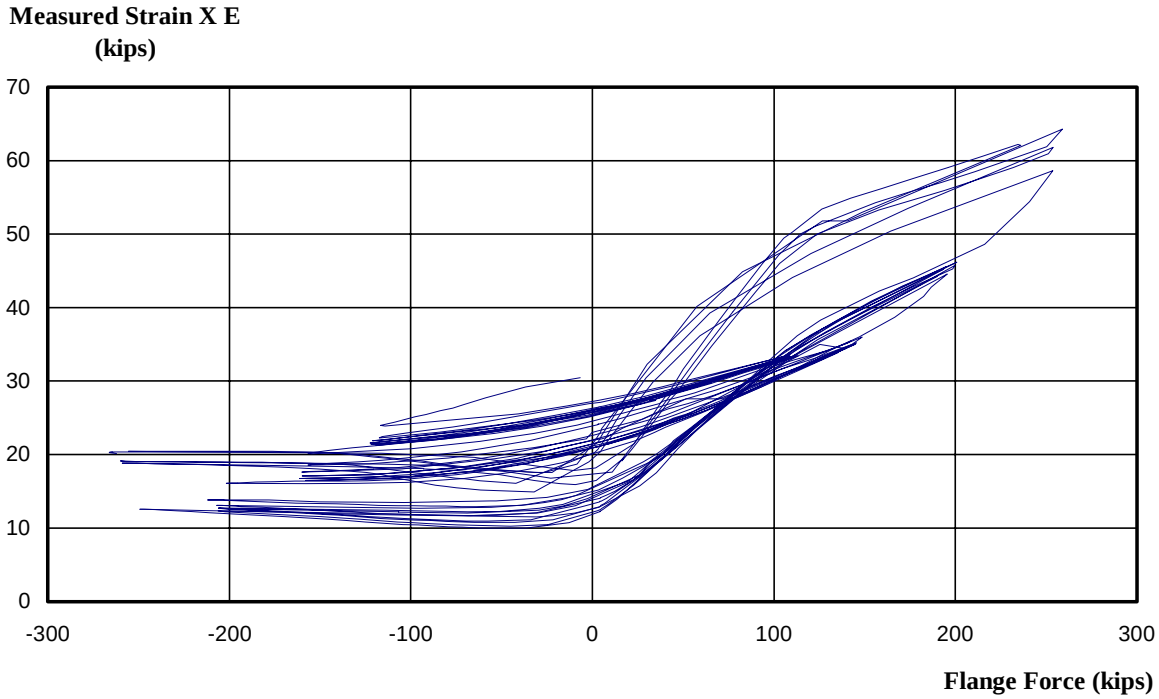

Measured Bolt Strain X E vs. Flange Force-Bolt 6
MRE1/3-7/8-1/2-55

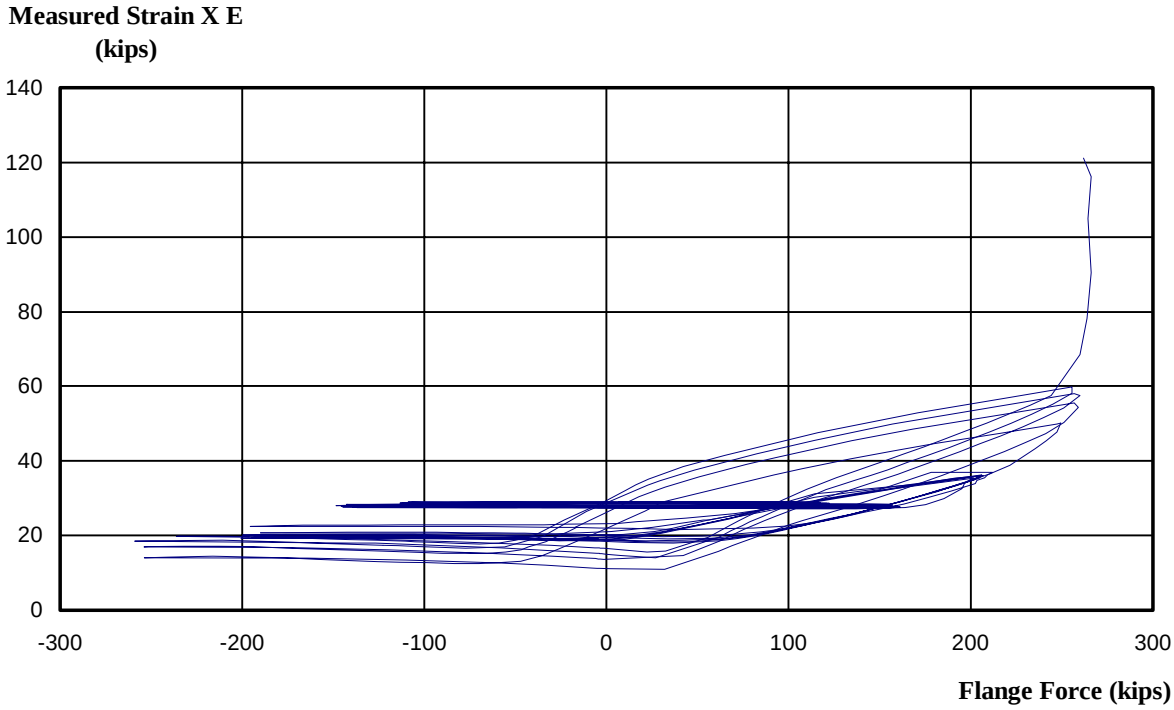

Measured Bolt Strain X E vs. Flange Force-Bolt 9
MRE1/3-7/8-1/2-55

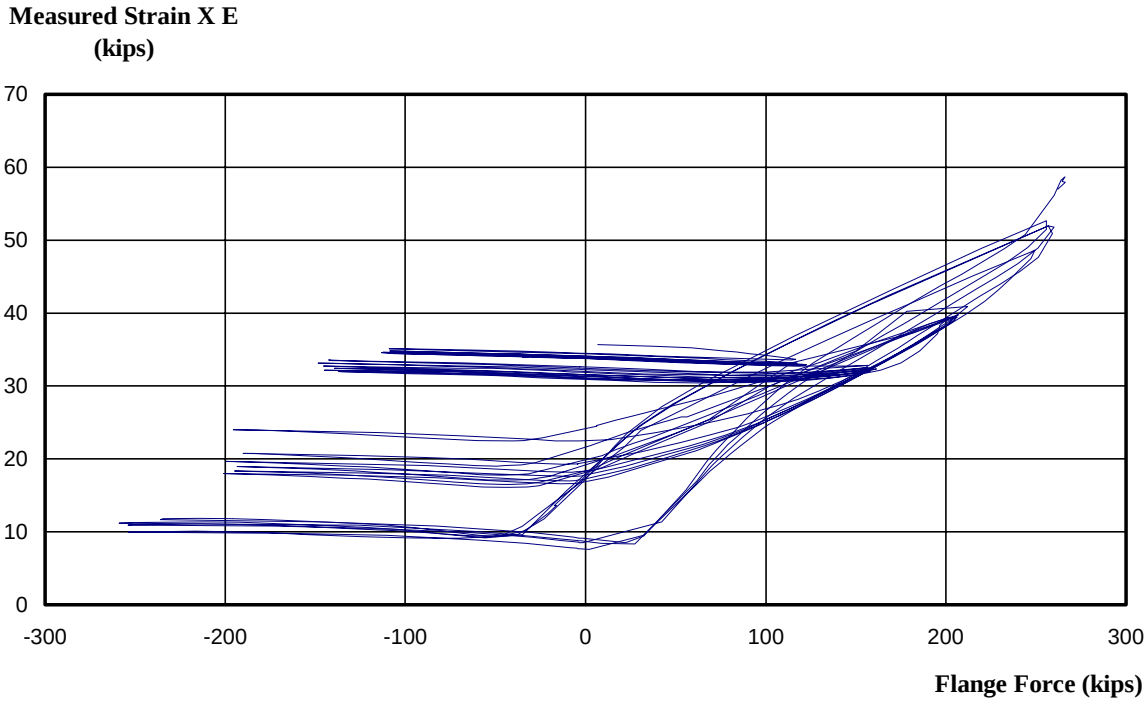

Measured Bolt Strain X E vs. Flange Force-Bolt 12
MRE1/3-7/8-1/2-55

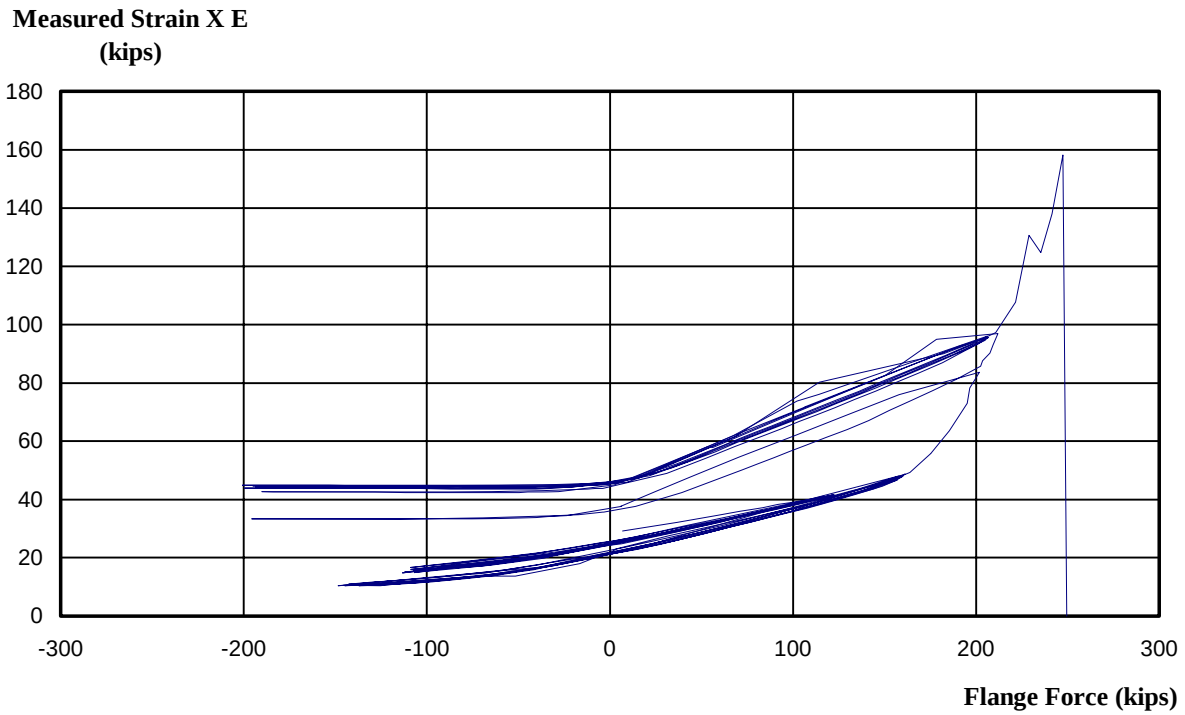

Measured Bolt Strain X E vs. Flange Force-Bolt 13
MRE1/3-7/8-1/2-55

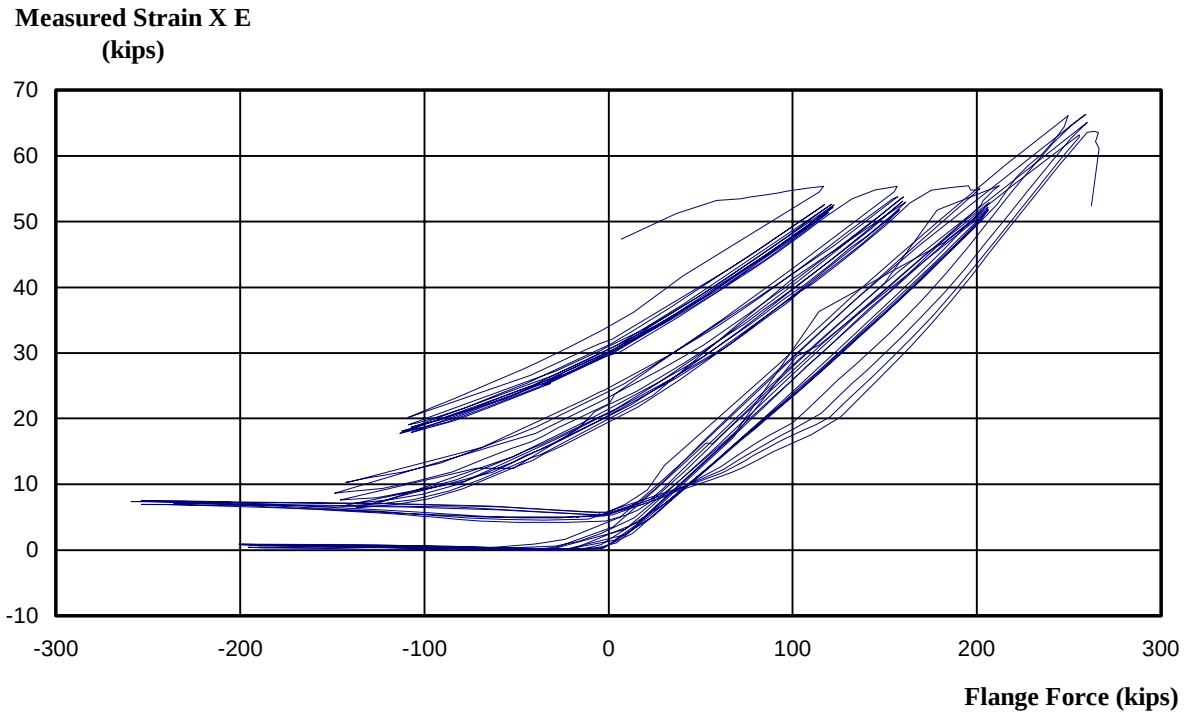

Measured Bolt Strain X E vs. Flange Force-Bolt 16
MRE1/3-7/8-1/2-55

APPENDIX D

FOUR BOLT EXTENDED UNSTIFFENED RESULTS AND TEST DATA

Summary

4E-7/8-1/2-55

Predicted Capacities:

Moment Strength Predicted by Yield Line Analysis, M_{pl}……..610 ft-kips

Yield Stress of End Plate, F_y……..…62.0 ksi

Moment Strength Predicted by Bolt Rupture, M_q……708 ft-kips

Strength Results:

Maximum Moment From Test, M_u……..904 ft-kips

M_{pl} / M_u……0.67

M_q / M_u…….0.78

Rotation Results:

Maximum Total Rotation……0.0114 rad

Maximum Inelastic Rotation……...0.0046 rad

Number of Completed Cycles…….….18

Condition at End of Test…….…..Bolt Rupture (Bolt #3, #4)

List of Significant Observations During Testing:

- During the first load step (Max Rotation =0.00375 rad) six cycles were completed. The Load vs. Displacement plot remained linear, and the specimen remained in the elastic region of stress. The specimen was observed after the sixth cycle. The white wash indicated no yielding of the specimen.
- During the second load step (Max Rotation = 0.005 rad) six cycles were completed. The observations made were identical to those stated above, with the exception of slight yielding present at the inside and outside of both flanges around the bolts, on the end-plate side of the connection. A small amount of separation of the end-plate from the column flange at the girder flange was observed at zero load.
- Six cycles were also completed at the third load step (Max Rotation = 0.0075 rad). While increasing load on the second half of the first load cycle, the bolt gage number read "offscale", indicating that the bolt had begun strain hardening. The "Moment vs. Rotation" curve begins to roll over slightly, indicating the yielding of the end-plate.

- At the fourth load step, (Max Rotation = 0.01 rad), only 75 % of the first loading cycle was completed before bolts #3, and #4 ruptured in tension. The shear failure of the end plate at the top flange of the connection then ruptured completely.

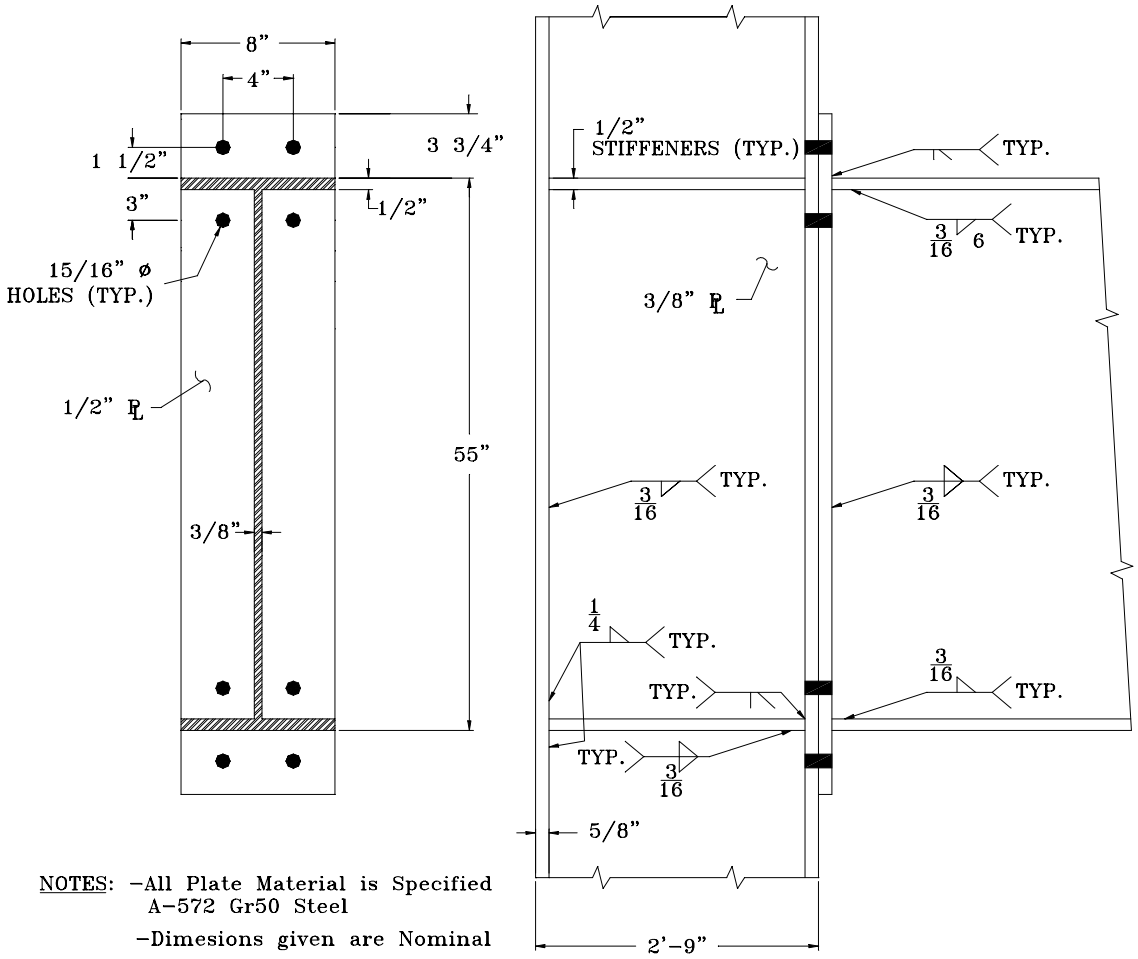

4E-7/8-1/2-55-Connection Details

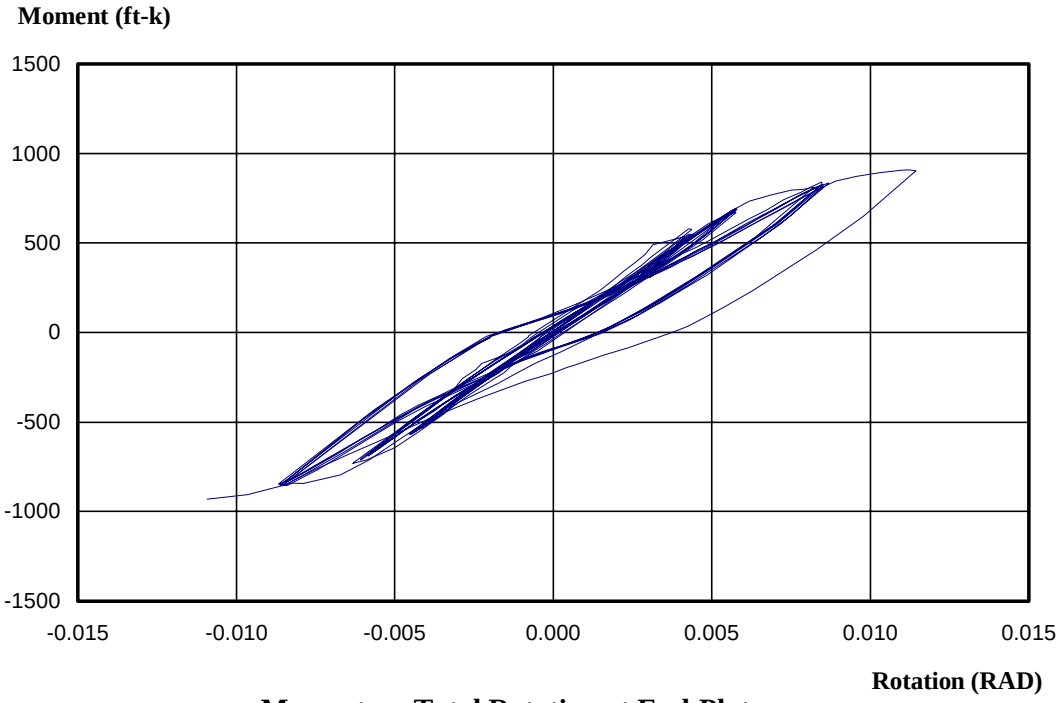

Moment vs. Total Rotation at End-Plate
4E-7/8-1/2-55

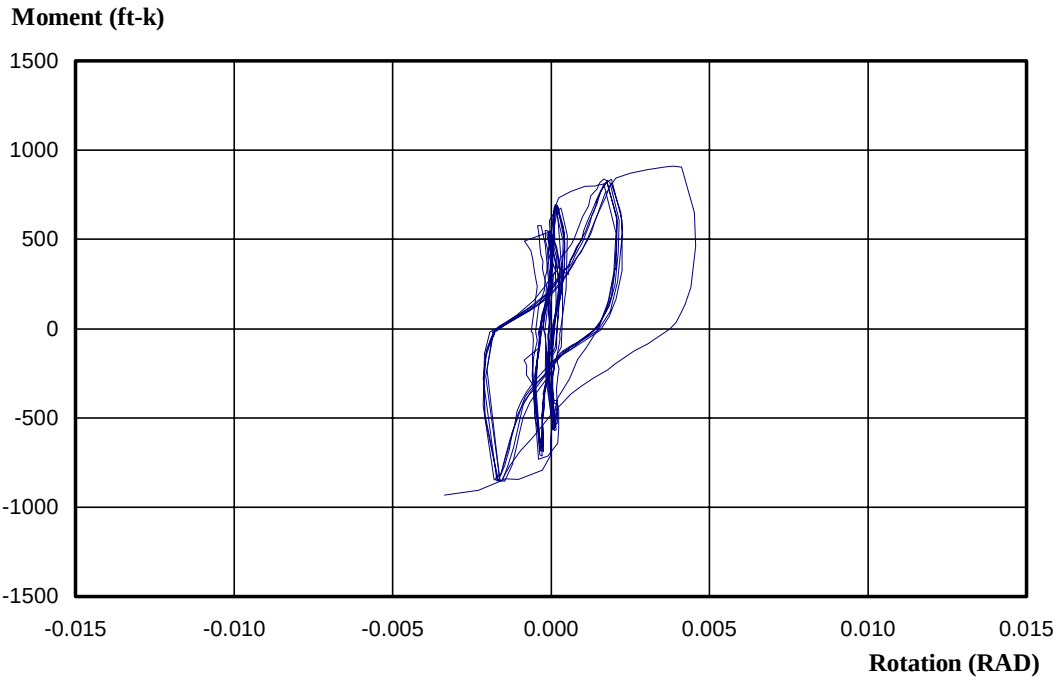

Moment at End Plate vs. Inelastic Rotation at End-Plate
4E-7/8-1/2-55

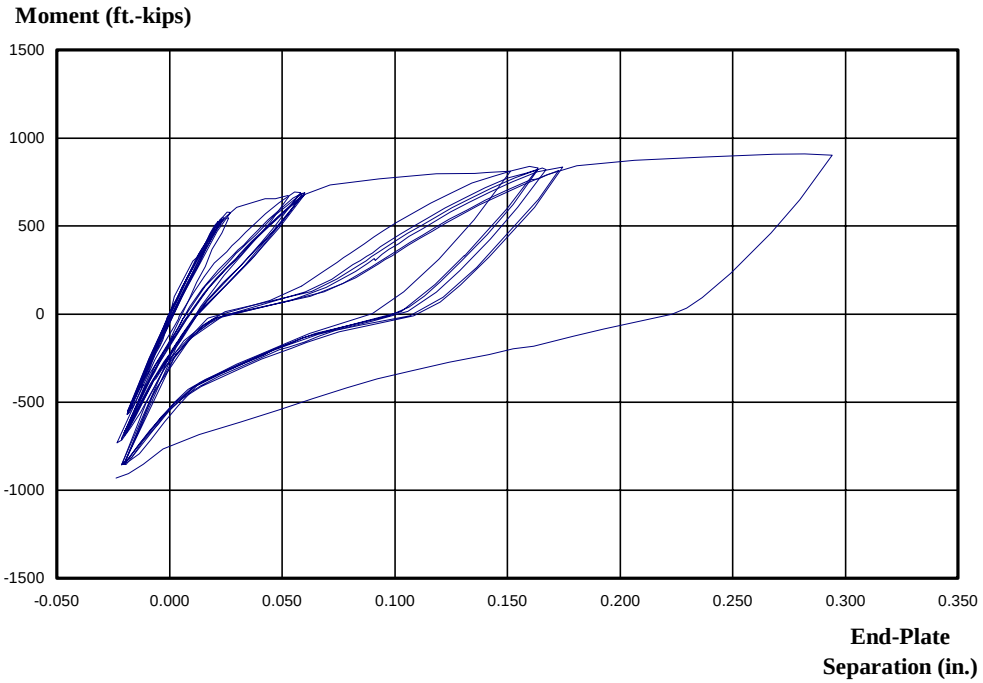

Moment at End-Plate vs. End Plate Separation at Top Flange
4E-7/8-1/2-55

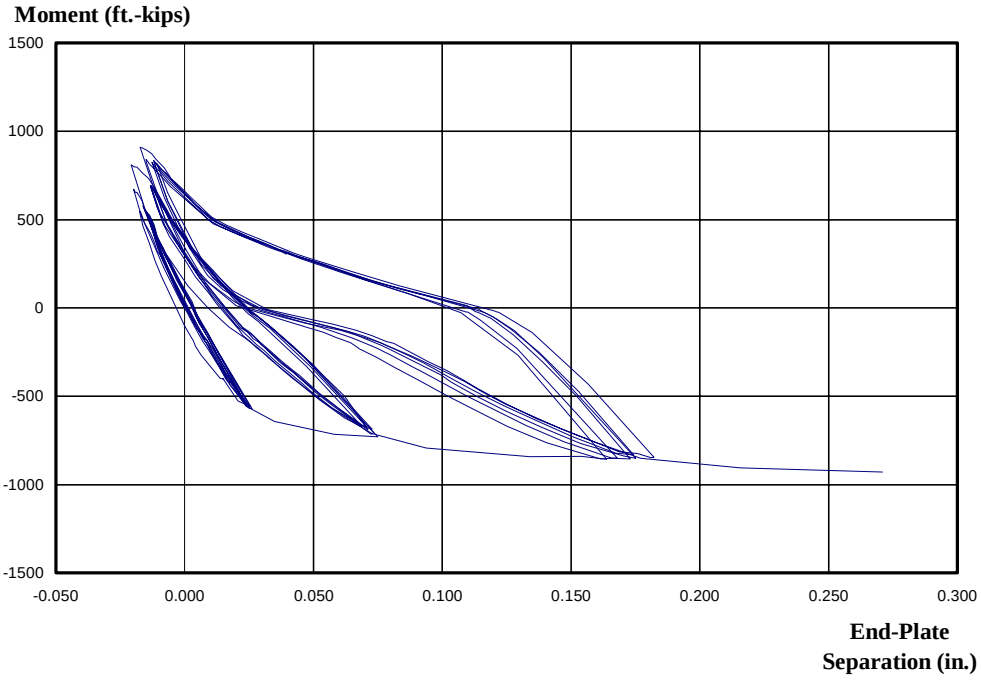

Moment at End-Plate vs. End Plate Separation at Bottom Flange
4E-7/8-1/2-55

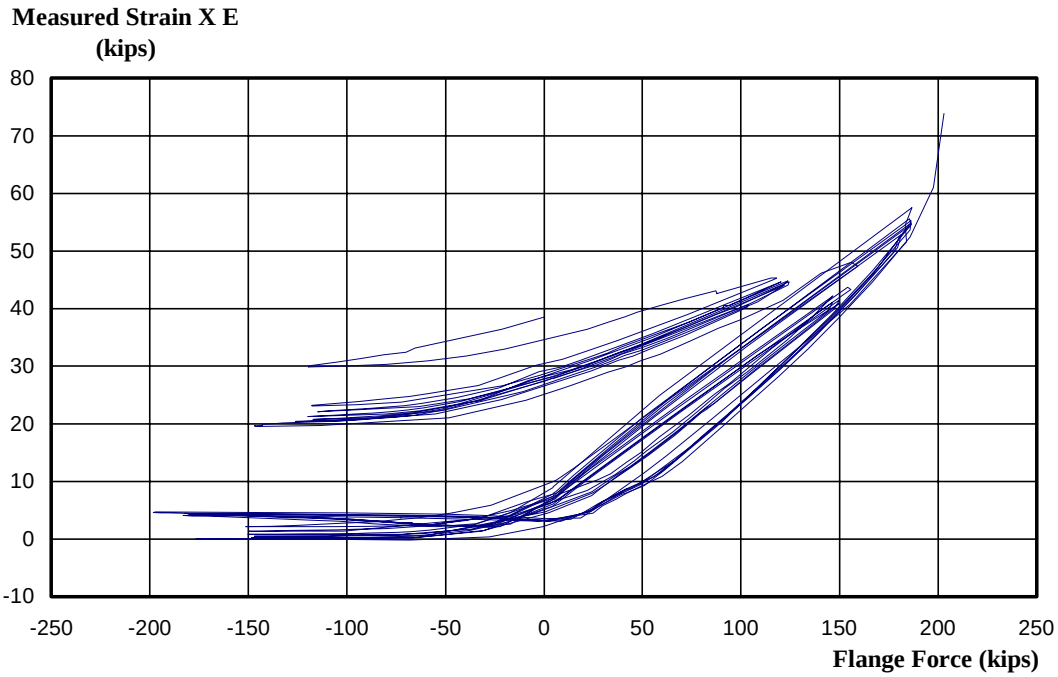

Measured Bolt Strain X E vs. Flange Force-Bolt 1
4E-7/8-1/2-55

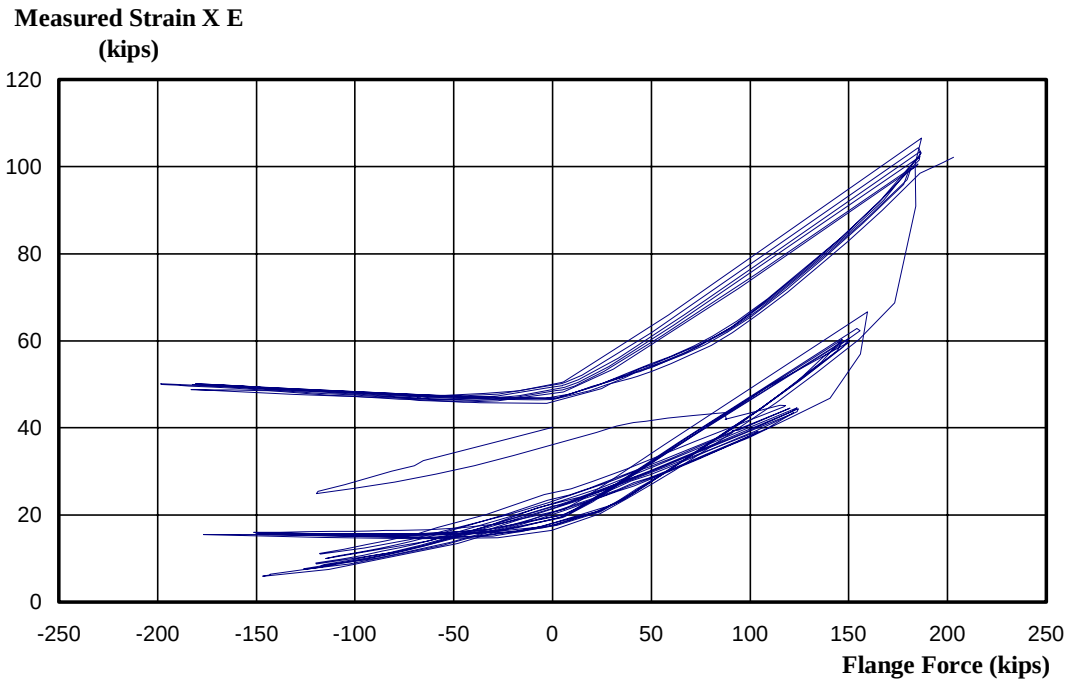

Measured Bolt Strain X E vs. Flange Force-Bolt 2
4E-7/8-1/2-55

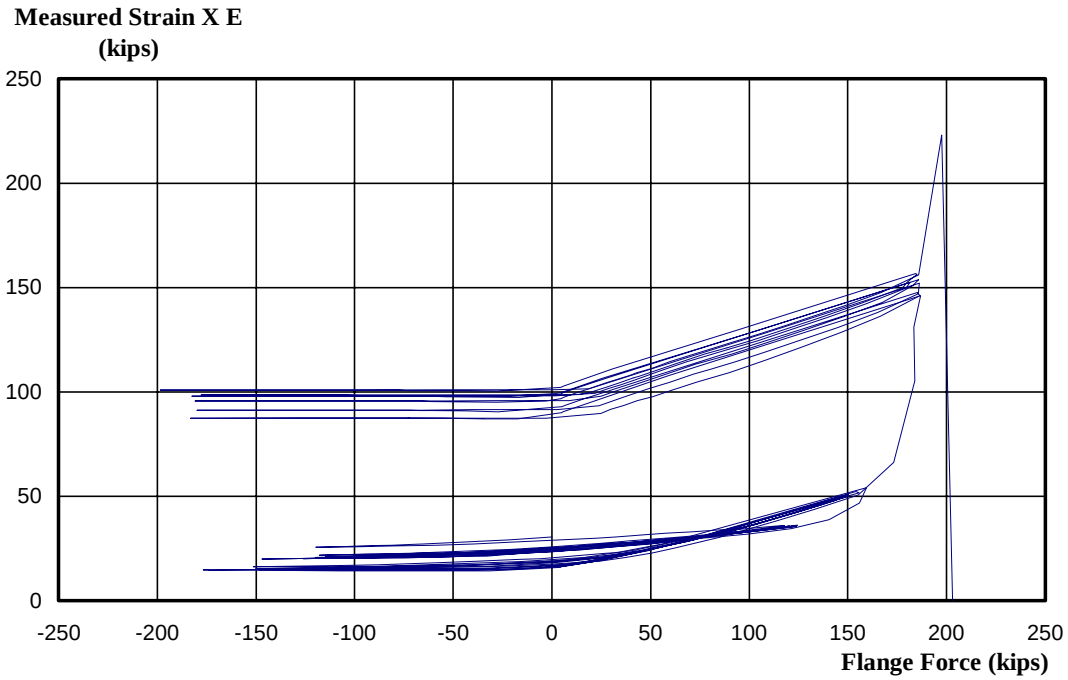

Measured Bolt Strain X E vs. Flange Force-Bolt 3
4E-7/8-1/2-55

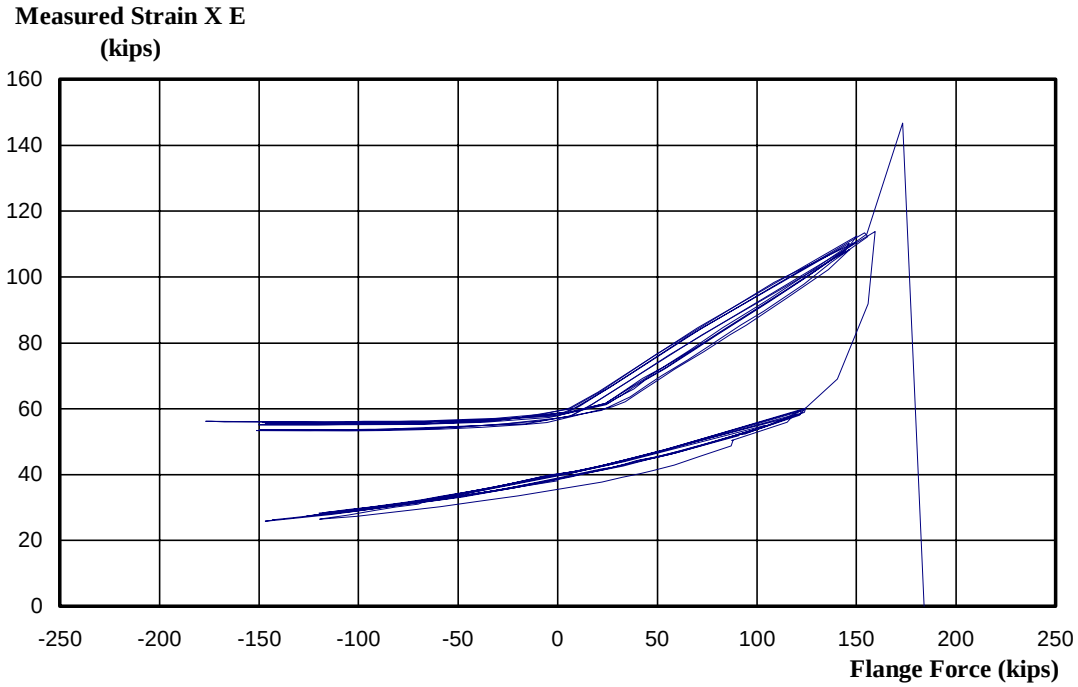

Measured Bolt Strain X E vs. Flange Force-Bolt 4
4E-7/8-1/2-55

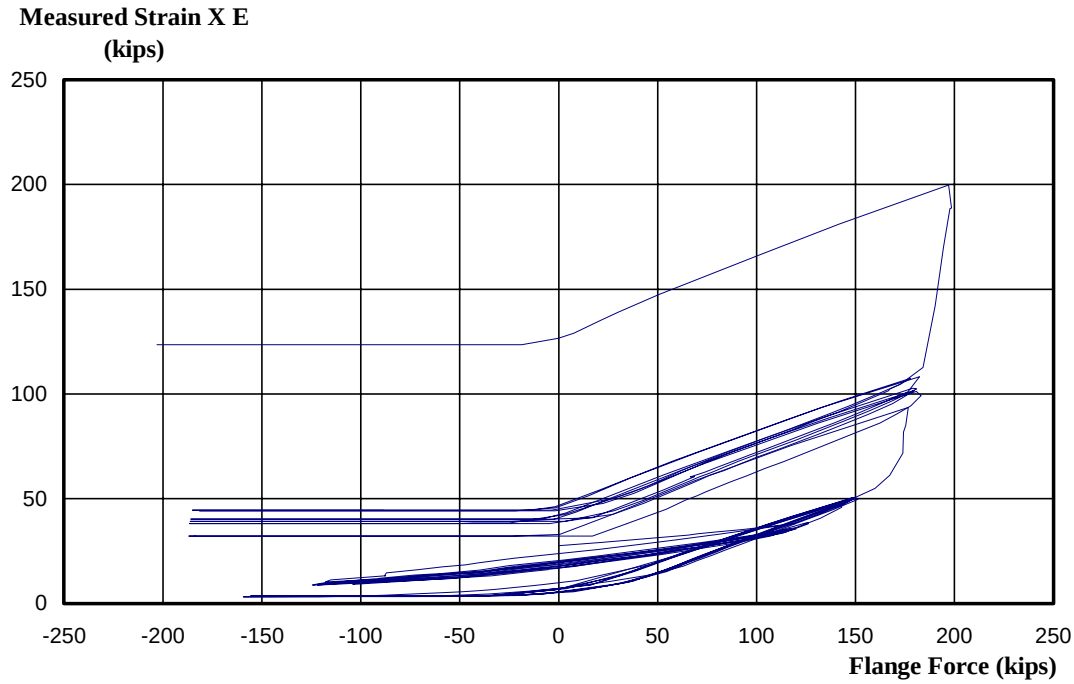

Measured Bolt Strain X E vs. Flange Force-Bolt 5
4E-7/8-1/2-55

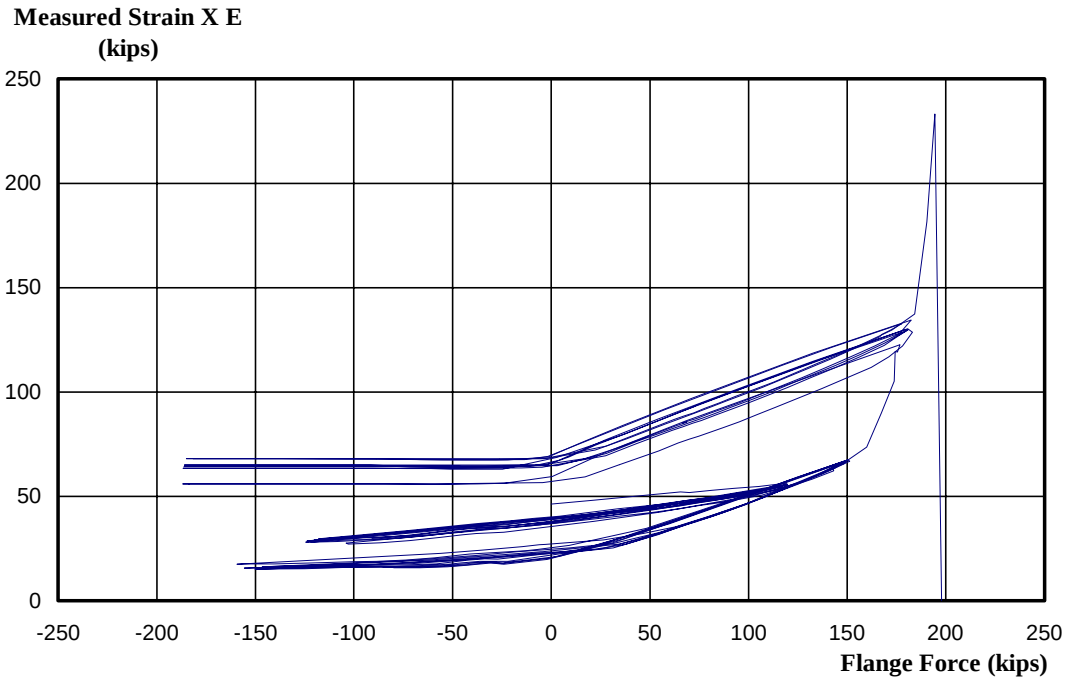

Measured Bolt Strain X E vs. Flange Force-Bolt 6
4E-7/8-1/2-55

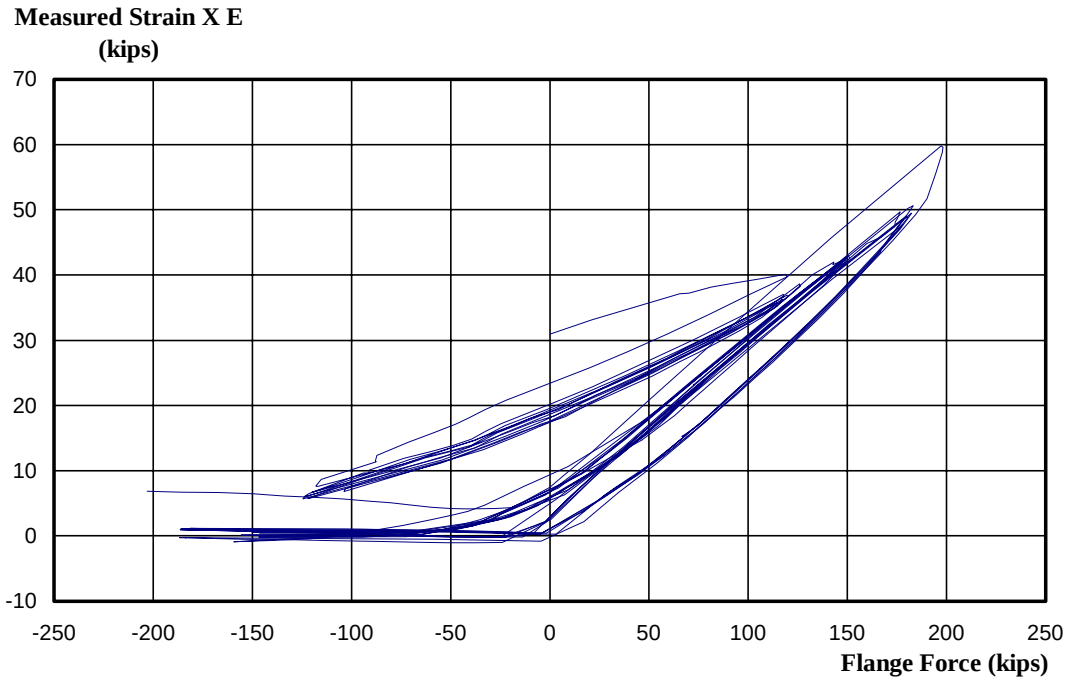

Measured Bolt Strain X E vs. Flange Force-Bolt 7
4E-7/8-1/2-55

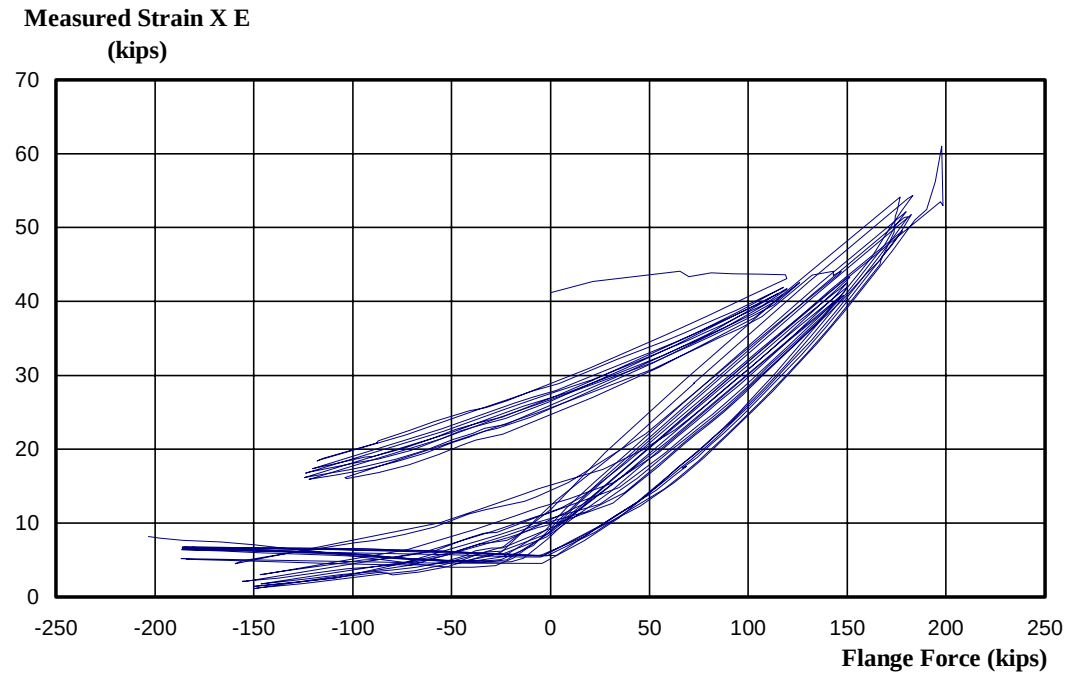

Measured Bolt Strain X E vs. Flange Force-Bolt 8
4E-7/8-1/2-55

APPENDIX E

STRENGTH PREDICTION EXAMPLES

Four Bolt Extended Stiffened Prediction Example
(4ES-7/8-1/2-24a Test 1)

Measured Connection Dimensions

$h := 24.0 \cdot in$ $b_f := 8.0 \cdot in$ $t_f := 0.321 \cdot in$

$p_t := 1.644 \cdot in$ $p_f := 1.323 \cdot in$ $g := 3.248 \cdot in$

$p_{ext} := 2.958 \cdot in$ $d_e := 1.635 \cdot in$ $w := 2.938 \cdot in$

$d_b := 1.0 \cdot in$ $t_p := 0.496 \cdot in$ $T_b := 51 \cdot k$ Tbl J3.1, AISC(1986)

Yield Stresses

Nominal Bolt Yield Stress: $F_{yb} := 90 \cdot ksi$

Measured End-Plate Yield Stress: $F_{py} := 62.71 \cdot ksi$

$$m_p := \frac{\left(F_{py} \cdot t_p^{\,2}\right)}{4} \quad \text{(Eqn. 2.11)}$$

$m_p = 3.857 \circ \frac{k \cdot in}{in}$

$$P_t := \frac{\pi \cdot d_b^{\,2} \cdot F_{yb}}{4}$$

$P_t = 70.686 \circ k$

Find M_{pl}:

$$s := \left(\frac{1}{2}\right) \cdot \sqrt{b_f \cdot g} \quad \text{(Eqn. 2.4)}$$

$s = 2.549 \circ in$

$d_e = 1.635 \circ in$

Case 1: ($s < d_e$)

$$M_{PL1} := 4 \cdot m_p \cdot \left[\left(\frac{b_f}{2}\right) \cdot \left(\frac{1}{p_f} + \frac{1}{s}\right) + \left(p_f + s\right) \cdot \left(\frac{2}{g}\right)\right] \cdot \left[\left(h - p_t\right) + \left(h + p_f\right)\right] \quad \text{(Eqn. 2.6)}$$

$M_{PL1} = 427.67 \circ ft \cdot k$

Case 2: ($s>d_e$)

$$M_{PL2} := 4 \cdot m_p \cdot \left[\left(\frac{b_f}{2} \right) \cdot \left(\frac{1}{p_f} + \frac{1}{2 \cdot s} \right) + \left(p_f + d_e \right) \cdot \left(\frac{2}{g} \right) \right] \cdot \left[\left(h - p_t \right) + \left(h + p_f \right) \right] \qquad \text{(Eqn. 2.8)}$$

$M_{PL2} = 345.081 \cdot k \cdot ft$

Find Controlling Yield-Line Solution Strength

$$M_{PL} := if\left(s < d_e, M_{PL1}, M_{PL2} \right)$$

$M_{PL} = 345.081 \cdot k \cdot ft$

Find M_q:

(Use Modified Kennedy Method)

$\beta := 0.6$

$$a := 3.682 \cdot in \cdot \left(\frac{t_p}{d_b} \right)^3 - .085 \cdot in \qquad \text{(Eqn. 2.23)}$$

$a = 0.364 \cdot in$

$$F_1 := \frac{b_f \cdot t_p^{\,2} \cdot F_{py}}{4 \cdot p_f \cdot \sqrt{1 + \left(\frac{3 \cdot t_p^{\,2}}{16 \cdot p_f^{\,2}} \right)}} \qquad \text{(Eqn. 2.29)}$$

$F_1 = 23.021 \cdot k$

$$F_{11} := \frac{\left[t_p^{\,2} \cdot F_{py} \cdot \left[.85 \cdot \left(\frac{b_f}{2} \right) + .8 \cdot w \right] + \frac{\left(\pi \cdot d_b^{\,3} \cdot F_{yb} \right)}{8} \right]}{2 \cdot p_f} \qquad \text{(Eqn. 2.30)}$$

$F_{11} = 46.885\ k$

$$Q_{max} := \frac{w \cdot t_p^{\,2}}{4 \cdot a} \cdot \sqrt{F_{py}^{\,2} - 3 \cdot \left(\frac{F_{11}}{2 \cdot w \cdot t_p} \right)^2} \qquad \text{(Eqn. 2.34)}$$

$Q_{max} = 27.867\ k$

**Plate is considered thin since $P_t > F_{11} / 2$. Therefore the maximum prying force, Q_{max}, given above applies.

.

$$Mq := \left(\frac{h}{12 \cdot \frac{in}{ft}} \right) \cdot \left[\left(P_t - Q_{max} \right) \cdot \frac{2}{\beta} \right]$$

$Mq = 285.461\ k \cdot ft$

RESULTS:

$M_{PL} = 345.081\ k \cdot ft$

$Mq = 285.461\ k \cdot ft$

Maximum Applied Moment: $Mu := 420\ ft - k$

Multiple Row 1/3 Extended Prediction Example

(MRE1/3-7/8-5/8-55 Test 1)

Connection Dimensions

$h := 55.0 \cdot in$ $b_f := 8.063 \cdot in$ $t_f := 0.501 \cdot in$

$p_t := 1.989 \cdot in$ $p_{t3} := 7.999 \cdot in$ $g := 4.015 \cdot in$

$p_f := 1.488 \cdot in$ $p_b := 3.005 \cdot in$ $p_{b1.3} := 6.010 \cdot in$

$w := 3.094 \cdot in$ $p_{ext} := 3.498 \cdot in$ $d_e := 2.010 \cdot in$

$d_b := .875 \cdot in$ $t_p := 0.615 \cdot in$ $T_b := 39 \cdot k$ Tbl J3.1, AISC(1986)

Yield Stresses

Nominal Bolt Yield Stress: $F_{yb} := 90 \cdot ksi$

Measured End-Plate Yield Stress: $F_{py} := 60.4 \cdot ksi$

$m_p := \frac{\left(F_{py} \cdot t_p^{2}\right)}{4}$ (Eqn. 2.11) $m_p = 5.711 \circ \frac{k \cdot in}{in}$

$P_t := \frac{\pi \cdot d_b^{2} \cdot F_{yb}}{4}$ $P_t = 54.119 \circ k$

Find M_{pl}:

Check Mechanism 1:

$u1 := \left(\frac{1}{2}\right) \cdot \sqrt{b_f \cdot g \cdot \left(\frac{h - p_{t3}}{h - p_t}\right)}$ (Eqn. 2.15) $u1 = 2.679 \circ in$

$M_{PL1} := 4 \cdot m_p \cdot \left[\left(\frac{b_f}{2}\right) \cdot \left(\frac{1}{2} + \frac{h}{p_f} + \frac{h - p_t}{p_f} + \frac{h - p_{t3}}{u1}\right) + \frac{2}{g} \cdot \left(p_f + p_{b1.3} + u1\right) \cdot \left(h - p_t\right)\right]$

(Eqn

2.17)

$M_{PL1} = 1.207 \cdot 10^{3}$ k·ft

Check Mechanism 2:

$u2 := \left(\frac{1}{2}\right) \cdot \sqrt{b_f \cdot g}$ (Eqn. 2.19) $u2 = 2.845$ in

$$M_{PL2} := 4 \cdot m_p \cdot \left[\left(\frac{b_f}{2}\right) \cdot \left(\frac{1}{2} + \frac{h}{p_f} + \frac{h - p_t}{p_f} + \frac{h - p_{t3}}{u2}\right) + \left[\left(\frac{2}{g}\right) \left(p_f + p_{b1.3}\right)\right] \cdot \left(h - t_f\right) \ldots + \left(\frac{2 \cdot u2}{g}\right) \cdot \left(h - p_{t3}\right) + \frac{g}{2} \right]$$

(Eqn. 2.13)

$M_{PL2} = 1.206 \cdot 10^{3}$ k·ft

Find Controlling Yield-Line Solution Strength

$m := \left[M_{PL1} \quad M_{PL2} \right]$

$M_{PL} := \min(m)$

$M_{PL} = 1.206 \cdot 10^{3}$ k·ft

Find M_q:

(Use Modified Kennedy Method)

$\beta := 0.35$

$a := 3.682 \cdot \text{in} \cdot \left(\frac{t_p}{d_b}\right)^{3} - .085 \cdot \text{in}$ (Eqn. 2.23)

$a = 1.193$ in

$$F_1 := \frac{b_f \cdot t_p^2 \cdot F_{py}}{4 \cdot p_f \cdot \sqrt{1 + \left(\frac{3 \cdot t_p^2}{16 \cdot p_f^2}\right)}}$$ (Eqn. 2.29)

$F_1 = 30.463$ k

$$F_{11} := \frac{\left[t_p^2 \cdot F_{py} \cdot \left[.85 \cdot \left(\frac{b_f}{2}\right) + .8 \cdot w\right] + \frac{\left(\pi \cdot d_b^3 \cdot F_{yb}\right)}{8}\right]}{2 \cdot p_f}$$ (Eqn. 2.30)

$F_{11} = 53.262$ k

$$Q_{max} := \frac{w \cdot t_p^2}{4 \cdot a} \cdot \sqrt{F_{py}^2 - 3 \cdot \left(\frac{F_{11}}{2 \cdot w \cdot t_p}\right)^2}$$ (Eqn. 2.34)

$Q_{max} = 13.561$ k

**Plate is considered thin since $P_t > F_{11} / 2$. Therefore the maximum prying force, Q_{max}, given above applies.

.

$$Mq := \left(\frac{h}{12 \cdot \frac{in}{ft}}\right) \cdot \left[\left(P_t - Q_{max}\right) \cdot \frac{2}{\beta}\right]$$

$Mq = 1.062 \cdot 10^3$ k·ft

RESULTS:

$M_{PL} = 1.206 \cdot 10^3$ k·ft

$Mq = 1.062 \cdot 10^3$ k·ft

Maximum Applied Moment: $Mu := 1523$ ft – k

Four Bolt Extended Unstiffened Prediction Example
(4E-7/8-1/2-55)

Connection Dimensions

$h := 55.0 \cdot in$ $b_f := 8.015 \cdot in$ $t_f := 0.502 \cdot in$

$g := 4.022 \cdot in$ $p_t := 2.025 \cdot in$ $p_f := 1.533 \cdot in$

$p_{ext} := 3.497 \cdot in$ $w := 3.070 \cdot in$

$d_b := .875 \cdot in$ $t_p := 0.499 \cdot in$ $T_b := 39 \cdot k$ Tbl J3.1, AISC(1986)

Yield Stresses

Nominal Bolt Yield Stress: $F_{yb} := 90 \cdot ksi$

Measured End-Plate Yield Stress: $F_{py} := 62.0 \cdot ksi$

$m_p := \frac{\left(F_{py} \cdot t_p^{\,2}\right)}{4}$ (Eqn. 2.11)

$m_p = 3.86 \circ \frac{k \cdot in}{in}$

$P_t := \frac{\pi \cdot d_b^{\,2} \cdot F_{yb}}{4}$

$P_t = 54.119 \circ k$

Find M_{pl}:

$s := \left(\frac{1}{2}\right) \cdot \sqrt{b_f \cdot g}$ (Eqn. 2.4)

$s = 2.839 \circ in$

$M_{PL} := 4 \cdot m_p \cdot \left[\left[\left(\frac{b_f}{2}\right) \cdot \left(\frac{1}{p_f} + \frac{1}{s}\right) + \left(p_f + s\right) \cdot \left(\frac{2}{g}\right)\right] \cdot \left(h - p_t\right) + \left(\frac{b_f}{2}\right) \cdot \left(\frac{1}{2} + \frac{h}{p_f}\right)\right]$ (Eqn. 2.21)

$M_{PL} = 610.081 \circ k \cdot ft$

Find M_q:

(Use Modified Kennedy Method)

$\beta := 0.5$

$$a := 3.682 \cdot in \cdot \left(\frac{t_p}{d_b}\right)^3 - .085 \cdot in \qquad \text{(Eqn. 2.23)}$$

$a = 0.598 \cdot in$

$$F_1 := \frac{b_f \cdot t_p^{\,2} \cdot F_{py}}{4 \cdot p_f \cdot \sqrt{1 + \left(\frac{3 \cdot t_p^{\,2}}{16 \cdot p_f^{\,2}}\right)}} \qquad \text{(Eqn. 2.29)}$$

$F_1 = 19.981 \cdot k$

$$F_{11} := \frac{\left[t_p^{\,2} \cdot F_{py} \cdot \left[.85 \cdot \left(\frac{b_f}{2}\right) + .8 \cdot w\right] + \frac{\left(\pi \cdot d_b^{\,3} \cdot F_{yb}\right)}{8}\right]}{2 \cdot p_f} \qquad \text{(Eqn. 2.30)}$$

$F_{11} = 37.241 \cdot k$

$$Q_{max} := \frac{w \cdot t_p^{\,2}}{4 \cdot a} \cdot \sqrt{F_{py}^{\,2} - 3 \cdot \left(\frac{F_{11}}{2 \cdot w \cdot t_p}\right)^2} \qquad \text{(Eqn. 2.34)}$$

$Q_{max} = 18.64 \cdot k$

**Plate is considered thin since $P_t > F_{11} / 2$. Therefre the maximum prying force, Q_{max}, given above applies.

$$Mq := \left(\frac{h}{12 \cdot \frac{in}{ft}}\right) \cdot \left[\left(P_t - Q_{max}\right) \cdot \frac{2}{\beta}\right]$$

$Mq = 650.454\ k \cdot ft$

RESULTS:

$$M_{PL} = 610.081\ k \cdot ft$$

$$Mq = 650.454\ k \cdot ft$$

Maximum Applied Moment: $Mu := 904\ ft - k$

VITA

John C. Ryan, Jr. was born in Slidell, Louisiana on February 19, 1975. After graduating from high school in 1993, he began work on a Bachelor of Science in Civil Engineering at Louisiana State University, Baton Rouge, Louisiana. In the fall of 1996, he began an exchange program at Virginia Polytechnic Institute and State University, Blacksburg, Virginia for one semester. The exchange was extended to two semesters, at the end of which, John transferred to Virginia Tech, where he completed his Bachelor of Science in Civil Engineering in May 1998. He immediately began work on a Master of Science in Civil Engineering, which was completed in September 1999. John will begin working for Anderson Consulting in Atlanta Georgia in October 1999.